THE TOTAL SYNTHESIS OF (+)-INELEGANOLIDE, THE LYCOJAPOMINE ALKALOIDS, AND A NEW STRATEGY FOR RADICAL DEOXYGENATION

Thesis by

Benjamin Martin Gross

In Partial Fulfillment of the Requirements

for the Degree of

Doctor of Philosophy



CALIFORNIA INSTITUTE OF TECHNOLOGY

Pasadena, California

2026

(Defended January 26, 2026)

© 2026

Benjamin Martin Gross
ORCID: 0000-0002-9124-2317

All Rights Reserved

Dedicated to

my family, friends, professors and mentors

that supported me throughout the years

ACKNOWLEDGEMENTS

I want to thank Prof. Brian Stoltz for serving as my PhD advisor. My time at Caltech, including my scientific as well as personal progress, would not have been the same without him. Over the course of my graduate studies, I have come to realize and cherish how special it is to have an advisor that wants the best for you. I thank him for wholeheartedly taking me into his research group and encouraging me in the many ways he has. I have come to be in awe of what it means to keep a research group like his running successfully for over 20 years (I can imagine it's not always easy!). His approach to leadership and his patience has been an inspiration, especially towards the later years of my graduate school. I will always remain grateful for his unwavering support. I would also like to thank Erna, Harry and Teddy, for always welcoming Somya and me with open arms and for all the conversations we got to share.

I would like to thank Prof. Hosea Nelson, Prof. Daniel Semlow and Prof. Greg Fu for serving as my thesis committee. I appreciate the time that they have all put in, sitting through my ideas in candidacy and proposal exams and supporting me throughout my time at Caltech. I would also like to thank Prof. Sarah Reisman, who played a crucial role in recruiting me to Caltech in the first place. Even though I was not a member of her research group, the interactions we had over the years meant a lot to me. I want to thank her for always believing in me and taking an interest in the science I conducted. Even though she likes to say: "You don't owe me anything, Ben!"- I will always be grateful for her support.

When I started on the ineleganolide project, people always told me: "You should talk to Scott."- and I did. Scott always took an interest in my ideas and the project with pure enthusiasm and joy. I want to thank him for his support on all the HPLC runs and

excitement we shared when isolating natural products. I had so much fun working alongside him, joking and talking. Thank you also to his wife Silva for always welcoming Somya and me- I will miss the wonderful Christmas parties.

I would like to thank Dr. David Vander Velde, and Dr. Rajan Paranji, for maintaining and running the NMR facility. It has been great to get to know both and work as a GLA alongside them, learning about the intricacies of NMR instruments. I would also like thank Dr. Michael Takase for running the X-ray facility and his persistence when collecting data from my often 'very small' crystals.

I would like to thank all the members of the Stoltz and Reisman group that I have interacted with over the years. I want to thank Yujia, Jordan, Emily, Simon, and many more for first welcoming me to Caltech during my summer rotation and helping me get set up in lab. I want to thank Nick Hafeman, for selling me on the 'cembranoid natural products' and for his enthusiasm and openness when I first joined the group. I would also especially like to thank my 'hood mates' Elliot and Hao. Both of them are exceptional scientists that take a real, dedicated interest in chemistry- which I have always appreciated. I will think fondly of all the times they would both listen to my ideas (sometimes more philosophical), and all the laughs we shared. I would also like to thank Samir, for his friendliness and endless encouragement. I miss just going over a bay and shooting the breeze with him. I want to thank Elijah for joining the lab, and the adjacent bay, taking a chance in listening to my suggestions. It has been great to interact with him- his enthusiasm and interest for synthesis has been motivating and I am sure he will continue to do great in graduate school. I am excited to follow the future of the lab and the next generation of graduate students.

Adrian, Chloe, Jonathan, Bryce, Sara, Maddie- I am excited to see all of their projects unfold.

I would also like to thank Sophia Razavi, for her dedication and enthusiasm while working on the titanium project with me over the summer. It has been a great time working with her- I am sure she will continue to do great things.

There are many more people that I can think of: Adrian de Almenara, Christian, Kevin, Jay, Farbod, Kali, Angel, Melinda, Veronica, Trevor Butcher, Yutaro, Liam and the list goes on and on. Thank you all for the support, great or small, and talks, short or long, that have shaped my time throughout graduate school.

I would like to thank Prof. Martin Oestreich, for teaching me organic chemistry from the ground-up and shaping me in a way that has made my career in chemistry possible. I think fondly of my time in Berlin and looking back am always grateful for all the chances and support that he has provided me with.

I would like to thank Prof. Christopher Vanderwal, for welcoming me into his lab at UCI and for his tremendous support in applying for graduate school and beyond. The time at UCI was transformative for me and has forever shaped my interest in total synthesis and chemistry as a whole. I would also like to thank Darius Vrubliauskas for mentoring me during that time and building me up with his unwavering determination. I consider myself fortunate to have worked alongside him and all the things he has taught me.

All throughout, graduate studies and life in general would not have been possible without the help and guidance of my family. I want to thank Margie and John for taking me in during my time in Irvine and for always being there for Somya and me. It is so special to have you in my life. Thank you for all the love you have shown us and for always having

an open door and ear for us. Thank you also to Leslie, Greg, Laura, Dean, Amy, Jack, Will, Tommy, Lulu, Ben and Macy. I am fortunate to have you all as part of my family here in California.

I want to thank Tanya and Drew for welcoming me into their family and for their support. I am thankful for all the time, the laughter, and holidays we got to share together with Winston and Olive and look forward to many more.

I want to thank my parents, Kathrin and Dietmar, for their support throughout my PhD and everything that they have done for me. I know it is not always easy being so far apart- their love, encouragement and faith we share shaped me in a way that is beyond words. I want to also thank my brothers, Maximilian and Jonathan, and Marie and Madeleine for their support. I am so thankful to have you all in my life. It has been a blessing, and I look forward to many more memories together.

Last, but not least, I would like to express my love for my wife, Somya. I never thought we would be where we are today. I am so thankful to have you alongside me and for all the times you stood by me throughout my PhD. It would be pretty lonely without you, and I feel so blessed to have you in my life.

ABSTRACT

Organic chemistry is an enabling science, that has given scientist the ability to construct and manipulate small molecules. The relationship that bridges the classic study of chemical reactivity and synthesis at the molecular level with the broader field of the life sciences continues to flourish and has expanded its impact tremendously. The study of complex, bioactive small molecules, their synthesis, and the development of new reactions has laid the foundation for many of these advancements to build upon. The contents of this thesis contribute to this goal and hope to be of use for future generations and the development of the field.

The first chapter describes the total synthesis of the furanobutenolide-derived norcembranoid diterpenoid ineleganolide, a secondary metabolite produced by sinularia soft corals. Displaying cytotoxic bioactivity, the chemical structure has intrigued chemists for several decades. We describe a successful synthesis of the natural product in 14 steps, enabled by several unique cascade reactions.

The second chapter details the total synthesis of Lycojapomine A and B, two members of the lycopodium alkaloids. To achieve a practical and concise synthetic route, we developed a photoreaction for the stepwise dearomatization of a pyrrole heterocycle. Building off the simple and easily accessible starting material, we can synthesize each of the complex target molecule in 13 steps.

Inspired by the previously utilized photochemistry, the third chapter details a new catalytic method for the generation of alkyl radicals directly from alcohols. We achieved this transformation by photo irradiation of a titanium porphyrin catalyst and showcase its ability to deoxygenate several different alcohols, by generation of the carbon-centered radical.

PUBLISHED CONTENT AND CONTRIBUTIONS

1. Gross, B. M.; Han, S.-J.; Stoltz, B. M. A Convergent Total Synthesis of (+)-Ineleganolide. *J. Am. Chem. Soc.* **2023**, *145*, 7763–7767. DOI: 10.1021/jacs.3c02142

   B.M.G. contributed to project conceptualization, experimental investigation, data analysis and preparation of the manuscript.

2. Gross, B. M.; Stoltz, B. M. Convenient access to a strained bicyclic enone: A concise and improved formal synthesis of ineleganolide. *Tetrahedron Lett.* **2024**, *140*, 155011. DOI: 10.1016/j.tetlet.2024.155011

   B.M.G. contributed to project conceptualization, experimental investigation, data analysis and preparation of the manuscript.

3. Gross, B. M.; Stoltz, B. M. Concise Syntheses of Lycojapomine Alkaloids Enabled by Radical Dearomatization of a Pyrrole. *J. Am. Chem. Soc.* **2025**, *147*, 20200–20204. DOI: 10.1021/jacs.5c05721

   B.M.G. contributed to project conceptualization, experimental investigation, data analysis and preparation of the manuscript.

4. Gross, B. M.; Razavi, S.; de Almenara, A. J.; Stoltz, B. M. Radical Deoxygenation of Alcohols via Visible Light Irradiation of a Titanium Porphyrin Catalyst. *Submitted for publication*.

   B.M.G. contributed to project conceptualization, experimental investigation, data analysis and preparation of the manuscript.

TABLE OF CONTENTS

Dedication iii
Acknowledgements iv
Abstract viii
Published Content and Contributions ix
Table of Contents x
List of Figures xiii
List of Schemes xviii
List of Tables xix
List of Abbreviations xxi

CHAPTER 1 ***1***
The Total Synthesis of Ineleganolide

1.1 Introduction 1
1.2 Previous Research Considerations 2
1.3 Retrosynthetic Analysis 5
1.4 Synthesis of Fragments 6
1.5 Fragment Coupling and Completion of the Synthesis 10
1.6 Conclusion 14
1.7 Experimental Section 15
1.7.1 Materials and Methods 15
1.7.2 Synthesis of Starting Materials 16
1.7.3 Experimental Procedures 17
1.8 References and Notes 40

APPENDIX 1 ***46***
Spectra Relevant to Chapter 1

APPENDIX 2 ***83***
X-Ray Crystallography Reports Relevant to Chapter 1

A2.1 General Experimental Information 84
A2.2 X-Ray Crystal Structure Analysis of **31** 84
A2.3 X-Ray Crystal Structure Analysis of **33** 105

A2.4 X-Ray Crystal Structure Analysis of **1** 117

CHAPTER 2 ***128***
Total Synthesis of Lycojapomine A & B

2.1 Introduction 128
2.2 Retrosynthetic Strategy: Pyrrole Dearomatization 129
2.3 Photocatalytic Radical Addition 130
2.4 Annulation Cascade to form the Core Structure 133
2.5 Divergent Aldol Reaction and Completion of the Synthesis 136
2.6 Conclusion 137
2.7 Experimental Section 138
2.7.1 Materials and Methods 138
2.7.2 Experimental Procedures 139
2.8 References and Notes 154

APPENDIX 3 ***159***
Spectra Relevant to Chapter 2

CHAPTER 3 ***182***
Radical Deoxygenation of Alcohols by a Titanium Porphyrin Catalyst

3.1 Introduction 182
3.2 Reaction Optimization 185
3.3 Evaluation of Substrate Generality 187
3.4 Mechanistic Investigations 190
3.5 Use in Giese Addition and Cross-coupling 193
3.6 Conclusion 193
3.7 Experimental Section 194
3.7.1 Materials and Methods 194
3.7.2 Experimental Procedures 196
3.7.2.1 Syntheis of $Ti(TPP)Cl_2$ 196
3.7.2.2 General Reaction Procedure A 197
3.7.2.3 Substrates for Deoxygenation 198
3.7.2.4 Synthetic Derivatives 214
3.7.2.5 Mechanistic Experiments 218
3.7.2.6 Giese Addition and Cross-coupling 220

3.8 References and Notes.....223

APPENDIX 4 ***234***
Spectra Relevant to Chapter 3

ABOUT THE AUTHOR ***272***

LIST OF FIGURES

CHAPTER 1
The Total Synthesis of Ineleganolide

Figure 1.1.1. Structures of representative furanobutenolide-derived diterpenoids.....1
Figure 1.5.3. X-ray structure of **1** 14

APPENDIX 1
Spectra Relevant to Chapter 1

Figure A1.1. ^{1}H NMR (600 MHz, $CDCl_3$) of compound **18** 47
Figure A1.2. Infrared spectrum (Thin Film, NaCl) of compound **18** 48
Figure A1.3. ^{13}C NMR (100 MHz, $CDCl_3$) of compound **18** 48
Figure A1.4. ^{1}H NMR (600 MHz, $CDCl_3$) of compound **19** 49
Figure A1.5. Infrared spectrum (Thin Film, NaCl) of compound **19** 50
Figure A1.6. ^{13}C NMR (100 MHz, $CDCl_3$) of compound **19** 50
Figure A1.7. ^{1}H NMR (600 MHz, $CDCl_3$) of compound **39** 51
Figure A1.8. Infrared spectrum (Thin Film, NaCl) of compound **39** 52
Figure A1.9. ^{13}C NMR (100 MHz, $CDCl_3$) of compound **39** 52
Figure A1.10. ^{1}H NMR (600 MHz, $CDCl_3$) of compound **21** 53
Figure A1.11. Infrared spectrum (Thin Film, NaCl) of compound **21** 54
Figure A1.12. ^{13}C NMR (125 MHz, $CDCl_3$) of compound **21** 54
Figure A1.13. ^{1}H NMR (600 MHz, $CDCl_3$) of compound **22** 55
Figure A1.14. Infrared spectrum (Thin Film, NaCl) of compound **22** 56
Figure A1.15. ^{13}C NMR (125 MHz, $CDCl_3$) of compound **22** 56
Figure A1.16. ^{1}H NMR (600 MHz, $CDCl_3$) of compound **28** 57
Figure A1.17. Infrared spectrum (Thin Film, NaCl) of compound **28** 58
Figure A1.18. ^{13}C NMR (100 MHz, $CDCl_3$) of compound **28** 58
Figure A1.19. ^{1}H NMR (600 MHz, $CDCl_3$) of compound **16** 59
Figure A1.20. Infrared spectrum (Thin Film, NaCl) of compound **16** 60
Figure A1.21. ^{13}C NMR (100 MHz, $CDCl_3$) of compound **16** 60
Figure A1.22. ^{1}H NMR (400 MHz, $CDCl_3$) of compound **26** 61
Figure A1.23. Infrared spectrum (Thin Film, NaCl) of compound **26** 62
Figure A1.24. ^{13}C NMR (100 MHz, $CDCl_3$) of compound **26** 62

Figure A1.25. ^{1}H NMR (400 MHz, $CDCl_3$) of compound **27** 63
Figure A1.26. Infrared spectrum (Thin Film, NaCl) of compound **27** 64
Figure A1.27. ^{13}C NMR (100 MHz, $CDCl_3$) of compound **27** 64
Figure A1.28. ^{1}H NMR (400 MHz, $CDCl_3$) of compound **41** 65
Figure A1.29. Infrared spectrum (Thin Film, NaCl) of compound **41** 66
Figure A1.30. ^{13}C NMR (100 MHz, $CDCl_3$) of compound **41** 66
Figure A1.31. ^{1}H NMR (400 MHz, $CDCl_3$) of compound **42** 67
Figure A1.32. Infrared spectrum (Thin Film, NaCl) of compound **42** 68
Figure A1.33. ^{13}C NMR (100 MHz, $CDCl_3$) of compound **42** 68
Figure A1.34. ^{1}H NMR (600 MHz, $CDCl_3$) of compound **15** 69
Figure A1.35. Infrared spectrum (Thin Film, NaCl) of compound **15** 70
Figure A1.36. ^{13}C NMR (100 MHz, $CDCl_3$) of compound **15** 70
Figure A1.37. ^{1}H NMR (600 MHz, $CDCl_3$) of compound **31** 71
Figure A1.38. Infrared spectrum (Thin Film, NaCl) of compound **31** 72
Figure A1.39. ^{13}C NMR (100 MHz, $CDCl_3$) of compound **31** 72
Figure A1.40. ^{1}H NMR (600 MHz, $CDCl_3$) of compound **43** 73
Figure A1.41. Infrared spectrum (Thin Film, NaCl) of compound **43** 74
Figure A1.42. ^{13}C NMR (125 MHz, $CDCl_3$) of compound **43** 74
Figure A1.43. ^{1}H NMR (600 MHz, $CDCl_3$) of compound **32** 75
Figure A1.44. Infrared spectrum (Thin Film, NaCl) of compound **32** 76
Figure A1.45. ^{13}C NMR (125 MHz, $CDCl_3$) of compound **32** 76
Figure A1.46. ^{1}H NMR (400 MHz, $CDCl_3$) of compound **33** 77
Figure A1.47. Infrared spectrum (Thin Film, NaCl) of compound **33** 78
Figure A1.48. ^{13}C NMR (100 MHz, $CDCl_3$) of compound **33** 78
Figure A1.49. ^{1}H NMR (600 MHz, $CDCl_3$) of compound **34** 79
Figure A1.50. Infrared spectrum (Thin Film, NaCl) of compound **34** 80
Figure A1.51. ^{13}C NMR (100 MHz, $CDCl_3$) of compound **34** 80
Figure A1.52. ^{1}H NMR (400 MHz, $CDCl_3$) of compound **1** 81
Figure A1.53. Infrared spectrum (Thin Film, NaCl) of compound **1** 82
Figure A1.54. ^{13}C NMR (100 MHz, $CDCl_3$) of compound **1** 82

APPENDIX 2

X-Ray Crystallography Reports Relevant to Chapter 1

Figure A2.2.1. X-ray crystal structure of compound **31** 84
Figure A2.3.1. X-ray crystal structure of compound **33** 105

Figure A2.4.1. X-ray crystal structure of compound **1** 117

CHAPTER 2
Total Synthesis of Lycojapomine A & B

Figure 2.2.1. (A) Structure of Lycojapomine A (**44**) and B (**45**) and proposed retrosynthetic elements. (B) Concept of reductive functionalization of a pyrrole. 129
Figure 2.3.1. Synthesis of starting material **48** 131
Figure 2.4.2. Potential pathways and considerations for cascade ring annulation 134

APPENDIX 3
Spectra Relevant to Chapter 2

Figure A3.1. ^{1}H NMR (400 MHz, $CDCl_3$) of compound **46** 160
Figure A3.2. Infrared spectrum (Thin Film, NaCl) of compound **46** 161
Figure A3.3. ^{13}C NMR (101 MHz, $CDCl_3$) of compound **46** 161
Figure A3.4. ^{1}H NMR (400 MHz, $CDCl_3$) of compound **48** 162
Figure A3.5. Infrared spectrum (Thin Film, NaCl) of compound **48** 163
Figure A3.6. ^{13}C NMR (101 MHz, $CDCl_3$) of compound **48** 163
Figure A3.7. ^{1}H NMR (600 MHz, $CDCl_3$) of compound **49** (*trans*) 164
Figure A3.8. Infrared spectrum (Thin Film, NaCl) of compound **49** (*trans*) 165
Figure A3.9. ^{13}C NMR (101 MHz, $CDCl_3$) of compound **49** (*trans*) 165
Figure A3.10. ^{1}H NMR (400 MHz, $CDCl_3$) of compound **49** (*cis*) 166
Figure A3.11. Infrared spectrum (Thin Film, NaCl) of compound **49** (*cis*) 167
Figure A3.12. ^{13}C NMR (101 MHz, $CDCl_3$) of compound **49** (*cis*) 167
Figure A3.13. ^{1}H NMR (400 MHz, $CDCl_3$) of compound **52** 168
Figure A3.14. Infrared spectrum (Thin Film, NaCl) of compound **52** 169
Figure A3.15. ^{13}C NMR (101 MHz, $CDCl_3$) of compound **52** 169
Figure A3.16. ^{1}H NMR (400 MHz, $CDCl_3$) of compound **53** 170
Figure A3.17. Infrared spectrum (Thin Film, NaCl) of compound **53** 171
Figure A3.18. ^{13}C NMR (101 MHz, $CDCl_3$) of compound **53** 171
Figure A3.19. ^{1}H NMR (400 MHz, $CDCl_3$) of compound **59** 172
Figure A3.20. Infrared spectrum (Thin Film, NaCl) of compound **59** 173
Figure A3.21. ^{13}C NMR (101 MHz, $CDCl_3$) of compound **59** 173
Figure A3.22. ^{1}H NMR (400 MHz, $CDCl_3$) of compound **60** 174
Figure A3.23. Infrared spectrum (Thin Film, NaCl) of compound **60** 175

Figure A3.24. ^{13}C NMR (101 MHz, $CDCl_3$) of compound **60** 175
Figure A3.25. ^{1}H NMR (600 MHz, CD_3OD) of compound **61** 176
Figure A3.26. Infrared spectrum (Thin Film, NaCl) of compound **61** 177
Figure A3.27. ^{13}C NMR (101 MHz, CD_3OD) of compound **61** 177
Figure A3.28. ^{1}H NMR (600 MHz, CD_3OD) of compound **45** 178
Figure A3.29. Infrared spectrum (Thin Film, NaCl) of compound **45** 179
Figure A3.30. ^{13}C NMR (101 MHz, CD_3OD) of compound **45** 179
Figure A3.31. ^{1}H NMR (600 MHz, CD_3OD) of compound **44** 180
Figure A3.32. Infrared spectrum (Thin Film, NaCl) of compound **44** 181
Figure A3.33. ^{13}C NMR (101 MHz, CD_3OD) of compound **44** 181

CHAPTER 3
Radical Deoxygenation of Alcohols by a Titanium Porphyrin Catalyst

Figure 3.1.1. Evolution of a titanium porphyrin catalyst for deoxygenation 183
Figure 3.3.1. Substrate scope for radical deoxygenation 188
Figure 3.3.2. Implementation of deoxygenation method in synthesis 190
Figure 3.4.1. Mechanistic control experiments 191
Figure 3.4.2. Preliminary mechanistic proposal 192
Figure 3.5.1. Interception of radical for Giese addition and Nickel cross-coupling 193
Figure 3.7.2.1.1. UV-Vis spectrum of $Ti(TPP)Cl_2$ 197
Figure 3.7.2.5.1. Mass trace analysis of adduct **69e** 219

APPENDIX 4
Spectra Relevant to Chapter 3

Figure A4.1. ^{1}H NMR (600 MHz, C_6D_6) of **$Ti(TPP)Cl_2$** 235
Figure A4.2. ^{1}H NMR (400 MHz, $CDCl_3$) of compound **69b** 236
Figure A4.3. ^{1}H NMR (400 MHz, $CDCl_3$) of compound **69c** 237
Figure A4.4. ^{1}H NMR (400 MHz, $CDCl_3$) of compound **71b** 238
Figure A4.5. ^{1}H NMR (400 MHz, $CDCl_3$) of compound **72b** 239
Figure A4.6. ^{1}H NMR (400 MHz, $CDCl_3$) of compound **73b** 240
Figure A4.7. ^{1}H NMR (400 MHz, $CDCl_3$) of compound **74b** 241
Figure A4.8. ^{1}H NMR (400 MHz, $CDCl_3$) of compound **76b** 242
Figure A4.9. ^{1}H NMR (400 MHz, $CDCl_3$) of compound **77b** 243
Figure A4.10. ^{1}H NMR (400 MHz, $CDCl_3$) of compound **78b** 244
Figure A4.11. ^{1}H NMR (500 MHz, $CDCl_3$) of compound **79b** 245

Figure A4.12. ^{1}H NMR (600 MHz, $CDCl_3$) of compound **80b** 246
Figure A4.13. ^{1}H NMR (600 MHz, $CDCl_3$) of compound **81b** 247
Figure A4.14. ^{1}H NMR (400 MHz, $CDCl_3$) of compound **82b** 248
Figure A4.15. ^{1}H NMR (400 MHz, $CDCl_3$) of compound **83b** 249
Figure A4.16. ^{1}H NMR (400 MHz, $CDCl_3$) of compound **84b** 250
Figure A4.17. ^{1}H NMR (400 MHz, $CDCl_3$) of compound **88b**, **88c**, **88d** 251
Figure A4.18. ^{1}H NMR (600 MHz, $CDCl_3$) of compound **90b**, **90c**, **90d** 252
Figure A4.19. ^{1}H NMR (400 MHz, $CDCl_3$) of compound **93b** 253
Figure A4.20. Infrared spectrum (Thin Film, NaCl) of compound **93b** 254
Figure A4.21. ^{13}C NMR (101 MHz, $CDCl_3$) of compound **93b** 254
Figure A4.22. ^{1}H NMR (400 MHz, $CDCl_3$) of compound **95b** 255
Figure A4.23. ^{1}H NMR (400 MHz, $CDCl_3$) of compound **97b** 256
Figure A4.24. ^{13}C NMR (101 MHz, $CDCl_3$) of compound **97b** 257
Figure A4.25. ^{1}H NMR (400 MHz, $CDCl_3$) of compound **98a** 258
Figure A4.26. Infrared spectrum (Thin Film, NaCl) of compound **98a** 259
Figure A4.27. ^{13}C NMR (101 MHz, $CDCl_3$) of compound **98a** 259
Figure A4.28. ^{1}H NMR (400 MHz, $CDCl_3$) of compound **98b** 260
Figure A4.29. Infrared spectrum (Thin Film, NaCl) of compound **98b** 261
Figure A4.30. ^{13}C NMR (101 MHz, $CDCl_3$) of compound **98b** 261
Figure A4.31. ^{1}H NMR (400 MHz, $CDCl_3$) of compound **99** 262
Figure A4.32. ^{1}H NMR (600 MHz, $CDCl_3$) of compound **100a** 263
Figure A4.33. ^{1}H NMR (600 MHz, $CDCl_3$) of compound **101** 264
Figure A4.34. ^{1}H NMR (600 MHz, $CDCl_3$) of **HE-d$_2$** 265
Figure A4.35. ^{1}H NMR (400 MHz, $CDCl_3$) of compound **69d** 266
Figure A4.36. ^{1}H NMR (400 MHz, $CDCl_3$) of compound **102** 267
Figure A4.37. Infrared spectrum (Thin Film, NaCl) of compound **102** 268
Figure A4.38. ^{13}C NMR (101 MHz, $CDCl_3$) of compound **102** 268
Figure A4.39. ^{1}H NMR (400 MHz, $CDCl_3$) of compound **103** 269
Figure A4.40. Infrared spectrum (Thin Film, NaCl) of compound **103** 270
Figure A4.41. ^{13}C NMR (101 MHz, $CDCl_3$) of compound **103** 270
Figure A4.42. ^{1}H NMR (600 MHz, $CDCl_3$) of compound **104** 271

LIST OF SCHEMES

CHAPTER 1
The Total Synthesis of Ineleganolide

Scheme 1.2.1. Biomimetic and bioinspired synthesis of **1** by Pattenden and Wood 2
Scheme 1.2.2. Previous approach to (-)-**1** by Stoltz and co-workers 4
Scheme 1.2.3. Previous approach to (-)-**1** by Vanderwal and co-workers 4
Scheme 1.2.4. Successful oxa-Michael and epimerization cascade by Fürstner in 2024 5
Scheme 1.3.1. Retrosynthesis of (+)-ineleganolide 6
Scheme 1.4.1. First-generation synthesis of enone **16**. 7
Scheme 1.4.2. Second-generation synthesis of enone **16** 9
Scheme 1.5.1. Completion of the total synthesis of Ineleganolide (**1**) 11
Scheme 1.5.2. Mechanistic proposal for air-oxidation to intermediate **33** 12
Scheme 1.7.2.1. Route to carboxylic acid **5**, Ref [17] 16
Scheme 1.7.2.2. Route to aldehyde **17**, Ref [20] and [21] 17

CHAPTER 2
Total Synthesis of Lycojapomine A & B

Scheme 2.4.1. Synthetic sequence to access the Lycojapomine core structure 133
Scheme 2.5.1. Oxidative cleavage and divergent aldol reaction to access **44** and **45** 136

LIST OF TABLES

APPENDIX 2

X-Ray Crystallography Reports Relevant to Chapter 1

Table A2.2.2. Crystal data and structure refinement for compound **31** 84

Table A2.2.3. Atomic coordinates ($\times 10^4$) and equivalent isotropic displacement parameters ($Å^2 \times 10^3$) for compound **31**. U(eq) is defined as one third of the trace of the orthogonalized U^{ij} tensor 85

Table A2.2.4. Bond lengths [Å] and angles [°] for compound **31** 87

Table A2.2.5. Anisotropic displacement parameters ($Å^2 \times 10^3$) for compound **31**. The anisotropic displacement factor exponent takes the form: $-2p^2[h^2a^{*2}U^{11} + \ldots + 2hka^*b^*U^{12}]$ 96

Table A2.2.6. Hydrogen coordinates (x 10^4) and isotropic displacement parameters ($Å^2 \times 10^3$) for compound **31** 98

Table A2.2.7. Torsion angles [°] for compound **31** 99

Table A2.2.8. Hydrogen bonds for compound **31** [Å and °] 104

Table A2.3.2. Crystal data and structure refinement for compound **33** 105

Table A2.3.3. Atomic coordinates ($\times 10^4$) and equivalent isotropic displacement parameters ($Å^2 \times 10^3$) for compound **33**. U(eq) is defined as one third of the trace of the orthogonalized U^{ij} tensor 106

Table A2.3.4. Bond lengths [Å] and angles [°] for compound **31** 107

Table A2.3.5. Anisotropic displacement parameters ($Å^2 \times 10^3$) for compound **33**. The anisotropic displacement factor exponent takes the form: $-2p^2[h^2a^{*2}U^{11} + \ldots + 2hka^*b^*U^{12}]$ 111

Table A2.3.6. Hydrogen coordinates (x 10^4) and isotropic displacement parameters ($Å^2 \times 10^3$) for compound **33** 112

Table A2.3.7. Torsion angles [°] for compound **33** 113

Table A2.3.8. Hydrogen bonds for compound **33** [Å and °] 116

Table A2.4.2. Crystal data and structure refinement for compound **1** 117

Table A2.4.3. Atomic coordinates ($\times 10^4$) and equivalent isotropic displacement parameters ($Å^2 \times 10^3$) for compound **1**. U(eq) is defined as one third of the trace of the orthogonalized U^{ij} tensor 118

Table A2.4.4. Bond lengths [Å] and angles [°] for compound **1** 119

Table A2.4.5. Anisotropic displacement parameters ($Å^2 \times 10^3$) for compound **1**. The anisotropic displacement factor exponent takes the form: $-2p^2[h^2a^{*2}U^{11} + \ldots + 2hka^*b^*U^{12}]$ 123

Table A2.4.6. Hydrogen coordinates (x 10^4) and isotropic displacement parameters ($Å^2 \times 10^3$) for compound **1** 124
Table A2.4.7. Torsion angles [°] for compound **1** 125

CHAPTER 2
Total Synthesis of Lycojapomine A & B

Table 2.3.2. Optimization of dearomative intramolecular radical addition 132

CHAPTER 3
Radical Deoxygenation of Alcohols by a Titanium Porphyrin Catalyst

Table 3.2.1. Optimization of reaction conditions 186

LIST OF ABBREVIATIONS

Å	Ångstrom
λ	wavelength
μ	micro
μwave	microwave
$[\alpha]_D$	specific rotation at wavelength of sodium D line
°C	degrees Celsius
Ac	acetyl
AcOH	acetic acid
An	*para*-anisoyl
APCI	atmospheric pressure chemical ionization
aq	aqueous
Ar	aryl
atm	atmosphere
Bn	benzyl
Boc	*tert*-butyloxycarbonyl
bp	boiling point
br	broad
Bu	butyl
Bz	benzoyl
c	concentration for specific rotation measurements (g/100 mL)
calc'd	calculated
CAN	ceric ammonium nitrate
cat	catalytic

cm^{-1}	wavenumber(s)
COD	1,5-cyclooctadiene
Cp	cyclopentadienyl
Cy	cyclohexyl
d	doublet
D	deuterium
dba	dibenzylideneacetone
DBU	1,8-diazabicyclo[5.4.0]undec-7-ene
DCE	1,2-dichloroethane
DIBAL	diisobutylaluminum hydride
DMA	*N*,*N*-dimethylacetamide
DMAP	4-dimethylaminopyridine
DMF	*N*,*N*-dimethylformamide
DMP	Dess-Martin periodinane
DMSO	dimethyl sulfoxide
dr	diastereomeric ratio
e.g.	for example (Latin exempli gratia)
ee	enantiomeric excess
equiv	equivalent(s)
ESI	electrospray ionization
Et	ethyl
EtOAc	ethyl acetate
FAB	fast atom bombardment
FD	field desorption
g	gram(s)
GC	gas chromatography
h	hour(s)

HE	Hantzsch ester
HFIP	1,1,1,3,3,3-hexafluoropropan-2-ol
HMDS	1,1,1,3,3,3-hexamethyldisilazane
HMPA	hexamethylphosphoramide
HPLC	high-performance liquid chromatography
HRMS	high-resolution mass spectroscopy
Hz	hertz
i-Bu	isobutyl
i.e.	that is (Latin id est)
IBX	2-iodoxybenzoic acid
IPA	isopropanol, 2-propanol
i-Pr	isopropyl
IR	infrared (spectroscopy)
J	coupling constant
K	Kelvin(s) (absolute temperature)
kcal	kilocalorie
L	liter; neutral ligand
LC–MS	liquid chromatography–mass spectrometry
LDA	lithium diisopropylamide
m	multiplet; milli
m	meta
M	metal; molar; molecular ion
m/z	mass to charge ratio
m-CPBA	*meta*-chloroperoxybenzoic acid
Me	methyl
mg	milligram(s)
MHz	megahertz

min	minute(s)
MM	mixed method
mol	mole(s)
mp	melting point
Ms	methanesulfonyl (mesyl)
MS	molecular sieves
MTBE	methyl *tert*-butyl ether
NBS	*N*-bromosuccinimide
n-Bu	butyl
NCS	*N*-chlorosuccinimide
ND	not determined
NMP	*N*-methyl-2-pyrrolidone
NMR	nuclear magnetic resonance
NR	no reaction detected
Nu^-	nucleophile
o	ortho
p	para
Pd/C	palladium on carbon
PG	protecting group
Ph	phenyl
pH	hydrogen ion concentration in aqueous solution
Phth	phthaloyl
Piv	pivaloyl
ppm	parts per million
Pr	propyl
p-TsOH	*para*-toluenesulfonic acid
Py	pyridine

q	quartet
R	generic for any atom or functional group
Ref.	reference
s	singlet
t	triplet
TBAF	tetrabutylammonium fluoride
TBS	*tert*-butyldimethylsilyl
t-Bu	*tert*-butyl
Tf	trifluoromethanesulfonyl (triflyl)
TFA	trifluoroacetic acid
TFAA	trifluoroacetic anhydride
TFE	2,2,2-trifluoroethanol
THF	tetrahydrofuran
TLC	thin-layer chromatography
TMP	2,2,6,6-tetramethylpiperidine
TMS	trimethylsilyl
TOF	time-of-flight
TosMIC	*para*-toluenesulfonylmethyl isocyanide
t_R	retention time
Ts	*p*-toluenesulfonyl (tosyl)
UV	ultraviolet
v/v	volume to volume
w	weak
w/v	weight to volume
w/w	weight to weight
X	anionic ligand or electronegative element

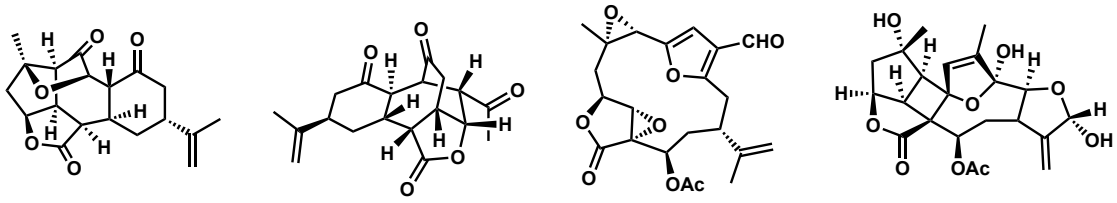
CHAPTER 1

The Total Synthesis of Ineleganolide †

1.1 INTRODUCTION

The cembranoid and norcembranoid diterpenoids represent a large family of natural products isolated from soft coral species.[1] Because of their unique, highly complex structures, the furanobutenolide-derived diterpenoids have received considerable attention from synthetic chemists over the past decades, which has given rise to new reaction developments in synthetic chemistry.[2] They have furthermore served as a proving ground in retrosynthetic planning and in delivering useful amounts of material for potential further investigations into their bioactivity.[3] A subclass of these molecules contain a macrocyclic structure, as represented by the neurotoxin lophotoxin (**3**), which functions as an irreversible inhibitor of the nicotinic acetylcholine receptor (Figure 1.1.1).[4,5]

Figure 1.1.1 *Structures of representative furanobutenolide-derived diterpenoids.*



Biosynthetically, these macrocycles are suggested to engage in further modifications to give rise to more dense polycyclic structures. Showcase examples of these architectures

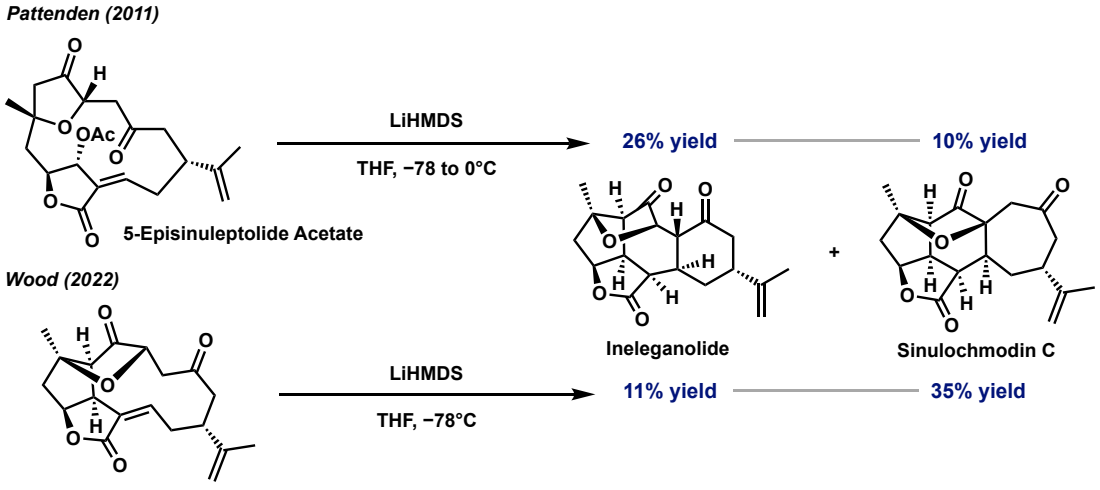
† Portions of this chapter have been reproduced and modified with permission from Gross, B. M.; Han, S.-J.; Stoltz, B. M. *J. Am. Chem. Soc.* **2023**, *145*, 7763–7767 under CC-BY 4.0; Gross, B. M.; Stoltz, B. M. *Tetrahedron Lett.* **2024**, *140*, 155011. © 2023 American Chemical Society, 2024 Elsevier Ltd.

are reflected in horiolide (**2**) or bielschowskysin (**4**), which shows promising cytotoxicity against non-small cell lung cancer and renal cancer.[6] Another flagship member of this class, ineleganolide (**1**), was isolated from the Formosan soft coral Sinularia inelegans by Duh and co-workers in 1999.[7] It has shown preliminary cytotoxicity against P-380 leukeumia cell lines, but further insights into its bioactivity remain undisclosed.

1.2 PREVIOUS RESEARCH CONSIDERATIONS

Structurally, ineleganolide contains a highly rigid oxidized framework that bears a key central seven-membered ring, a remote isopropenyl group, and a bridging *β*-keto tetrahydrofuran moiety. Because of its unique and challenging framework, the synthesis of ineleganolide had remained an unsolved challenge over the past two decades, despite efforts by the groups of Vanderwal,[8] Nicolaou,[9] Gaich,[10] Romo,[11] Moeller,[12] and our group.[13] Only in 2022, shortly before our published research, did Wood and co-workers showcase the first total synthesis of ineleganolide (Scheme 1.2.1).[14]

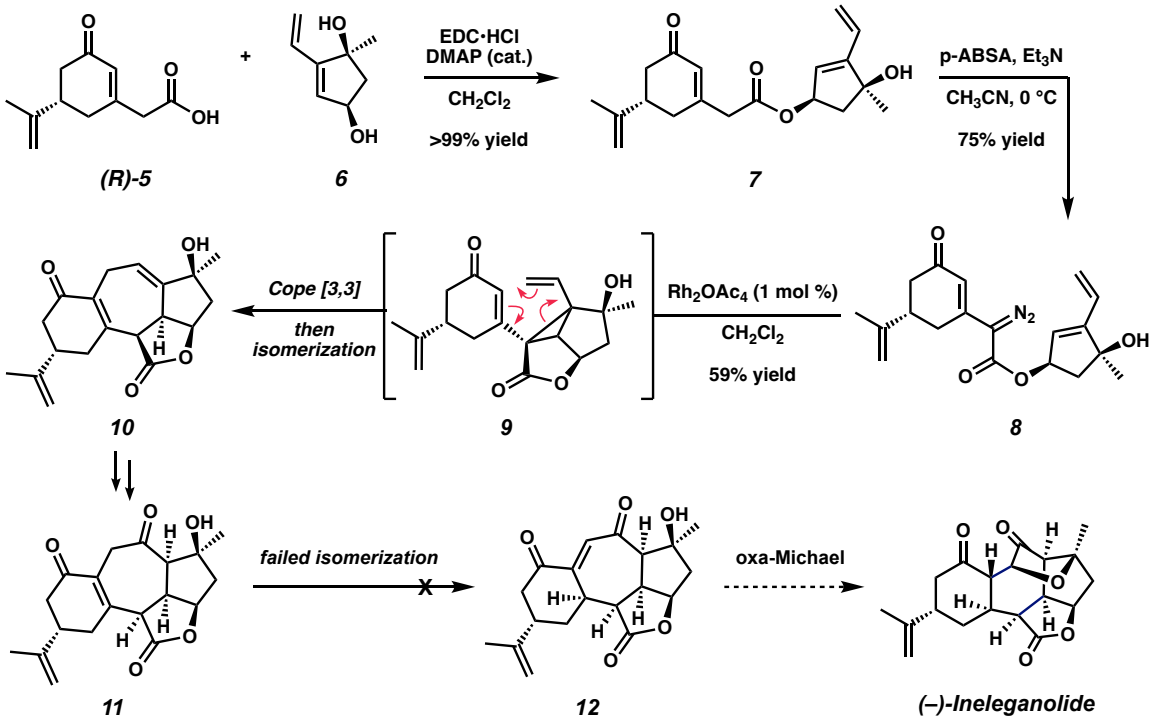
Scheme 1.2.1 *Biomimetic and bioinspired synthesis of* ***1*** *by Pattenden and Wood.*



As one of the earliest reports on synthetic success to target ineleganolide, Pattenden and co-workers had shown the conversion of the natural product 5-episinuleptolide acetate to ineleganolide upon treatment with strong base.[15] Believed to undergo a double Michael addition cascade, they isolated ineleganolide along with its isomer sinulochmodin C. The Wood group achieved the first total synthesis of ineleganolide in 2022, by elegantly constructing a macrocyclic precursor from commercial starting materials. They were able to form the last bond by inducing a similar transannular Michael addition, which gave rise to sinulochmodin C in 35% yield and ineleganolide in 11% yield, respectively.

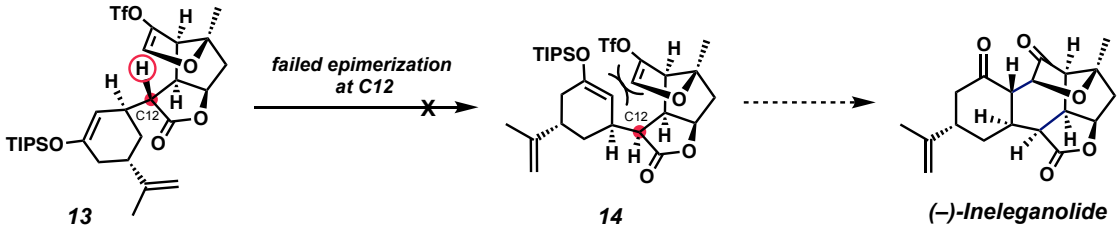
In our own research group, the effort to achieve the synthesis of ineleganolide had been a long-standing project that led to numerous advances in reaction development (Scheme 1.2.2).[16,17] Previous group members established a route to carboxylic acid (*R*)-**5** from (*R*)-norcarvone, and displayed diol **6** over a 15-step sequence from commercial starting materials. Esterification with carbodiimide gave the ester **7** in excellent yield, which can be converted to the diazo species **8**. To construct the cycloheptane core of the target molecule, **8** was treated with a rhodium catalyst which induced carbenoid formation and cyclopropanation, giving strained intermediate **9**. This intermediate subsequently underwent divinyl cyclopropane rearrangement to give compound **10** upon olefin isomerization. Using oxidation state manipulations, **10** was converted to **11** over a multi-step sequence. However, the advanced structure **11** proved challenging to manipulate, namely isomerization of the alkene into conjugation with both ketones failed under numerous conditions. This step was viewed as crucial to complete the synthesis, having proposed oxa-Michael addition of the tertiary alcohol to complete the synthesis of **1**. It was later found computationally that this exact approach was flawed.[16]

Scheme 1.2.2 *Previous approach to (-)-**1** by Stoltz and co-workers.*



Complementary to our group's research, Vanderwal and co-workers had published their extensive efforts to synthesize **1** (Scheme 1.2.3).[8] Having constructed the advanced intermediate **13**, they proposed to close the central seven-membered ring by addition of the silyl enol ether into a latent oxocarbenium ion.

Scheme 1.2.3 *Previous approach to (-)-**1** by Vanderwal and co-workers.*

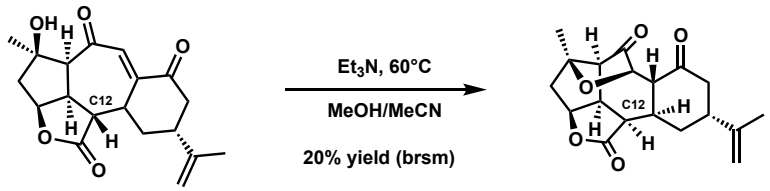


Before attempting to achieve this transformation, they ran into a stereochemical problem with compound **13**. Having synthesized the incorrect epimer at the C12 carbon, they were unable to invert the stereocenter to give the desired conformation depicted in structure **14**.

Due to presumed steric clash of the C4 and C5 carbon, they deemed this epimerization and strategic approach systematically flawed.

Following the publication of our total synthesis detailed in this chapter, the group of Fürstner reported successful conversion of the revised structure of scabrolide B to ineleganolide in 2024, by an oxa-Michael and epimerization cascade (Scheme 1.2.4).[18] Key to this success was the epimeric carbon at C12 of scabrolide B, which presumably allowed for oxa-Michael addition to occur. Followingly, the product undergoes a final epimerization to the correct stereochemical configuration found in ineleganolide.

Scheme 1.2.4 *Successful oxa-Michael and epimerization cascade by Fürstner in 2024.*



Scabrolide B
[*revised structure*]

Ineleganolide (1)

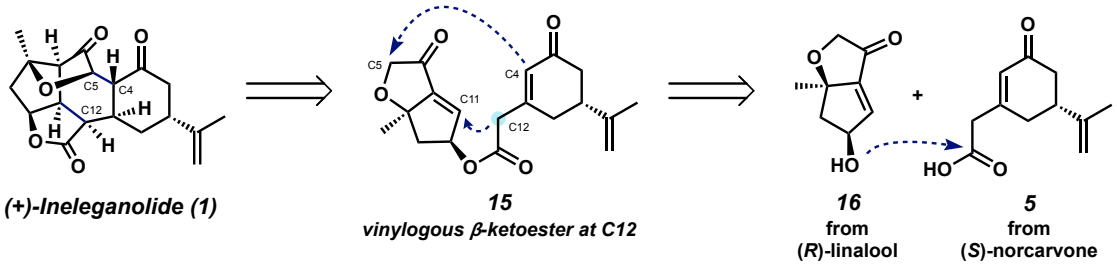
Maimone and co-workers independently followed up with their own unique strategy for the synthesis of **1**, published in 2025.[19]

1.3 RETROSYNTHETIC ANALYSIS

In our own research, issues surrounding the central seven-membered ring and constructing the ether bridge at a late stage had halted previous efforts.[16,17] This sparked the idea of constructing the central seven-membered ring at a later stage, and instead having the tetrahydrofuran motif introduced early. Therefore, we envisioned disconnecting through the C4−C5 bond as the final step and constructing the seven-membered ring last (Scheme

1.3.1). Originally, we imagined this bond formation could potentially be achieved by a cross-enolate coupling process.

Scheme 1.3.1 *Retrosynthesis of (+)-ineleganolide.*



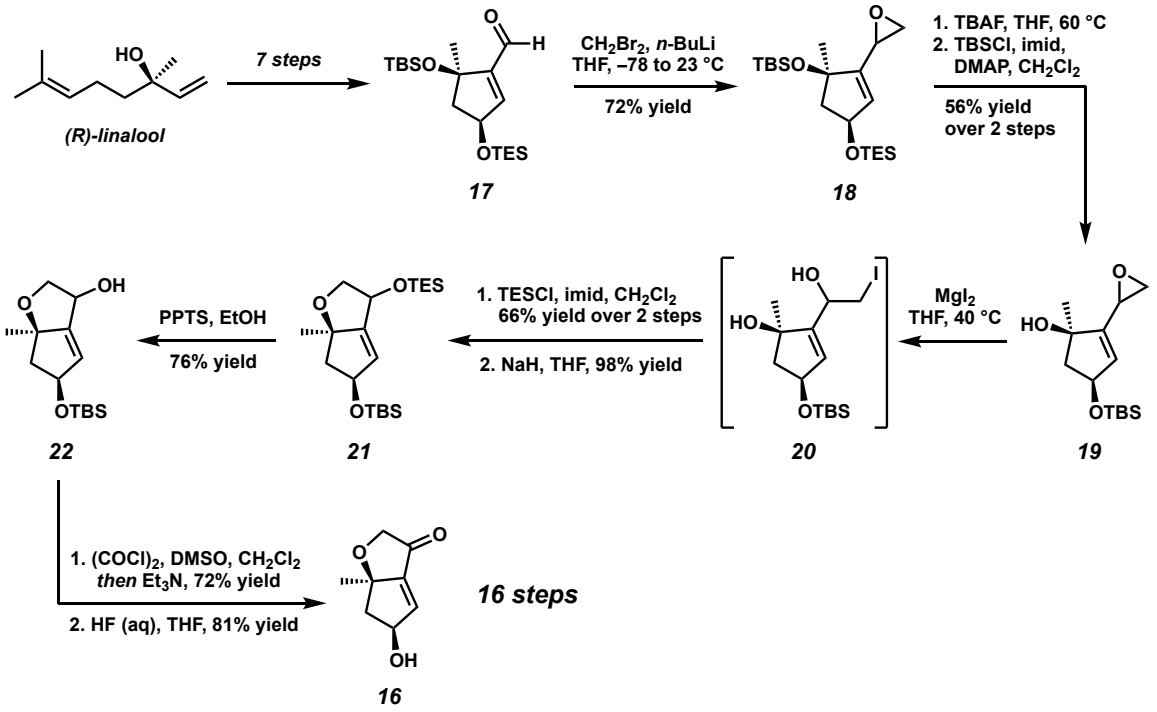
Inspired by our previous research and, specifically, the work of Vanderwal and co-workers, we planned our route back to the precursor **15** to set the stereochemistry at C12 through a Michael addition.[8] As a vinylogous *β*-keto ester, we envisioned that the lowered acidity of the C12 proton would thereby provide an epimerizable handle. Disconnecting **15** through an esterification, we were left with two fragments, carboxylic acid **5** and alcohol **16**.

1.4 SYNTHESIS OF FRAGMENTS

We were able to derive these from (−)-linalool and (+)-norcarvone, respectively, which resulted in an overall convergent and stereospecific synthesis. To synthesize bicyclic enone **16**, we began from (R)-linalool (Scheme 1.4.1). Aldehyde **17** was readily available through previously developed chemistry established by the Maimone group and our group, respectively.[20,21] This route proved to be highly scalable to access aldehyde **17** in sufficient quantities (>70 g prepared). We next focused our attention on building the essential *β*-keto tetrahydrofuran moiety present in bicycle **16**. This proved challenging because of the highly strained nature of enone **16**. Initially, extensive efforts of an intra-molecular cyclization of the tertiary alcohol onto an *α*-functionalized ketone showed no success. We

envisioned that oxidizing to the ketone later would alleviate the induced strain and allow for the intramolecular cyclization to occur. This idea proved to be successful, as the cyclization onto a β-functionalized secondary alcohol was possible.

Scheme 1.4.1 *First-generation synthesis of enone* ***16***.



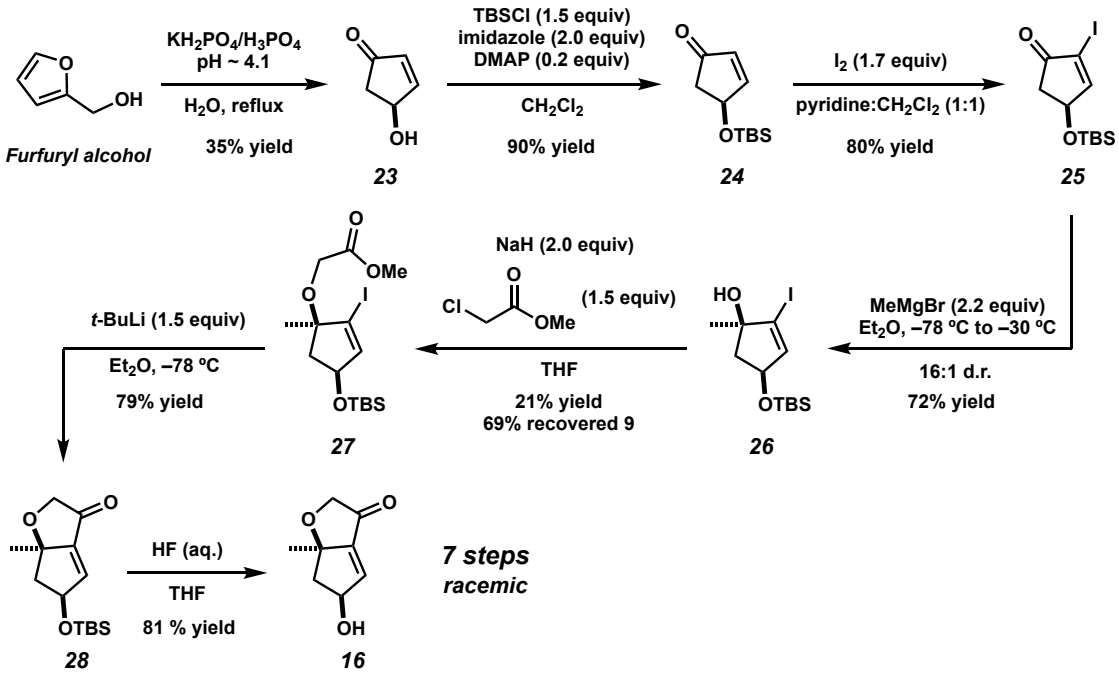
We converted aldehyde **17** to the corresponding epoxide **18** using dibromomethane as the one carbon source. Removal of both silyl groups by treatment of **18** with TBAF, followed by selective silylation of the resulting secondary alcohol with TBSCl, revealed the tertiary alcohol **19**. Treatment of epoxide **19** with magnesium diiodide revealed the intermediary iodohydrin **20**. Protection of the incipient secondary alcohol as the corresponding silyl ether proved necessary since cyclization in the presence of the unprotected secondary alcohol failed, even with excess amounts of base. Upon silylation, however, intramolecular substitution of the alkyl iodide by the tertiary alkoxide occurred at room temperature to afford bicycle **21** in excellent yield (98%). Selective deprotection of the triethyl silyl ether

under mild acidic conditions gave alcohol **22**, which was oxidized to the enone under Swern conditions in 72% yield. Lastly, deprotection employing aqueous HF yielded **16** in 81% yield. Other deprotection conditions proved unsuccessful because of the presumed high reactivity and instability of enone **16** as an electrophilic Michael acceptor.

Although this route allowed us to introduce chirality at the tertiary alcohol early in the sequence, the excessive use of protecting groups and redox manipulations led to a lengthy sequence of 16 steps to get to compound **16**. One of the challenges in constructing building block **16** is its highly strained structure. Presumably, the planar conformation of the enone required for π-orbital overlap induces significant strain into the fused [5-5] ring system. The shorter C–O bond lengths of the embedded tetrahydrofuran moiety serve to further intensify this effect. In our hands, enone **16** often behaved as the chemical equivalent of a wound-up spring. As an exceptional Michael-acceptor, we observed 1,4-addition with numerous nucleophiles or rapid decomposition, even under mild reaction conditions. However, when the allylic alcohol was protected as a bulky silyl ether, the compounds stability was significantly improved.

In looking for a better route, we considered how we could simultaneously construct the enone and β-keto tetrahydrofuran. We imagined that retrosynthetic disconnection of the C-sp^2/C-sp^2 bond through an intramolecular 1,2-addition could lead to a more direct synthesis of **16**. We hypothesized that collapse of the tetrahedral intermediate would provide a sufficient thermodynamic driving force to induce the strain of the enone moiety. Ultimately this proved to be a successful strategy, reducing the length of our route to only seven steps from commercial starting materials, employing only two protecting group (PG) manipulations (Scheme 1.4.2).

Scheme 1.4.2 *Second-generation synthesis of enone* ***16***.



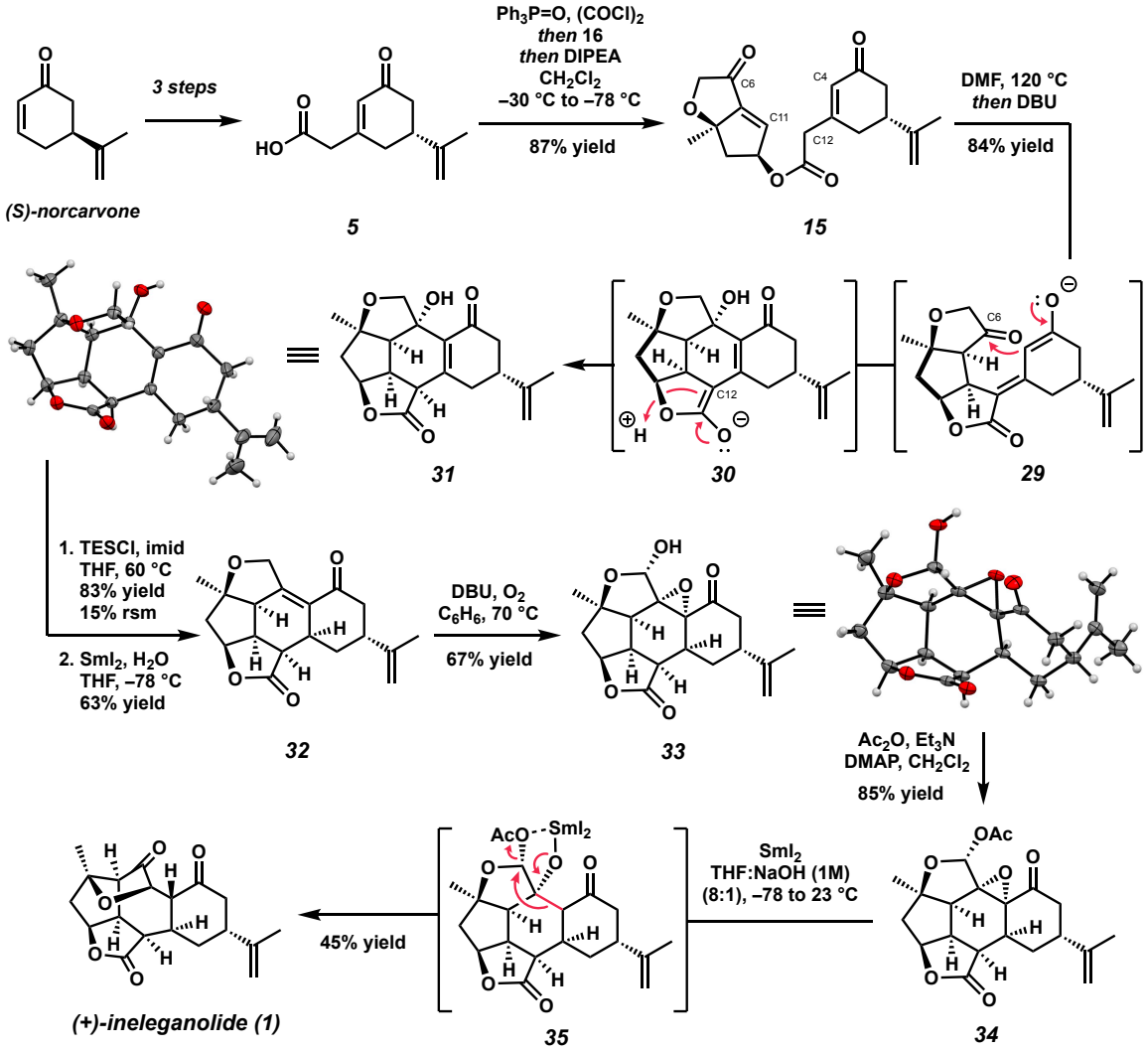
Our sequence was initiated in targeting the intermediate tertiary alcohol **26**, which was previously known in the literature.[22] Starting from furfuryl alcohol, we can readily display cyclopentenone **23** via the known Piancatelli-rearrangement.[23] Due to the ease of access, we set out with the racemic mixture of compound **23** to investigate the forward route. The allylic alcohol of **23** can be converted to the silyl ether **24**. Subsequent α-iodination of the enone occurred in great yield to give vinyl iodide **25**.[24] Next, we preformed 1,2-addition using methyl magnesium bromide. Under cryogenic conditions, we could achieve an excellent diastereoselectivity of 16:1, favoring the syn-arrangement of oxygenation in **26**. With the tertiary alcohol in place, we sought to alkylate using methyl chloroacetate. Deprotonation with sodium hydride followed by allylation was successful, producing compound **27** in 21% yield, with 69% recovered starting material. In trying to improve this yield, we evaluated numerous solvents and different conditions, such as K_2CO_3/acetonitrile, potassium hydride/18-crown-6 or methyl bromoacetate as electrophile

for example. Unfortunately, most of these conditions led to no product formation and complete decomposition of the starting material. With the vinyl iodide **27** in place, lithium-halogen exchange occurred rapidly and gave clean conversion to our desired enone **28** in 79% isolated yield. It is noteworthy to point out that we had initially synthesized the analogous vinyl bromide, where lithium-halogen exchange and 1,2-addition occurred to give product **28** successfully, yet in a diminished 18% yield. Deprotecting with our previously developed conditions, we can now access the racemic building block **16** in only seven steps from commercial starting materials.

1.5 FRAGMENT COUPLING AND COMPLETION OF THE SYNTHESIS

Carboxylic acid **5** could be accessed through a protocol previously employed by our group, which utilizes (S)-norcarvone as an enantioenriched starting material.[17] With acid **5** and alcohol **16** in hand, we turned to develop conditions for esterification. This proved challenging because of (1) the acidic α-proton of the acid **5** and (2) the instability of enone **16** toward a amine bases or nucleophiles (Et_3N, DIPEA, DMAP, pyridine, etc.), thereby leading to decomposition within minutes. As such, a broad range of esterification reagents were evaluated (i.e., EDC, DIC, Yamaguchi's reagent, Otera's catalyst, etc.) but failed to yield any desired product. We eventually developed specific conditions to overcome these issues by activating the acid as the triphenylphosphonium salt at low temperatures,[25] which reacted with alcohol **16** within seconds upon addition of a base, to afford ester **15** in 87% yield. Next, we investigated the intramolecular Michael addition. While we were evaluating conditions, ester **15** appeared unstable to various bases and induced the formation of an array of unidentified side products upon reaction.

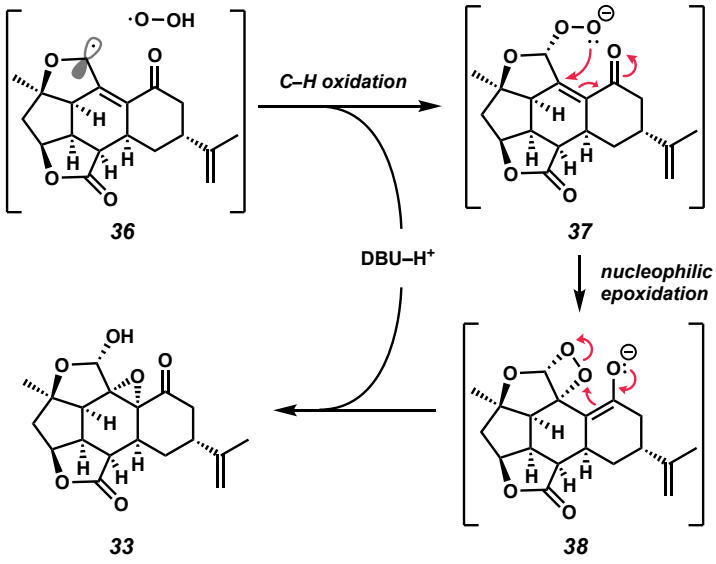
Scheme 1.5.1 *Completion of the total synthesis of Ineleganolide (**1**).*



To our surprise, treatment of ester **15** with DBU at 23 °C gave trace amounts of an unexpected pentacycle (**31**), the structure of which was determined by X-ray crystallography and resulted from not only Michael addition but a subsequent aldol cyclization, as well. We were able to optimize this process by preheating a solution of the ester **15** in DMF at high temperatures (i.e., 120 °C) and adding DBU in one portion. Under this protocol the reaction then proceeded within minutes to smoothly give **31** in 84% yield, thereby suppressing previous side products. Mechanistically, we believe that a Michael

addition occurs first to form the C12−C11 bond. The second proton at C12 can be abstracted again to give the conjugated enolate **29**. The extended enolate can then undergo aldol addition at C4 with the neighboring ketone and isomerize to give rise to intermediate **30**. Being sp^2-hybridized, the enolate at C12 is preferentially protonated from the convex face, thereby giving **31** as a single diastereomer. Overall, this Michael addition and aldol cascade forges two bonds and four stereocenters as a single diastereomer in high yield, which crucially provides the correct stereochemistry at C12. With this result in hand, we could envision a path toward ring expansion and completion of the natural product. To this end, protection of the tertiary alcohol as the silyl ether facilitated reduction of the tetrasubstituted enone under samarium diiodide conditions and subsequent elimination to enone **32**.[17] While attempting an allylic oxidation at C5, we discovered that enone **32** undergoes a unique air oxidation under basic conditions to produce the epoxide hemiacetal **33** (Scheme 1.5.2).

Scheme 1.5.2 *Mechanistic proposal for air-oxidation to intermediate **33**.*

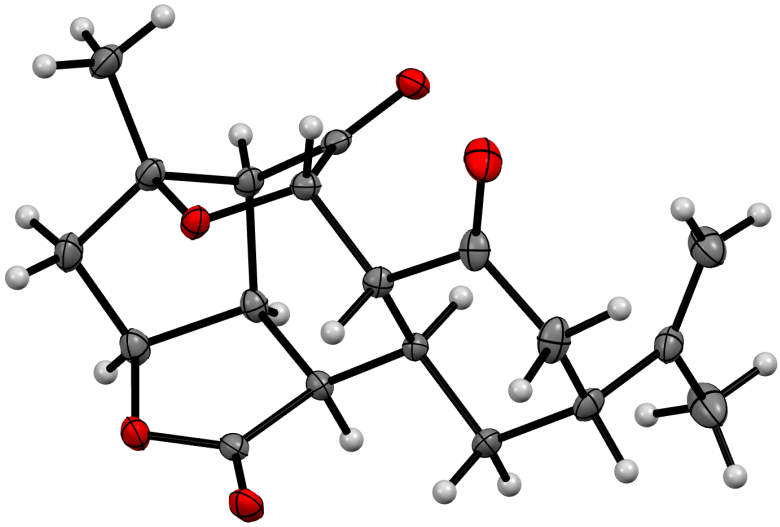


We were surprised by this nearly unprecedented reaction[26] and speculate that triplet oxygen can facilitate a radical H atom abstraction to form the highly stabilized captodative radical **36** on the γ-position of the enone. Upon radical recombination, an initial peroxide can be formed, which can be deprotonated to form compound **37**. Under basic conditions, the peroxyanion **37** can then undergo intramolecular nucleophilic epoxidation with the enone to give intermediate **38**, which converts to the final product **33**. After optimization, **33** could be reliably obtained in 67% yield, because it is highly sensitive to the stirring rate and oxygen atmosphere.

Having the correct oxidation pattern in place, we planned to construct the crucial C4−C5 bond through reductive opening of the epoxide and a subsequent semipinacol shift. We deemed the odds in our favor and predicted good antiperiplanar orbital overlap between the shifting carbon−carbon bond and hemiacetal leaving group. Additionally, the ability to form a stabilized oxocarbenium ion could also be beneficial. Initial investigations showed that epoxide opening typically leads to elimination of the resulting tertiary alcohol. Conversion of hemiacetal **33** to the acetate **34** provided the initial lead, and reductive opening of **34** with samarium diiode provided trace amounts of ineleganolide, which indicates that the semipinacol rearrangement proceeded in the same pot as the epoxide opening. We then extensively evaluated additives and temperatures and found that addition of an aqueous 1 M sodium hydroxide solution as relatively high pH proton source significantly improved the yield. Although several mechanistic scenarios are possible, we deemed the existence of intermediate **35** to be crucial, with samarium potentially engaging as a Lewis acid to promote the rearrangement.[27] The basicity of the proton source could provide improved conditions to protonate the initially forming samarium enolate without

protonating the tertiary alcohol too rapidly and forcing elimination. Quickly warming up from−78 to 23 °C gave (+)-ineleganolide **1** in 45% isolated yield. While the isolation paper initially provides an X-ray structure of ineleganolide, lower resolution prevented determination of absolute stereochemistry.[7] This led us to obtain a higher- resolution crystal structure that further confirms the absolute stereochemistry of the naturally occurring enantiomer (+)-ineleganolide, in accordance with observations by Wood[14] and Pattenden[15] (Figure 1.5.3).

Figure 1.5.3 *X-ray structure of* ***1***.



1.6 CONCLUSION

In conclusion, we have completed the total synthesis of (+)-ineleganolide in an overall longest linear sequence of 23 steps from (−)-linalool and 14 steps with a revised route starting from furfuryl alcohol. We based our convergent strategy on the union of two fragments, thereby providing a concise endgame with only seven total steps from our coupling partners **5** and **16**. We were able to access a highly strained enone **16** and develop

underutilized esterification conditions for sensitive substrates by employing triphenyl phosphine oxide and oxalyl chloride as activating reagents. Furthermore, we realized an exceptional Michael addition and aldol cascade by constructing a crucial pentacyclic intermediate as a single diastereomer (i.e., **15** → **31**). In the later stage, we discovered a unique air oxidation and epoxidation sequence to install the needed oxidation pattern (i.e., **32** → **33**). Reductive opening of acetoxy epoxide **34** with samarium diiode induced a semi-pinacol shift in the same pot to furnish (+)-ineleganolide (**1**) in good yield. We envision that the developed chemistry can be utilized in solving future problems in the synthesis of related compounds and enable further investigations into the bioactivity of the cembranoid and norcembranoid diterpenoids, specifically (+)-ineleganolide.

1.7 EXPERIMENTAL SECTION

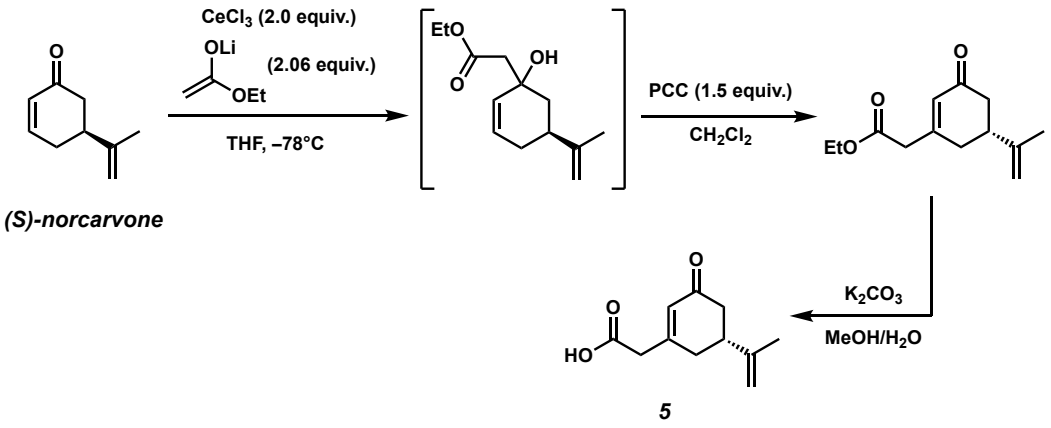
1.7.1 MATERIALS AND METHODS

Unless otherwise stated, reactions were performed in flame-dried glassware under an argon or nitrogen atmosphere using dry, deoxygenated solvents. Solvents were dried by passage through an activated alumina column under argon.[28] Reaction progress was monitored by thin-layer chromatography (TLC). TLC was performed using E. Merck silica gel 60 F254 precoated glass plates (0.25 mm) and visualized by UV fluorescence quenching, p-anisaldehyde, or $KMnO_4$ staining. Silicycle SiliaFlash® P60 Academic Silica gel (particle size 40–63 μm) was used for flash chromatography. ^{1}H NMR spectra were recorded on Varian Inova 500 MHz and 600 MHz and Bruker 400 MHz spectrometers and are reported relative to residual $CHCl_3$ (δ 7.26 ppm), C_6D_6 (δ 7.16 ppm) or CD3OD (δ 3.31 ppm). ^{13}C NMR spectra were recorded on a Varian Inova 500 MHz spectrometer (125 MHz) and

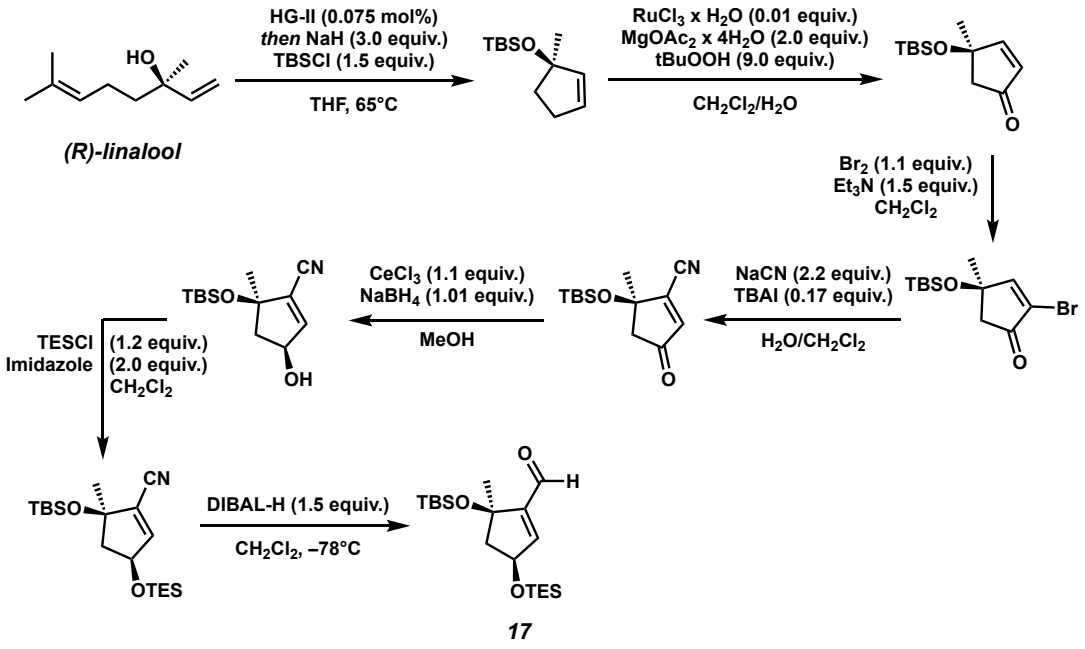
Bruker 400 MHz spectrometers (100 MHz) and are reported relative to $CHCl_3$ (δ 77.16 ppm), C_6D_6 (δ 128.06 ppm) or CD_3OD (δ 49.01 ppm). Data for ^1H NMR are reported as follows: chemical shift (δ ppm) (multiplicity, coupling constant (Hz), integration). Multiplicities are reported as follows: s = singlet, d = doublet, t = triplet, q = quartet, p = pentet, sept = septuplet, m = multiplet, br s = broad singlet, br d = broad doublet. Data for ^{13}C NMR are reported in terms of chemical shifts (δ ppm). IR spectra were obtained by use of a Perkin Elmer Spectrum BXII spectrometer or Nicolet 6700 FTIR spectrometer using thin films deposited on NaCl plates and reported in frequency of absorption (cm^{-1}). Optical rotations were measured with a Jasco P-2000 polarimeter operating on the sodium D-line (589 nm), using a 100 mm path- length cell. High resolution mass spectra (HRMS) were obtained using an Agilent 6200 Series TOF with an Agilent G1978A Multimode source in electrospray ionization (ESI+) mode.

1.7.2 SYNTHESIS OF STARTING MATERIALS

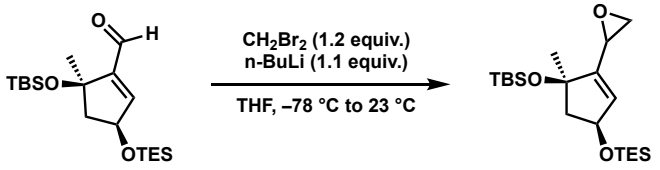
Scheme 1.7.2.1 *Route to carboxylic acid* ***5****, Ref [17].*



Scheme 1.7.2.2 *Route to aldehyde* ***17****, Ref [20] and [21].*

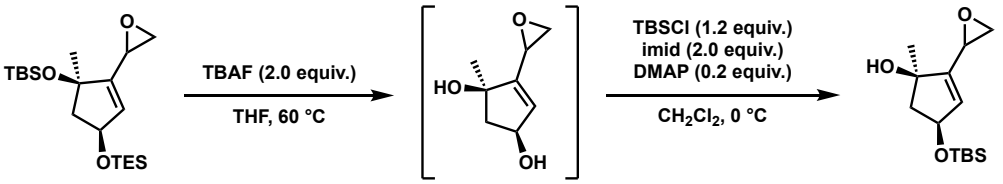


1.7.3 EXPERIMENTAL PROCEDURES



Epoxide 18: In a flame dried round-bottom flask, Aldehyde **17** (9.4 g, 25.3 mmol, 1.0 equiv.) was dissolved in THF (125 mL, 0.2 M) and CH_2Br_2 (2.1 mL, 30.1 mmol, 1.2 equiv.) was added in one portion. The solution was cooled to –78 °C in a dry ice/acetone bath and *n*-BuLi (2.5 M in hexanes, 10.6 mL, 27.6 mmol, 1.1 equiv.) was added dropwise over the course of one hour. The reaction mixture was left to stir in the dry ice/acetone bath and let warm to 23 °C overnight (12 h). After consumption of starting material as determined by TLC, saturated aqueous NH_4Cl was added, the layers separated, and the aqueous layer was

extracted with EtOAc (3x). The combined organic extracts were dried over Na_2SO_4, and the solvent evaporated under reduced pressure. The crude product was purified by flash chromatography on silica gel (hexanes → 5% Et_2O/hexanes) to afford the title compound **18** as a pale-yellow oil (7.0 g, 18.2 mmol, 72% yield). ***18*** *was isolated as an inconsequential mixture of diastereomers (ratio ~2:1). Signals for the major diastereomer are reported*; ^{1}H NMR (600 MHz, $CDCl_3$) δ 5.47 (s, 1H), 4.62 – 4.58 (m, 1H), 3.37 (s, 1H), 2.98 – 2.95 (m, 1H), 2.74 (dd, *J* = 6.0, 2.7 Hz, 1H), 2.44 (dd, *J* = 12.2, 6.8 Hz, 1H), 1.95 (dd, *J* = 12.2, 6.5 Hz, 1H), 1.38 (s, 3H), 0.95 (t, *J* = 7.9 Hz, 9H), 0.86 (s, 9H), 0.60 (q, *J* = 7.9 Hz, 6H), 0.11 (s, 3H), 0.09 (s, 3H); ^{13}C NMR (100 MHz, $CDCl_3$) δ 149.8, 127.3, 82.1, 73.3, 53.1, 49.9, 47.0, 28.6, 25.8, 18.0, 6.9, 4.8, -2.0, -2.4; IR (neat film, NaCl) 2955, 2885, 2855, 1471, 1461, 1359, 1251, 1118, 1004, 834, 739, 671, 645 cm^{-1}; HRMS (ESI+): m/z calc'd for $C_{14}H_{25}SiO_2$ $[M–OTBS]^+$: 253.1618, found 253.1610; $[\alpha]_D^{23}$ + 7.7 (*c* 0.20, $CHCl_3$).

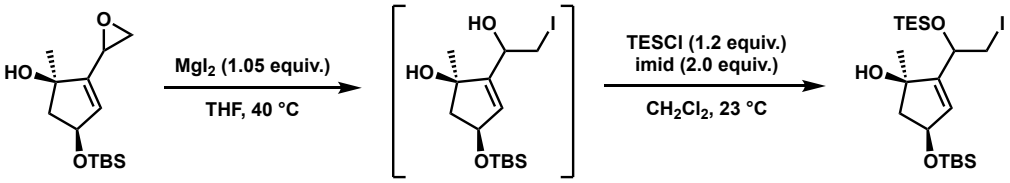


18 ***19***

Tertiary Alcohol 19: A round-bottom flask was charged with **18** (12.1 g, 31.4 mmol, 1.0 equiv.) and dissolved in THF (314 mL, 0.1 M). TBAF (1M in THF, 62.9 mL, 2.0 equiv.) was added and the solution heated to 60 °C. After 3h, full consumption of starting material was observed by TLC and the solution was left to cool to 23 °C. The reaction mixture was diluted with hexanes (50 mL) and flushed over a plug of silica gel, eluting with a mixture

of EtOAc/Hexanes (9:1). The solvent was evaporated under reduced pressure, and the crude diol (3.8 g) isolated as a yellow oil which was directly used in the next step.

The intermediate diol (3.8 g, 24.3 mmol, 1.0 equiv.) was dissolved in CH_2Cl_2 (243 mL, 0.1 M), and imidazole (3.3 g, 48.6 mmol, 2.0 equiv.) added in one portion. The solution was cooled to 0°C, after which TBSCl (4.4 g, 29.2 mmol, 1.2 equiv.) and DMAP (0.59 g, 4.86 mmol, 0.2 equiv.) were subsequently added. The solution was stirred for 1 h, quenched with a saturated aqueous solution of $NaHCO_3$, and the aqueous layer extracted with EtOAc (3x). The combined organic extracts were washed with brine, dried over Na_2SO_4 and the solvent evaporated under reduced pressure. The crude product was purified by flash chromatography on silica gel (20% EtOAc/hexanes), to yield tertiary alcohol **19** (4.8 g, 17.7 mmol, 56% over two steps) as a yellow oil. ***19*** *was isolated as an inconsequential mixture of diastereomers (ratio ~2:1). Signals for the major diastereomer are reported*; ^{1}H NMR (600 MHz, $CDCl_3$) δ 5.68 (s, 1H), 4.63 – 4.58 (m, 1H), 3.47 (s, 1H), 3.02 – 2.98 (m, 1H), 2.87 – 2.82 (m, 1H), 2.41 (dd, *J* = 13.3, 6.5 Hz, 1H), 2.21 – 2.13 (m, 1H), 1.90 – 1.83 (m, 1H), 1.41 (s, 3H), 0.88 (s, 9H), 0.07 (s, 6H); ^{13}C NMR (100 MHz, $CDCl_3$) δ 148.1, 131.1, 81.0, 73.2, 52.7, 49.4, 47.4, 25.9, 18.2, -4.5, -4.5; IR (neat film, NaCl) 2956, 2855, 1614, 1460, 1422, 1360, 1252, 1166, 1079, 1064, 898, 834, 776, 759, 748, 662 621 cm^{-1}; HRMS (ESI+): m/z calc'd for $C_{14}H_{25}SiO_2$ $[M–OH]^+$: 253.1618, found 253.1611; $[\alpha]_D^{25}$ + 11.5 (*c* 0.15, $CHCl_3$).

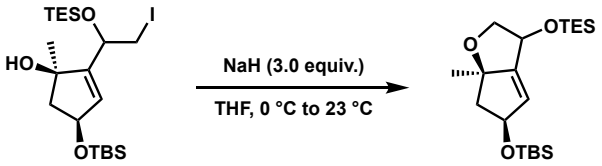


19 ***20*** ***39***

Alkyliodide 39: A flame dried round-bottom flask was charged with **19** (4.8 g, 17.7 mmol, 1.0 equiv.) and transferred into a glovebox. The starting material was dissolved in THF (89 mL, 0.2 M) and anhydrous MgI_2 (5.17 g, 18.6 mmol, 1.05 equiv.) was added in one portion. The flask was sealed with a rubber septum and transferred outside the glovebox. The flask was kept under N_2, placed in a heating mantel set to 40 °C and the reaction mixture stirred for 14 h. H_2O was added, and the aqueous phase extracted with EtOAc (3x). The combined organic extracts were washed with brine, dried over Na_2SO_4 and the solvent evaporated under reduced pressure to yield the crude diol **20** (7.05 g) as a yellow oil, which was directly used in the next step.

Diol **10** (7.05 g, 17.7 mmol, 1.0 equiv.) was dissolved in CH_2Cl_2 (177 mL, 0.1 M), imidazole (2.4 g, 35.4 mmol, 2.0 equiv.) added in one portion and the reaction mixture cooled to 0 °C. TESCl (3.5 mL, 21.2 mmol, 1.2 equiv.) was added dropwise and the reaction mixture stirred for 10 minutes. Brine was added, the phases separated, and the aqueous phase extracted with Et_2O (3x). The combined organic extracts were dried over Na_2SO_4, and the solvent evaporated under reduced pressure. The crude product was purified by flash chromatography on silica gel (hexanes → 10% Et_2O/hexanes) to yield alkyliodide **39** (5.94 g, 11.6 mmol, 66% over two steps) as a yellow oil. ***39*** *was isolated as an inconsequential mixture of diastereomers. Signals for the major diastereomer are reported*; ^{1}H NMR (600 MHz, $CDCl_3$) δ 5.89 (s, 1H), 4.58 – 4.55 (m, 1H), 4.31 – 4.28 (m,

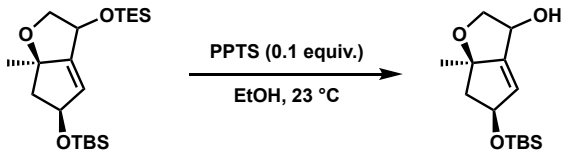
1H), 3.59 (dd, *J* = 10.2, 3.9 Hz, 1H), 3.35 (dd, *J* = 10.1, 6.4 Hz, 1H), 2.23 (dd, *J* = 13.2, 6.0 Hz, 1H), 1.88 (dd, *J* = 13.2, 3.0 Hz, 1H), 1.33 (s, 3H), 0.97 (t, *J* = 7.9 Hz, 9H), 0.88 (s, 9H), 0.66 – 0.58 (m, 6H), 0.08 (s, 6H); ^{13}C NMR (100 MHz, $CDCl_3$) δ 151.7, 132.3, 80.5, 72.7, 69.1, 52.5, 25.9, 25.3, 18.2, 15.3, 7.0, 5.0, -4.3, -4.6; IR (neat film, NaCl) 2956, 2929, 2879, 1362, 1098, 1004, 834, 736, 652 cm^{-1}; HRMS (ESI+): m/z calc'd for $C_{20}H_{40}ISi_2O_2$ $[M–OH]^+$: 495.1606, found 495.1600; $[\alpha]_D^{25}$ + 4.31 (*c* 0.20, $CHCl_3$).



39 ***21***

Bicycle 21: A flame dried round-bottom flask was charged with alkyl iodide **39** (5.94 g, 11.59 mmol, 1.0 equiv.), dissolved in THF (0.013 M, 891 mL) and cooled to 0°C. NaH (60% in mineral oil, 1.4 g, 34.7 mmol, 3.0 equiv.) was added portion wise, after which the ice bath was removed and the reaction stirred at 23°C for 2.5 hours, until full consumption of starting material as determined by TLC. The reaction was quenched with a saturated aqueous solution of NH_4Cl, and the aqueous layer extracted with EtOAc (3x). The combined organic extracts were dried over Na_2SO_4, and the solvent evaporated under reduced pressure. The crude product was purified by flash chromatography on silica gel (hexanes → 10% Et_2O/hexanes) to yield the title compound **21** (4.4 g, 11.4 mmol, 98%) as a colorless oil; ***21*** *was isolated as an inconsequential mixture of diastereomers. Signals for the major diastereomer are reported*; ^{1}H NMR (600 MHz, $CDCl_3$) δ 5.61 (s, 1H), 5.02 (t, *J* = 6.3 Hz, 1H), 4.62 (d, *J* = 3.1 Hz, 1H), 4.11 (dd, *J* = 9.5, 4.7 Hz, 1H), 4.00 (dd, *J* = 9.6,

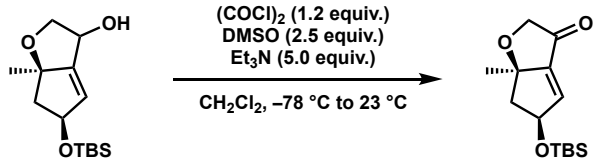
1.8 Hz, 1H), 2.44 (dd, *J* = 11.6, 5.5 Hz, 1H), 1.87 (dd, *J* = 11.6, 7.4 Hz, 1H), 1.39 (s, 3H), 0.95 (t, *J* = 7.9 Hz, 9H), 0.89 (s, 9H), 0.60 (q, *J* = 7.9 Hz, 6H), 0.09 (s, 3H), 0.07 (s, 3H); ^{13}C NMR (125 MHz, $CDCl_3$) δ 151.3, 128.7, 90.0, 79.3, 78.2, 68.1, 54.5, 26.0, 24.9, 18.3, 6.8, 4.8, -4.4, -4.6; IR (neat film, NaCl) 2955, 2878, 2856, 1463, 1456, 1362, 1251, 1102, 1051, 1003, 895, 862, 831, 779, 728 cm^{-1}; HRMS (ESI+): m/z calc'd for $C_{20}H_{41}Si_2O_3$ $[M+H]^+$: 385.2589, found 385.2579; $[\alpha]_D^{25}$ + 12.7 (*c* 0.15, $CHCl_3$).



21 ***22***

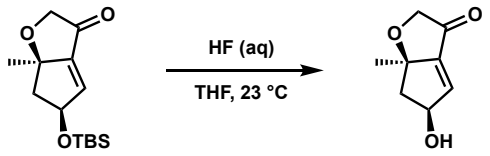
Allylic alcohol 22: A round-bottom flask was charged with **21** (2.25g, 5.85 mmol, 1.0 equiv.) and dissolved in EtOH (58 mL, 0.1 M). PPTS (147.0 mg, 0.585 mmol, 0.1 equiv.) was added in one portion and the reaction mixture stirred for 1 h. After nearly full consumption of starting material as determined by TLC, a saturated aqueous solution of $NaHCO_3$ was added. The aqueous layer was extracted with EtOAc (3x), the combined organic extracts dried over Na_2SO_4, and the solvent evaporated under reduced pressure. The crude product was purified by flash chromatography on silica gel (hexanes → 20% EtOAc/hexanes) to yield the title compound **22** (1.2 g, 4.4 mmol, 76%) as a colorless oil; ***22*** *was isolated as an inconsequential mixture of diastereomers. Signals for the major diastereomer are reported;* ^{1}H NMR (600 MHz, $CDCl_3$) δ 5.74 (s, 1H), 5.03 (t, *J* = 6.5 Hz, 1H), 4.73 (dd, *J* = 4.8, 1.9 Hz, 1H), 4.15 (dd, *J* = 10.0, 4.9 Hz, 1H), 4.06 (dd, *J* = 10.1, 1.8 Hz, 1H), 2.45 (dd, *J* = 11.6, 5.5 Hz, 1H), 1.93 (s, 1H), 1.90 (dd, *J* = 11.6, 7.5 Hz, 1H), 1.41 (s, 3H), 0.89 (s, 9H), 0.09 (s, 3H), 0.07 (s, 3H); ^{13}C NMR (125 MHz, $CDCl_3$) δ 150.7,

130.2, 89.9, 79.3, 77.2, 68.0, 54.7, 25.9, 25.1, 18.3, -4.4, -4.6; IR (neat film, NaCl) 3402, 2931, 2857, 1471, 1360, 1260, 1213, 1185, 1097, 1047, 977, 828, 775, 674 cm^{-1}; HRMS (ESI+): m/z calc'd for $C_{14}H_{27}SiO_3$ $[M+H]^+$: 271.1724, found 271.1719; $[\alpha]_D^{25}$ + 33.7 (*c* 0.06, $CHCl_3$).



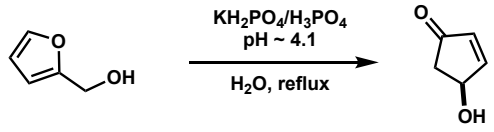
22 ***28***

Enone 28: In a flame dried round-bottom, a solution of DMSO (0.78 mL, 11.0 mmol, 2.5 equiv.) in CH_2Cl_2 (44.3 mL) was cooled to –78 °C and oxalyl chloride (0.45 mL, 5.31 mmol, 1.2 equiv.) was added dropwise. After stirring at the same temperature for 15 minutes, alcohol **22** (1.2 g, 4.4 mmol, 1.0 equiv.) was added as a solution in CH_2Cl_2 (44.3 mL). The reaction mixture was stirred for 1 hour at –78 °C, after which Et_3N (3.1 mL, 22.1 mmol, 5.0 equiv.) was added and the reaction mixture let warm to 23 °C. The solvent was evaporated under reduced pressure and the crude mixture purified by flash chromatography on silica gel (hexanes → 10% EtOAc/hexanes). The title compound **28** (854 mg, 3.18 mmol, 72%) was obtained as a colorless oil; ^1H NMR (600 MHz, $CDCl_3$) δ 6.48 (s, 1H), 5.18 (t, *J* = 6.6 Hz, 1H), 4.26 (d, *J* = 17.1 Hz, 1H), 4.21 (d, *J* = 17.1 Hz, 1H), 2.64 (dd, *J* = 11.8, 5.6 Hz, 1H), 2.27 (dd, *J* = 11.9, 8.0 Hz, 1H), 1.39 (s, 3H), 0.90 (s, 9H), 0.11 (s, 3H), 0.10 (s, 3H); ^{13}C NMR (100 MHz, $CDCl_3$) δ 200.1, 146.4, 138.8, 90.5, 80.0, 74.0, 55.6, 25.8, 22.9, 18.2, -4.5, -4.7; IR (neat film, NaCl) 2955, 2930, 2857, 1732, 1645, 1362, 1258, 1103, 1035, 865, 834, 779, 651 cm^{-1}; HRMS (ESI+): m/z calc'd for $C_{14}H_{25}SiO_3$ $[M+H]^+$: 269.1567, found 269.1561; $[\alpha]_D^{23}$ – 48.0 (*c* 0.50, $CHCl_3$).



28 ***16***

Alcohol 16: A round-bottom flask was charged with **28** (420 mg, 1.56 mmol, 1.0 equiv.) and dissolved in THF (15 mL, 0.1 M), after which an aqueous solution of HF (45%, 0.6 mL) was added dropwise. After stirring at 23 °C for 5 hours, the reaction was quenched with a saturated aqueous solution of $NaHCO_3$. The aqueous layer was extracted with EtOAc (3x), the combined organic extracts dried over Na_2SO_4, and the solvent evaporated under reduced pressure. The crude product was purified by flash chromatography on silica gel (30% EtOAc/hexanes) to yield the title compound **16** (196 mg, 1.27 mmol, 81%) as a white solid; ^{1}H NMR (600 MHz, $CDCl_3$) δ 6.55 (s, 1H), 5.22 (t, *J* = 6.9 Hz, 1H), 4.28 (d, *J* = 17.2 Hz, 1H), 4.23 (d, *J* = 17.2 Hz, 1H), 2.78 (dd, *J* = 12.0, 5.7 Hz, 1H), 2.20 (dd, *J* = 12.1, 8.0 Hz, 1H), 1.40 (s, 3H); ^{13}C NMR (100 MHz, $CDCl_3$) δ 200.0, 147.3, 137.6, 90.7, 79.9, 74.0, 55.0, 22.7; IR (neat film, NaCl) 3435, 2921, 2852, 1749, 1220 cm^{-1}; HRMS (ESI+): m/z calc'd for $C_8H_{11}O_3$ $[M+H]^+$: 155.0703, found 155.0700; $[\alpha]_D^{23}$ – 15.0 (*c* 0.30, $CHCl_3$).



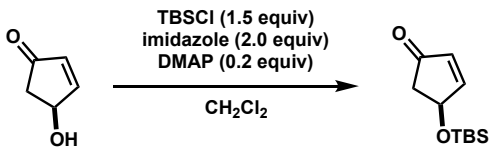
Furfuryl alcohol ***23***

Cyclopentenone 23: Prepared according to a known literature procedure.[2] Deionized water (509 mL, 0.4M), furfuryl alcohol (20 g, 203.8 mmol, 1.0 equiv.) and 6.25 g of

KH_2PO_4 were placed in a round bottom flask equipped with a reflux condenser. The pH was measured with a handheld pH-Meter and H_3PO_4 was added until the pH was measured to be ~4.1. The solution was placed under inert atmosphere and was degassed by bubbling argon through the solution for 1 hour. Subsequently the reaction mixture was heated to reflux for 72 hours, and complete consumption of starting material was observed by GC-MS. The reaction mixture was cooled to room temperature and washed once with EtOAc. The aqueous layer was evaporated under reduced pressure, diluted with EtOAc and the salts filtered off. The organic layer was evaporated under reduced pressure to yield product **23** (6.9 g, 70.3 mmol, 35% yield) as a colorless oil.

^{1}H NMR (300 MHz, $CDCl_3$) δ 7.57 (dd, *J* = 5.7, 2.3 Hz, 1H), 6.22 (dd, *J* = 5.7, 1.3 Hz, 1H), 5.05 (dtd, *J* = 6.0, 2.3, 1.3 Hz, 1H), 3.44 (br s, 1H), 2.78 (dd, *J* = 18.5, 6.1 Hz, 1H), 2.28 (dd, *J* = 18.5, 2.2 Hz, 1H).

The spectroscopic data matches those previously reported.[23]



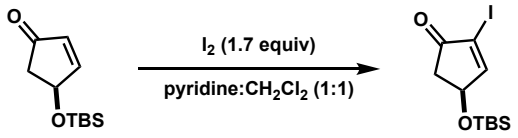
23 ***24***

Silyl Ether 24: Prepared according to a known literature procedure.[3] Allylic alcohol **23** (7.0 g, 71 mmol, 1.0 equiv.) was placed in a round bottom flask and dissolved in dichloromethane (355 mL, 0.2 M). Imidazole (9.6 g, 142 mmol, 2.0 equiv.), TBSCl (16 g, 107 mmol, 1.5 equiv.) and DMAP (1.7 g, 14.2 mmol, 0.2 equiv.) were added and the reaction mixture stirred at 20 °C for 6 hours. After complete consumption of starting material, water was added to the reaction mixture and the aqueous phase extracted with

Et_2O (3x). The combined organic layers were washed with brine, dried over Na_2SO_4 and the solvent evaporated under reduced pressure. The crude product was purified by flash chromatography on silica gel (0 → 10% EtOAc/Hexanes) to yield product **24** (13.5 g, 64 mmol, 90% yield) as a colorless oil.

^{1}H NMR (300 MHz, $CDCl_3$) δ 7.45 (ddd, *J* = 5.7, 2.3, 0.7 Hz, 1H), 6.18 (ddd, *J* = 5.6, 1.3, 0.7 Hz, 1H), 4.98 (dd, *J* = 3.7, 1.6 Hz, 1H), 2.70 (ddd, *J* = 18.2, 5.9, 0.7 Hz, 1H), 2.24 (ddd, *J* = 18.2, 2.2, 0.7 Hz, 1H), 0.90 (s, 9H), 0.13 (s, 3H), 0.12 (s, 3H).

The spectroscopic data matches those previously reported.[29]

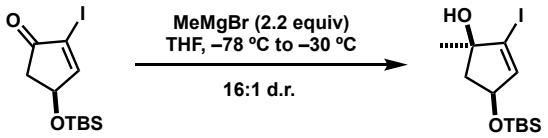


24 ***25***

Vinyl iodide 25: Prepared according to a known literature procedure.[4] Starting material **24** (1.0 g, 4.7 mmol, 1.0 equiv.) was dissolved in a mixture of dichloromethane/pyridine (8 mL/8 mL) and cooled to 0 °C in an ice bath. A solution of iodine (2.0 g, 8.0 mmol, 1.7 equiv.) in a mixture of dichloromethane/pyridine (9.5 mL/9.5 mL) was added dropwise over the course of 1 h. The mixture was then allowed to warm to room temperature and stirred for another hour. Upon complete consumption of starting material as determined by TLC, aqueous HCl (1M) was added and the aqueous layer extracted with CH_2Cl_2 (2x). The combined organic layers were washed with a sat. aqueous solution of $Na_2S_2O_3$, brine and dried over Na_2SO_4. The crude product was purified by flash column chromatography on silica gel (0 → 10% EtOAc/Hexanes) to yield the product **25** as a yellow oil (1.28 g, 3.8 mmol, 80% yield).

^{1}H NMR (600 MHz, $CDCl_3$) δ 7.80 (d, *J* = 2.5 Hz, 1H), 4.95 (d, *J* = 6.1 Hz, 1H), 2.86 (dd, *J* = 18.2, 6.0 Hz, 1H), 2.35 (ddd, *J* = 18.2, 2.2, 0.7 Hz, 1H), 0.91 (s, 9H), 0.14 (s, 3H), 0.13 (s, 3H).

The spectroscopic data matches those previously reported.[30]

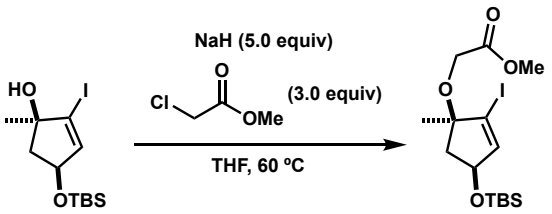


25 ***26***

Alcohol 26: Vinyl iodide **25** (300 mg, 0.88 mmol, 1.0 equiv.) was placed in a vial equipped with a stir bar, sealed, evacuated, and backfilled with N_2 (3x). The starting material was dissolved in THF (8.8 mL, 0.1 M) and cooled to –78 °C in a dry ice/acetone bath. MeMgBr (3M in Et_2O, 0.35 mL, 1.05 mmol, 1.2 equiv) was added dropwise over the course of 5 min and the reaction mixture warmed and kept at temperature between –40 °C and –30 °C. After 1 h, another equivalent of MeMgBr (3M in Et_2O, 0.3 mL) was added and the reaction stirred for another hour at the same temperature. After full consumption of SM as indicated by TLC, a solution of sat. aq. NH_4Cl was added, and the reaction mixture warmed to room temperature. The aqueous layer was extracted with EtOAc (3x) and the combined organic layers dried over Na_2SO_4. The crude product was purified by flash column chromatography on silica gel (0 → 15% EtOAc/Hexanes) to yield the product **26** as a yellow oil (225 mg, 0.64 mmol, 72% yield).

^{1}H NMR (400 MHz, $CDCl_3$) δ 6.16 (d, *J* = 2.2 Hz, 1H), 4.60 (ddd, *J* = 6.6, 4.4, 2.1 Hz, 1H), 2.48 (dd, *J* = 13.3, 6.8 Hz, 1H), 2.17 (s, 1H), 1.91 (dd, *J* = 13.3, 4.4 Hz, 1H), 1.24 (s, 3H), 0.88 (s, 9H), 0.07 (s, 6H); ^{13}C NMR (125 MHz, $CDCl_3$) δ 143.2, 113.8, 82.7, 75.6,

48.2, 27.4, 25.9, 18.2, -4.6, -4.6; IR (neat film, NaCl) 3423, 2954, 2929, 2856, 1743, 1604, 1471, 1359, 1255, 1087, 960, 824, 776, 681, 651 cm^{-1}; HRMS (ESI+): m/z calc'd for $C_{12}H_{22}SiOI$ $[M–OH]^+$: 337.0480, found 337.0482.

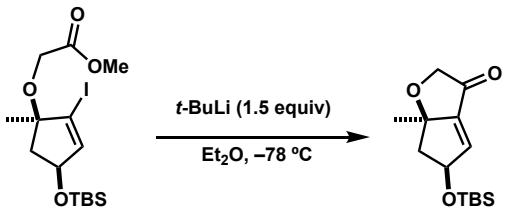


26 ***27***

Methyl Ester 27: Starting material **26** (183 mg, 0.516 mmol, 1.0 equiv.) was placed in a vial and dissolved in THF (3.4 mL, 0.15 M). Sodium hydride (60% in mineral oil, 103 mg, 2.58 mmol, 5.0 equiv.) was added and the reaction stirred for 10 minutes at room temperature. Methyl chloroacetate (0.135 mL, 1.55 mmol, 3.0 equiv.) was added dropwise and the reaction mixture heated to 60 °C for 3 hours. The reaction mixture was cooled to room temperature and quenched with a sat. aq. solution of $NaHCO_3$. The aqueous layer was extracted with Et_2O (3x), the combined organic layers dried over Na_2SO_4, and the solvent evaporated under reduced pressure. The crude product was purified by flash column chromatography on silica gel (0 → 10% EtOAc/Hexanes) to yield the product **27** as a colorless oil (44.5 mg, 0.11 mmol, 21% yield) along with reisolated starting material **26** (126 mg, 0.35 mmol, 69% yield).

^1H NMR (600 MHz, $CDCl_3$) δ 6.31 (dd, *J* = 2.3, 0.5 Hz, 1H), 4.75 – 4.31 (m, 1H), 4.12 (d, *J* = 16.4 Hz, 1H), 3.99 (d, *J* = 16.4 Hz, 1H), 3.73 (s, 3H), 2.35 (dd, *J* = 14.7, 7.5 Hz, 1H), 1.92 (dd, *J* = 14.7, 3.0 Hz, 1H), 1.34 (s, 3H), 0.87 (s, 9H), 0.07 (s, 3H), 0.06 (s, 3H); ^{13}C NMR (125 MHz, $CDCl_3$) δ 171.3, 146.1, 109.7, 88.9, 75.1, 61.9, 51.9, 42.3, 28.1, 25.9,

18.2, -4.6, -4.7; IR (neat film, NaCl) 2955, 2928, 2856, 1741, 1648, 1462, 1361, 1257, 1103, 1035, 837, 778 cm^{-1}; HRMS (ESI+): m/z calc'd for $C_{12}H_{22}SiOI$ [M–OCH_2COOMe]$^+$: 337.0480, found 337.0488.

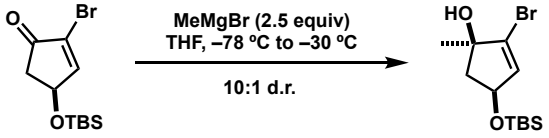


27 ***28***

Enone 28: Starting material **27** (20 mg, 0.048 mmol, 1.0 equiv.) was placed in a vial, capped, equipped with a stir bar, evacuated, and backfilled with N_2 (3x). Et_2O (4.8 mL, 0.01 M) was added, and the reaction mixture cooled to –78 °C in a dry ice/acetone bath. A solution of *t*-BuLi (1.7M in pentane, 0.072 mmol, 0.042 mL) was added dropwise to the reaction mixture and the solution stirred for 30 minutes, before the reaction was quenched with a sat. aq. solution of $NaHCO_3$ and subsequently warmed to room temperature. The aqueous layer was extracted with Et_2O (3x), and the combined organic layers dried over Na_2SO_4. The solvent was evaporated under reduced pressure and the crude product purified by flash column chromatography on silica gel (0 → 10% EtOAc/Hexanes) to yield the product **28** as a colorless oil (10.2 mg, 0.038 mmol, 79% yield).

^{1}H NMR (600 MHz, $CDCl_3$) δ 6.48 (s, 1H), 5.18 (t, *J* = 6.6 Hz, 1H), 4.26 (d, *J* = 17.1 Hz, 1H), 4.21 (d, *J* = 17.1 Hz, 1H), 2.64 (dd, *J* = 11.8, 5.6 Hz, 1H), 2.27 (dd, *J* = 11.9, 8.0 Hz, 1H), 1.39 (s, 3H), 0.90 (s, 9H), 0.11 (s, 3H), 0.10 (s, 3H).

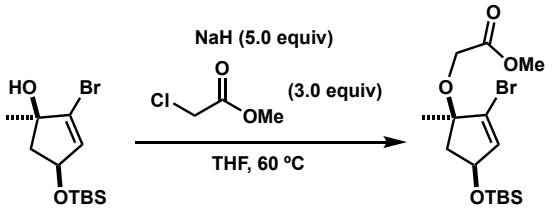
The spectroscopic data matches those previously reported.[5]



40 ***41***

Alcohol 41: Vinyl bromide **40** (500 mg, 1.71 mmol, 1.0 equiv.) was placed in a round bottom flask with a stir bar, sealed, evacuated, and backfilled with N_2 (3x). The starting material was dissolved in Et_2O (17 mL, 0.1 M) and cooled to –78 °C in a dry ice/acetone bath. MeMgBr (3M in Et_2O, 0.85 mL, 2.56 mmol, 1.5 equiv) was added dropwise over the course of 5 min and the reaction mixture warmed and kept at temperature between –40 °C and –30 °C. After 1 h another equivalent of MeMgBr (3M in Et_2O, 0.3 mL) was added and the reaction stirred for another hour at the same temperature. After full consumption of SM as indicated by TLC, a solution of sat. aq. NH_4Cl was added, and the reaction mixture warmed to room temperature. The aqueous layer was extracted with EtOAc (3x) and the combined organic layers dried over Na_2SO_4. The crude product was purified by flash column chromatography on silica gel (0 → 15% EtOAc/Hexanes) to yield the product **41** as a yellow oil (363 mg, 1.18 mmol, 69% yield).

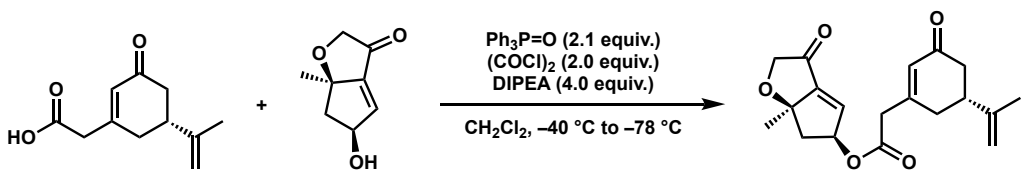
^{1}H NMR (400 MHz, $CDCl_3$) δ 5.94 (d, *J* = 2.2 Hz, 1H), 4.60 (ddd, *J* = 6.5, 3.9, 2.2 Hz, 1H), 2.49 (dd, *J* = 13.4, 6.8 Hz, 1H), 1.95 (dd, *J* = 13.4, 4.0 Hz, 1H), 1.32 (s, 3H), 0.88 (s, 9H), 0.08 (s, 6H); ^{13}C NMR (125 MHz, $CDCl_3$) δ 134.9, 81.1, 73.2, 49.6, 26.2, 25.9, 18.2, -4.6, -4.6; IR (neat film, NaCl) 3423, 2954, 2930, 2857, 1618, 1358, 1254, 1087, 970, 901, 820, 777 cm^{-1}; HRMS (ESI+): m/z calc'd for $C_{12}H_{22}SiOBr$ $[M–OH]^+$: 291.0598, found 291.0605.



41 ***42***

Methyl Ester 42: Starting material **41** (220 mg, 0.714 mmol, 1.0 equiv.) was placed in a vial and dissolved in THF (7 mL, 0.1 M). Sodium hydride (60% in mineral oil, 142 mg, 3.57 mmol, 5.0 equiv.) was added and the reaction stirred for 10 minutes at room temperature. Methyl chloroacetate (0.183 mL, 2.1 mmol, 3.0 equiv.) was added dropwise and the reaction mixture heated to 60 °C for 3 hours. The reaction mixture was cooled to room temperature and quenched with a sat. aq. solution of $NaHCO_3$. The aqueous layer was extracted with Et_2O (3x), the combined organic layers dried over Na_2SO_4, and the solvent evaporated under reduced pressure. The crude product was purified by flash column chromatography on silica gel (0 → 10% EtOAc/Hexanes) to yield the product **42** as a colorless oil (67 mg, 0.18 mmol, 25% yield) along with reisolated starting material **41** (132 mg, 0.43 mmol, 60% yield).

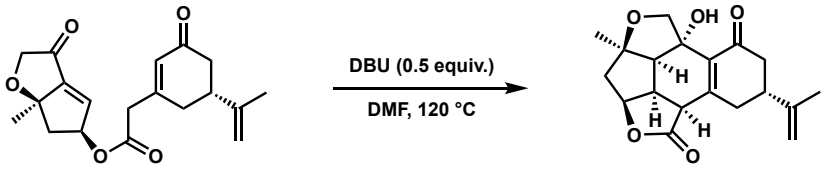
^{1}H NMR (600 MHz, $CDCl_3$) δ 6.08 (dd, J = 2.4, 0.6 Hz, 1H), 4.56 (d, J = 7.3 Hz, 1H), 4.15 (d, J = 16.3 Hz, 1H), 4.00 (d, J = 16.3 Hz, 1H), 3.73 (s, 3H), 2.38 (dd, J = 14.8, 7.4 Hz, 1H), 1.97 (dd, J = 14.8, 2.7 Hz, 1H), 1.41 (s, 3H), 0.87 (s, 9H), 0.07 (s, 3H), 0.06 (s, 3H); ^{13}C NMR (125 MHz, $CDCl_3$) δ 171.3, 137.9, 131.5, 87.3, 72.5, 62.0, 52.0, 44.0, 26.8, 25.9, 18.1, -4.6, -4.7; IR (neat film, NaCl) 3503, 2954, 2857, 1740, 1619, 1471, 1359, 1251, 1118, 1060, 1036, 972, 900, 840, 777 cm^{-1}; HRMS (ESI+): m/z calc'd for $C_{12}H_{22}SiOBr$ $[M–OCH_2COOMe]^+$: 291.0598, found 291.0602.



5 ***16*** ***15***

Ester 15: A flame dried round-bottom flask was charged with triphenylphosphine oxide (478 mg, 1.7 mmol, 2.1 equiv.) and dissolved in CH_2Cl_2 (3.3 mL). The reaction mixture was cooled to –10 °C using a dry ice/acetone bath, and oxalyl chloride (0.14 mL, 1.65 mmol, 2.0 equiv.) was added dropwise. After stirring at the same temperature for 10 minutes, the reaction mixture was cooled to –40 °C, after which acid **5** (323 mg, 1.65 mmol, 2.0 equiv.) was added dropwise as a solution in CH_2Cl_2 (1.0 mL). The mixture was stirred for exactly 10 minutes, while the temperature of the dry ice/acetone bath was monitored with a thermostat and kept between –35 °C to –40 °C. Subsequently, the reaction mixture was cooled to –78 °C, after which alcohol **16** (127 mg, 0.8 mmol, 1.0 equiv.) was added as a solution in CH_2Cl_2 (1.0 mL). Following directly, a solution of diisopropylethylamine (0.53 mL, 3.3 mmol, 4.0 equiv.) in CH_2Cl_2 (0.5 mL) was added dropwise to the reaction mixture and stirred at –78 °C for 10 minutes. The reaction mixture was quenched at the same temperature with a saturated aqueous solution of NH_4Cl and let warm to 23 °C. The aqueous layer was extracted with EtOAc (3x), the combined organic extracts dried over Na_2SO_4, and the solvent evaporated under reduced pressure. The crude product was purified by flash chromatography on silica gel (30% EtOAc/hexanes) to yield the title compound **15** (235 mg, 0.71 mmol, 87%) as a colorless oil; ^{1}H NMR (600 MHz, $CDCl_3$) δ 6.45 (s, 1H), 6.04 (t, *J* = 7.1 Hz, 1H), 5.96 (s, 1H), 4.83 (s, 1H), 4.77 (s, 1H), 4.31 (d, *J* = 17.3 Hz, 1H), 4.25 (d, *J* = 17.2 Hz, 1H), 3.29 (s, 2H), 2.81 (dd, *J* = 12.2, 6.0 Hz, 1H), 2.72 (ddt, *J* = 14.1, 9.6, 4.9 Hz, 1H), 2.54 (dd, *J* = 16.3, 3.9 Hz, 1H), 2.46 – 2.39 (m, 2H), 2.35

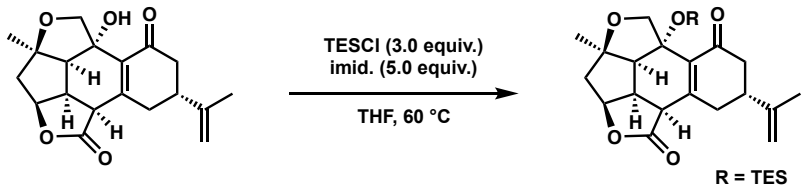
– 2.28 (m, 2H), 1.76 (s, 3H), 1.44 (s, 3H); ^{13}C NMR (100 MHz, $CDCl_3$) δ 199.1, 198.8, 168.6, 155.4, 149.3, 146.0, 132.4, 128.9, 111.2, 90.5, 81.5, 74.3, 50.9, 43.0, 42.2, 41.9, 34.9, 22.9, 20.6; IR (neat film, NaCl) 2976, 1660, 1136, 1028, 988, 889, 735, 658 cm^{-1}; HRMS (ESI+): m/z calc'd for $C_{19}H_{23}O_5$ $[M+H]^+$: 331.1540, found 331.1535; $[\alpha]_D^{23}$ – 91.6 (*c* 0.50, $CHCl_3$).



15 ***31***

Tertiary Alcohol 31: In a flame dried round-bottom flask, **15** (228 mg, 0.69 mmol, 1.0 equiv.) was dissolved in dry DMF (69 mL, 0.01 M) under N_2 atmosphere and heated in a heating mantel set to 120°C for 10 minutes. DBU (51.6 μL, 0.34 mmol, 0.5 equiv.) was added in one portion via syringe and the reaction mixture stirred for 5 minutes. The reaction mixture was consequently cooled to 23°C and a saturated aqueous solution of NH_4Cl and EtOAc was added. The phases were separated, and the aqueous layer extracted with EtOAc (3x). The combined organic extracts were washed with a 10% aqueous solution of LiCl (3x), then brine, dried over Na_2SO_4 and the solvent evaporated under reduced pressure. The crude product was purified via flash chromatography on silica gel (50% EtOAc/hexanes) and the title compound **31** (193 mg, 0.58 mmol, 84%) isolated as a white solid. ^{1}H NMR (600 MHz, $CDCl_3$) δ 5.52 (s, 1H), 5.03 (t, *J* = 6.1 Hz, 1H), 4.85 (s, 1H), 4.79 (s, 1H), 4.20 (d, *J* = 9.9 Hz, 1H), 3.62 (d, *J* = 10.0 Hz, 1H), 3.53 (d, *J* = 9.8 Hz, 1H), 3.26 (ddd, *J* = 12.3, 9.9, 6.4 Hz, 1H), 3.06 (dd, *J* = 18.0, 4.7 Hz, 1H), 2.84 (ddt, *J* =

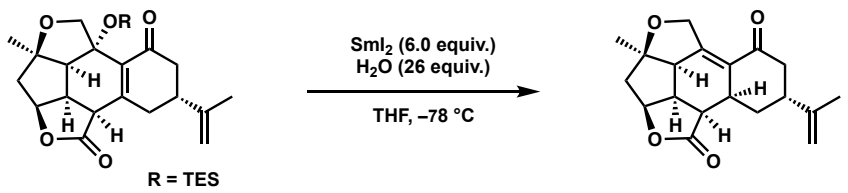
14.8, 9.0, 4.2 Hz, 1H), 2.63 – 2.51 (m, 4H), 2.50 – 2.41 (m, 1H), 2.01 (dd, *J* = 15.9, 5.8 Hz, 1H), 1.78 (s, 3H), 1.55 (s, 3H); ^{13}C NMR (100 MHz, $CDCl_3$) δ 201.9, 173.9, 151.4, 145.7, 134.8, 111.3, 95.0, 85.7, 83.5, 80.6, 59.7, 46.1, 44.4, 43.7, 41.2, 40.3, 36.4, 24.2, 20.5; IR (neat film, NaCl) 3458, 3082, 2971, 1755, 1655, 1360, 1114, 1062, 897, 733 cm^{-1}; HRMS (ESI+): m/z calc'd for $C_{19}H_{21}O_4$ $[M–OH]^+$: 313.1434, found 331.1435; $[\alpha]_D^{23}$ + 14.3 (*c* 1.00, $CHCl_3$).



31 ***43***

Silyl ether 43: In a vial, **31** (100 mg, 0.3 mmol, 1.0 equiv.) was dissolved in THF (3 mL, 0.1 M) and imidazole (102 mg, 1.5 mmol, 5.0 equiv.) added in one portion. Subsequently, TESCl (152 μL, 0.9 mmol, 3.0 equiv.) was added dropwise. The vial was sealed with a plastic cap and placed in a heating block set to 60 °C. After stirring for exactly 3 h, the reaction mixture was flushed over a plug of silica gel, eluting with EtOAc. After the solvent was removed under reduced pressure, the crude product was purified by flash chromatography on silica gel (20% EtOAc/hexanes → 60% EtOAc/hexanes) to give the title compound **43** (112 mg, 0.25 mmol, 83%) as a white solid, along with reisolated starting material **31** (15 mg, 0.045 mmol, 15%); ^{1}H NMR (600 MHz, $CDCl_3$) δ 5.01 (t, *J* = 6.4 Hz, 1H), 4.84 (s, 1H), 4.79 (s, 1H), 4.28 (d, *J* = 10.2 Hz, 1H), 3.86 (d, *J* = 10.2 Hz, 1H), 3.41 (d, *J* = 10.4 Hz, 1H), 3.24 (td, *J* = 11.2, 6.8 Hz, 1H), 3.15 (dd, *J* = 17.7, 4.8 Hz, 1H), 2.95 – 2.77 (m, 1H), 2.66 – 2.43 (m, 4H), 2.36 (dd, *J* = 17.7, 11.3 Hz, 1H), 1.97 (dd, *J* =

15.6, 6.0 Hz, 1H), 1.78 (s, 3H), 1.50 (s, 3H), 0.90 (t, J = 7.9 Hz, 9H), 0.50 (q, J = 7.9 Hz, 6H). ^{13}C NMR (125 MHz, $CDCl_3$) δ 197.4, 174.1, 146.4, 146.2, 138.1, 110.6, 93.7, 85.1, 83.6, 80.1, 60.8, 44.6, 44.5, 43.3, 42.1, 38.3, 35.8, 22.8, 20.5, 7.1, 6.2; IR (neat film, NaCl) 2955, 1766, 1682, 1372, 1116, 1004, 735, 627 cm^{-1}; HRMS (ESI+): m/z calc'd for $C_{19}H_{21}O_4$ [M–OTES]$^+$: 313.1434, found 331.1442; $[\alpha]_D^{23}$ + 10.4 (*c* 0.20, $CHCl_3$).

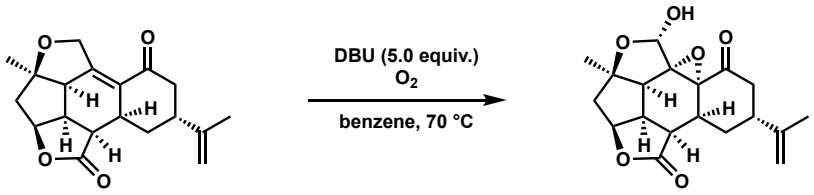


43 ***32***

Preparation of Samariumdiiode (0.1 M in THF): Samarium metal (325 mg, 2.16 mmol, 1.7 equiv.) was freshly filed and the resulting fine powder submitted in a Schlenk tube. The tube was set under vacuum and flame-dried, letting it cool back down to 23 °C. THF (125 mL, 0.1 M) was added, followed by EtI_2 (350 mg, 1.24 mmol, 1.0 equiv.). The reaction mixture was stirred for 10 h, becoming dark blue in color, before it was used. The stock solution was kept under N_2 and sealed with a stopcock, storing it for up to two months without observing any loss of reactivity.

Enone 32: A vial was charged with Silylether **43** (19.2 mg, 0.04 mmol, 1.0 equiv.), dissolved in dry THF (0.4 mL, 0.1 M), the reaction mixture cooled to –78 °C with a dry ice/acetone bath and H_2O (17.3 μL, 0.96 mmol, 24.0 equiv.) added dropwise. SmI_2 (0.1 M in THF, 2.6 mL, 6.0 equiv.) was slowly added down the side of the reaction flask and the dark blue reaction mixture stirred for exactly 2 hours at the same temperature. The dry ice/acetone bath was removed and replaced with an ice bath to let the reaction mixture

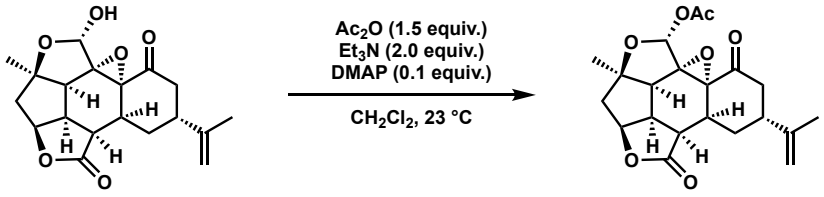
slowly warm up to 0 °C. After one hour, the reaction was quenched with a mixture of a saturated aqueous solution of $Na_2S_2O_3$ and hexanes (4 mL, 1:8). After stirring for 2 minutes, Na_2SO_4 was added and the mixture filtered over a plug of silica gel, eluting with EtOAc. The solvent was evaporated under reduced pressure and the crude product purified by flash chromatography on silica gel (20% EtOAc/hexanes → 30% EtOAc/hexanes) to yield the title compound **32** (8.0 mg, 0.025 mmol, 63%) as a white foam; ^{1}H NMR (600 MHz, $CDCl_3$) δ 4.96 – 4.89 (m, 2H), 4.85 (td, *J* = 7.6, 3.8 Hz, 1H), 4.82 (s, 1H), 4.51 (s, 1H), 3.38 (td, *J* = 9.7, 7.8 Hz, 1H), 2.99 (dd, *J* = 10.0, 3.9 Hz, 1H), 2.94 (ddd, *J* = 14.3, 10.7, 4.0 Hz, 1H), 2.82 (s, 1H), 2.71 – 2.50 (m, 4H), 2.21 (dd, *J* = 15.6, 7.5 Hz, 1H), 2.14 – 2.07 (m, 1H), 2.01 (dd, *J* = 15.7, 4.0 Hz, 1H), 1.80 (s, 3H), 1.48 (s, 3H); ^{13}C NMR (125 MHz, $CDCl_3$) δ 197.4, 177.2, 156.8, 146.0, 127.5, 111.9, 89.9, 82.6, 71.0, 53.6, 44.2, 43.7, 43.5, 42.2, 38.0, 34.7, 26.5, 25.9, 22.2; IR (neat film, NaCl) 2922, 1761, 1616, 1315, 1110, 950, 798, 637 cm^{-1}; HRMS (ESI+): m/z calc'd for $C_{19}H_{23}O_4$ $[M+H]^+$: 315.1591, found 315.1588; $[\alpha]_D^{23}$ + 10.1 (*c* 0.15, $CHCl_3$).



32 ***33***

Hemiacetal 33: A vial was charged with starting material **32** (8.0 mg, 0.025 mmol, 1.0 equiv.), dissolved in benzene (2.5 mL, 0.01 M) and DBU (20 µL, 0.12 mmol, 5.0 equiv.) added dropwise. The head space of the vial was briefly flushed with a blow of oxygen (1 second) and sealed shut with a plastic cap. The vial was placed in a preheated

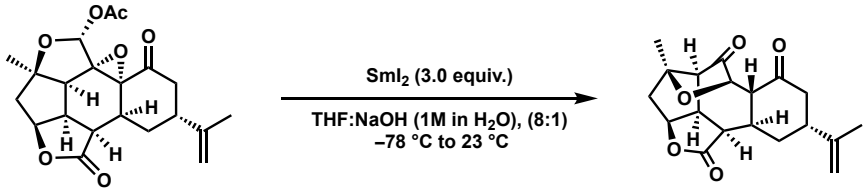
heating block set to 70 °C and stirred for 3 h until full consumption of starting material was observed as determined by TLC. The reaction mixture was directly purified by flash chromatography on silica gel (hexanes → EtOAc/hexanes/acetone, 4:5:1) to yield the title compound **33** (5.8 mg, 0.016 mmol, 67%) as a white foam. ***Note:*** *The reaction was very sensitive to the speed of stirring; being kept low (around 200 to 300 rpm), as a loss in yield was observed at higher rates*; ^{1}H NMR (400 MHz, $CDCl_3$) δ 5.60 (s, 1H), 4.98 (s, 1H), 4.87 (t, *J* = 5.0 Hz, 1H), 4.71 (s, 1H), 3.19 (ddd, *J* = 10.8, 8.1, 5.0 Hz, 1H), 3.07 (dd, *J* = 17.2, 5.0 Hz, 1H), 2.99 (dt, *J* = 6.3, 3.2 Hz, 2H), 2.86 – 2.75 (m, 1H), 2.74 – 2.62 (m, 2H), 2.54 (d, *J* = 10.8 Hz, 1H), 2.37 (dddd, *J* = 14.0, 9.6, 4.3, 2.6 Hz, 1H), 2.13 – 2.02 (m, 1H), 1.87 (dd, *J* = 16.1, 5.0 Hz, 1H), 1.81 (s, 3H), 1.71 (s, 3H); ^{13}C NMR (100 MHz, $CDCl_3$) δ 205.6, 176.6, 145.3, 112.7, 95.2, 93.7, 85.1, 74.4, 60.6, 50.4, 45.6, 45.4, 44.9, 44.5, 38.2, 35.5, 29.2, 28.6, 22.1; IR (neat film, NaCl) 3335, 2929, 1756, 1600, 1124, 1007, 735, 624 cm^{-1}; HRMS (ESI+): m/z calc'd for $C_{19}H_{21}O_5$ $[M+H]^+$: 329.1384, found 329.1383; $[\alpha]_D^{23}$ + 7.5 (*c* 0.23, $CHCl_3$).



33 ***34***

Acetal 34: A vial was charged with **33** (26.3 mg, 0.076 mmol, 1.0 equiv.) and dissolved in CH_2Cl_2 (0.76 mL, 0.1 M). Et_3N (21.2 μL, 0.15 mmol, 2.0 equiv.) and Acetic anhydride (10.7 μL, 0.11 mmol, 1.5 equiv.) were added dropwise. Subsequently, DMAP (0.9 mg, 0.0076 mmol, 0.1 equiv.) was added and the reaction stirred at 23 °C for 1.5 h. The crude

reaction mixture was directly purified by flash chromatography on silica gel (hexanes → EtOAc/hexanes/acetone, 4:5:1) and the title compound **34** (26.8 mg, 0.065 mmol, 85% yield) isolated as a white foam; ^{1}H NMR (600 MHz, $CDCl_3$) δ 6.56 (s, 1H), 4.97 (s, 1H), 4.87 (t, *J* = 5.0 Hz, 1H), 4.71 (s, 1H), 3.20 (ddd, *J* = 11.9, 8.0, 5.1 Hz, 1H), 3.06 (dd, *J* = 17.4, 5.1 Hz, 1H), 3.00 (dd, *J* = 8.3, 2.6 Hz, 1H), 2.99 – 2.95 (m, 1H), 2.79 (dt, *J* = 17.7, 3.1 Hz, 1H), 2.74 – 2.65 (m, 2H), 2.57 (d, *J* = 10.8 Hz, 1H), 2.43 – 2.32 (m, 1H), 2.11 (s, 3H), 2.10 – 2.04 (m, 1H), 1.87 (dd, *J* = 16.2, 5.0 Hz, 1H), 1.80 (s, 3H), 1.64 (s, 3H); ^{13}C NMR (100 MHz, $CDCl_3$) δ 204.4, 176.3, 169.6, 145.3, 112.6, 94.6, 93.8, 84.9, 72.0, 59.9, 50.4, 45.3, 45.1, 44.8, 44.6, 38.1, 35.6, 28.6, 28.5, 22.0, 21.4; IR (neat film, NaCl) 2929, 1748, 1715, 1362, 1228, 1131, 1080, 1005, 940, 736 cm^{-1}; HRMS (ESI+): m/z calc'd for $C_{21}H_{24}O_7Na$ $[M+Na]^+$: 411.1414, found 411.1412; $[\alpha]_D^{23}$ + 18.6 (*c* 0.12, $CHCl_3$).



34 ***(+)-Ineleganolide (1)***

(+)-Ineleganolide (1): A vial was charged with **34** (11.0 mg, 0.026 mmol, 1.0 equiv.), dissolved in THF (1.07 mL, 0.025 M) and the reaction mixture cooled to –78 °C in a dry ice/acetone bath. Aqueous NaOH (1M, 133 μL) was added dropwise, before SmI_2 (0.1 M in THF, 801 μL, 0.08 mmol, 3.0 equiv.) was added dropwise. The reaction mixture was stirred for 3 minutes, before the dry ice/acetone bath was removed. The reaction mixture was stirred for a total of another 3 minutes, while warming up to 23 °C, before it was quenched with a mixture of a saturated aqueous solution of $Na_2S_2O_3$ and hexanes (2 mL,

1:8). After stirring for 2 minutes, Na_2SO_4 was added and the mixture filtered over a plug of silica gel, eluting with EtOAc. The solvent was evaporated under reduced pressure and the crude product purified by preparative HPLC (Agilent Zorbax RX-SIL 5μm (SiO_2), Hexanes:CH_2Cl_2 (3:1) / iPrOH (10% → 25% over 7.5 min), flowrate: 7 mL/min, monitor wavelength = 206 nm, retention time = 3.9 min) to yield (+)-ineleganolide (**1**, 4.0 mg, 0.012 mmol, 45%) as a white solid; ^{1}H NMR (400 MHz, $CDCl_3$) δ 5.12 (t, *J* = 7.4 Hz, 1H), 5.07 (s, 1H), 4.94 (s, 1H), 4.62 (s, 1H), 3.42 (ddd, *J* = 12.1, 9.2, 7.6 Hz, 1H), 3.02 (dd, *J* = 12.0, 2.4 Hz, 1H), 3.00 (m, 1H), 2.78 (br s, 1H), 2.70 (d, *J* = 13.0 Hz, 1H), 2.64 (m, 1H), 2.59 (d, *J* = 9.3 Hz, 1H), 2.52 (d, *J* = 15.6 Hz, 1H), 2.25 (tt, *J* = 12.4, 2.8 Hz, 1H), 2.10 (dd, *J* = 15.5, 7.3 Hz, 1H), 1.78 (dq, *J* = 13.0, 2.8 Hz, 1H), 1.71 (s, 2H), 1.28 (s, 3H). ^{13}C NMR (100 MHz, $CDCl_3$) δ 212.2, 206.4, 176.1, 146.0, 113.8, 91.1, 83.1, 77.4, 62.5, 49.8, 47.0, 45.5, 44.4, 43.8, 40.4, 33.2, 32.7, 22.7, 20.2; IR (neat film, NaCl) 2935, 1759, 1705, 1372, 1322, 1213, 1184, 1026, 905, 835, 736 cm^{-1}; HRMS (ESI+): m/z calc'd for $C_{19}H_{23}O_5$ $[M+H]^+$: 331.1540, found 331.1538; $[\alpha]_D^{23}$ + 25.1 (*c* 0.22, $CHCl_3$).

1.8 REFERENCES AND NOTES

(1) Li, Y.; Pattenden, G. Perspectives on the Structural and Biosynthetic Interrelationships Between Oxygenated Furanocembranoids and Their Polycyclic Congeners Found in Corals. *Nat. Prod. Rep.* **2011**, *28*, 1269−1310.

(2) Craig, R. A., II; Stoltz, B. M. Polycyclic Furanobutenolide-Derived Cembranoid and Norcembranoid Natural Products: Biosynthetic Connections and Synthetic Efforts. *Chem. Rev.* **2017**, *117*, 7878−7909.

(3) For recent and selected examples of syntheses of the polycyclic furanobutenolide-derived diterpenoids, see: (a) Tang, B.; Bray, C. D.; Pattenden, G. A Biomimetic Total Synthesis of (+)-Intricarene. *Tetrahedron Lett.* **2006**, *47*, 6401−6404. (b) Roethle, P. A.; Hernandez, P. T.; Trauner, D. Exploring Biosynthetic Relationships Among Furanocembranoids: Synthesis of (−)-Bipinnatin J, (+)-Intricarene, (+)-Rubifolide, and (+)-Isoepilophodione B. *Org. Lett.* **2006**, *8*, 5901−5904. (c) Stichnoth, D.; Kölle, P.; Kimbrough, T. J.; Riedle, E.; de Vivie-Riedle, R.; Trauner, D. Photochemical Formation of Intricarene. *Nat. Commun.* **2014**, *5*, 5597. (d) Hafeman, N. J.; Loskot, S. A.; Reimann, C. E.; Pritchett, B. P.; Virgil, S. C.; Stoltz, B. M. The Total Synthesis of (−)-Scabrolide A. *J. Am. Chem. Soc.* **2020**, *142*, 8585−8590. (e) Meng, Z.; Fürstner, A. Total Syntheses of Scabrolide A and Nominal Scabrolide B. *J. Am. Chem. Soc.* **2022**, *144*, 1528−1533. (f) Truax, N. J.; Ayinde, S.; Liu, J. O.; Romo, D. Total Synthesis of Rameswaralide Utilizing a Pharmacophore- Directed Retrosynthetic Strategy. *J. Am. Chem. Soc.* **2022**, *144*, 18575−18585.

(4) Fenical, W.; Okuda, R.K.; Bandurraga, M.W.; Culver, P.; Jacobs, R.S. Lophotoxin: a Novel Neuromuscular Toxin from Pacific Sea Whips of the Genus Lophogorgia, *Science*, **1981**, *212*, 1512−1514.

(5) Groebe, D. R.; Abramson, S. N. Lophotoxin Is a Slow Binding Irreversible Inhibitor of Nicotinic Acetylcholine Receptors**,** *The Journal of Biological Chemistry,* **1995**, *270*, 281−286.

(6) Marrero, J.; Rodríguez, A. D.; Baran, P.; Raptis, R. G.; Sánchez, J. A.; Ortega-Barria, E.; Capson, T. L. Bielschowskysin, a Gorgonian-Derived Biologically Active Diterpene with an Unprecedented Carbon Skeleton, *Org. Lett.* **2006**, *10*, 1661−1664.

(7) (a) Duh, C. Y.; Wang, S. K.; Chia, M. C.; Chiang, M. Y. A Novel Cytotoxic Norditerpenoid from the Formosan Soft Coral *Sinularia Inelegans*, *Tetrahedron Lett.* **1999**, *40*, 6033– 6035. An additional isolation report of compound **1** was recently published: (b) Cui W.; Yang, M.; Li, H.; Li, S.; Yao, L.; Li, G.; Tang, W.; Wang, C.; Liang, L.; Guo, Y. Polycyclic furanobutenolide-derived norditerpenoids from the South China Sea soft corals Sinularia scabra and Sinularia polydactyla with immunosuppressive activity, *Bioorg. Chem.* **2019**, *94*, 103350.

(8) Horn, E. J.; Silverston, J. S.; Vanderwal, C. D. A Failed Late- Stage Epimerization Thwarts an Approach to Ineleganolide, *J. Org. Chem.* **2016**, *81*, 1819−1838.

(9) Pratt, B. A. The Design and Synthesis of Highly Potent Epothilone B Analogues and Progress toward the Total Synthesis of Sinularia Natural Products. Ph.D. Dissertation, The Scripps Research Institute, La Jolla, CA, 2008.

(10) Breunig, M. Studies toward the Total Synthesis of Macro- and Polycyclic Furanobutenolides and Formal Synthesis of (±)-Strictamine. Ph.D. Dissertation, Universität Konstanz, Konstanz, Germany, 2019.

(11) Liu, G. Beta-Lactones as Synthetic Vehicles in Natural Product Synthesis: Total Syntheses of Schulzeines B & C and Omphadiol, and Studies toward the Total Syntheses of Scabrolides A & B and Sinulochmodin C. Ph.D. Dissertation, Texas A & M University, College Station, TX, 2012.

(12) (a) Tang, F.; Moeller, K. D. Anodic Oxidations and Polarity: Exploring the Chemistry of Olefinic Radical Cations. *Tetrahedron* **2009**, *65*, 10863−10875. (b) Tang, F.; Moeller, K. D. Intramolecular Anodic Olefin Coupling Reactions: The Effect of Polarization on Carbon−Carbon Bond Formation. *J. Am. Chem. Soc.* **2007**, *129*, 12414−12415.

(13) For the previous work of our group see: (a) Roizen, J. L.; Jones, A. C.; Smith, R. C.; Virgil, S. C.; Stoltz, B. M. Model Studies To Access the [6,7,5,5]-Core of Ineleganolide Using Tandem Translactonization−Cope or Cyclopropanation−Cope Rearrangements as Key Steps. *J. Org. Chem.* **2017**, *82*, 13051−13067. (b) Craig, R. A.; Smith, R. C.; Roizen, J. L.; Jones, A. C.; Virgil, S. C.; Stoltz, B. M. Development of a Unified Enantioselective, Convergent Synthetic Approach Toward the Furanobutenolide-Derived Polycyclic Norcembranoid Diterpenes: Asymmetric Formation of the Polycyclic Norditerpenoid Carbocyclic Core by Tandem Annulation Cascade. *J. Org. Chem.* **2018**, *83*, 3467−3485. (c) Craig, R. A.; Smith, R. C.; Roizen, J. L.; Jones, A. C.; Virgil, S. C.; Stoltz, B. M. Unified Enantioselective, Convergent Synthetic Approach toward the Furanobutenolide-Derived Polycyclic

Norcem- branoid Diterpenes: Synthesis of a Series of Ineleganoloids by Oxidation-State Manipulation of the Carbocyclic Core. *J. Org. Chem.* **2019**, *84*, 7722−7746.

(14) (a) Tuccinardi, J. P.; Wood J. L. Total Syntheses of (+)-Ineleganolide and (−)-Sinulochmodin C. *J. Am. Chem. Soc.* **2022**, *144*, 20539−20547. (b) A similar macrocycle was also prepared by Sarlah and coworkers: Nesic, M.; Kincanon, M. M.; Ryffel, D. B.; Sarlah, D. A New Approach towards the Synthesis of Bielschowskysin: Synthesis and Photochemistry of an Advanced Macrocyclic Enedione Intermediate. *Tetrahedron* **2020**, *76*, No. 131318.

(15) Li, Y.; Pattenden, G. Biomimetic Syntheses of Ineleganolide and Sinulochmodin C from 5-Episinuleptolide via Sequences of Transannular Michael Reactions. *Tetrahedron* **2011**, *67*, 10045−10052.

(16) Cusumano, A. Q.; Houk, K. N.; Stoltz, B. M. Synthetic Strategy toward Ineleganolide: A Cautionary Tale. *Tetrahedron* **2021**, *93*, No. 132289.

(17) Craig, R. A.; Roizen, J. L.; Smith, R. C.; Jones, A. C.; Virgil, S. C.; Stoltz, B. M. Enantioselective, convergent synthesis of the ineleganolide core by a tandem annulation cascade. *Chem. Sci.* **2017**, *8*, 507−514.

(18) (a) Lin, D. S.; Späth, G.; Meng, Z.; Wieske, L. H. E.; Farès, C.; Fürstner, A. Total Synthesis of the Norcembranoid Scabrolide B and Its Transformation into Sinuscalide C, Ineleganolide, and Horiolide. *J. Am. Chem. Soc.* **2024**, *146*, 24250−24256. Also see: (b) Simmons, E. J.; Ryffel, D. B.; Lopez, D. A.; Boyko, Y. D.; Sarlah, D. Total Syntheses of Scabrolide B, Ineleganolide, and Related Norcembranoids. *J. Am. Chem. Soc.* **2025**, *147*, 130−135.

(19) Yu, K.; Gorou, A.; Huang, D.; Maimone, T. J. Short, Enantioselective Total Synthesis of (+)-Ineleganolide, *J. Am. Chem. Soc.* **2025**, *ASAP*.

(20) Brill, Z. G.; Grover, H. K.; Maimone, T. J. Enantioselective Synthesis of an Ophiobolin Sesterterpene via a Programmed Radical Cascade. *Science* **2016**, *352*, 1078−1082.

(21) Hafeman, N. J.; Chan, M.; Fulton, T. J.; Alexy, E. J.; Loskot, S. A.; Virgil, S. C.; Stoltz, B. M. Asymmetric Total Synthesis of Havellockate. *J. Am. Chem. Soc.* **2022**, *144*, 20232−20236.

(22) Saitman, A.; Theodorakis, E. A.; Synthesis of a Highly Functionalized Core of Verrillin. *Org. Lett.* **2013**, *15*, 2410–2413.

(23) Watson, T. J. N.; Curran, T. T.; Hay, D. A.; Shah, R. S.; Wenstrup, D. L.; Webster, M. E. Development of the Carbocyclic Nucleoside MDL 201449A: A Tumor Necrosis Factor-α Inhibitor. *Org. Proc. Res. Dev.* **1998**, *2*, 357–365.

(24) Myers, A. G.; Dragovich, P. S.; A Reaction Cascade Leading to 1,6-Didehydro[10]annulene → 1,5-Dehydronaphthalene Initiated by Thiol Addition. *J. Am. Chem. Soc.* **1993**, *115*, 7021–7022.

(25) Jia, M.; Jiang, L.; Niu, F.; Zhang, Y.; Sun, X. A novel and highly efficient esterification process using triphenylphosphine oxide with oxalyl chloride. *R. Soc. Open Sci.* **2018**, *5*, 171988.

(26) To the best of our knowledge, the only similar observations we found were (a) by Vanderwal and co-workers during the synthesis of the pseudopterosins and (b) by Newhouse, Yin and co-workers during the development of a copper-catalyzed aerobic oxidation: (a) Ramella, V.; Roosen, P. C.; Vanderwal, C. D. Concise Formal

Synthesis of the Pseudopterosins via Anionic Oxy-Cope/Transannular Michael Addition Cascade. *Org. Lett.* **2020**, *22*, 2883–2886. (b) Zhang, H.-J.; Schuppe, A. W.; Pan, S.-T.; Chen, J.-X.; Wang, B.-R.; Newhouse, T. R.; Yin, L. Copper-Catalyzed Vinylogous Aerobic Oxidation of Unsaturated Compounds with Air. *J. Am. Chem. Soc.* **2018**, *140*, 5300−5310.

(27) For a review on the semi-pinacol shift in natural product synthesis see: Song, Z. L.; Fan, C. A.; Tu, Y. Q. Semipinacol Rearrangement in Natural Product Synthesis. *Chem. Rev.* **2011**, *111*, 7523.

(28) Pangborn, A. M.; Giardello, M. A.; Grubbs, R. H.; Rosen, R. K.; Timmers, F. J. Safe and Convenient Procedure for Solvent Purification. *Organometallics* **1996**, *15*, 1518–1520.

(29) Jacobo, S. H. et al. Total Synthesis of 8,12-*iso*-iP$F_{3\alpha}$-VI, an EPA-Derived Isoprostane: Stereoselective Introduction of the Fifth Asymmetric Center. *J. Org. Chem.* **2006**, *71*, 1370–1379.

(30) Kimbrough, J. R. et al. Synthesis of tetranor-PGE_1: A urinary metabolite of prostaglandins E_1 and E_2, *Tetrahedron Lett.* **2020**, *61*, 151922.

APPENDIX 1

Spectra Relevant to Chapter 1:

The Total Synthesis of Ineleganolide

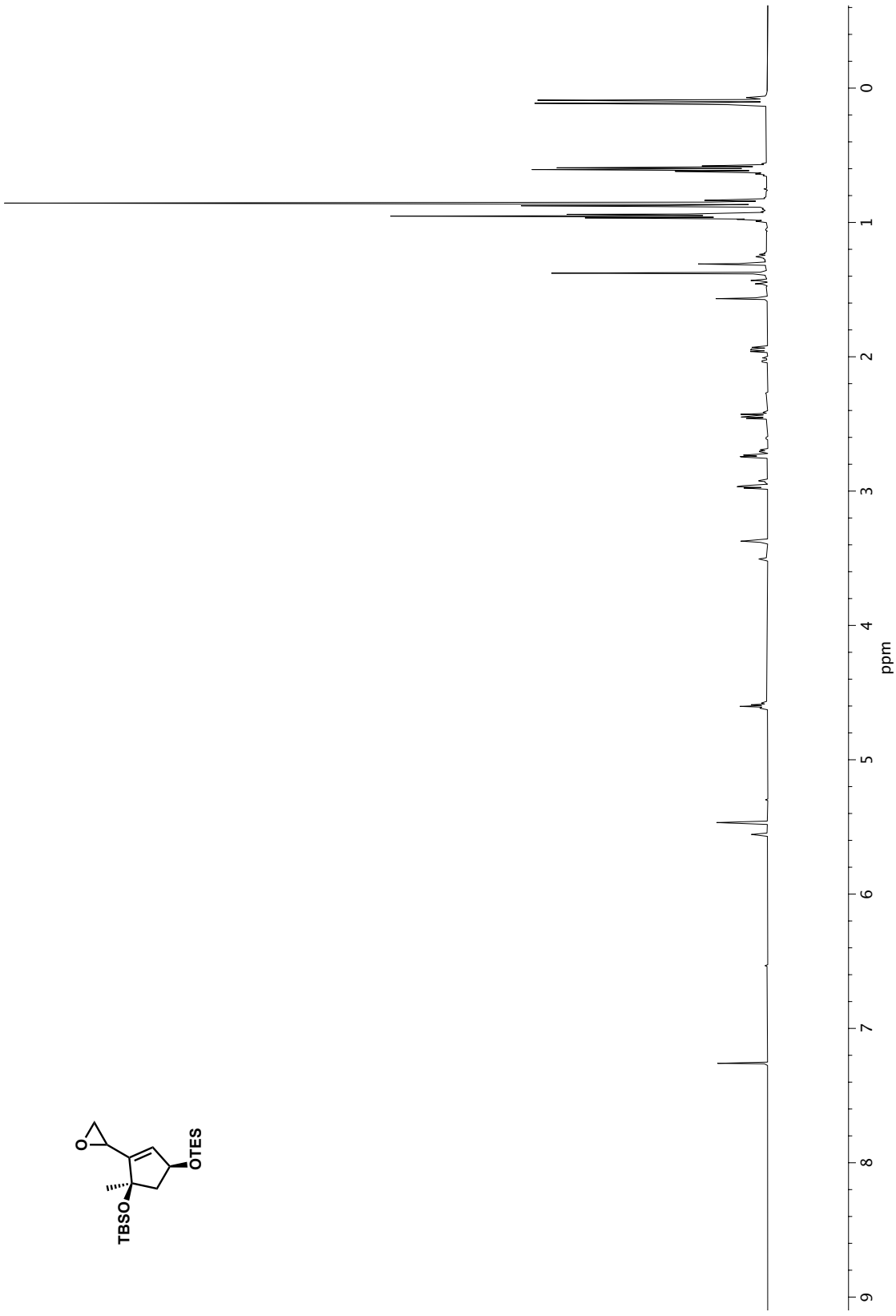


Figure A1.1. ^{1}H NMR (600 MHz, $CDCl_3$) of compound **18**.

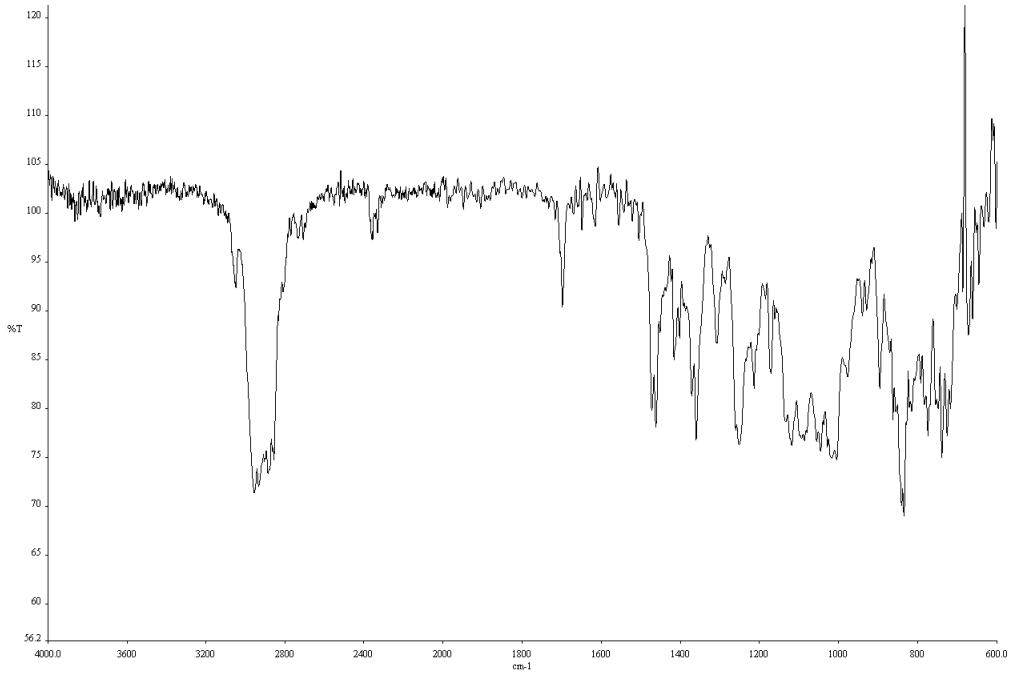


Figure A1.2. Infrared spectrum (Thin Film, NaCl) of compound **18**.

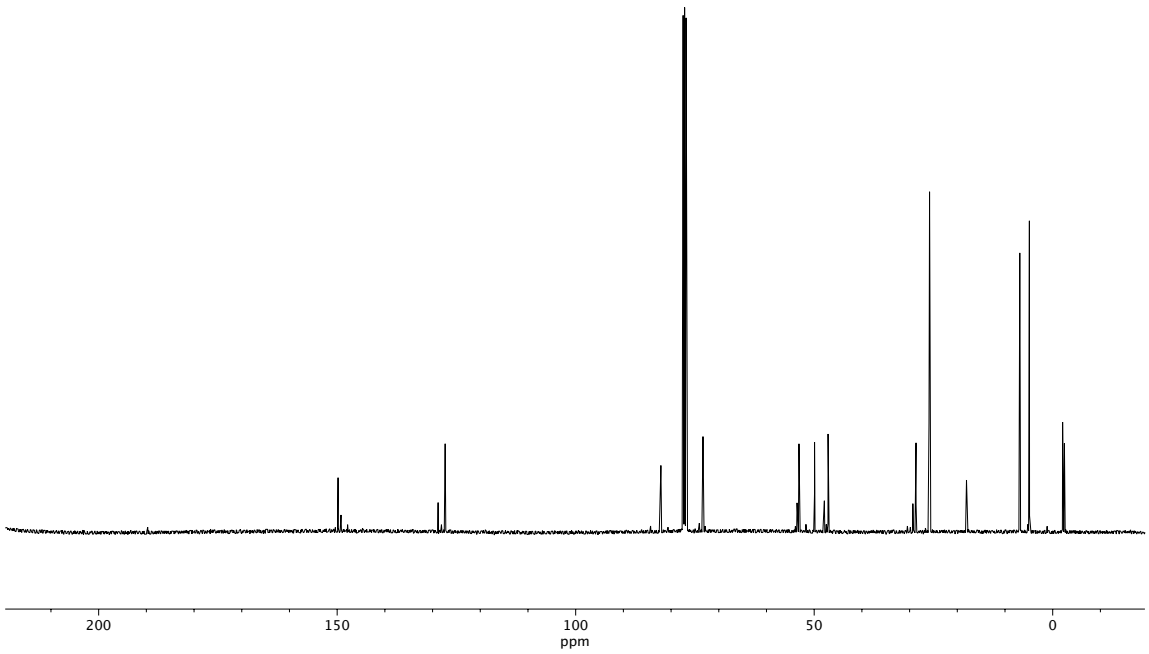


Figure A1.3. ^{13}C NMR (100 MHz, $CDCl_3$) of compound **18**.

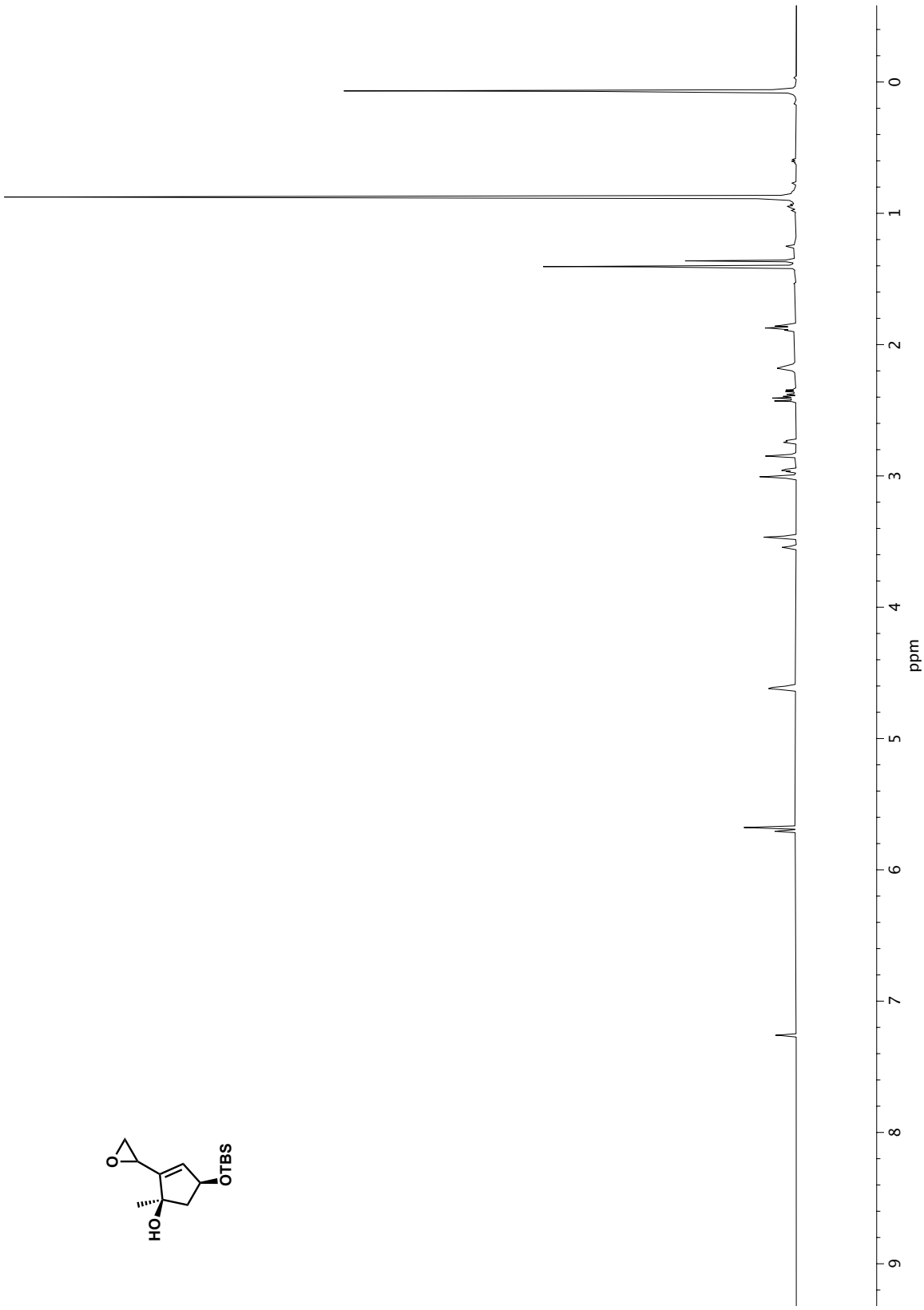


Figure A1.4. ^{1}H NMR (600 MHz, $CDCl_3$) of compound **19**.

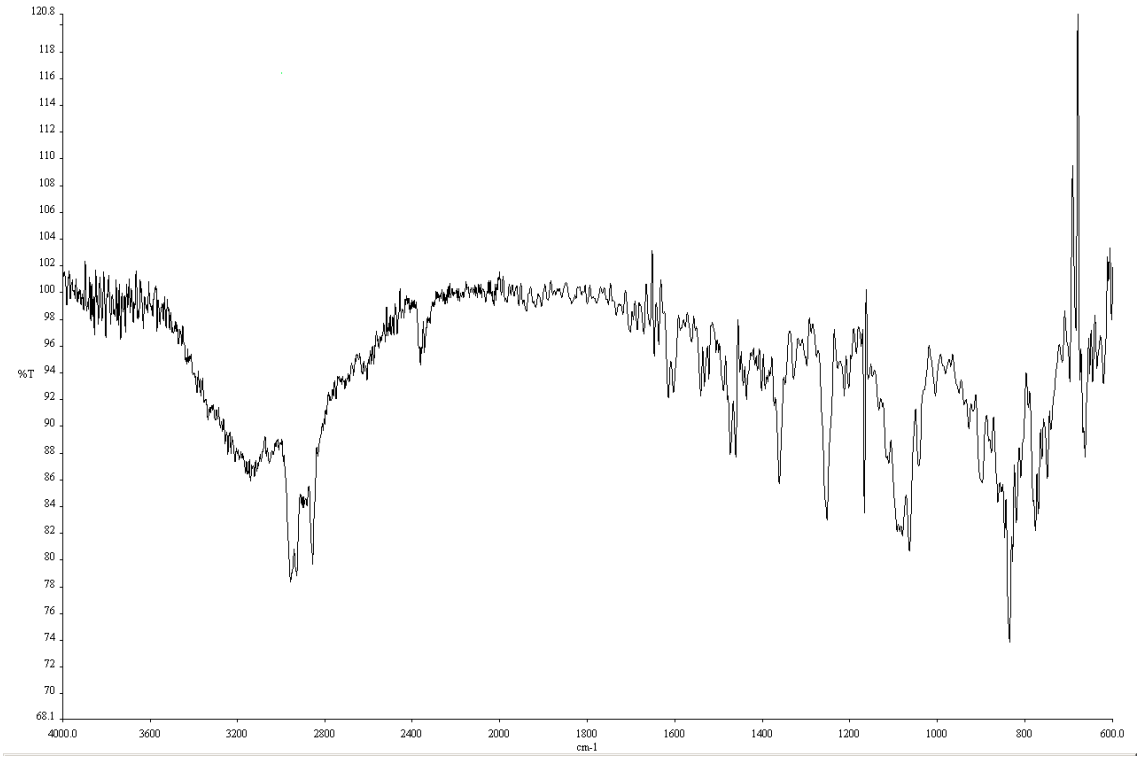


Figure A1.5. Infrared spectrum (Thin Film, NaCl) of compound **19**.

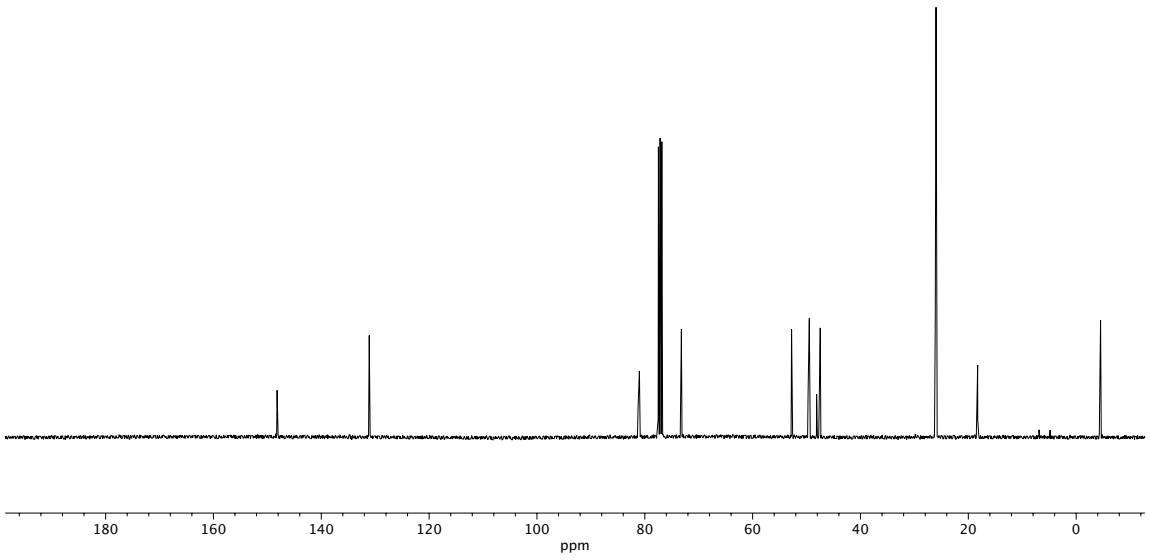


Figure A1.6. ^{13}C NMR (100 MHz, $CDCl_3$) of compound **19**.

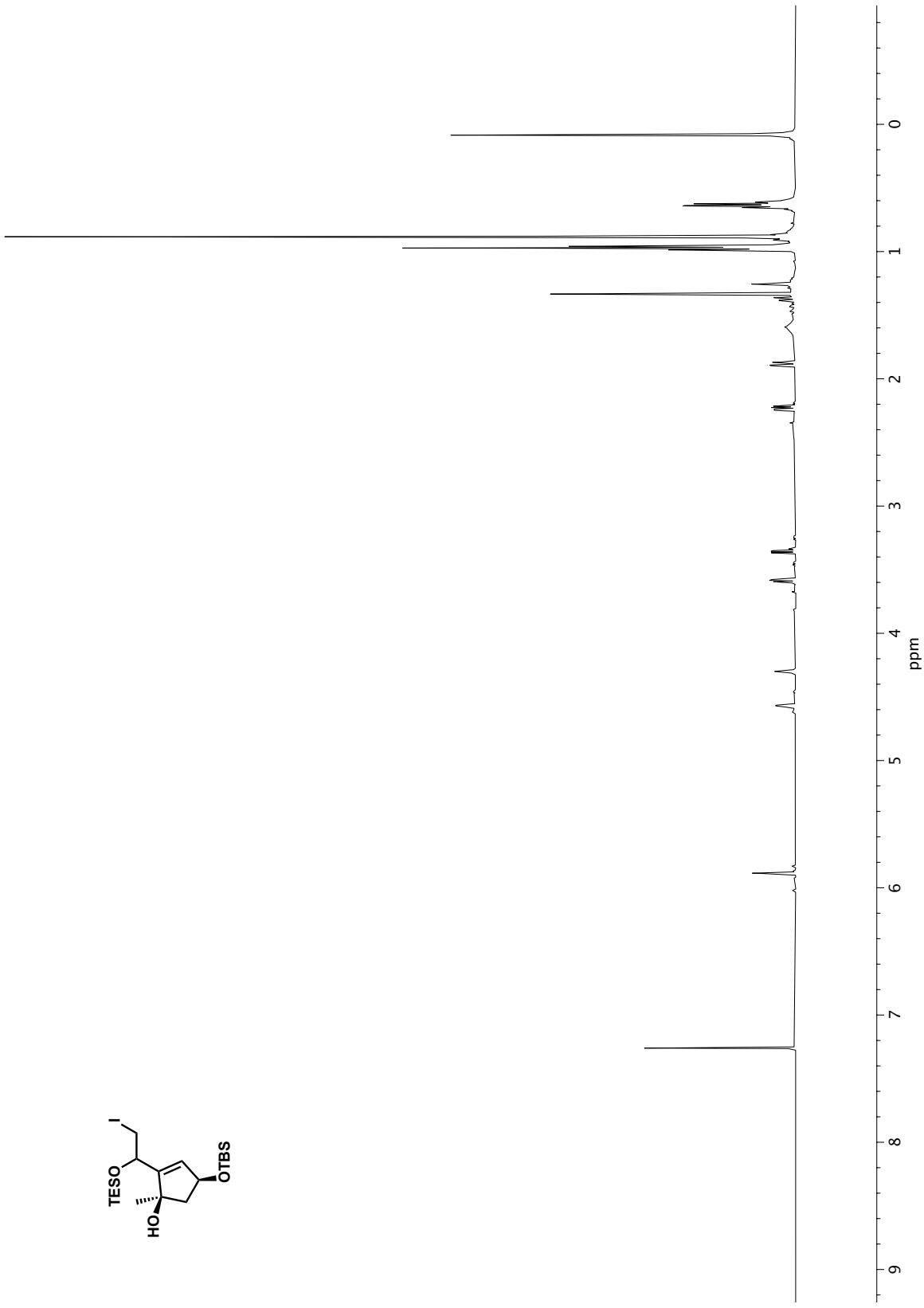


Figure A1.7. ^{1}H NMR (600 MHz, $CDCl_3$) of compound **39**.

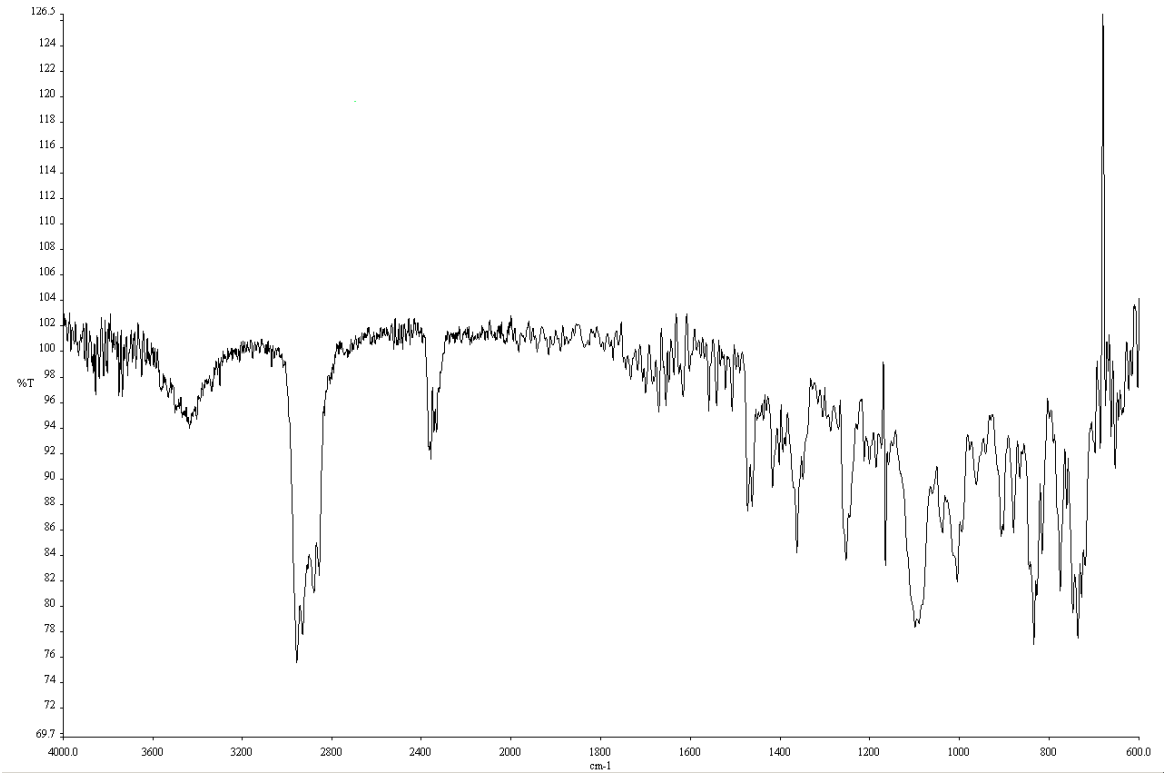


Figure A1.8. Infrared spectrum (Thin Film, NaCl) of compound **39**.

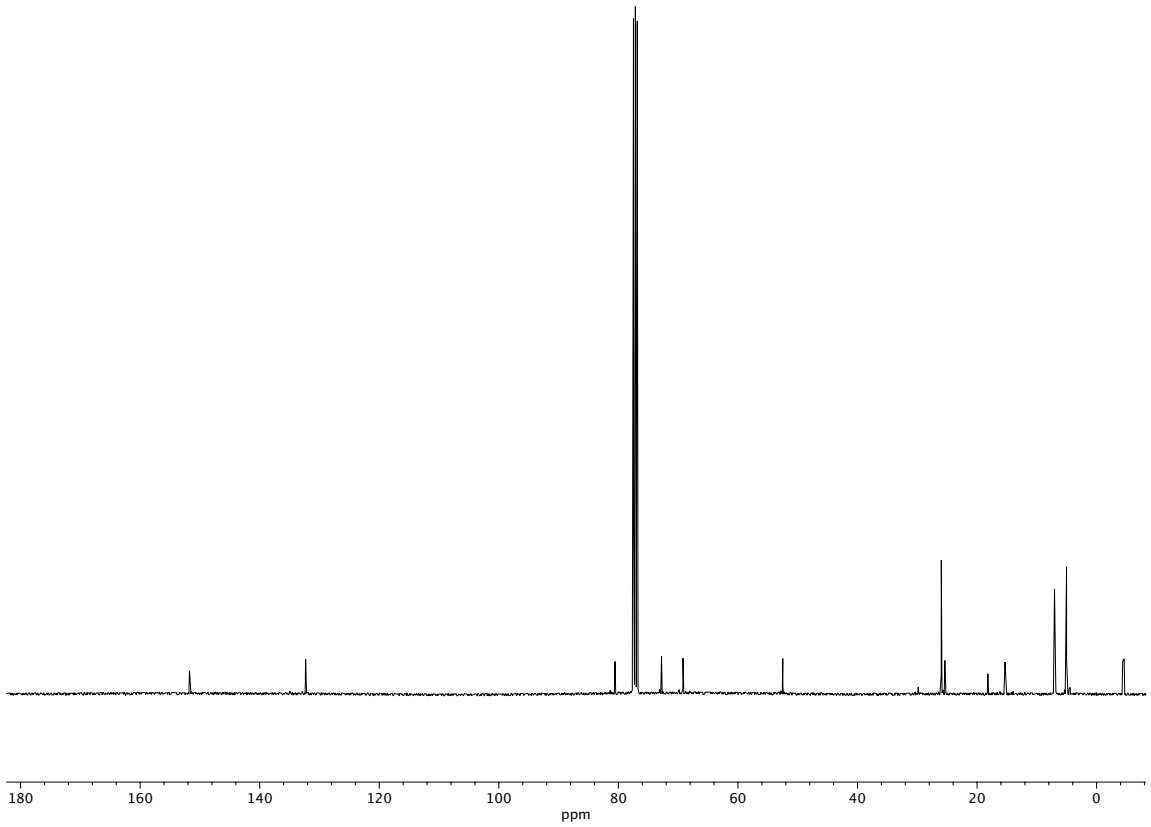


Figure A1.9. ^{13}C NMR (100 MHz, $CDCl_3$) of compound **39**.

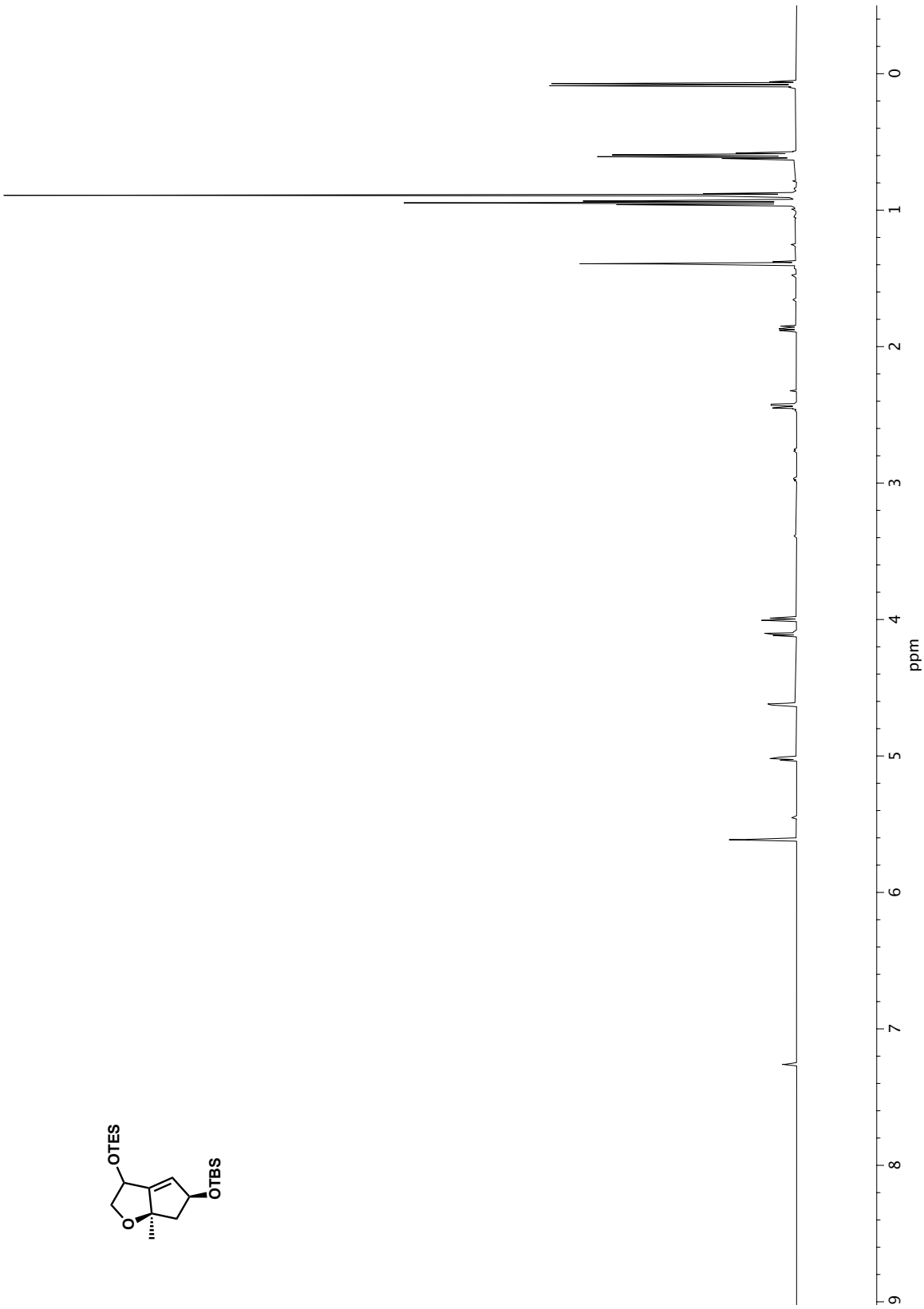


Figure A1.10. ^{1}H NMR (600 MHz, $CDCl_3$) of compound **21**.

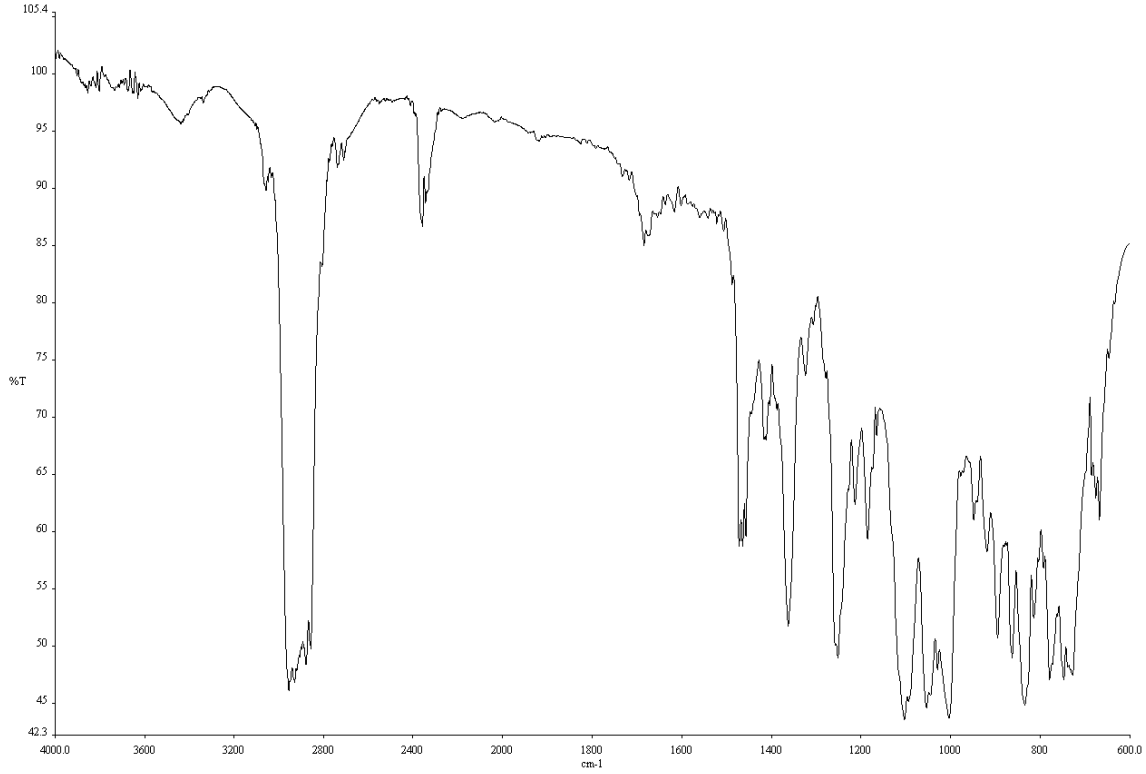


Figure A1.11. Infrared spectrum (Thin Film, NaCl) of compound **21**.

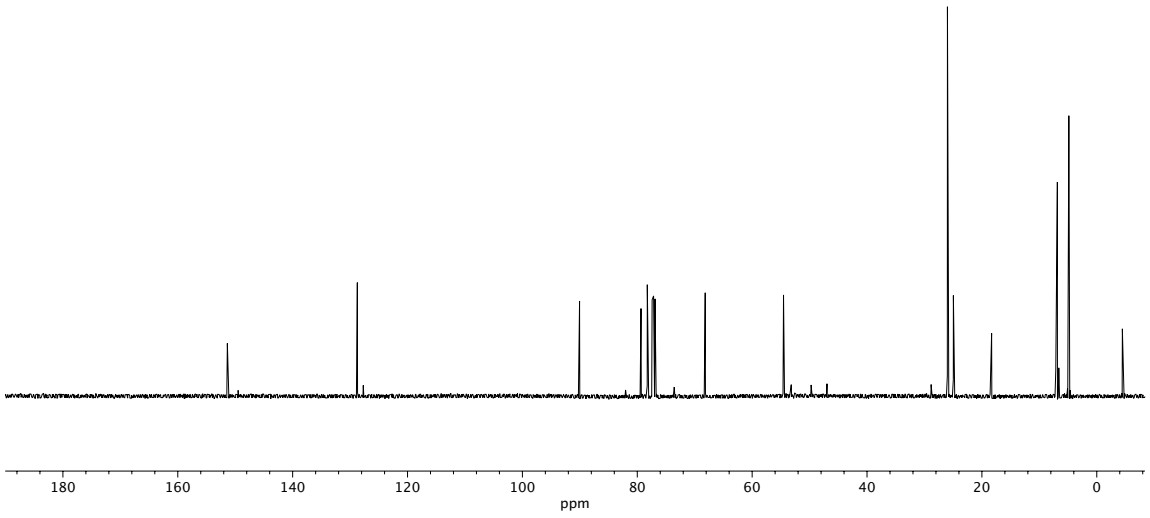


Figure A1.12. ^{13}C NMR (125 MHz, $CDCl_3$) of compound **21**.

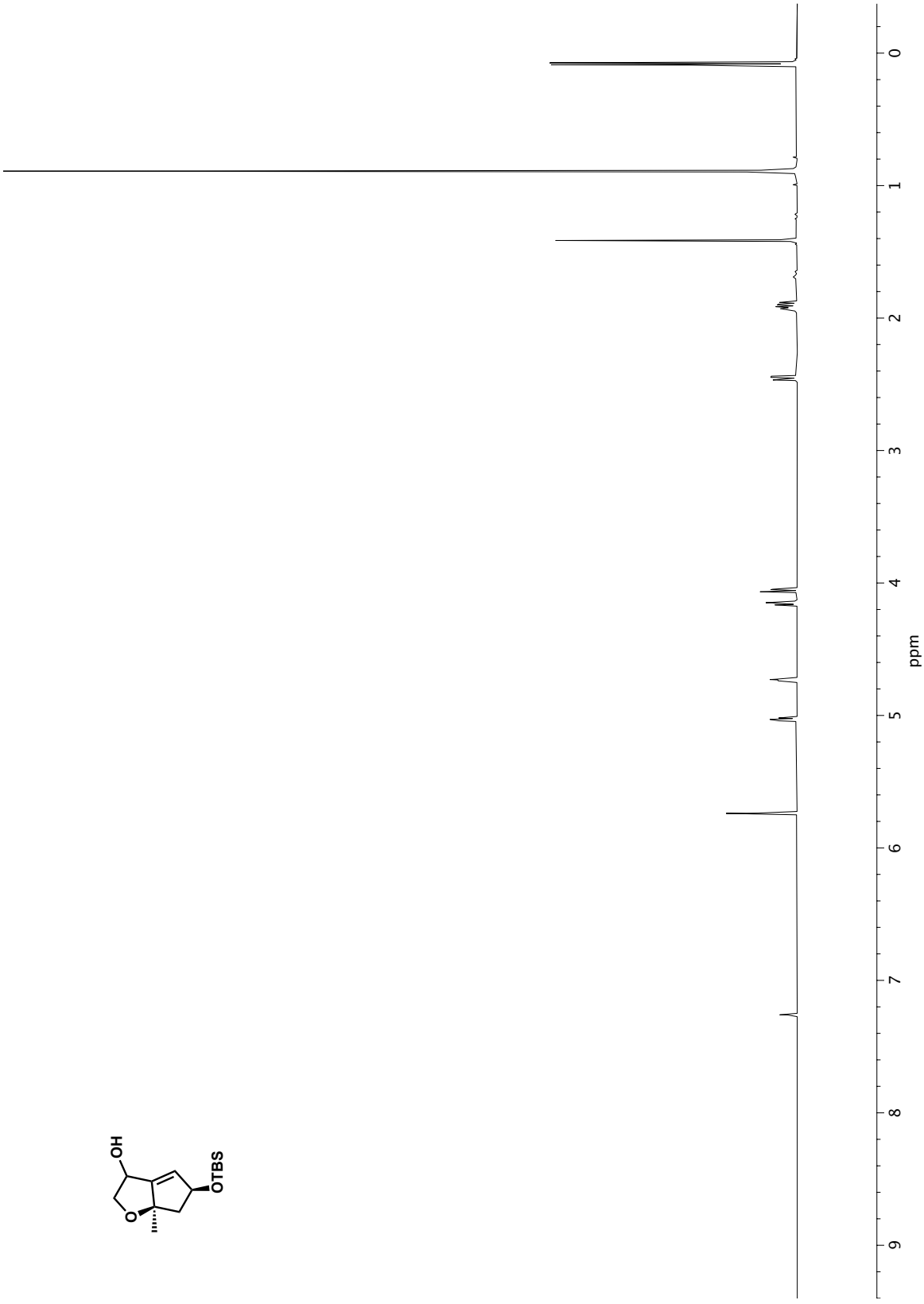


Figure A1.13. ^{1}H NMR (600 MHz, $CDCl_3$) of compound **22**.

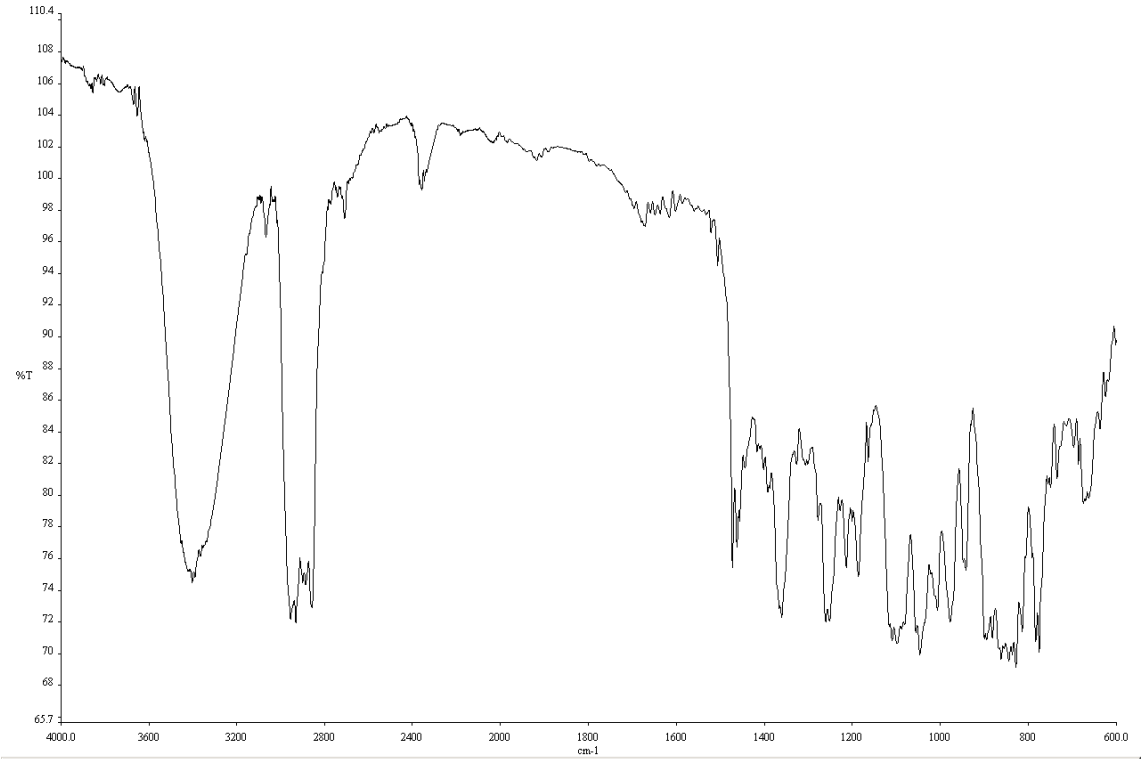


Figure A1.14. Infrared spectrum (Thin Film, NaCl) of compound **22**.

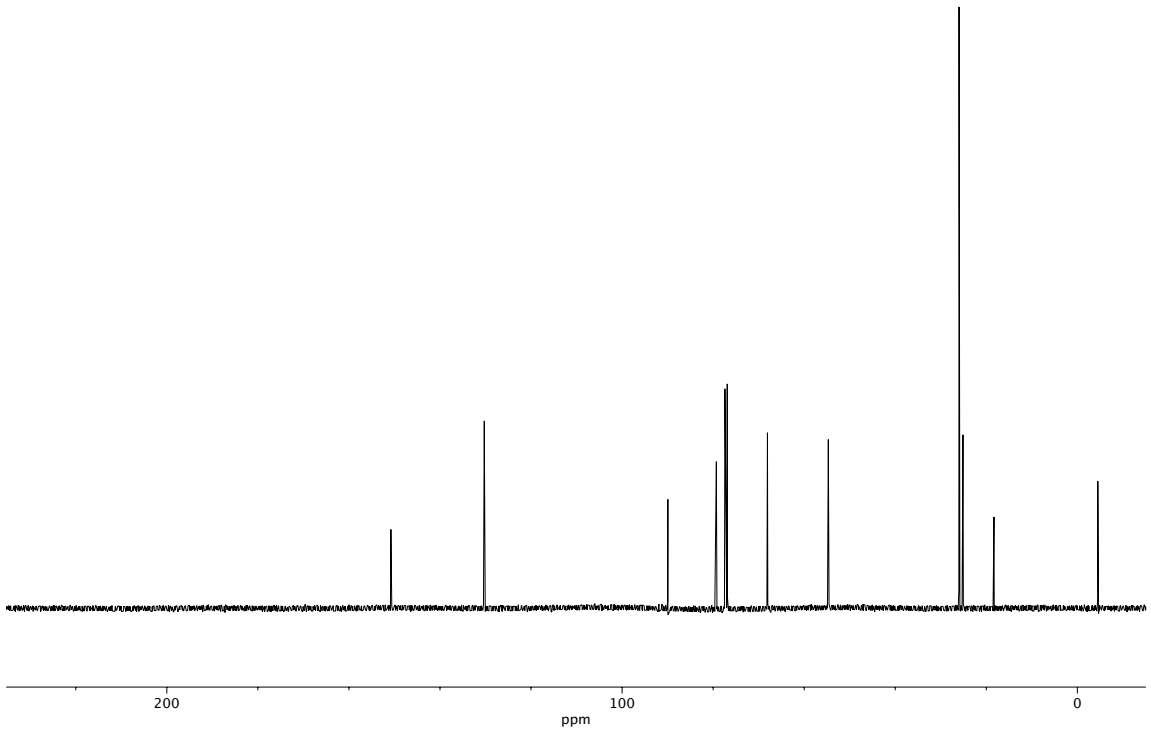


Figure A1.15. ^{13}C NMR (125 MHz, $CDCl_3$) of compound **22**.

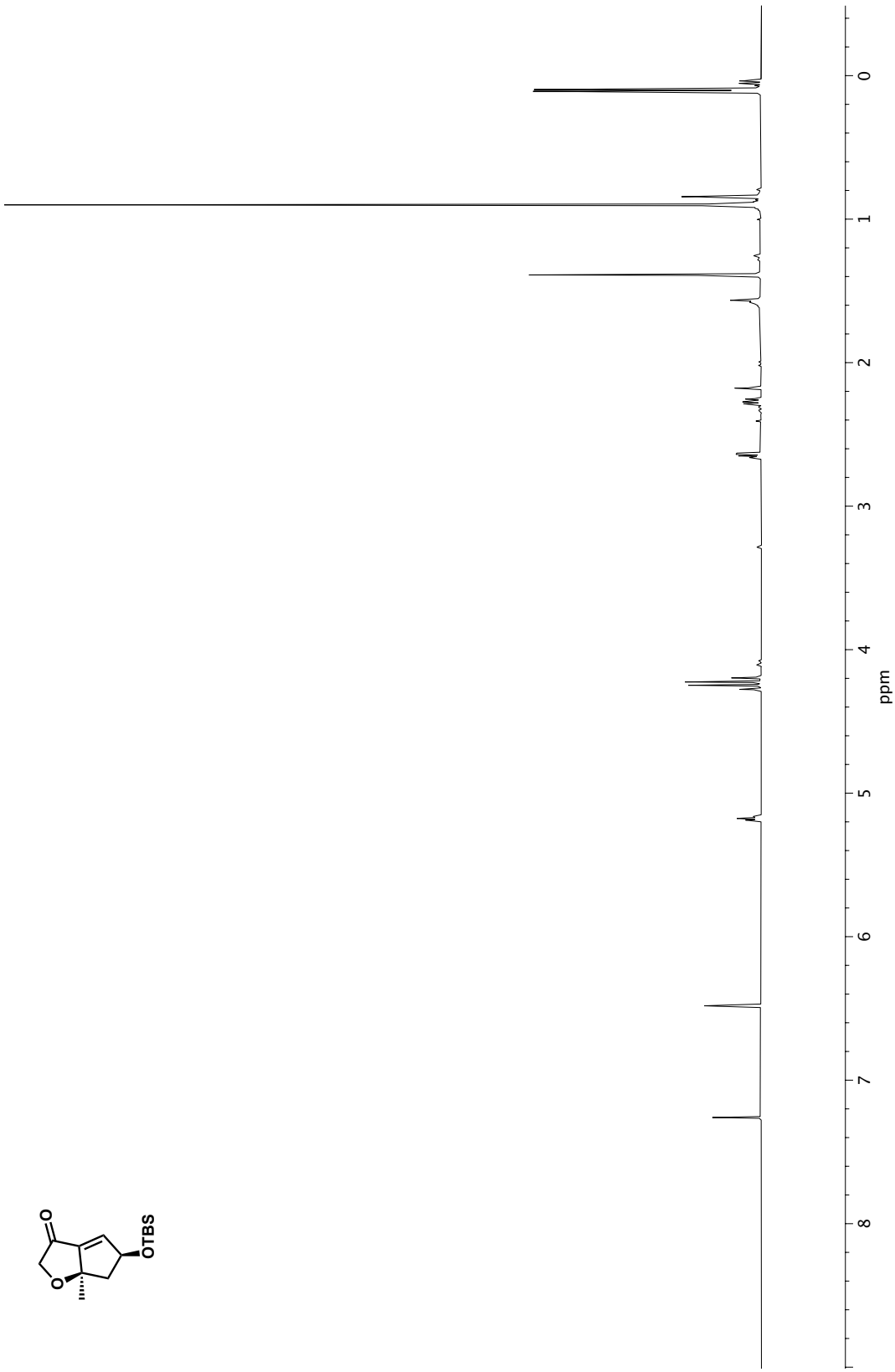


Figure A1.16. ^{1}H NMR (600 MHz, $CDCl_3$) of compound **28**.

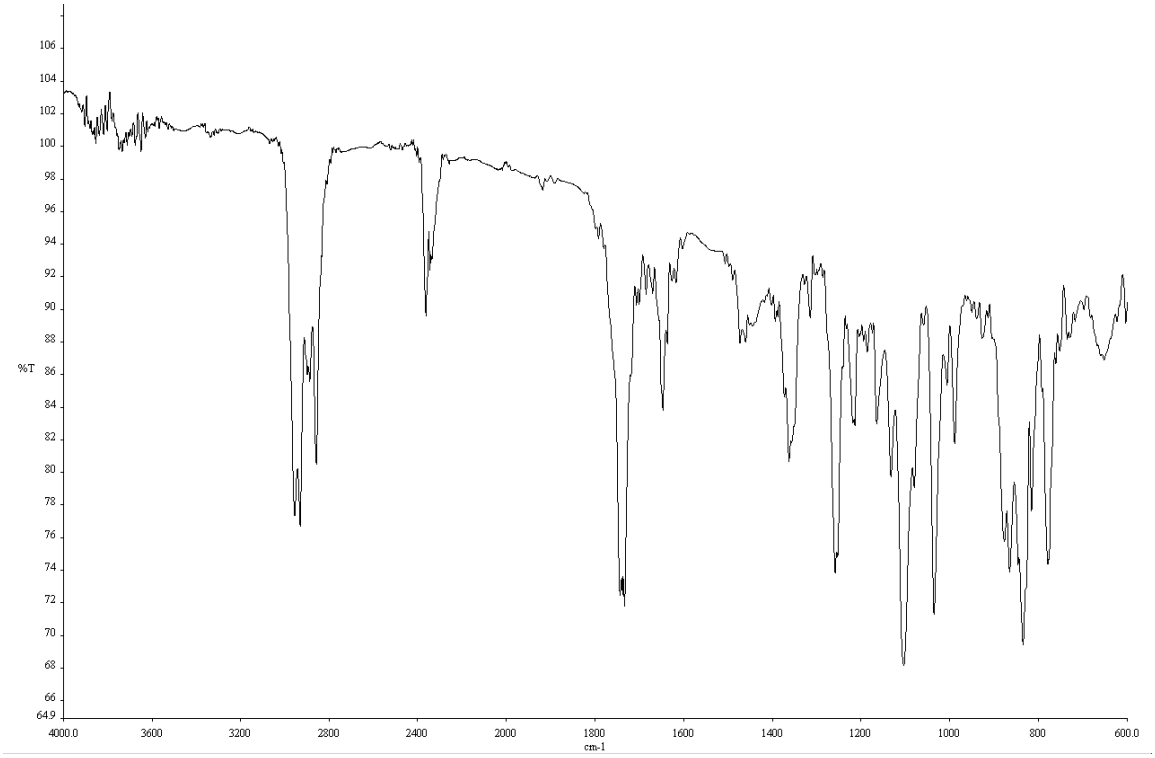


Figure A1.17. Infrared spectrum (Thin Film, NaCl) of compound **28**.

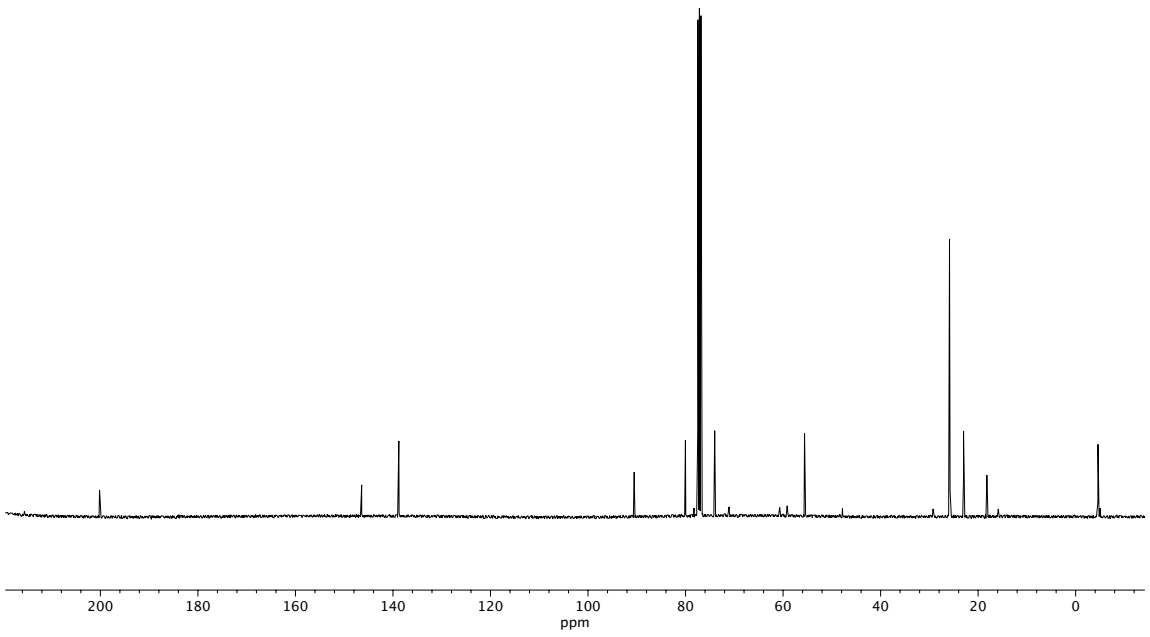


Figure A1.18. ^{13}C NMR (100 MHz, $CDCl_3$) of compound **28**.

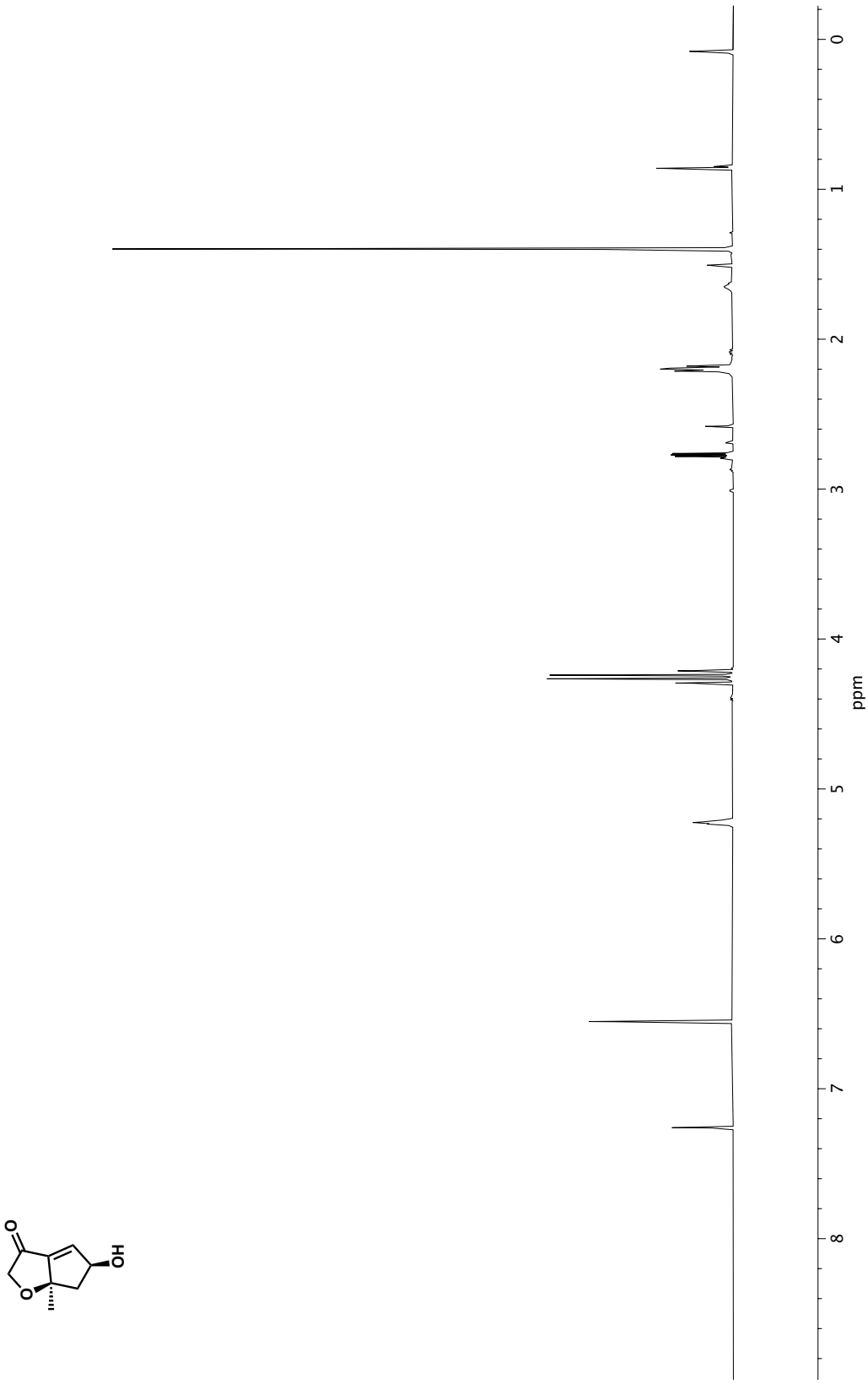


Figure A1.19. ^{1}H NMR (600 MHz, $CDCl_3$) of compound **16**.

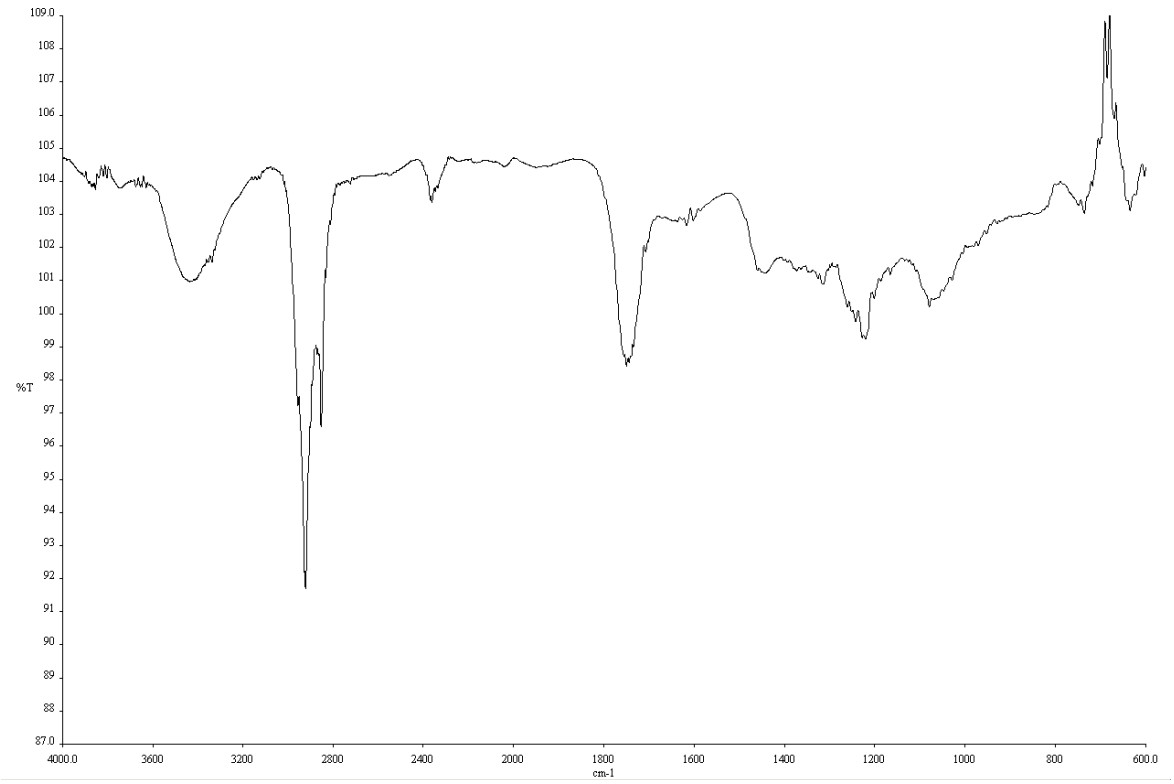


Figure A1.20. Infrared spectrum (Thin Film, NaCl) of compound **16**.

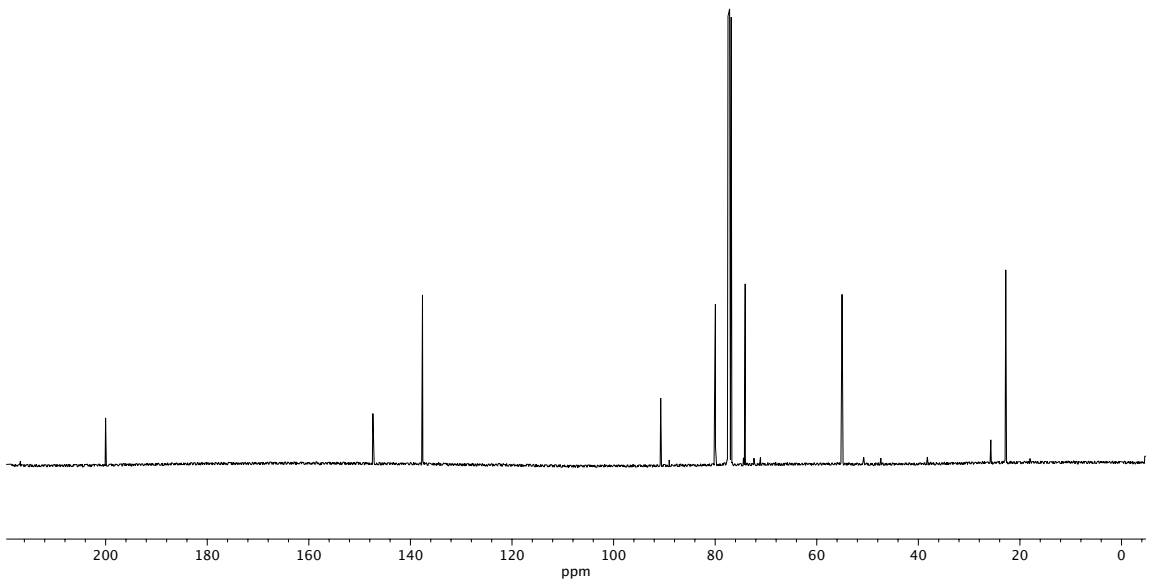


Figure A1.21. ^{13}C NMR (100 MHz, $CDCl_3$) of compound **16**.

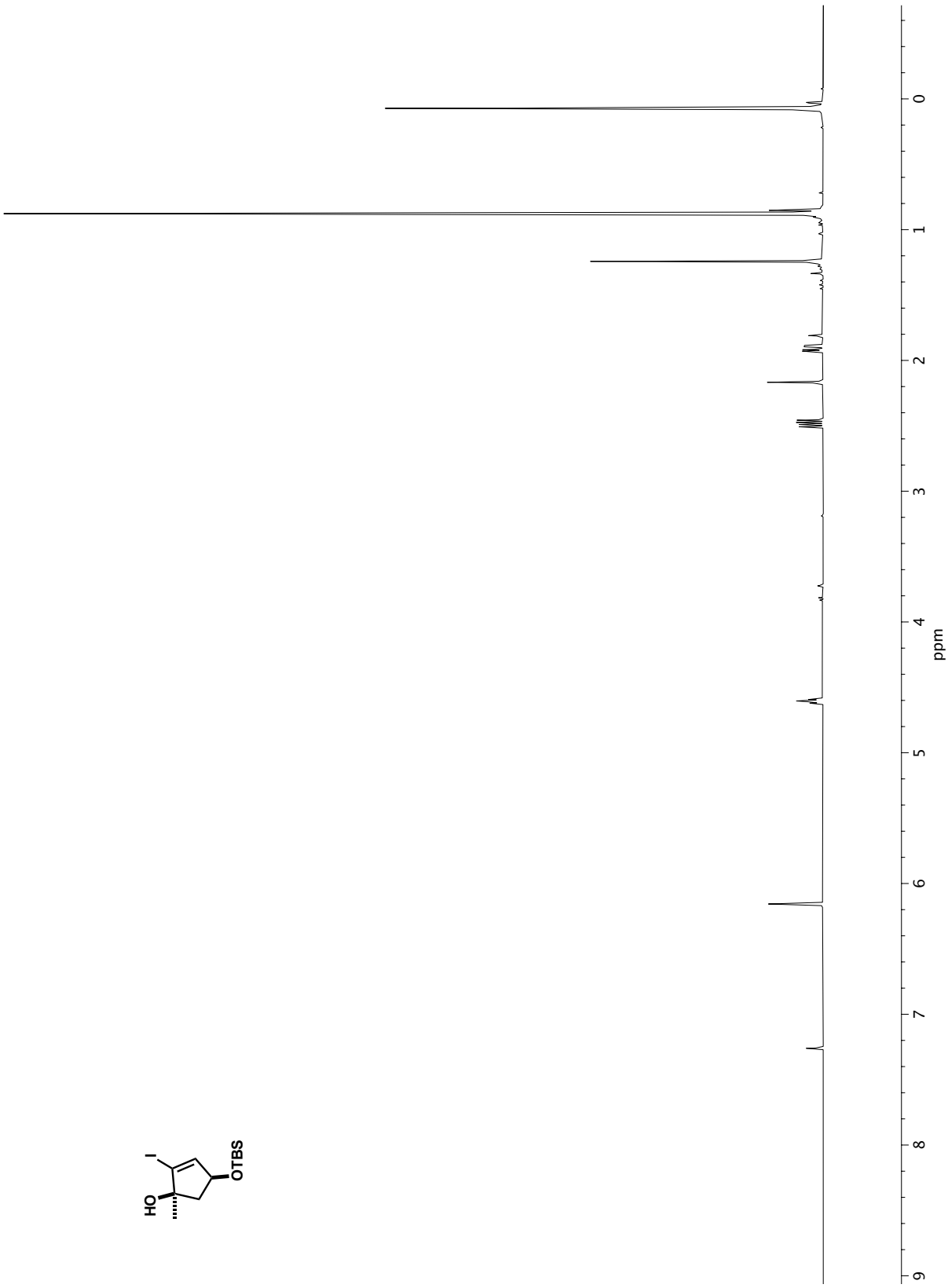


Figure A1.22. ^{1}H NMR (400 MHz, $CDCl_3$) of compound **26**.

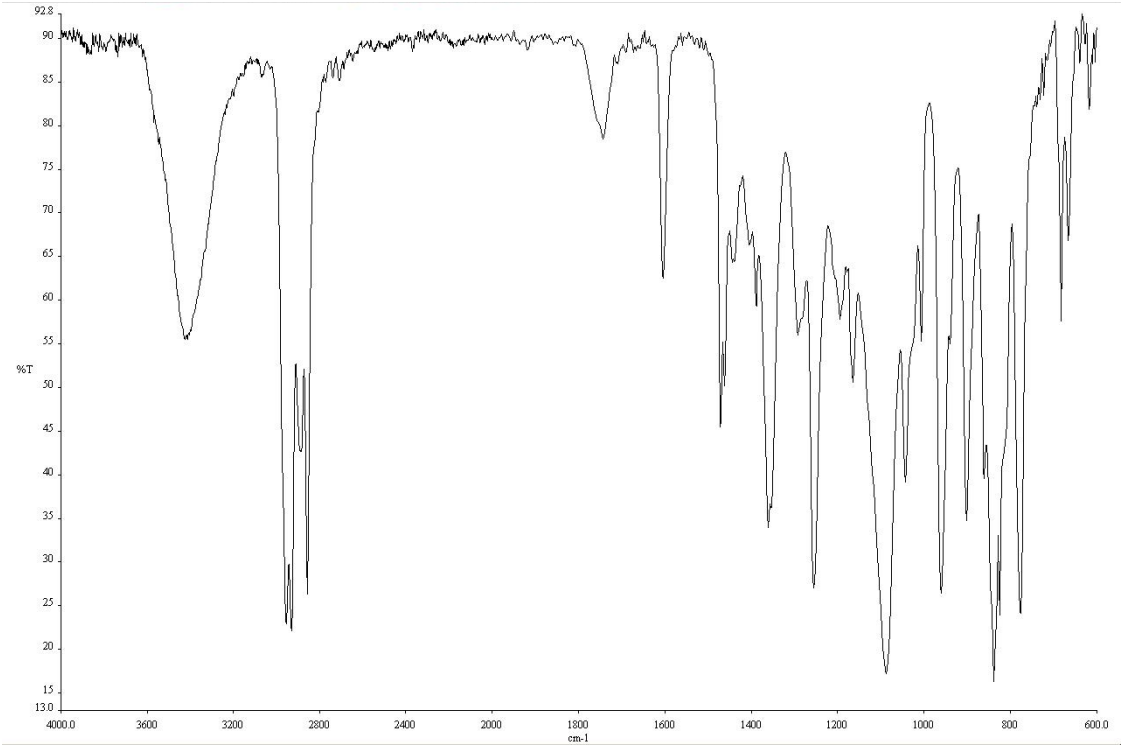


Figure A1.23. Infrared spectrum (Thin Film, NaCl) of compound **26**.

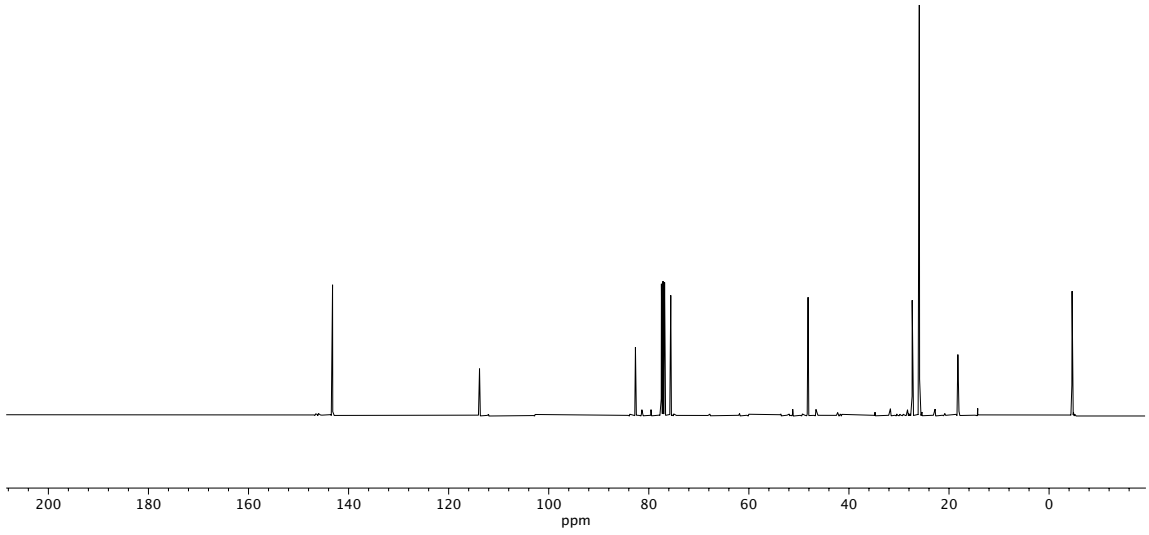


Figure A1.24. ^{13}C NMR (100 MHz, $CDCl_3$) of compound **26**.

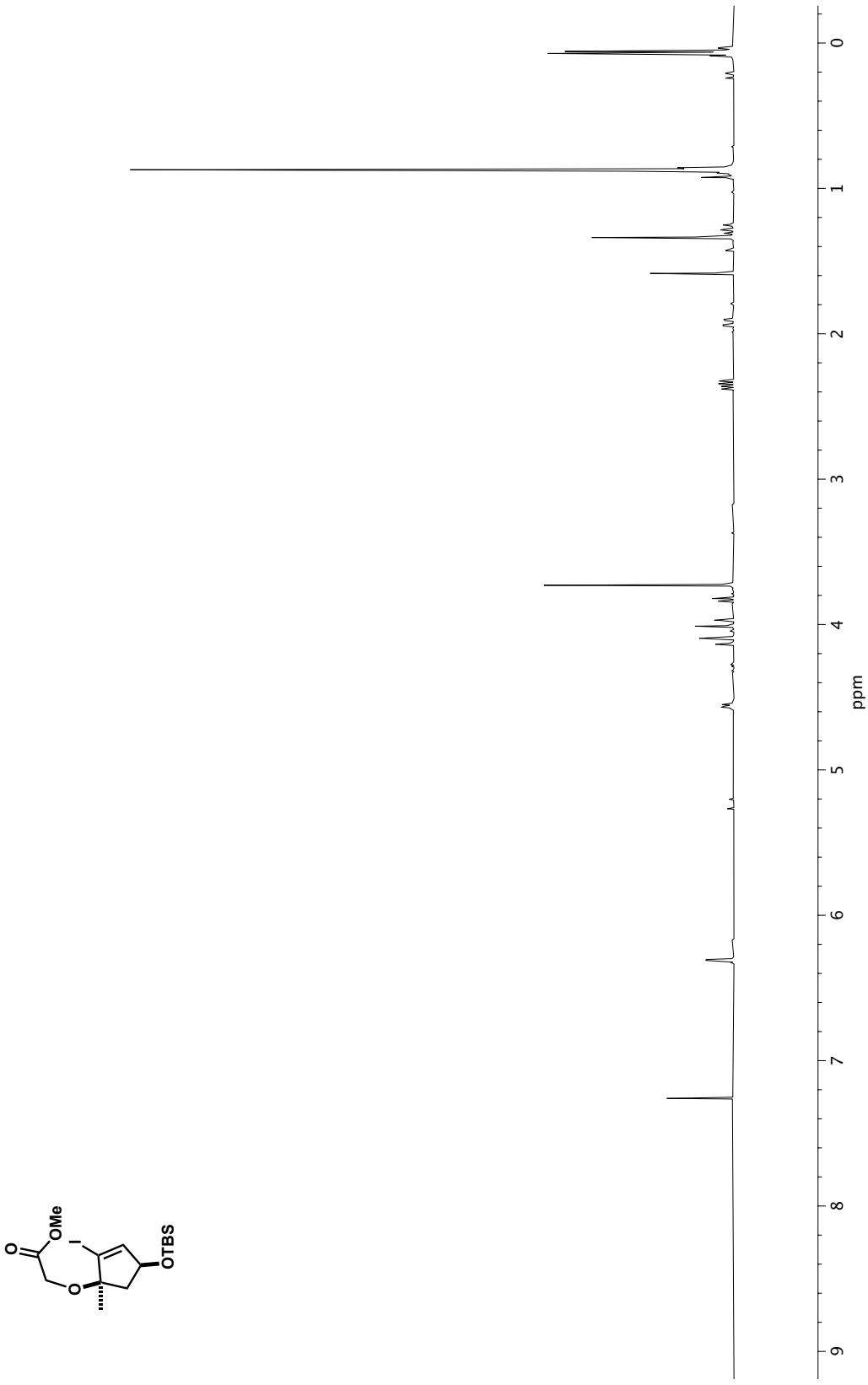


Figure A1.25. ^{1}H NMR (400 MHz, $CDCl_3$) of compound **27**.

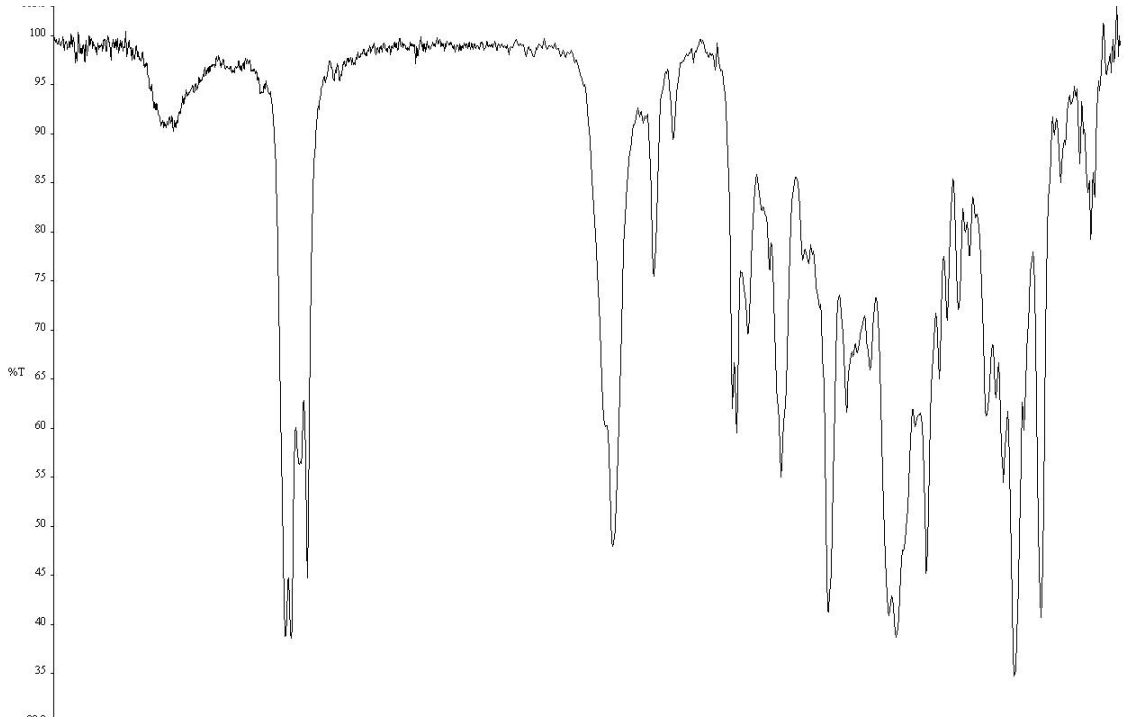


Figure A1.26. Infrared spectrum (Thin Film, NaCl) of compound **27**.

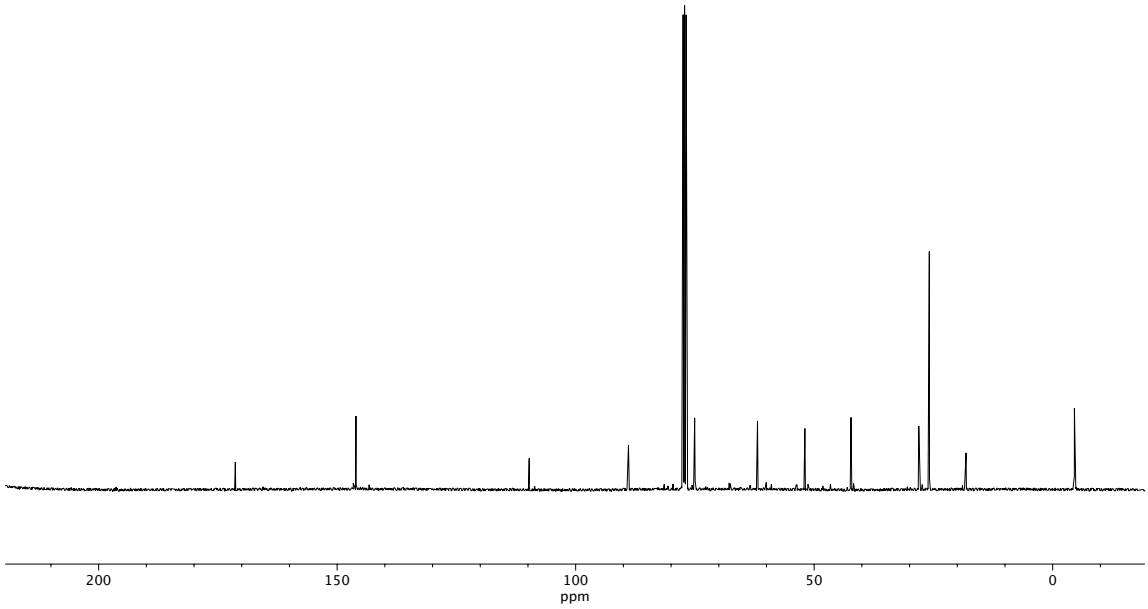


Figure A1.27. ^{13}C NMR (100 MHz, $CDCl_3$) of compound **27**.

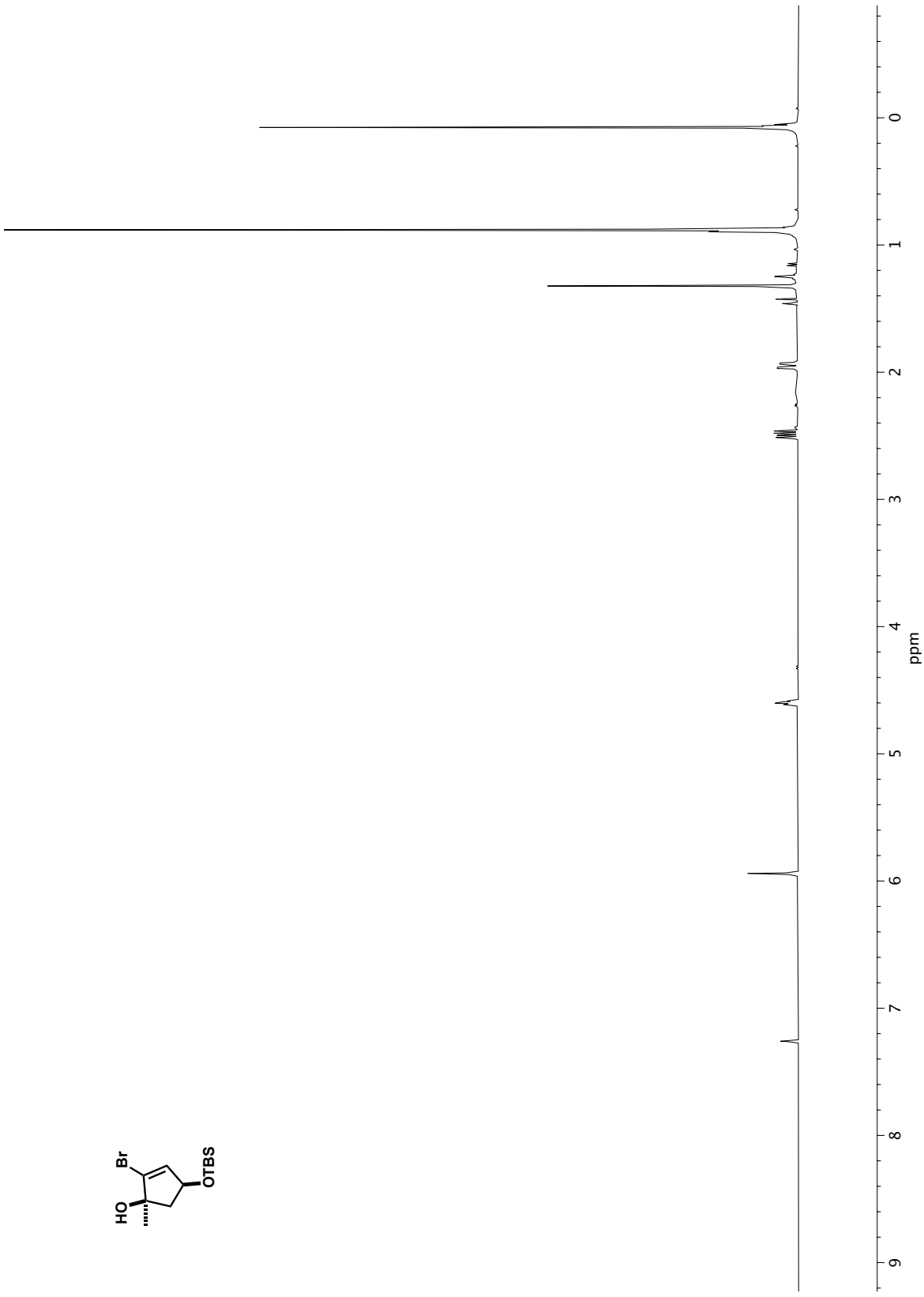


Figure A1.28. ^{1}H NMR (400 MHz, $CDCl_3$) of compound **41**.

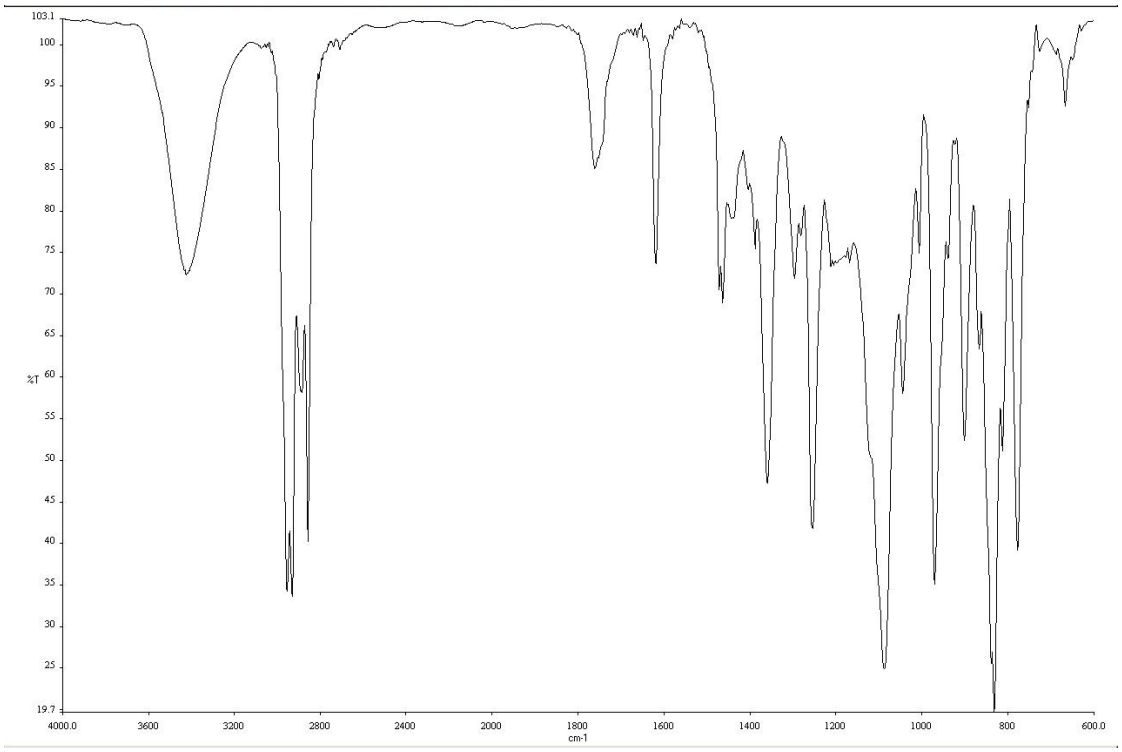


Figure A1.29. Infrared spectrum (Thin Film, NaCl) of compound **41**.

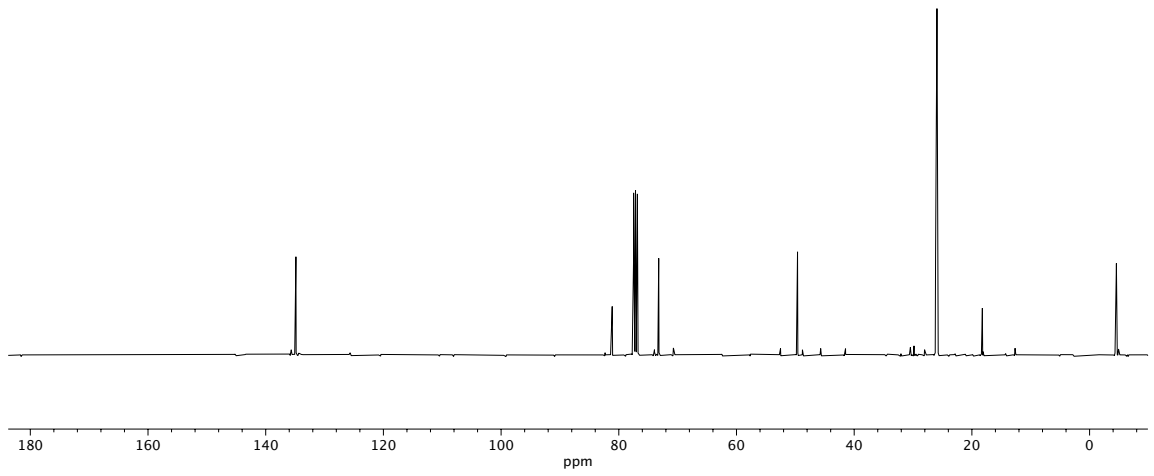


Figure A1.30. ^{13}C NMR (100 MHz, $CDCl_3$) of compound **41**.

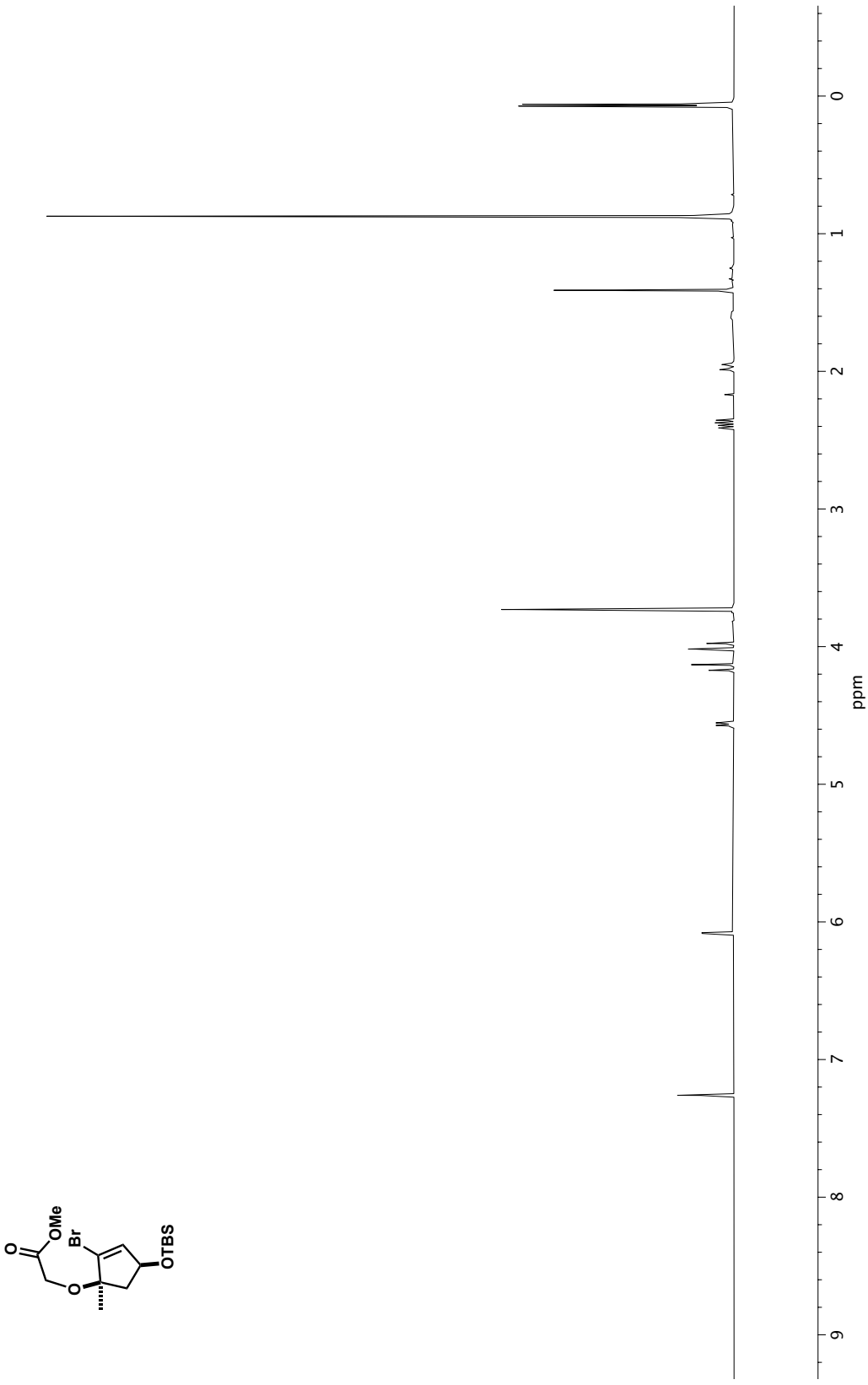


Figure A1.31. ^{1}H NMR (400 MHz, $CDCl_3$) of compound **42**.

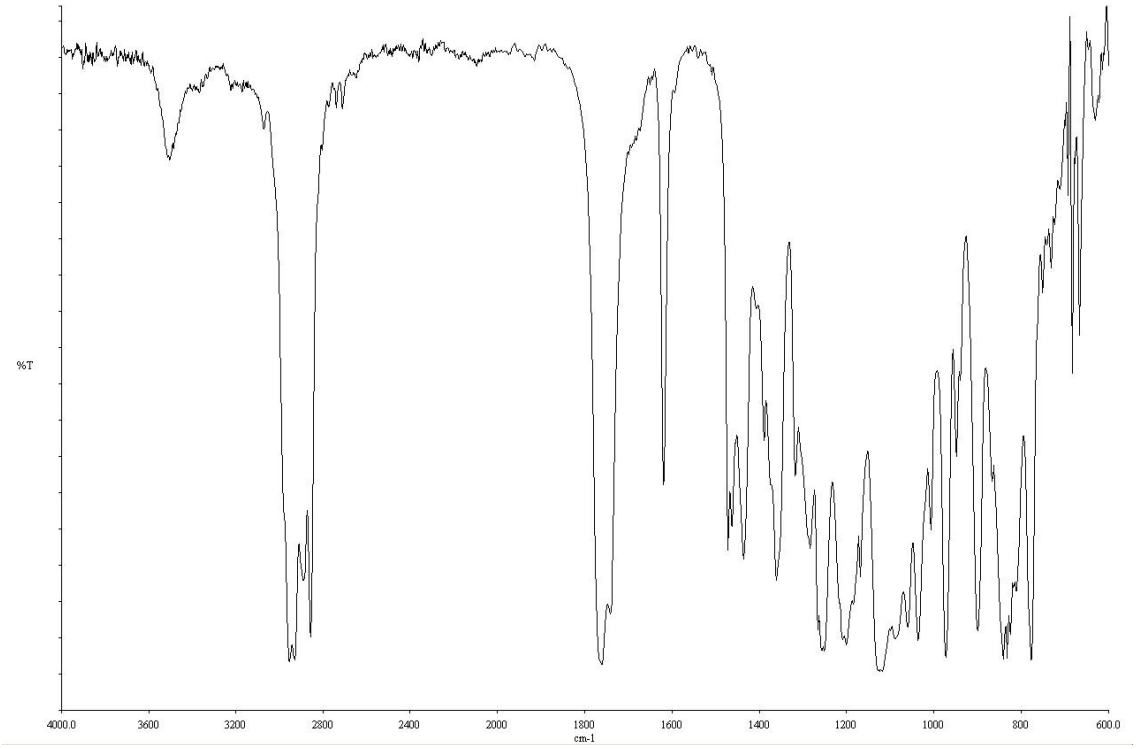


Figure A1.32. Infrared spectrum (Thin Film, NaCl) of compound **42**.

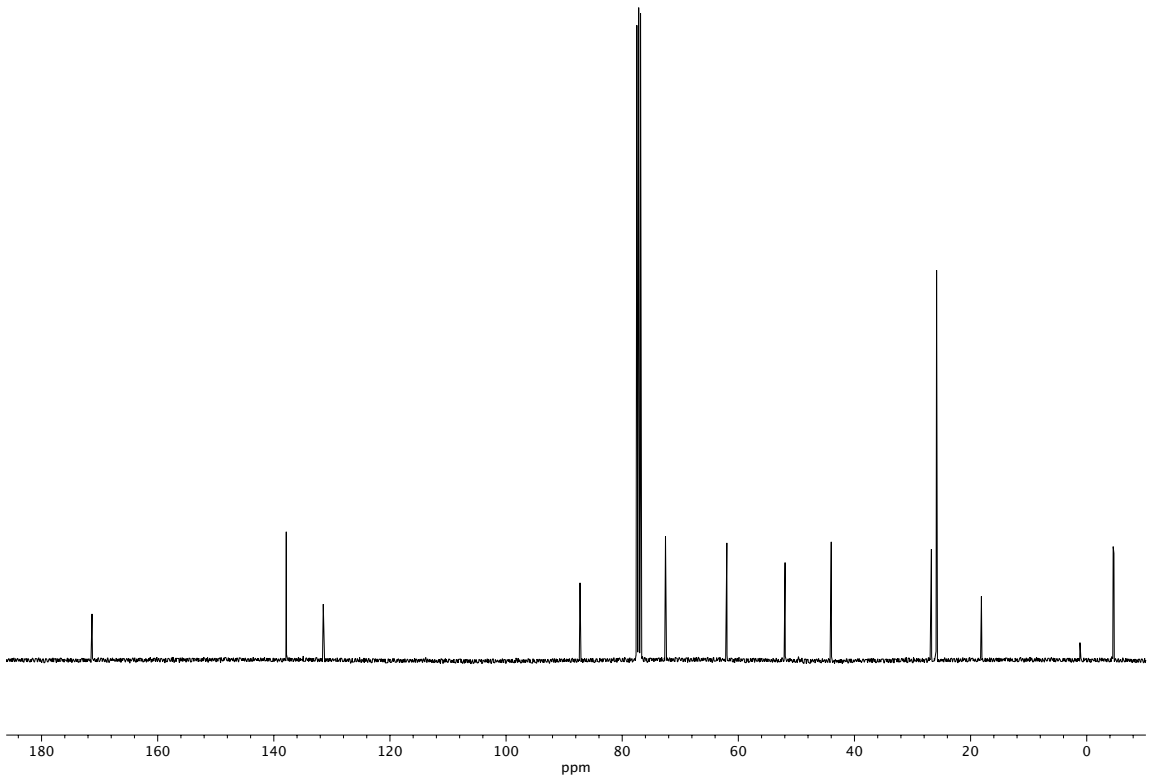


Figure A1.33. ^{13}C NMR (100 MHz, $CDCl_3$) of compound **42**.

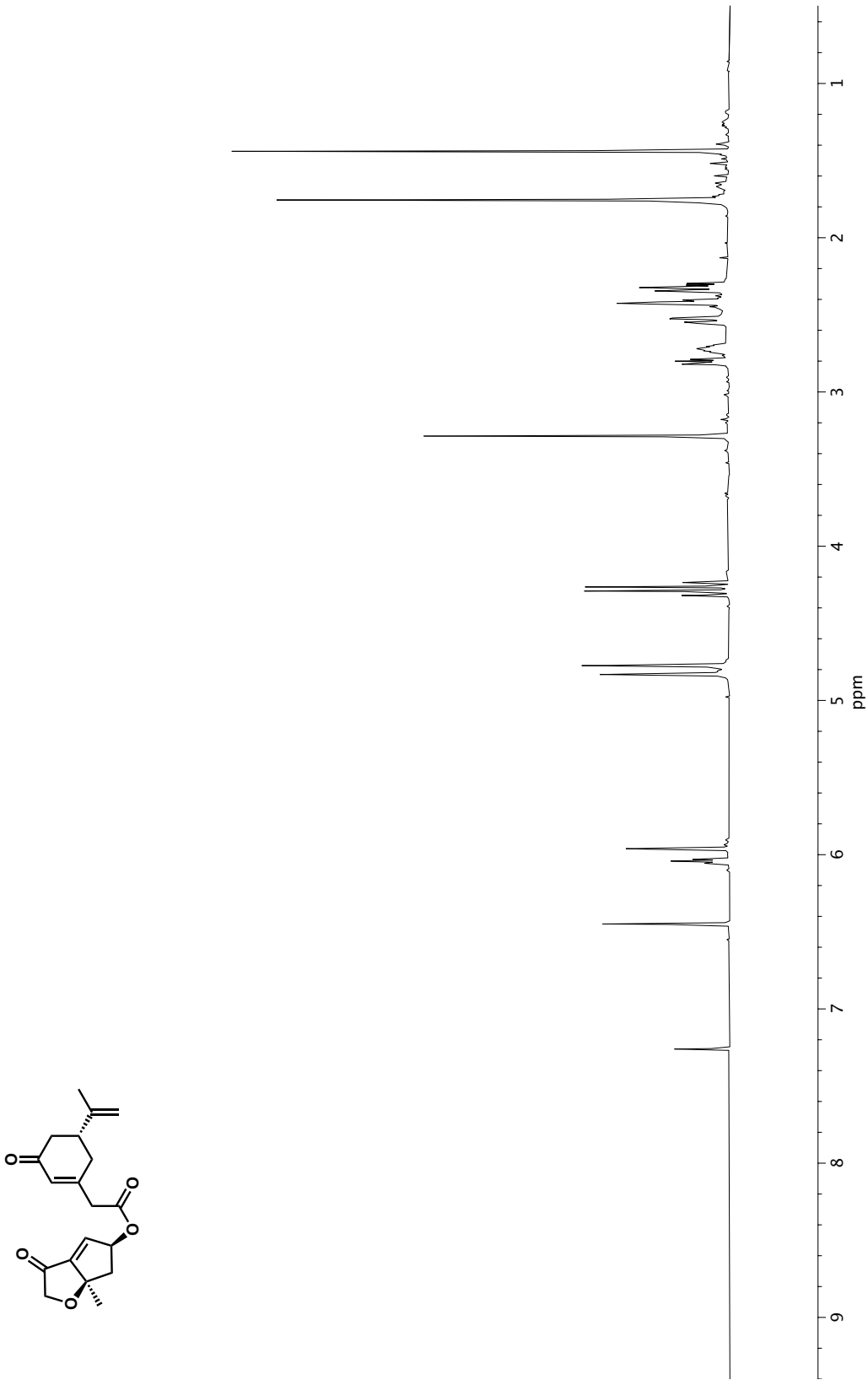


Figure A1.34. ^{1}H NMR (600 MHz, $CDCl_3$) of compound **15**.

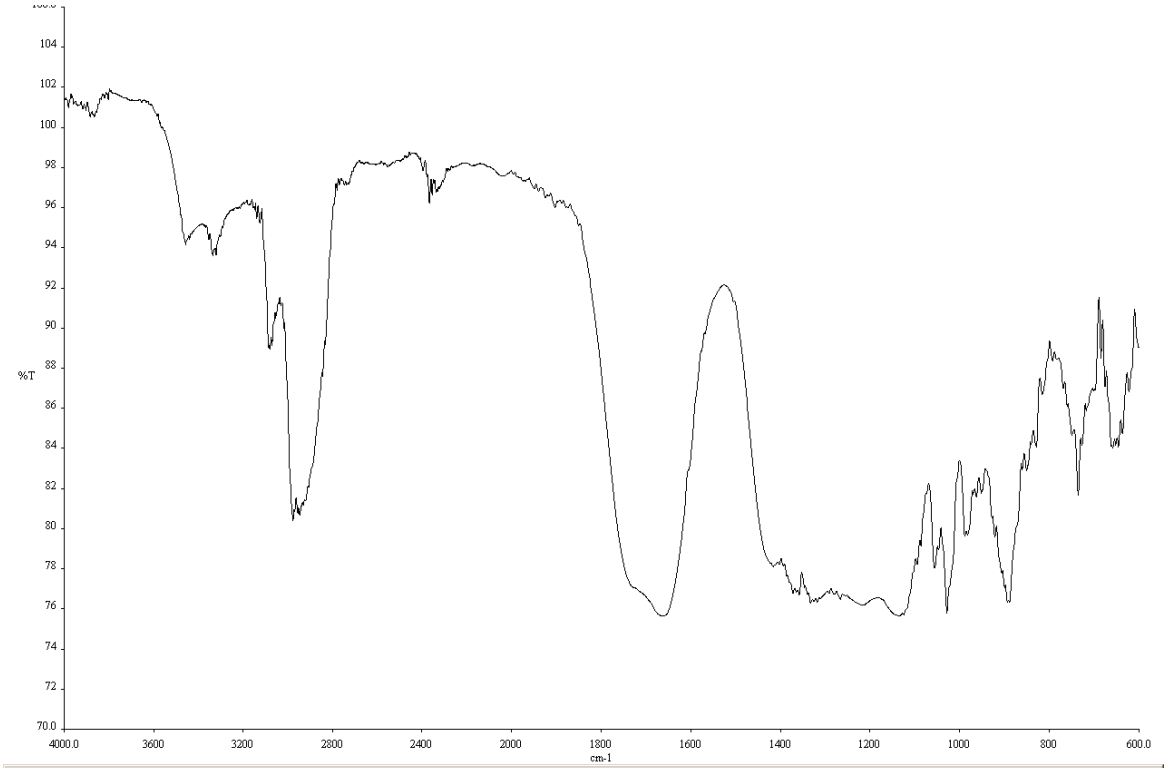


Figure A1.35. Infrared spectrum (Thin Film, NaCl) of compound **15**.

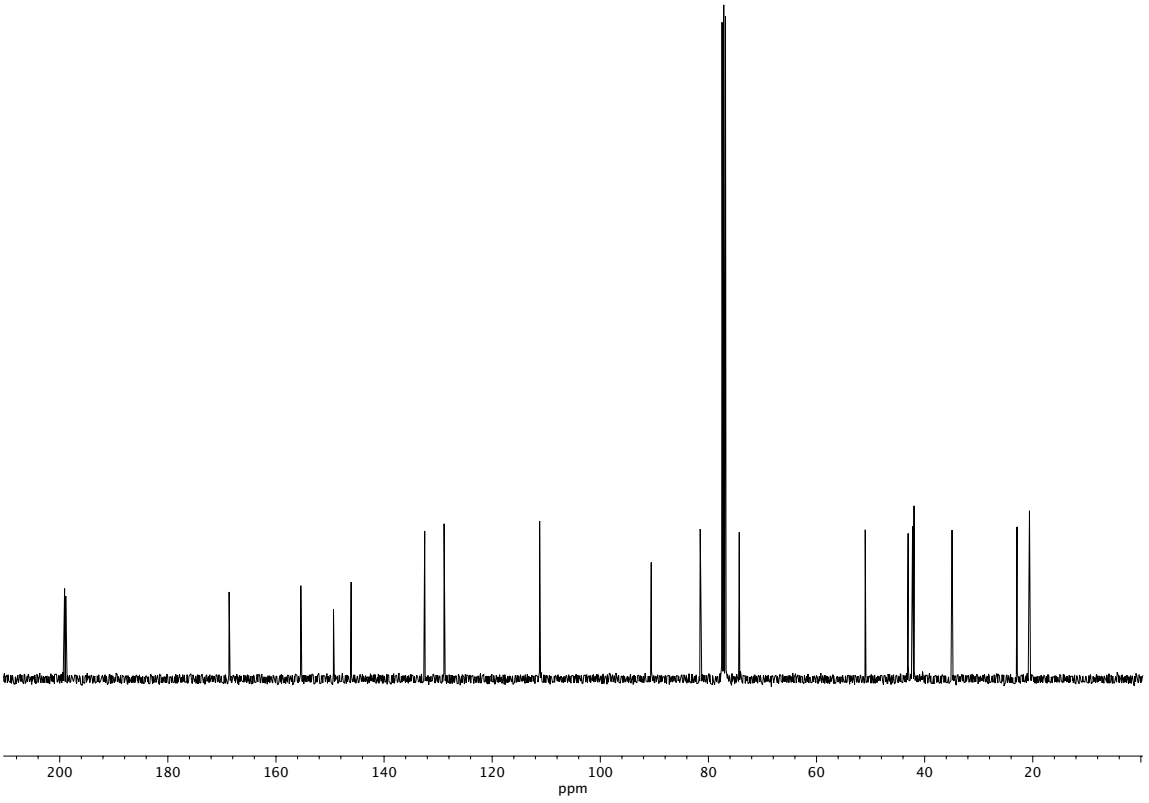


Figure A1.36. ^{13}C NMR (100 MHz, $CDCl_3$) of compound **15**.

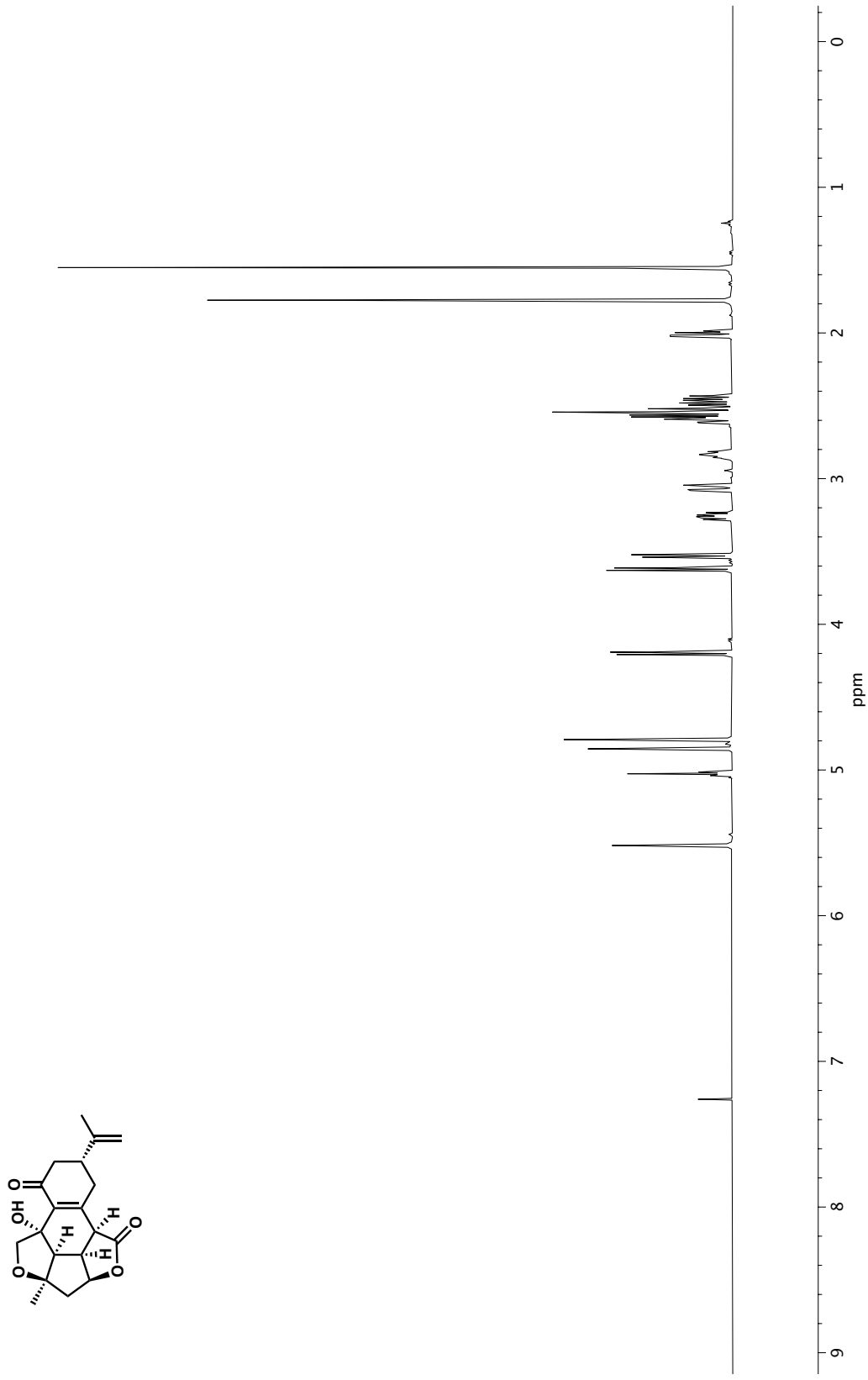


Figure A1.37. ^{1}H NMR (600 MHz, $CDCl_3$) of compound **31**.

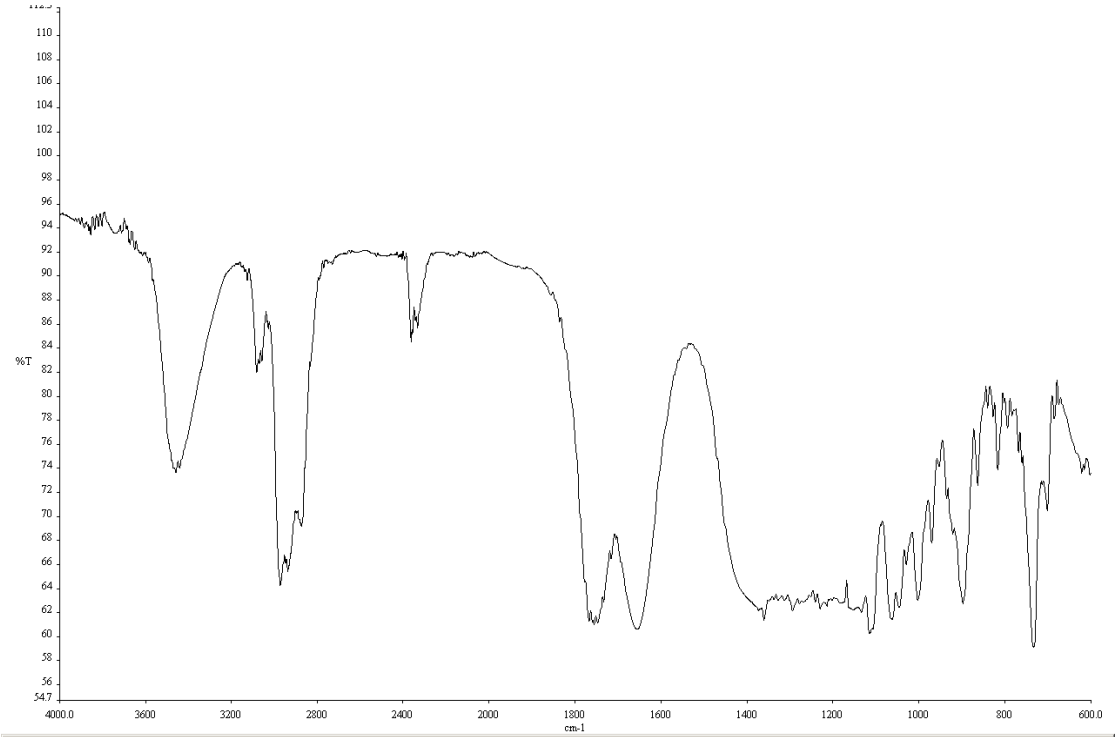


Figure A1.38. Infrared spectrum (Thin Film, NaCl) of compound **31**.

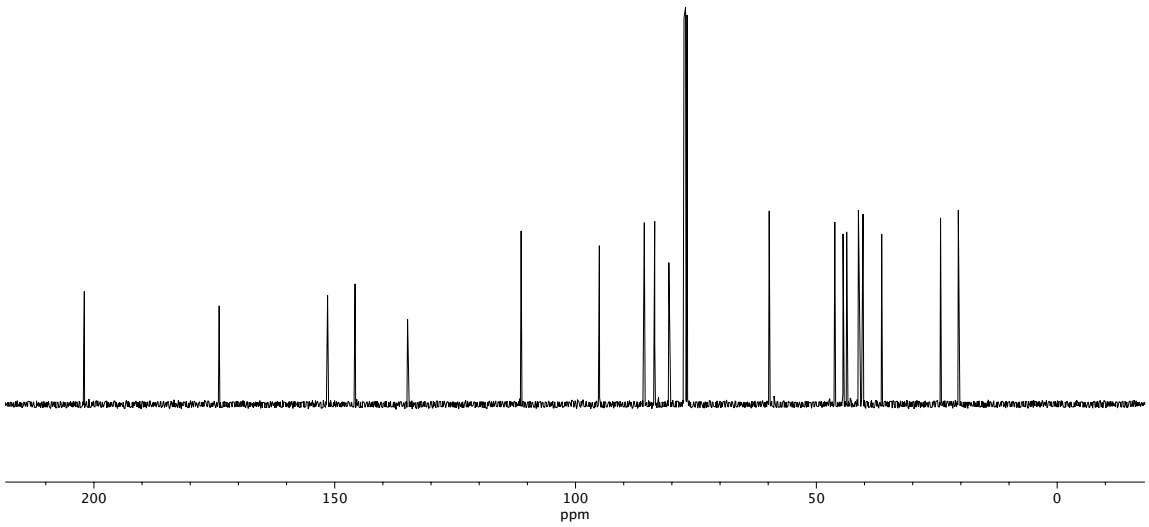


Figure A1.39. ^{13}C NMR (100 MHz, $CDCl_3$) of compound **31**.

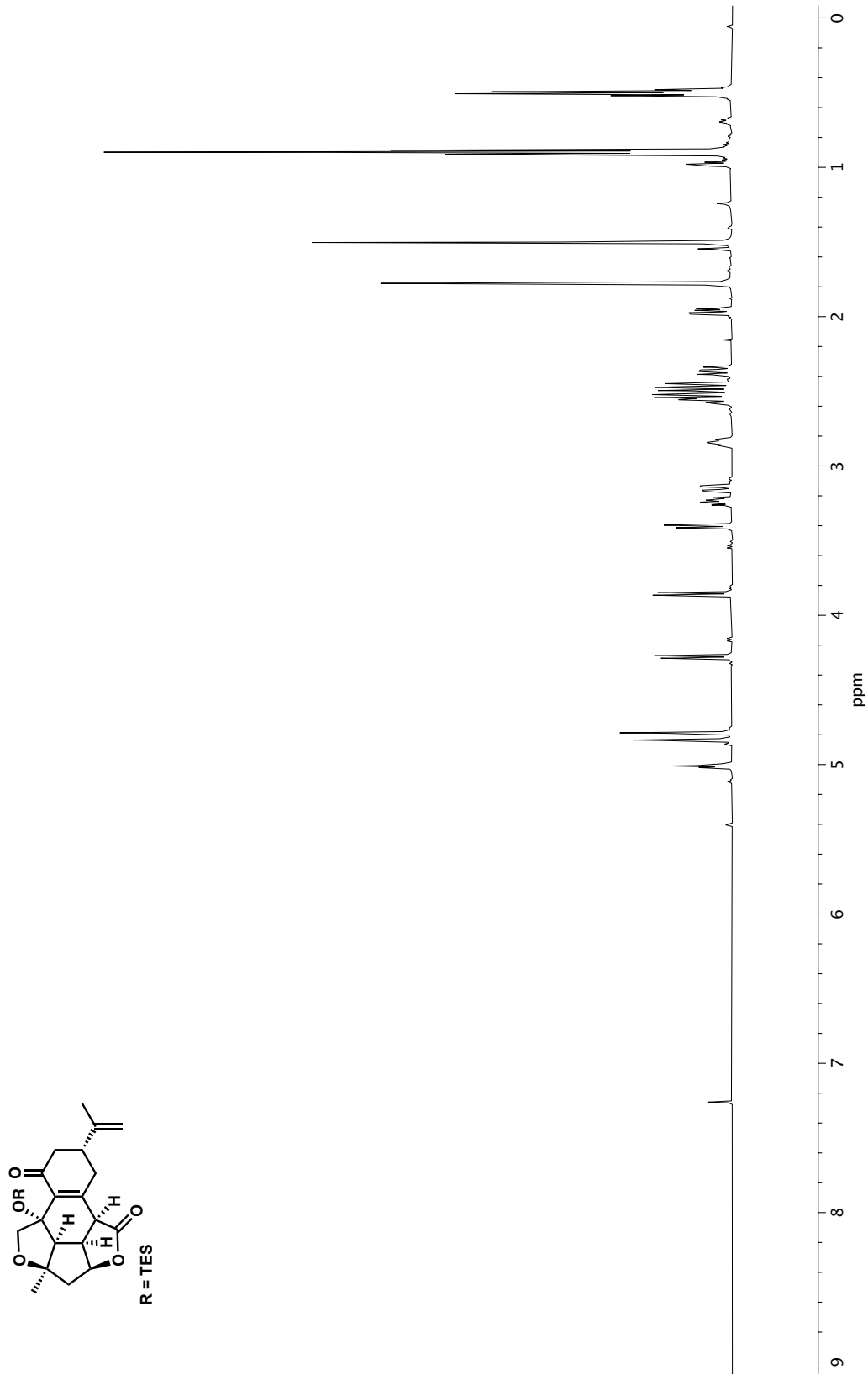


Figure A1.40. ^{1}H NMR (600 MHz, $CDCl_3$) of compound **43**.

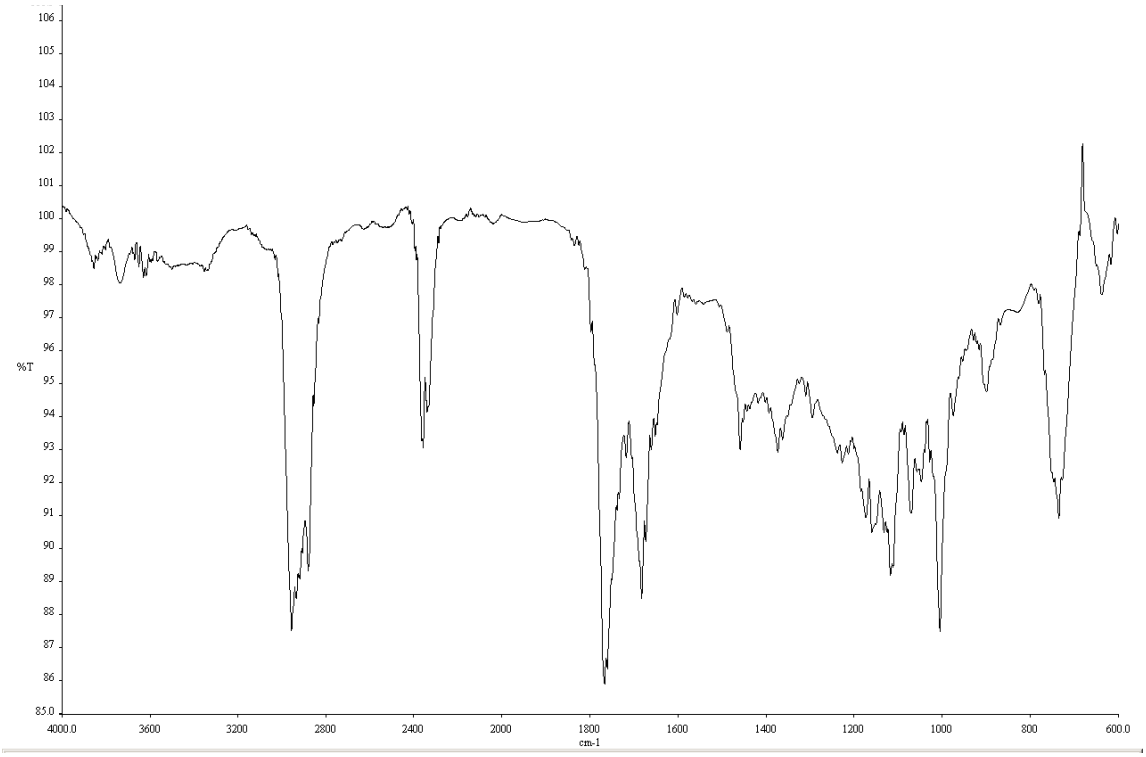


Figure A1.41. Infrared spectrum (Thin Film, NaCl) of compound **43**.

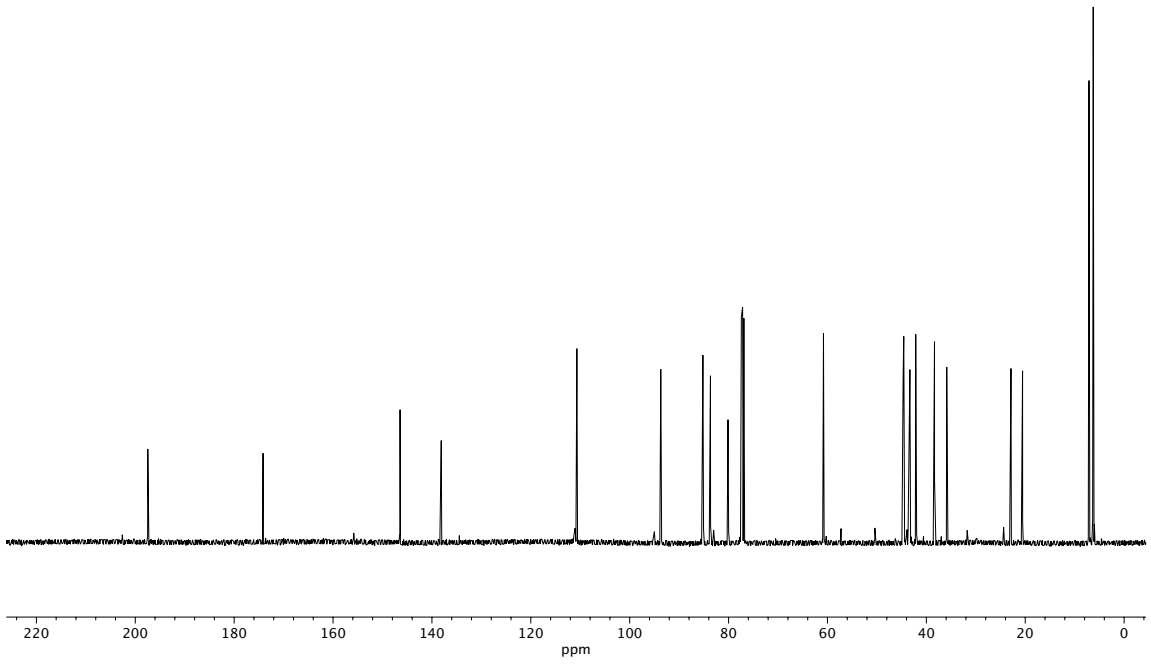


Figure A1.42. ^{13}C NMR (125 MHz, $CDCl_3$) of compound **43**.

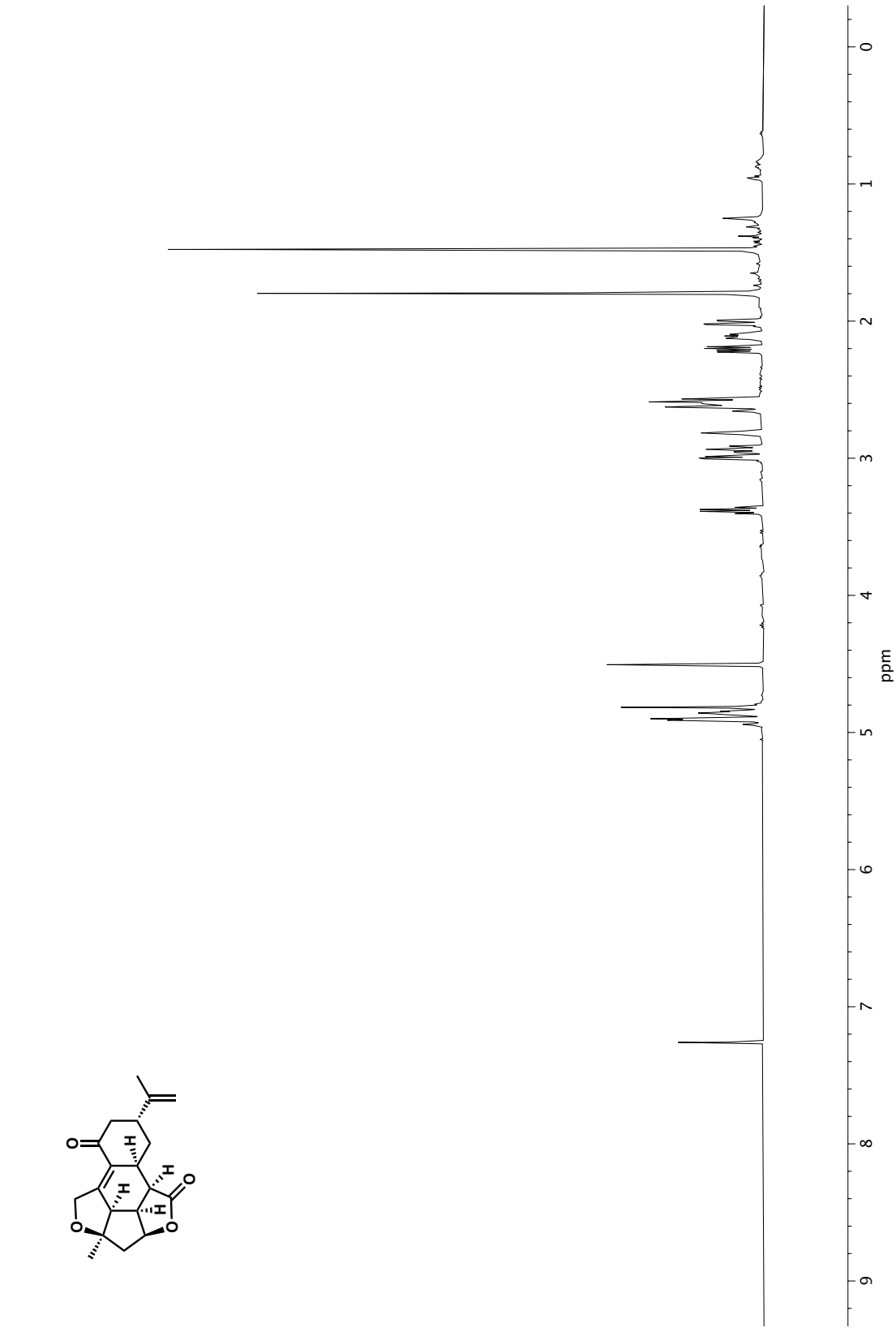


Figure A1.43. ^{1}H NMR (600 MHz, $CDCl_3$) of compound **32**.

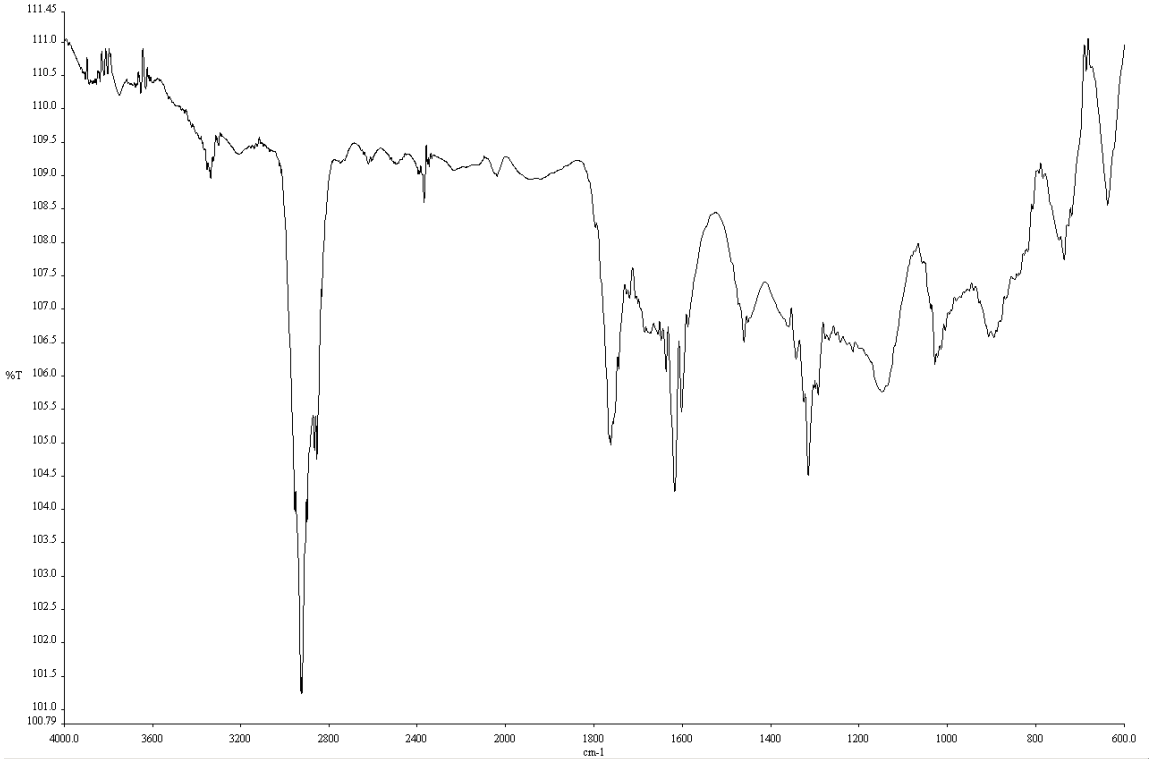


Figure A1.44. Infrared spectrum (Thin Film, NaCl) of compound **32**.

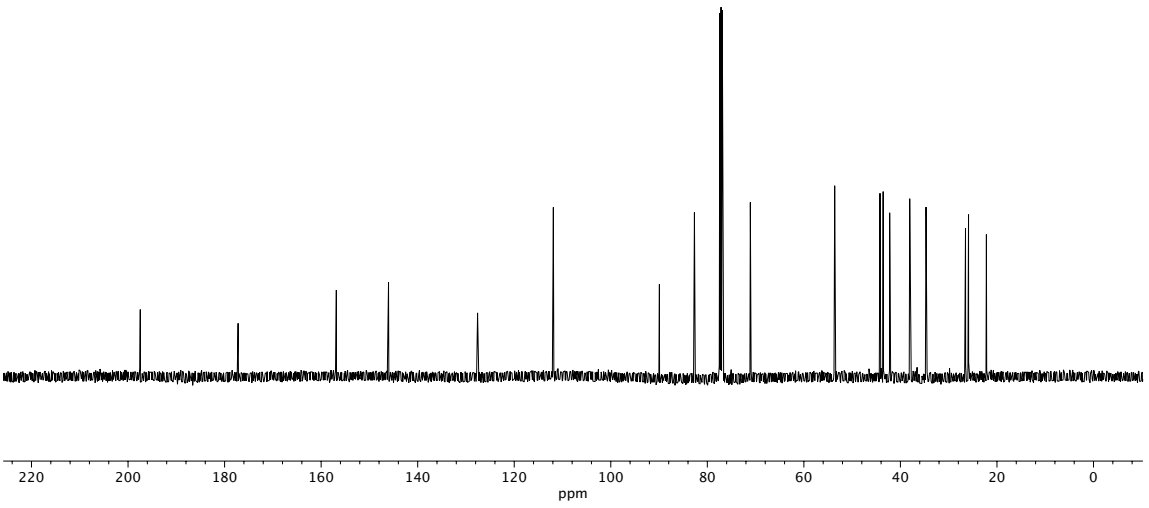


Figure A1.45. ^{13}C NMR (125 MHz, $CDCl_3$) of compound **32**.

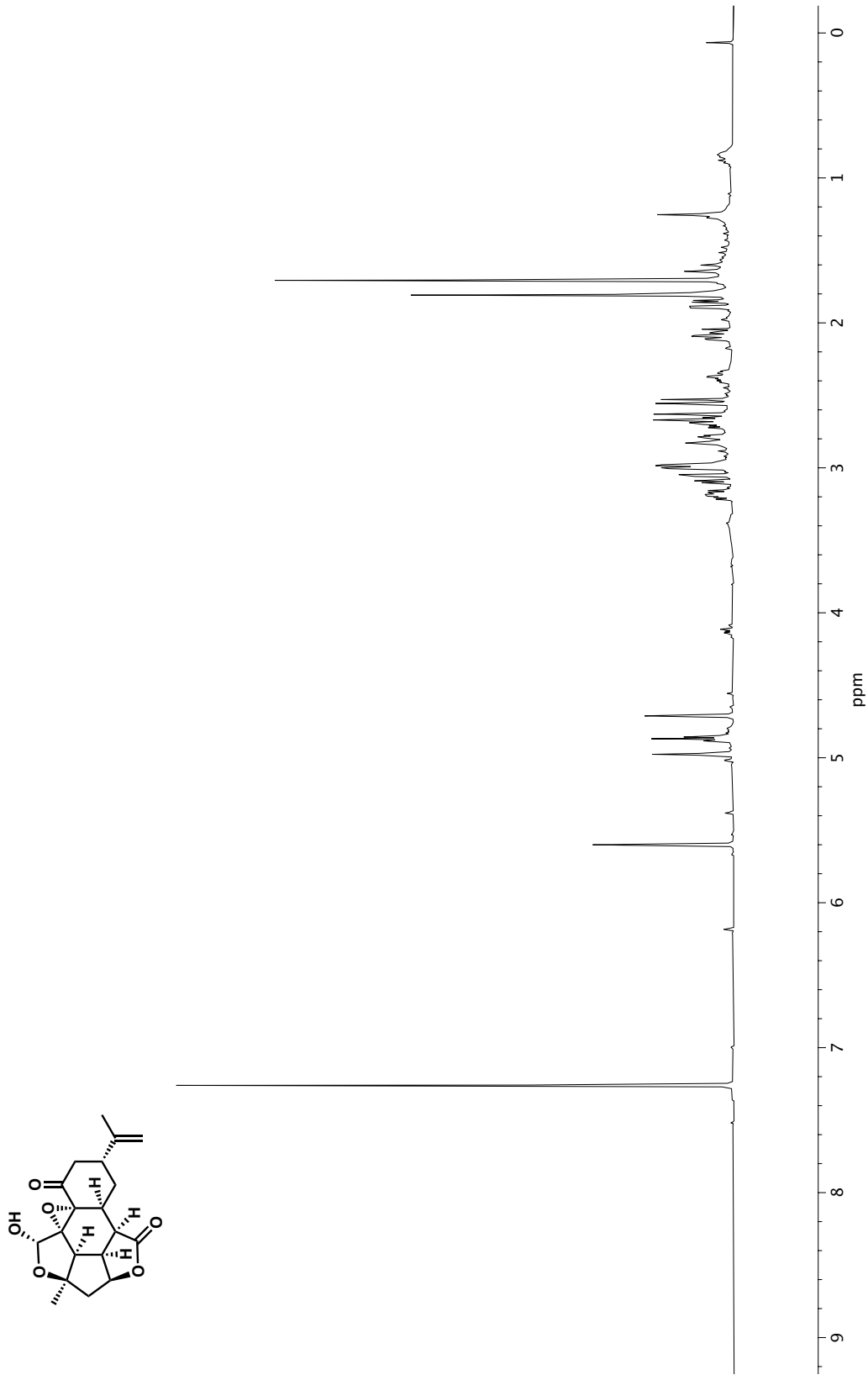


Figure A1.46. ^{1}H NMR (400 MHz, $CDCl_3$) of compound **33**.

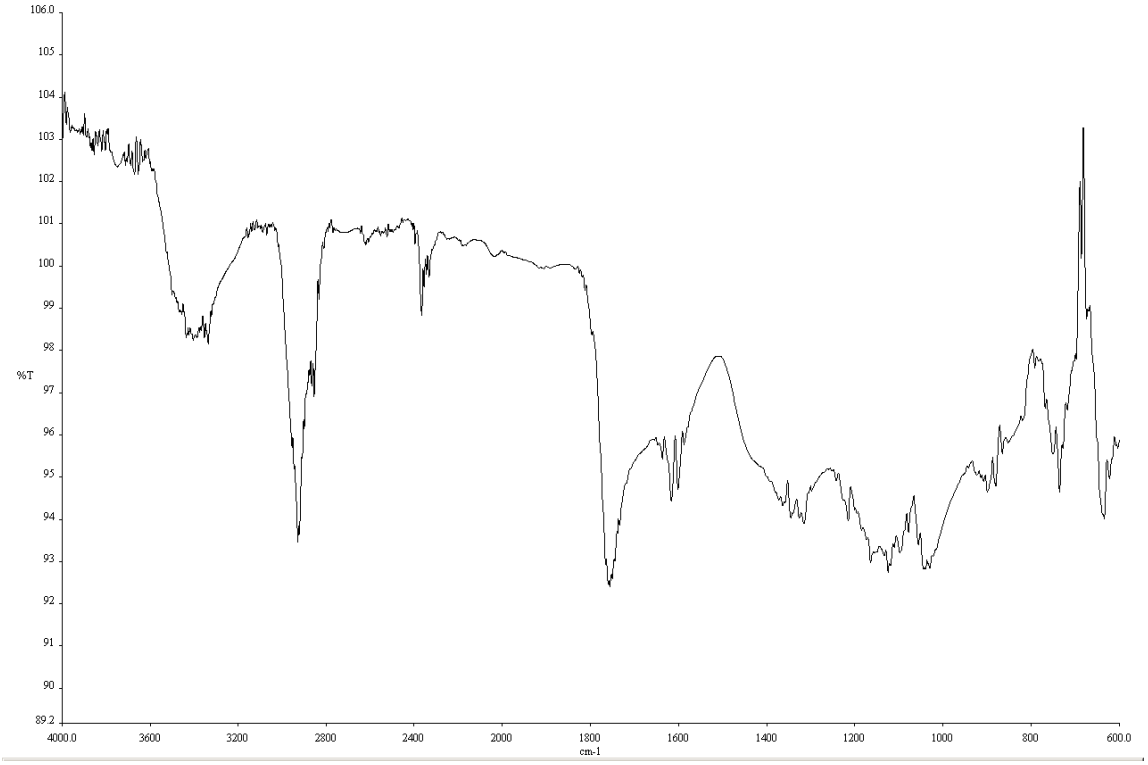


Figure A1.47. Infrared spectrum (Thin Film, NaCl) of compound **33**.

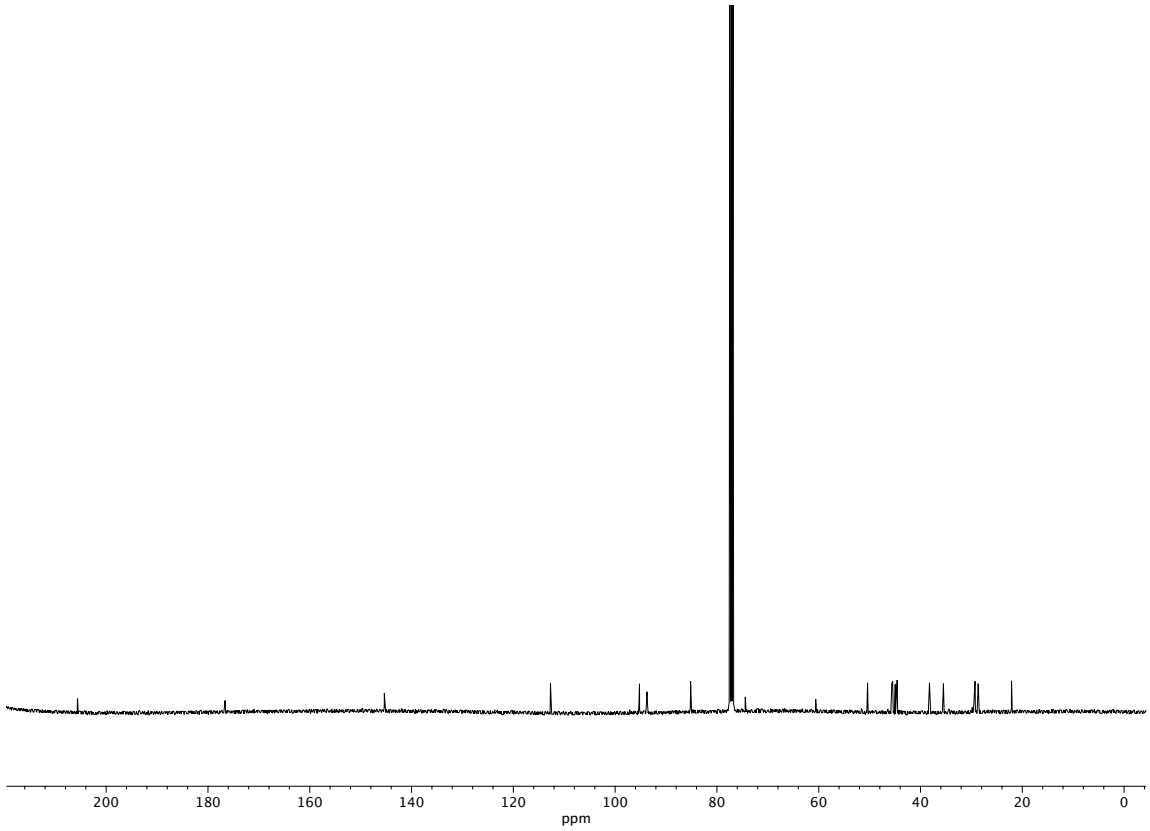


Figure A1.48. ^{13}C NMR (100 MHz, $CDCl_3$) of compound **33**.

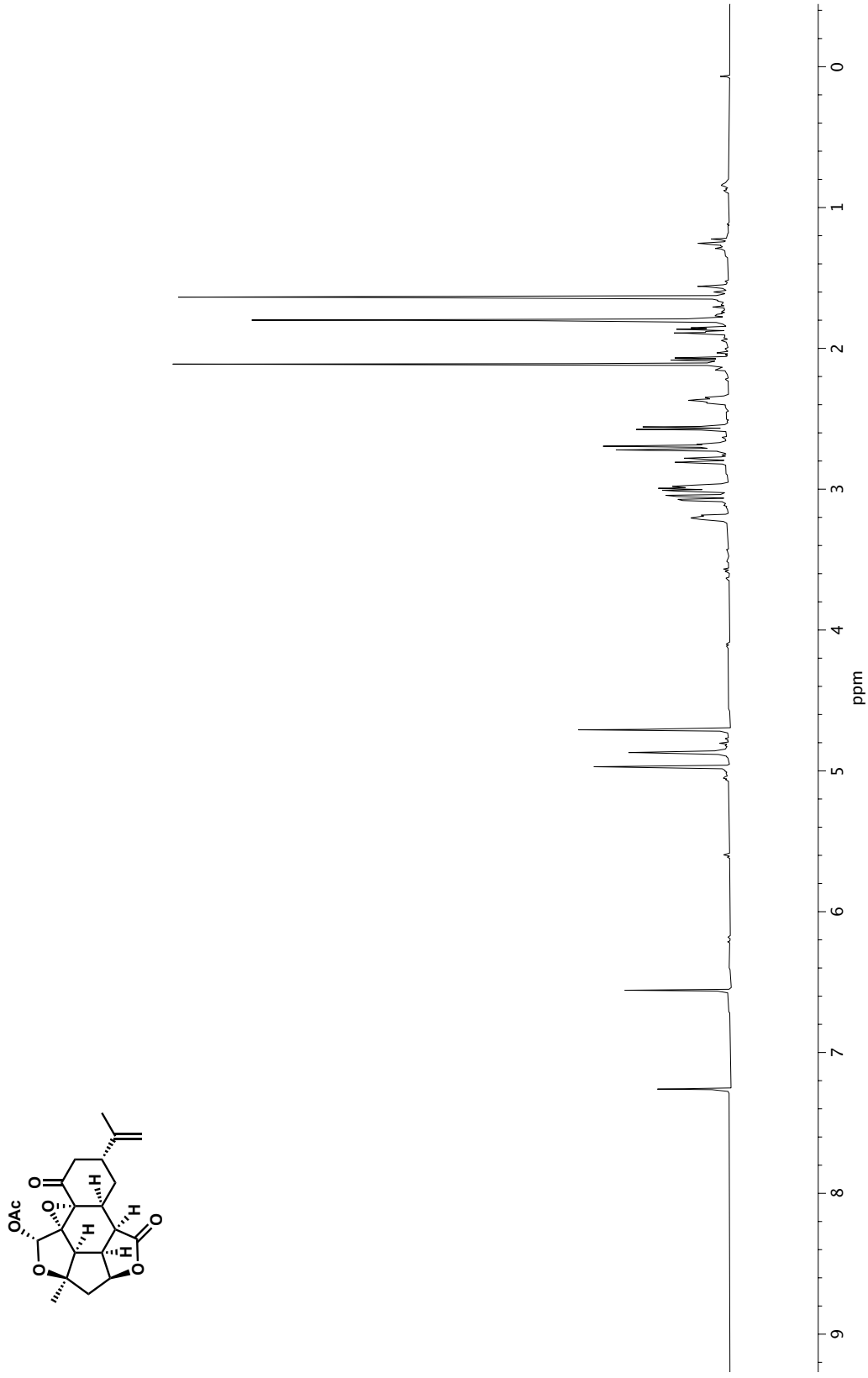


Figure A1.49. ^{1}H NMR (600 MHz, $CDCl_3$) of compound **34**.

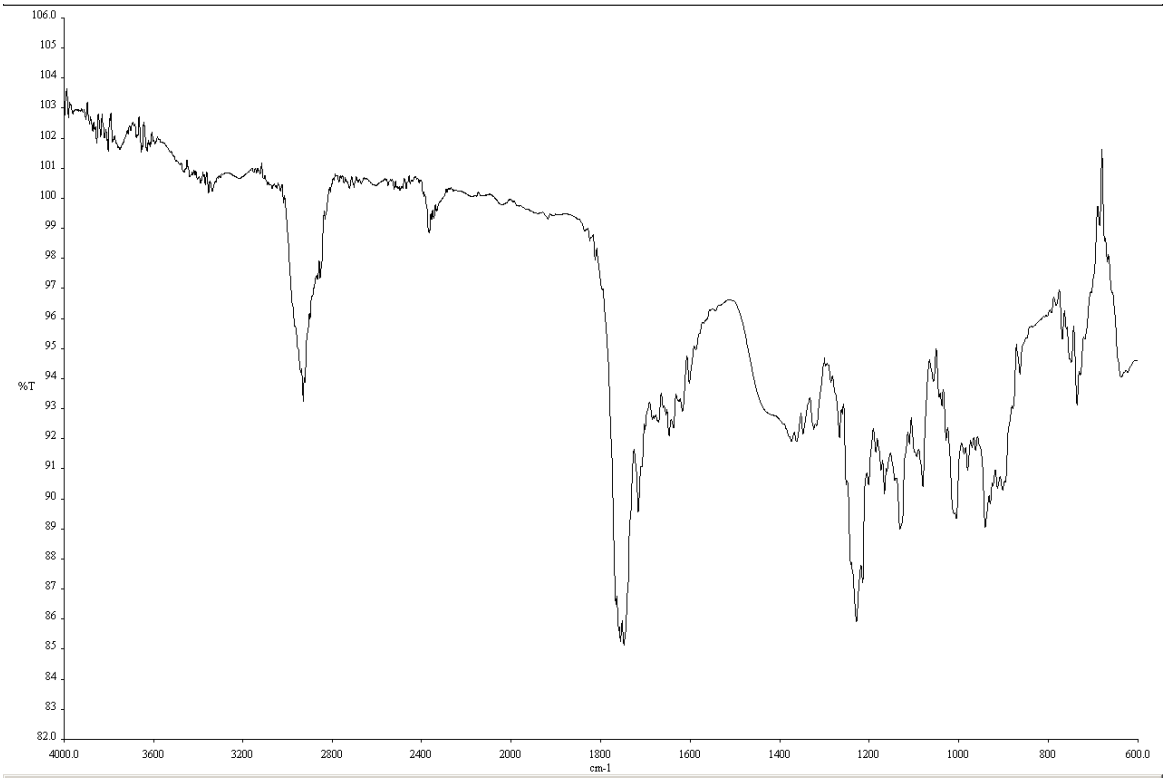


Figure A1.50. Infrared spectrum (Thin Film, NaCl) of compound **34**.

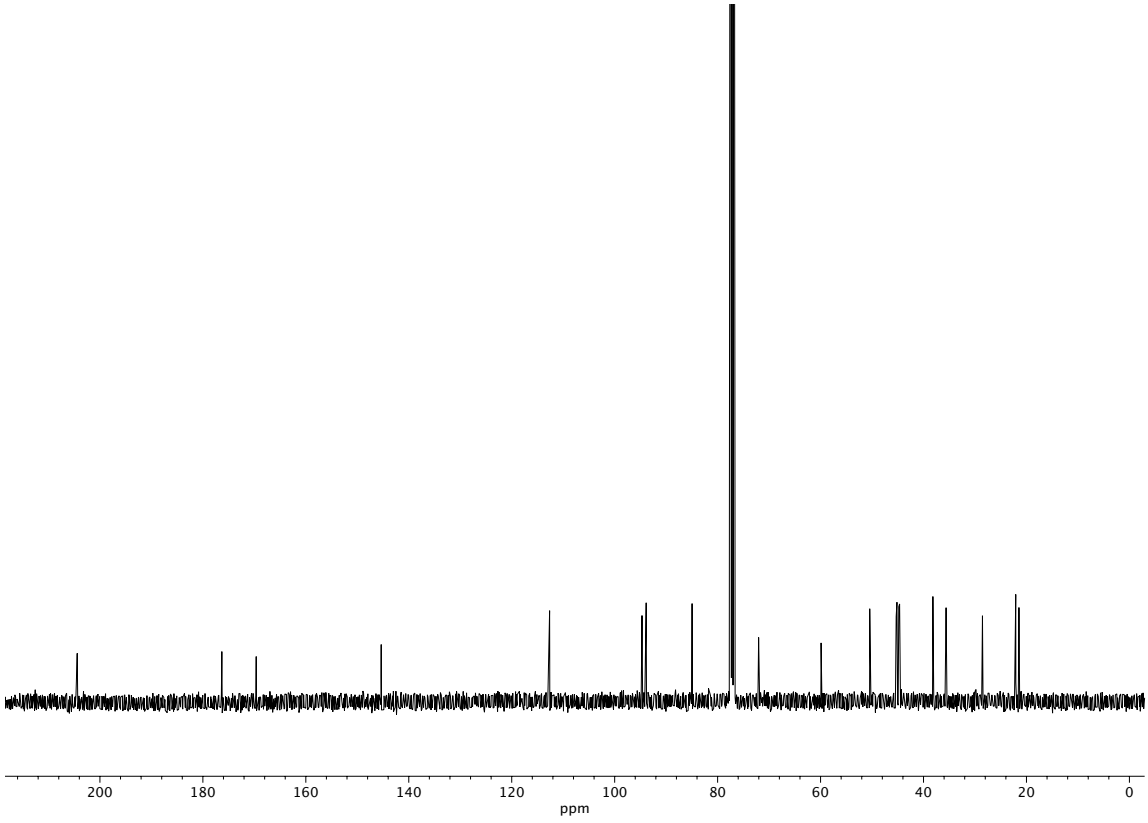


Figure A1.51. ^{13}C NMR (100 MHz, $CDCl_3$) of compound **34**.

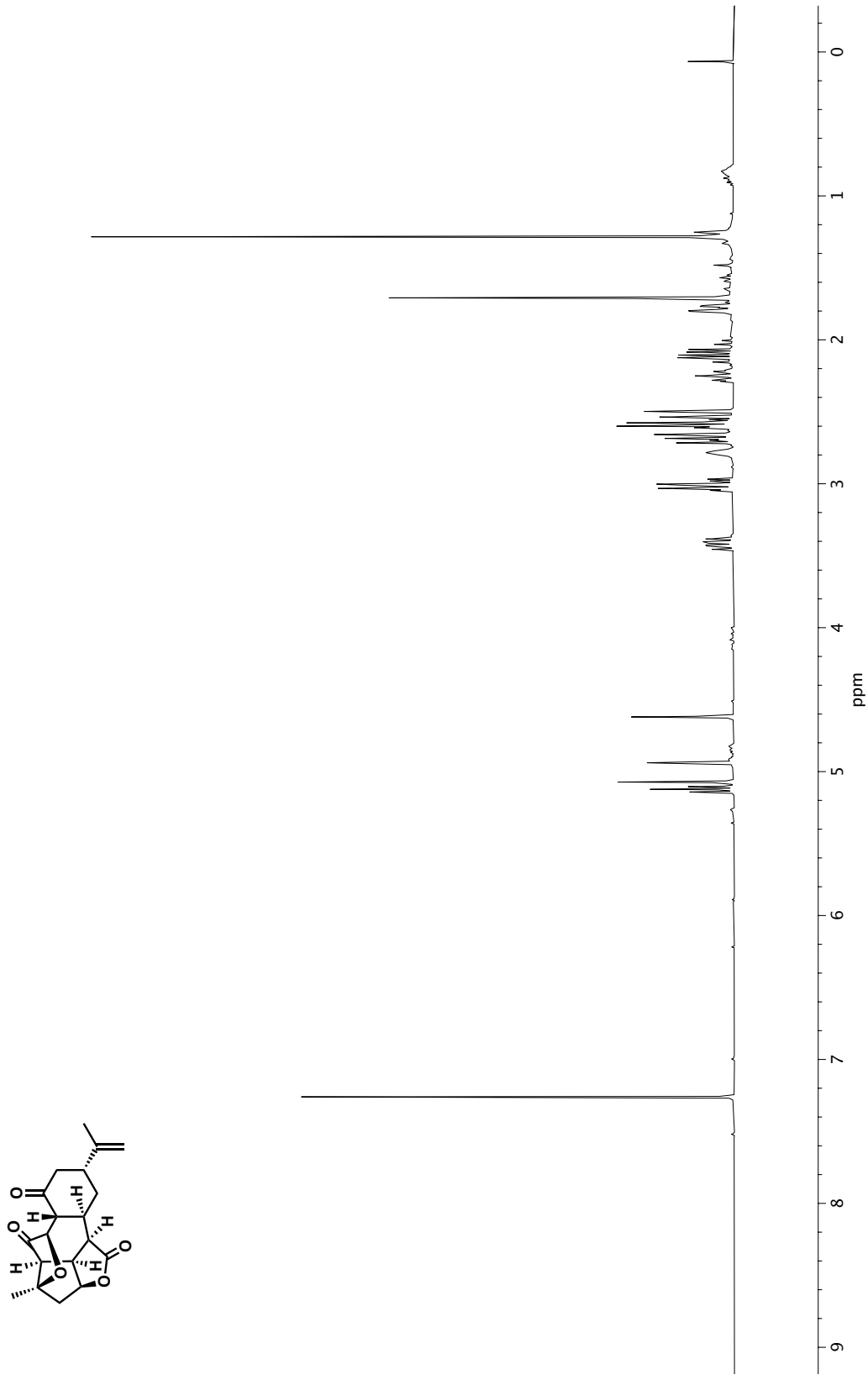


Figure A1.52. ^{1}H NMR (400 MHz, $CDCl_3$) of compound **1**.

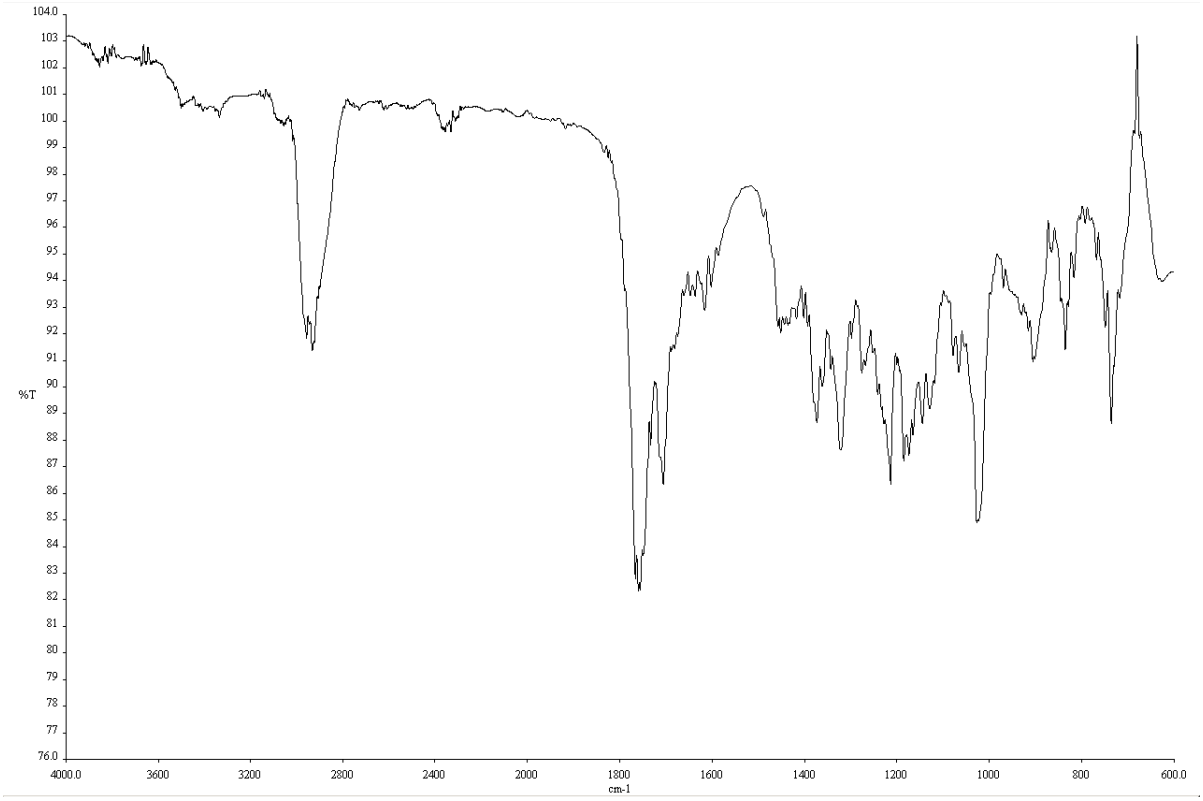


Figure A1.53. Infrared spectrum (Thin Film, NaCl) of compound **1**.

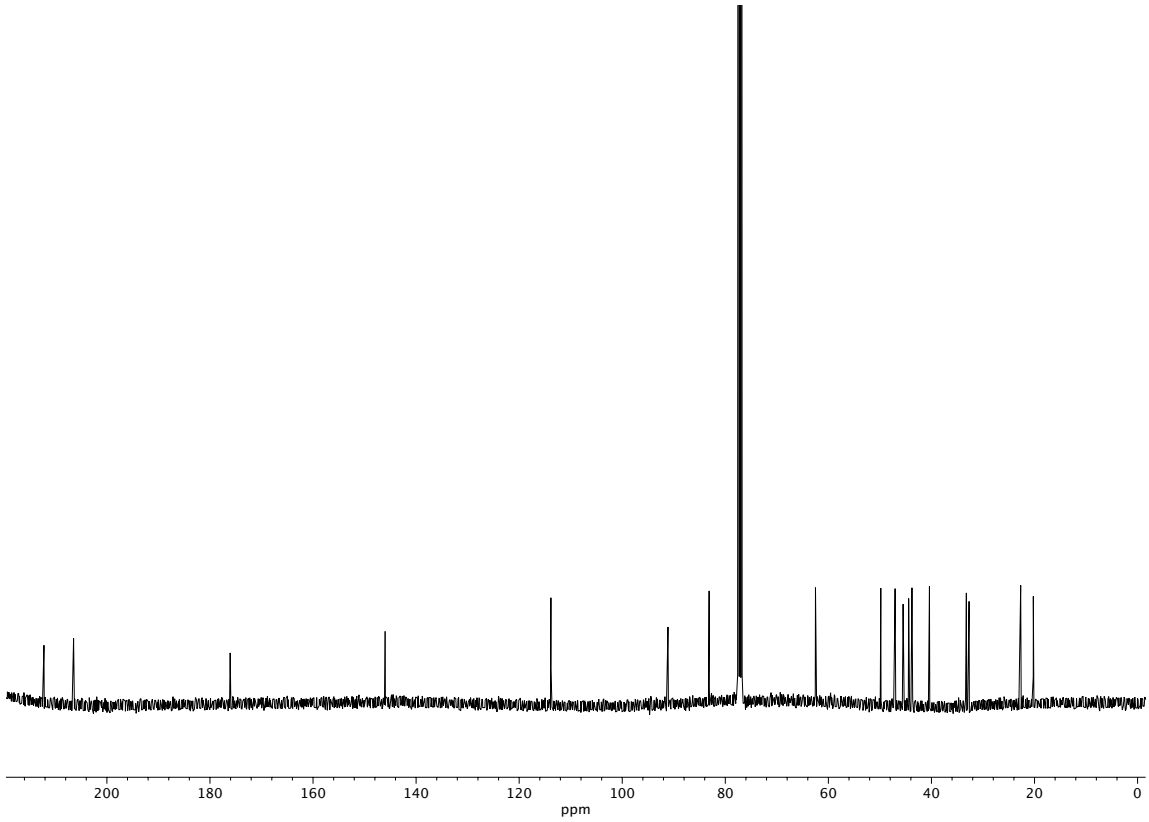


Figure A1.54. ^{13}C NMR (100 MHz, $CDCl_3$) of compound **1**.

APPENDIX 2

X-Ray Crystallography Reports Relevant to Chapter 1:

The Total Synthesis of Ineleganolide

A2.1 GENERAL EXPERIMENTAL INFORMATION

Low-temperature diffraction data (ϕ-and ω-scans) were collected a Bruker AXS D8 VENTURE KAPPA diffractometer coupled to a PHOTON II CPAD detector with Cu *K*a radiation (l = 1.54178 Å) from an IμS micro-source. The structure was solved by direct methods using SHELXS and refined against F^2 on all data by full-matrix least squares with SHELXL-2019 using established refinement techniques. All non-hydrogen atoms were refined anisotropically. All hydrogen atoms were included into the model at geometrically calculated positions and refined using a riding model. The isotropic displacement parameters of all hydrogen atoms were fixed to 1.2 times the *U* value of the atoms they are linked to (1.5 times for methyl groups).

A2.2 X-RAY CRYSTAL STRUCTURE OF COMPOUND 31

Figure A2.2.1 *X-ray crystal structure of compound* ***31***.

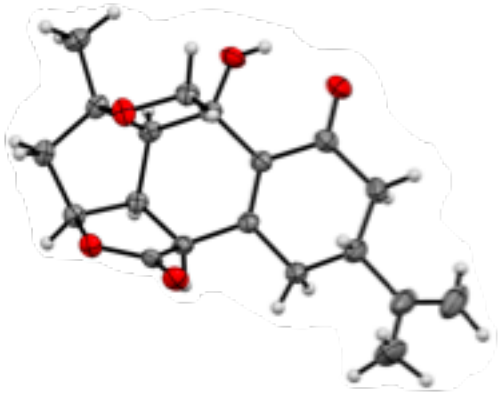


Table A2.2.2 *Crystal data and structure refinement for compound* ***31***.

Empirical formula	$C_{38}H_{44}O_{10}$
Formula weight	660.73
Temperature	100(2) K
Wavelength	1.54178 Å
Crystal system	Monoclinic

Space group	$P2_1$	
Unit cell dimensions	a = 5.4379(6) Å	a= 90°.
	b = 20.759(2) Å	b= 93.475(6)°.
	c = 14.7956(10) Å	g = 90°.
Volume	1667.2(3) $Å^3$	
Z	2	
Density (calculated)	1.316 Mg/m^3	
Absorption coefficient	0.778 mm^{-1}	
F(000)	704	
Crystal size	0.200 x 0.100 x 0.050 mm^3	
Theta range for data collection	2.992 to 74.571°.	
Index ranges	-6<=h<=6, -25<=k<=25, -18<=l<=18	
Reflections collected	30860	
Independent reflections	6591 [R(int) = 0.0626]	
Completeness to theta = 67.679°	98.8 %	
Absorption correction	Semi-empirical from equivalents	
Max. and min. transmission	0.7538 and 0.5987	
Refinement method	Full-matrix least-squares on F^2	
Data / restraints / parameters	6591 / 123 / 472	
Goodness-of-fit on F^2	1.043	
Final R indices [I>2sigma(I)]	R1 = 0.0388, wR2 = 0.0957	
R indices (all data)	R1 = 0.0462, wR2 = 0.0984	
Absolute structure parameter	0.12(13)	
Extinction coefficient	n/a	
Largest diff. peak and hole	0.186 and -0.159 e.$Å^{-3}$	

Table A2.2.3 *Atomic coordinates (x 10^4) and equivalent isotropic displacement parameters ($Å^2$x 10^3) for compound* ***31****. U(eq) is defined as one third of the trace of the orthogonalized U^{ij} tensor.*

	x	y	z	U(eq)
O(1)	2700(3)	6720(1)	8394(1)	27(1)
C(1)	3494(5)	6439(1)	9236(2)	25(1)
C(2)	6328(5)	6329(1)	9210(2)	22(1)

O(4)	6584(5)	5571(1)	10834(2)	43(1)
C(3)	6938(5)	5612(1)	9244(2)	23(1)
C(4)	7106(6)	5292(2)	10141(2)	34(1)
O(5)	7629(4)	6666(1)	9937(1)	29(1)
C(5)	7989(9)	4600(2)	10171(2)	49(1)
C(6)	6818(8)	4217(2)	9379(2)	39(1)
C(16)	7455(9)	3504(2)	9376(3)	51(1)
C(17)	9389(9)	3264(2)	9859(3)	58(1)
C(18)	5771(12)	3102(2)	8797(3)	68(1)
C(7)	7501(6)	4538(1)	8501(2)	28(1)
C(8)	7088(5)	5255(1)	8494(2)	22(1)
C(9)	6734(5)	5546(1)	7575(2)	21(1)
C(10)	4061(5)	5489(1)	7203(2)	22(1)
O(2)	3443(4)	6002(1)	6691(1)	24(1)
O(3)	2636(4)	5057(1)	7311(1)	30(1)
C(11)	5399(5)	6489(1)	6739(2)	23(1)
C(12)	4431(5)	7127(1)	7064(2)	26(1)
C(13)	4713(5)	7103(1)	8087(2)	23(1)
C(19)	4785(6)	7765(1)	8531(2)	32(1)
C(14)	6959(5)	6675(1)	8331(2)	20(1)
C(15)	7323(5)	6258(1)	7481(2)	21(1)
O(201)	-2721(3)	3099(1)	4780(1)	26(1)
C(201)	-2411(5)	3593(1)	4137(2)	22(1)
C(202)	340(5)	3599(1)	3953(2)	22(1)
O(204)	476(6)	4016(1)	2088(2)	46(1)
C(203)	1184(5)	4260(1)	3646(2)	24(1)
C(204)	1242(7)	4400(2)	2668(2)	34(1)
O(205)	857(4)	3101(1)	3328(1)	25(1)
C(205)	2297(9)	5037(2)	2402(2)	47(1)
C(206)	1569(8)	5574(2)	3041(2)	44(1)
C(216)	2690(30)	6220(6)	2760(11)	52(3)
C(217)	4390(17)	6547(4)	3206(8)	56(3)
C(218)	1320(30)	6465(5)	1912(7)	76(4)
C(16B)	1970(40)	6256(9)	2640(20)	37(4)
C(17B)	290(30)	6633(6)	2235(13)	45(4)
C(18B)	4630(30)	6430(7)	2733(18)	50(4)

C(207)	2438(7)	5404(2)	4000(2)	36(1)
C(208)	1749(5)	4727(1)	4253(2)	26(1)
C(209)	1661(5)	4603(1)	5250(2)	25(1)
C(210)	-888(5)	4742(1)	5581(2)	26(1)
O(202)	-1542(4)	4272(1)	6152(1)	27(1)
O(203)	-2238(4)	5184(1)	5384(2)	33(1)
C(211)	464(5)	3816(1)	6337(2)	26(1)
C(212)	-466(6)	3128(1)	6262(2)	29(1)
C(213)	-401(5)	2938(1)	5261(2)	24(1)
C(219)	15(6)	2217(1)	5126(2)	30(1)
C(214)	1552(5)	3379(1)	4862(2)	22(1)
C(215)	2197(5)	3910(1)	5567(2)	24(1)

Table A2.2.4 *Bond lengths [Å] and angles [°] for compound* ***31***.

O(1)-C(1)	1.419(3)
O(1)-C(13)	1.449(3)
C(1)-C(2)	1.561(4)
C(1)-H(1A)	0.9900
C(1)-H(1B)	0.9900
C(2)-O(5)	1.433(3)
C(2)-C(3)	1.524(4)
C(2)-C(14)	1.543(4)
O(4)-C(4)	1.225(4)
C(3)-C(8)	1.342(4)
C(3)-C(4)	1.483(4)
C(4)-C(5)	1.515(4)
O(5)-H(5O)	0.83(3)
C(5)-C(6)	1.523(5)
C(5)-H(5A)	0.9900
C(5)-H(5B)	0.9900
C(6)-C(16)	1.520(4)
C(6)-C(7)	1.526(4)

C(6)-H(6)	1.0000
C(16)-C(17)	1.333(7)
C(16)-C(18)	1.474(7)
C(17)-H(17A)	0.9500
C(17)-H(17B)	0.9500
C(18)-H(18A)	0.9800
C(18)-H(18B)	0.9800
C(18)-H(18C)	0.9800
C(7)-C(8)	1.506(4)
C(7)-H(7A)	0.9900
C(7)-H(7B)	0.9900
C(8)-C(9)	1.489(4)
C(9)-C(15)	1.522(4)
C(9)-C(10)	1.527(4)
C(9)-H(9)	1.0000
C(10)-O(3)	1.203(3)
C(10)-O(2)	1.338(3)
O(2)-C(11)	1.465(3)
C(11)-C(12)	1.515(4)
C(11)-C(15)	1.545(4)
C(11)-H(11)	1.0000
C(12)-C(13)	1.513(4)
C(12)-H(12A)	0.9900
C(12)-H(12B)	0.9900
C(13)-C(19)	1.522(4)
C(13)-C(14)	1.536(4)
C(19)-H(19A)	0.9800
C(19)-H(19B)	0.9800
C(19)-H(19C)	0.9800
C(14)-C(15)	1.548(4)
C(14)-H(14)	1.0000
C(15)-H(15)	1.0000
O(201)-C(201)	1.416(3)
O(201)-C(213)	1.450(3)
C(201)-C(202)	1.537(4)
C(201)-H(20A)	0.9900

C(201)-H(20B)	0.9900
C(202)-O(205)	1.427(3)
C(202)-C(203)	1.525(4)
C(202)-C(214)	1.532(4)
O(204)-C(204)	1.224(4)
C(203)-C(208)	1.345(4)
C(203)-C(204)	1.479(4)
C(204)-C(205)	1.504(5)
O(205)-H(05O)	0.82(3)
C(205)-C(206)	1.528(5)
C(205)-H(20C)	0.9900
C(205)-H(20D)	0.9900
C(206)-C(207)	1.510(5)
C(206)-C(216)	1.541(10)
C(206)-C(16B)	1.556(16)
C(206)-H(206)	1.0000
C(216)-C(217)	1.296(14)
C(216)-C(218)	1.507(14)
C(217)-H(21A)	0.9500
C(217)-H(21B)	0.9500
C(218)-H(21C)	0.9800
C(218)-H(21D)	0.9800
C(218)-H(21E)	0.9800
C(16B)-C(17B)	1.32(2)
C(16B)-C(18B)	1.49(2)
C(17B)-H(17C)	0.9500
C(17B)-H(17D)	0.9500
C(18B)-H(18D)	0.9800
C(18B)-H(18E)	0.9800
C(18B)-H(18F)	0.9800
C(207)-C(208)	1.506(4)
C(207)-H(20E)	0.9900
C(207)-H(20F)	0.9900
C(208)-C(209)	1.502(4)
C(209)-C(210)	1.526(4)
C(209)-C(215)	1.536(4)

C(209)-H(209)	1.0000
C(210)-O(203)	1.200(4)
C(210)-O(202)	1.352(4)
O(202)-C(211)	1.458(4)
C(211)-C(212)	1.518(4)
C(211)-C(215)	1.534(4)
C(211)-H(211)	1.0000
C(212)-C(213)	1.535(4)
C(212)-H(21F)	0.9900
C(212)-H(21G)	0.9900
C(213)-C(219)	1.530(4)
C(213)-C(214)	1.545(4)
C(219)-H(21H)	0.9800
C(219)-H(21I)	0.9800
C(219)-H(21J)	0.9800
C(214)-C(215)	1.543(4)
C(214)-H(214)	1.0000
C(215)-H(215)	1.0000

C(1)-O(1)-C(13)	107.8(2)
O(1)-C(1)-C(2)	106.7(2)
O(1)-C(1)-H(1A)	110.4
C(2)-C(1)-H(1A)	110.4
O(1)-C(1)-H(1B)	110.4
C(2)-C(1)-H(1B)	110.4
H(1A)-C(1)-H(1B)	108.6
O(5)-C(2)-C(3)	110.8(2)
O(5)-C(2)-C(14)	106.3(2)
C(3)-C(2)-C(14)	115.0(2)
O(5)-C(2)-C(1)	110.7(2)
C(3)-C(2)-C(1)	110.8(2)
C(14)-C(2)-C(1)	102.9(2)
C(8)-C(3)-C(4)	119.3(2)
C(8)-C(3)-C(2)	122.4(3)
C(4)-C(3)-C(2)	117.9(2)
O(4)-C(4)-C(3)	122.2(3)

O(4)-C(4)-C(5)	120.8(3)
C(3)-C(4)-C(5)	117.0(3)
C(2)-O(5)-H(5O)	105(3)
C(4)-C(5)-C(6)	110.8(3)
C(4)-C(5)-H(5A)	109.5
C(6)-C(5)-H(5A)	109.5
C(4)-C(5)-H(5B)	109.5
C(6)-C(5)-H(5B)	109.5
H(5A)-C(5)-H(5B)	108.1
C(16)-C(6)-C(5)	115.2(3)
C(16)-C(6)-C(7)	110.8(3)
C(5)-C(6)-C(7)	108.4(3)
C(16)-C(6)-H(6)	107.4
C(5)-C(6)-H(6)	107.4
C(7)-C(6)-H(6)	107.4
C(17)-C(16)-C(18)	122.8(4)
C(17)-C(16)-C(6)	122.4(4)
C(18)-C(16)-C(6)	114.8(4)
C(16)-C(17)-H(17A)	120.0
C(16)-C(17)-H(17B)	120.0
H(17A)-C(17)-H(17B)	120.0
C(16)-C(18)-H(18A)	109.5
C(16)-C(18)-H(18B)	109.5
H(18A)-C(18)-H(18B)	109.5
C(16)-C(18)-H(18C)	109.5
H(18A)-C(18)-H(18C)	109.5
H(18B)-C(18)-H(18C)	109.5
C(8)-C(7)-C(6)	113.2(2)
C(8)-C(7)-H(7A)	108.9
C(6)-C(7)-H(7A)	108.9
C(8)-C(7)-H(7B)	108.9
C(6)-C(7)-H(7B)	108.9
H(7A)-C(7)-H(7B)	107.8
C(3)-C(8)-C(9)	121.4(2)
C(3)-C(8)-C(7)	123.9(3)
C(9)-C(8)-C(7)	114.7(2)

C(8)-C(9)-C(15)	117.4(2)
C(8)-C(9)-C(10)	111.4(2)
C(15)-C(9)-C(10)	104.0(2)
C(8)-C(9)-H(9)	107.8
C(15)-C(9)-H(9)	107.8
C(10)-C(9)-H(9)	107.8
O(3)-C(10)-O(2)	121.8(2)
O(3)-C(10)-C(9)	128.0(2)
O(2)-C(10)-C(9)	110.1(2)
C(10)-O(2)-C(11)	111.3(2)
O(2)-C(11)-C(12)	110.7(2)
O(2)-C(11)-C(15)	106.3(2)
C(12)-C(11)-C(15)	106.2(2)
O(2)-C(11)-H(11)	111.2
C(12)-C(11)-H(11)	111.2
C(15)-C(11)-H(11)	111.2
C(13)-C(12)-C(11)	105.8(2)
C(13)-C(12)-H(12A)	110.6
C(11)-C(12)-H(12A)	110.6
C(13)-C(12)-H(12B)	110.6
C(11)-C(12)-H(12B)	110.6
H(12A)-C(12)-H(12B)	108.7
O(1)-C(13)-C(12)	107.4(2)
O(1)-C(13)-C(19)	111.2(2)
C(12)-C(13)-C(19)	113.6(2)
O(1)-C(13)-C(14)	102.3(2)
C(12)-C(13)-C(14)	106.5(2)
C(19)-C(13)-C(14)	115.0(2)
C(13)-C(19)-H(19A)	109.5
C(13)-C(19)-H(19B)	109.5
H(19A)-C(19)-H(19B)	109.5
C(13)-C(19)-H(19C)	109.5
H(19A)-C(19)-H(19C)	109.5
H(19B)-C(19)-H(19C)	109.5
C(13)-C(14)-C(2)	104.7(2)
C(13)-C(14)-C(15)	105.8(2)

C(2)-C(14)-C(15)	118.1(2)
C(13)-C(14)-H(14)	109.3
C(2)-C(14)-H(14)	109.3
C(15)-C(14)-H(14)	109.3
C(9)-C(15)-C(11)	103.2(2)
C(9)-C(15)-C(14)	115.5(2)
C(11)-C(15)-C(14)	106.9(2)
C(9)-C(15)-H(15)	110.3
C(11)-C(15)-H(15)	110.3
C(14)-C(15)-H(15)	110.3
C(201)-O(201)-C(213)	111.2(2)
O(201)-C(201)-C(202)	106.3(2)
O(201)-C(201)-H(20A)	110.5
C(202)-C(201)-H(20A)	110.5
O(201)-C(201)-H(20B)	110.5
C(202)-C(201)-H(20B)	110.5
H(20A)-C(201)-H(20B)	108.7
O(205)-C(202)-C(203)	112.6(2)
O(205)-C(202)-C(214)	105.2(2)
C(203)-C(202)-C(214)	114.1(2)
O(205)-C(202)-C(201)	110.0(2)
C(203)-C(202)-C(201)	111.9(2)
C(214)-C(202)-C(201)	102.3(2)
C(208)-C(203)-C(204)	119.6(3)
C(208)-C(203)-C(202)	120.8(3)
C(204)-C(203)-C(202)	119.5(2)
O(204)-C(204)-C(203)	122.1(3)
O(204)-C(204)-C(205)	120.6(3)
C(203)-C(204)-C(205)	117.3(3)
C(202)-O(205)-H(05O)	108(3)
C(204)-C(205)-C(206)	111.3(3)
C(204)-C(205)-H(20C)	109.4
C(206)-C(205)-H(20C)	109.4
C(204)-C(205)-H(20D)	109.4
C(206)-C(205)-H(20D)	109.4
H(20C)-C(205)-H(20D)	108.0

C(207)-C(206)-C(205)	109.4(3)
C(207)-C(206)-C(216)	110.6(6)
C(205)-C(206)-C(216)	110.3(8)
C(207)-C(206)-C(16B)	121.8(11)
C(205)-C(206)-C(16B)	112.4(12)
C(207)-C(206)-H(206)	108.8
C(205)-C(206)-H(206)	108.8
C(216)-C(206)-H(206)	108.8
C(217)-C(216)-C(218)	123.2(8)
C(217)-C(216)-C(206)	126.9(9)
C(218)-C(216)-C(206)	109.7(9)
C(216)-C(217)-H(21A)	120.0
C(216)-C(217)-H(21B)	120.0
H(21A)-C(217)-H(21B)	120.0
C(216)-C(218)-H(21C)	109.5
C(216)-C(218)-H(21D)	109.5
H(21C)-C(218)-H(21D)	109.5
C(216)-C(218)-H(21E)	109.5
H(21C)-C(218)-H(21E)	109.5
H(21D)-C(218)-H(21E)	109.5
C(17B)-C(16B)-C(18B)	122.7(14)
C(17B)-C(16B)-C(206)	127.2(15)
C(18B)-C(16B)-C(206)	110.1(12)
C(16B)-C(17B)-H(17C)	120.0
C(16B)-C(17B)-H(17D)	120.0
H(17C)-C(17B)-H(17D)	120.0
C(16B)-C(18B)-H(18D)	109.5
C(16B)-C(18B)-H(18E)	109.5
H(18D)-C(18B)-H(18E)	109.5
C(16B)-C(18B)-H(18F)	109.5
H(18D)-C(18B)-H(18F)	109.5
H(18E)-C(18B)-H(18F)	109.5
C(208)-C(207)-C(206)	112.5(3)
C(208)-C(207)-H(20E)	109.1
C(206)-C(207)-H(20E)	109.1
C(208)-C(207)-H(20F)	109.1

C(206)-C(207)-H(20F)	109.1
H(20E)-C(207)-H(20F)	107.8
C(203)-C(208)-C(209)	120.8(3)
C(203)-C(208)-C(207)	123.9(3)
C(209)-C(208)-C(207)	115.3(2)
C(208)-C(209)-C(210)	111.5(2)
C(208)-C(209)-C(215)	116.4(2)
C(210)-C(209)-C(215)	103.7(2)
C(208)-C(209)-H(209)	108.3
C(210)-C(209)-H(209)	108.3
C(215)-C(209)-H(209)	108.3
O(203)-C(210)-O(202)	121.5(3)
O(203)-C(210)-C(209)	128.4(3)
O(202)-C(210)-C(209)	110.1(2)
C(210)-O(202)-C(211)	111.3(2)
O(202)-C(211)-C(212)	110.8(2)
O(202)-C(211)-C(215)	105.3(2)
C(212)-C(211)-C(215)	106.4(2)
O(202)-C(211)-H(211)	111.4
C(212)-C(211)-H(211)	111.4
C(215)-C(211)-H(211)	111.4
C(211)-C(212)-C(213)	106.5(2)
C(211)-C(212)-H(21F)	110.4
C(213)-C(212)-H(21F)	110.4
C(211)-C(212)-H(21G)	110.4
C(213)-C(212)-H(21G)	110.4
H(21F)-C(212)-H(21G)	108.6
O(201)-C(213)-C(219)	106.9(2)
O(201)-C(213)-C(212)	110.2(2)
C(219)-C(213)-C(212)	112.9(2)
O(201)-C(213)-C(214)	105.9(2)
C(219)-C(213)-C(214)	114.8(2)
C(212)-C(213)-C(214)	105.9(2)
C(213)-C(219)-H(21H)	109.5
C(213)-C(219)-H(21I)	109.5
H(21H)-C(219)-H(21I)	109.5

C(213)-C(219)-H(21J)	109.5
H(21H)-C(219)-H(21J)	109.5
H(21I)-C(219)-H(21J)	109.5
C(202)-C(214)-C(215)	116.6(2)
C(202)-C(214)-C(213)	104.1(2)
C(215)-C(214)-C(213)	107.3(2)
C(202)-C(214)-H(214)	109.5
C(215)-C(214)-H(214)	109.5
C(213)-C(214)-H(214)	109.5
C(211)-C(215)-C(209)	103.4(2)
C(211)-C(215)-C(214)	106.6(2)
C(209)-C(215)-C(214)	115.6(2)
C(211)-C(215)-H(215)	110.3
C(209)-C(215)-H(215)	110.3
C(214)-C(215)-H(215)	110.3

Symmetry transformations used to generate equivalent atoms:

Table A2.2.5 *Anisotropic displacement parameters ($Å^2 x\ 10^3$) for compound **31**. The anisotropic displacement factor exponent takes the form: $-2p^2[h^2\ a^{*2}U^{11} + ... + 2hka^*\ b^*\ U^{12}]$*

	U^{11}	U^{22}	U^{33}	U^{23}	U^{13}	U^{12}
O(1)	16(1)	38(1)	28(1)	5(1)	2(1)	1(1)
C(1)	20(1)	29(1)	27(1)	2(1)	8(1)	3(1)
C(2)	17(1)	23(1)	24(1)	-3(1)	1(1)	2(1)
O(4)	73(2)	36(1)	21(1)	-1(1)	9(1)	7(1)
C(3)	20(1)	26(1)	23(1)	-1(1)	2(1)	3(1)
C(4)	46(2)	33(2)	23(2)	0(1)	3(1)	9(1)
O(5)	32(1)	32(1)	22(1)	-6(1)	-3(1)	-2(1)
C(5)	86(3)	38(2)	22(2)	6(1)	5(2)	24(2)
C(6)	63(2)	26(1)	31(2)	4(1)	16(2)	10(1)
C(16)	91(3)	26(2)	40(2)	9(1)	34(2)	15(2)
C(17)	78(3)	34(2)	66(3)	16(2)	29(2)	22(2)

C(18)	122(4)	28(2)	56(3)	-5(2)	12(3)	5(2)
C(7)	36(2)	24(1)	24(1)	0(1)	6(1)	7(1)
C(8)	20(1)	24(1)	23(1)	1(1)	4(1)	4(1)
C(9)	22(1)	21(1)	20(1)	-3(1)	4(1)	2(1)
C(10)	26(1)	23(1)	17(1)	-4(1)	0(1)	-2(1)
O(2)	22(1)	27(1)	25(1)	1(1)	-1(1)	-4(1)
O(3)	32(1)	28(1)	29(1)	-1(1)	0(1)	-11(1)
C(11)	21(1)	25(1)	24(1)	1(1)	2(1)	-3(1)
C(12)	22(1)	25(1)	30(1)	6(1)	1(1)	1(1)
C(13)	16(1)	24(1)	30(1)	1(1)	2(1)	1(1)
C(19)	36(2)	24(1)	36(2)	-3(1)	3(1)	7(1)
C(14)	13(1)	21(1)	26(1)	-2(1)	2(1)	-2(1)
C(15)	15(1)	24(1)	23(1)	1(1)	5(1)	0(1)
O(201)	15(1)	28(1)	34(1)	1(1)	1(1)	-2(1)
C(201)	15(1)	22(1)	29(1)	-4(1)	-1(1)	1(1)
C(202)	19(1)	24(1)	24(1)	-6(1)	1(1)	1(1)
O(204)	80(2)	31(1)	26(1)	-5(1)	-6(1)	-8(1)
C(203)	18(1)	27(1)	26(1)	-5(1)	3(1)	0(1)
C(204)	42(2)	32(2)	27(2)	-6(1)	4(1)	-1(1)
O(205)	28(1)	24(1)	25(1)	-7(1)	4(1)	2(1)
C(205)	75(3)	41(2)	25(2)	-6(1)	15(2)	-19(2)
C(206)	69(2)	30(2)	35(2)	-2(1)	13(2)	-14(2)
C(216)	91(9)	37(4)	30(4)	1(3)	11(5)	-22(5)
C(217)	93(5)	33(3)	40(5)	-2(3)	5(4)	-28(3)
C(218)	137(11)	47(5)	42(5)	12(4)	-9(6)	-33(6)
C(16B)	55(8)	27(6)	31(10)	-7(5)	19(7)	-6(5)
C(17B)	74(8)	23(5)	37(8)	3(5)	5(6)	-4(5)
C(18B)	64(7)	40(6)	46(11)	-2(6)	13(6)	-14(5)
C(207)	51(2)	30(2)	28(2)	-7(1)	14(1)	-16(1)
C(208)	22(1)	29(1)	27(1)	-5(1)	6(1)	-5(1)
C(209)	24(1)	26(1)	26(1)	-8(1)	5(1)	-7(1)
C(210)	26(1)	28(1)	23(1)	-10(1)	3(1)	-3(1)
O(202)	24(1)	28(1)	29(1)	-6(1)	7(1)	-4(1)
O(203)	35(1)	32(1)	33(1)	-6(1)	6(1)	6(1)
C(211)	24(1)	31(1)	24(1)	-2(1)	4(1)	-3(1)
C(212)	29(2)	29(1)	30(2)	1(1)	4(1)	0(1)

C(213)	17(1)	26(1)	30(1)	-2(1)	1(1)	1(1)
C(219)	31(2)	26(1)	35(2)	-2(1)	2(1)	4(1)
C(214)	13(1)	26(1)	28(1)	-3(1)	3(1)	2(1)
C(215)	14(1)	34(1)	23(1)	-3(1)	1(1)	-3(1)

Table A2.2.6 *Hydrogen coordinates (x 10^4) and isotropic displacement parameters (Å^{2}x 10^3) for compound* ***31***.

	x	y	z	U(eq)
H(1A)	2639	6024	9321	30
H(1B)	3134	6730	9741	30
H(5O)	7220(80)	6480(20)	10400(20)	44
H(5A)	7560	4399	10747	59
H(5B)	9804	4590	10147	59
H(6)	4990	4252	9408	47
H(17A)	9729	2815	9838	70
H(17B)	10427	3540	10223	70
H(18A)	6176	2647	8896	103
H(18B)	5949	3212	8160	103
H(18C)	4068	3181	8950	103
H(7A)	9259	4451	8409	34
H(7B)	6510	4343	7988	34
H(9)	7784	5301	7161	25
H(11)	6153	6537	6143	28
H(12A)	5394	7489	6830	31
H(12B)	2680	7184	6857	31
H(19A)	3242	7993	8372	48
H(19B)	6172	8012	8317	48
H(19C)	4989	7715	9190	48
H(14)	8444	6953	8456	24
H(15)	9028	6316	7275	25

H(20A)	-2911	4014	4381	27
H(20B)	-3424	3505	3572	27
H(05O)	470(70)	3231(19)	2813(19)	38
H(20C)	1691	5144	1776	56
H(20D)	4115	5005	2416	56
H(206)	-267	5613	3006	53
H(21A)	4833	6962	3000	67
H(21B)	5195	6371	3738	67
H(21C)	1823	6910	1799	114
H(21D)	-453	6450	1987	114
H(21E)	1719	6194	1398	114
H(17C)	762	7033	1986	54
H(17D)	-1387	6504	2191	54
H(18D)	5558	6145	2350	75
H(18E)	5239	6381	3366	75
H(18F)	4839	6877	2542	75
H(20E)	4252	5450	4069	43
H(20F)	1709	5710	4422	43
H(209)	2872	4896	5578	30
H(211)	1333	3899	6941	31
H(21F)	-2168	3099	6461	35
H(21G)	602	2838	6645	35
H(21H)	-1373	1976	5350	46
H(21I)	1543	2086	5461	46
H(21J)	140	2127	4480	46
H(214)	3061	3121	4755	27
H(215)	3952	3868	5802	29

Table A2.2.7 *Torsion angles [°] for compound* ***31***.

C(13)-O(1)-C(1)-C(2)	-31.1(3)
O(1)-C(1)-C(2)-O(5)	121.4(2)
O(1)-C(1)-C(2)-C(3)	-115.2(2)
O(1)-C(1)-C(2)-C(14)	8.2(3)
O(5)-C(2)-C(3)-C(8)	-145.2(3)

C(14)-C(2)-C(3)-C(8)	-24.7(4)
C(1)-C(2)-C(3)-C(8)	91.5(3)
O(5)-C(2)-C(3)-C(4)	41.3(3)
C(14)-C(2)-C(3)-C(4)	161.9(2)
C(1)-C(2)-C(3)-C(4)	-82.0(3)
C(8)-C(3)-C(4)-O(4)	-167.8(3)
C(2)-C(3)-C(4)-O(4)	5.9(5)
C(8)-C(3)-C(4)-C(5)	13.0(5)
C(2)-C(3)-C(4)-C(5)	-173.4(3)
O(4)-C(4)-C(5)-C(6)	138.4(4)
C(3)-C(4)-C(5)-C(6)	-42.3(5)
C(4)-C(5)-C(6)-C(16)	-176.3(3)
C(4)-C(5)-C(6)-C(7)	59.0(4)
C(5)-C(6)-C(16)-C(17)	-18.4(5)
C(7)-C(6)-C(16)-C(17)	105.1(4)
C(5)-C(6)-C(16)-C(18)	161.7(4)
C(7)-C(6)-C(16)-C(18)	-74.9(5)
C(16)-C(6)-C(7)-C(8)	-175.7(3)
C(5)-C(6)-C(7)-C(8)	-48.4(4)
C(4)-C(3)-C(8)-C(9)	175.2(3)
C(2)-C(3)-C(8)-C(9)	1.8(4)
C(4)-C(3)-C(8)-C(7)	-2.0(4)
C(2)-C(3)-C(8)-C(7)	-175.3(3)
C(6)-C(7)-C(8)-C(3)	21.0(4)
C(6)-C(7)-C(8)-C(9)	-156.4(3)
C(3)-C(8)-C(9)-C(15)	26.5(4)
C(7)-C(8)-C(9)-C(15)	-156.1(2)
C(3)-C(8)-C(9)-C(10)	-93.3(3)
C(7)-C(8)-C(9)-C(10)	84.1(3)
C(8)-C(9)-C(10)-O(3)	-35.0(4)
C(15)-C(9)-C(10)-O(3)	-162.5(3)
C(8)-C(9)-C(10)-O(2)	146.4(2)
C(15)-C(9)-C(10)-O(2)	18.9(3)
O(3)-C(10)-O(2)-C(11)	174.3(2)
C(9)-C(10)-O(2)-C(11)	-7.0(3)
C(10)-O(2)-C(11)-C(12)	-122.5(2)

C(10)-O(2)-C(11)-C(15)	-7.7(3)
O(2)-C(11)-C(12)-C(13)	87.4(3)
C(15)-C(11)-C(12)-C(13)	-27.5(3)
C(1)-O(1)-C(13)-C(12)	152.7(2)
C(1)-O(1)-C(13)-C(19)	-82.4(3)
C(1)-O(1)-C(13)-C(14)	40.8(3)
C(11)-C(12)-C(13)-O(1)	-78.7(3)
C(11)-C(12)-C(13)-C(19)	157.9(2)
C(11)-C(12)-C(13)-C(14)	30.3(3)
O(1)-C(13)-C(14)-C(2)	-33.9(2)
C(12)-C(13)-C(14)-C(2)	-146.4(2)
C(19)-C(13)-C(14)-C(2)	86.8(3)
O(1)-C(13)-C(14)-C(15)	91.6(2)
C(12)-C(13)-C(14)-C(15)	-21.0(3)
C(19)-C(13)-C(14)-C(15)	-147.8(2)
O(5)-C(2)-C(14)-C(13)	-100.7(2)
C(3)-C(2)-C(14)-C(13)	136.3(2)
C(1)-C(2)-C(14)-C(13)	15.8(3)
O(5)-C(2)-C(14)-C(15)	142.1(2)
C(3)-C(2)-C(14)-C(15)	19.1(3)
C(1)-C(2)-C(14)-C(15)	-101.5(2)
C(8)-C(9)-C(15)-C(11)	-145.6(2)
C(10)-C(9)-C(15)-C(11)	-21.9(3)
C(8)-C(9)-C(15)-C(14)	-29.4(3)
C(10)-C(9)-C(15)-C(14)	94.3(2)
O(2)-C(11)-C(15)-C(9)	18.7(3)
C(12)-C(11)-C(15)-C(9)	136.6(2)
O(2)-C(11)-C(15)-C(14)	-103.5(2)
C(12)-C(11)-C(15)-C(14)	14.4(3)
C(13)-C(14)-C(15)-C(9)	-110.1(2)
C(2)-C(14)-C(15)-C(9)	6.6(3)
C(13)-C(14)-C(15)-C(11)	4.0(3)
C(2)-C(14)-C(15)-C(11)	120.7(2)
C(213)-O(201)-C(201)-C(202)	20.2(3)
O(201)-C(201)-C(202)-O(205)	80.4(3)
O(201)-C(201)-C(202)-C(203)	-153.6(2)

O(201)-C(201)-C(202)-C(214)	-31.0(3)
O(205)-C(202)-C(203)-C(208)	-154.0(3)
C(214)-C(202)-C(203)-C(208)	-34.2(4)
C(201)-C(202)-C(203)-C(208)	81.4(3)
O(205)-C(202)-C(203)-C(204)	29.6(4)
C(214)-C(202)-C(203)-C(204)	149.4(3)
C(201)-C(202)-C(203)-C(204)	-95.0(3)
C(208)-C(203)-C(204)-O(204)	-171.4(3)
C(202)-C(203)-C(204)-O(204)	5.0(5)
C(208)-C(203)-C(204)-C(205)	8.8(5)
C(202)-C(203)-C(204)-C(205)	-174.8(3)
O(204)-C(204)-C(205)-C(206)	142.0(4)
C(203)-C(204)-C(205)-C(206)	-38.2(5)
C(204)-C(205)-C(206)-C(207)	57.7(5)
C(204)-C(205)-C(206)-C(216)	179.6(7)
C(204)-C(205)-C(206)-C(16B)	-163.7(9)
C(207)-C(206)-C(216)-C(217)	9(2)
C(205)-C(206)-C(216)-C(217)	-112(2)
C(207)-C(206)-C(216)-C(218)	-165.5(10)
C(205)-C(206)-C(216)-C(218)	73.3(13)
C(207)-C(206)-C(16B)-C(17B)	-128(3)
C(205)-C(206)-C(16B)-C(17B)	99(3)
C(207)-C(206)-C(16B)-C(18B)	55(2)
C(205)-C(206)-C(16B)-C(18B)	-78(2)
C(205)-C(206)-C(207)-C(208)	-48.7(4)
C(216)-C(206)-C(207)-C(208)	-170.3(8)
C(16B)-C(206)-C(207)-C(208)	177.4(11)
C(204)-C(203)-C(208)-C(209)	178.9(3)
C(202)-C(203)-C(208)-C(209)	2.5(4)
C(204)-C(203)-C(208)-C(207)	0.5(5)
C(202)-C(203)-C(208)-C(207)	-175.9(3)
C(206)-C(207)-C(208)-C(203)	20.7(5)
C(206)-C(207)-C(208)-C(209)	-157.8(3)
C(203)-C(208)-C(209)-C(210)	-89.1(3)
C(207)-C(208)-C(209)-C(210)	89.5(3)
C(203)-C(208)-C(209)-C(215)	29.6(4)

C(207)-C(208)-C(209)-C(215)	-151.8(3)
C(208)-C(209)-C(210)-O(203)	-42.0(4)
C(215)-C(209)-C(210)-O(203)	-168.1(3)
C(208)-C(209)-C(210)-O(202)	136.9(2)
C(215)-C(209)-C(210)-O(202)	10.8(3)
O(203)-C(210)-O(202)-C(211)	-175.8(2)
C(209)-C(210)-O(202)-C(211)	5.2(3)
C(210)-O(202)-C(211)-C(212)	-133.8(2)
C(210)-O(202)-C(211)-C(215)	-19.2(3)
O(202)-C(211)-C(212)-C(213)	86.5(3)
C(215)-C(211)-C(212)-C(213)	-27.5(3)
C(201)-O(201)-C(213)-C(219)	-123.5(2)
C(201)-O(201)-C(213)-C(212)	113.4(2)
C(201)-O(201)-C(213)-C(214)	-0.7(3)
C(211)-C(212)-C(213)-O(201)	-89.9(3)
C(211)-C(212)-C(213)-C(219)	150.6(2)
C(211)-C(212)-C(213)-C(214)	24.2(3)
O(205)-C(202)-C(214)-C(215)	156.8(2)
C(203)-C(202)-C(214)-C(215)	32.9(3)
C(201)-C(202)-C(214)-C(215)	-88.3(3)
O(205)-C(202)-C(214)-C(213)	-85.2(2)
C(203)-C(202)-C(214)-C(213)	150.8(2)
C(201)-C(202)-C(214)-C(213)	29.7(3)
O(201)-C(213)-C(214)-C(202)	-18.9(3)
C(219)-C(213)-C(214)-C(202)	98.8(3)
C(212)-C(213)-C(214)-C(202)	-136.0(2)
O(201)-C(213)-C(214)-C(215)	105.3(2)
C(219)-C(213)-C(214)-C(215)	-137.0(2)
C(212)-C(213)-C(214)-C(215)	-11.8(3)
O(202)-C(211)-C(215)-C(209)	24.6(3)
C(212)-C(211)-C(215)-C(209)	142.2(2)
O(202)-C(211)-C(215)-C(214)	-97.7(2)
C(212)-C(211)-C(215)-C(214)	19.9(3)
C(208)-C(209)-C(215)-C(211)	-144.1(2)
C(210)-C(209)-C(215)-C(211)	-21.2(3)
C(208)-C(209)-C(215)-C(214)	-27.9(3)

C(210)-C(209)-C(215)-C(214)	94.9(3)
C(202)-C(214)-C(215)-C(211)	111.3(3)
C(213)-C(214)-C(215)-C(211)	-4.9(3)
C(202)-C(214)-C(215)-C(209)	-3.0(3)
C(213)-C(214)-C(215)-C(209)	-119.2(3)

Symmetry transformations used to generate equivalent atoms:

Table A2.2.8 *Hydrogen bonds for compound* ***31*** *[Å and °].*

D-H...A	d(D-H)	d(H...A)	d(D...A)	<(DHA)
O(5)-H(5O)...O(4)	0.83(3)	2.04(3)	2.710(3)	138(4)
C(5)-H(5A)...O(204)#1	0.99	2.59	3.299(4)	128.6
C(9)-H(9)...O(202)#2	1.00	2.65	3.542(3)	149.2
C(9)-H(9)...O(203)#2	1.00	2.64	3.406(3)	133.5
C(12)-H(12A)...O(205)#3	0.99	2.43	3.342(3)	153.7
C(14)-H(14)...O(1)#2	1.00	2.37	3.119(3)	130.8
C(15)-H(15)...O(1)#2	1.00	2.65	3.288(3)	121.6
O(205)-H(05O)...O(204)	0.82(3)	1.95(3)	2.640(3)	141(4)
C(209)-H(209)...O(3)	1.00	2.60	3.206(3)	119.2
C(211)-H(211)...O(3)	1.00	2.56	3.146(3)	117.5
C(214)-H(214)...O(201)#2	1.00	2.29	3.178(3)	147.0
C(215)-H(215)...O(202)#2	1.00	2.61	3.542(3)	154.9

Symmetry transformations used to generate equivalent atoms:

#1 x+1,y,z+1 #2 x+1,y,z #3 -x+1,y+1/2,-z+1

A2.3 X-RAY CRYSTAL STRUCTURE OF COMPOUND 33

Figure A2.3.1 *X-ray crystal structure of compound* ***33***.

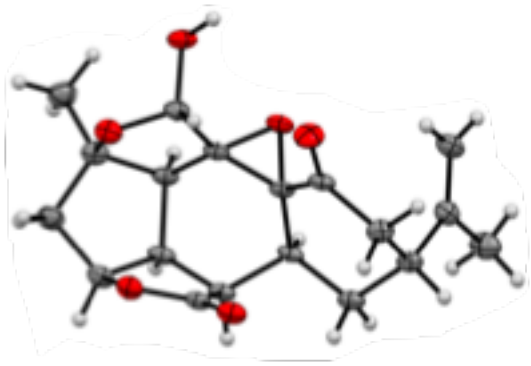


Table A2.3.2 *Crystal data and structure refinement for compound* ***33***.

Empirical formula	$C_{19}H_{22}O_6$	
Formula weight	346.36	
Temperature	100(2) K	
Wavelength	1.54178 Å	
Crystal system	Orthorhombic	
Space group	$P2_12_12_1$	
Unit cell dimensions	a = 6.0176(4) Å	a= 90°.
	b = 12.9933(17) Å	b= 90°.
	c = 20.752(2) Å	g = 90°.
Volume	1622.6(3) $Å^3$	
Z	4	
Density (calculated)	1.418 Mg/m^3	
Absorption coefficient	0.874 mm^{-1}	
F(000)	736	
Crystal size	0.300 x 0.300 x 0.050 mm^3	
Theta range for data collection	4.014 to 74.419°.	
Index ranges	-7<=h<=7, -14<=k<=16, -25<=l<=22	
Reflections collected	17915	
Independent reflections	3315 [R(int) = 0.0964]	
Completeness to theta = 67.679°	100.0 %	
Absorption correction	Semi-empirical from equivalents	
Max. and min. transmission	0.7538 and 0.4675	

Refinement method	Full-matrix least-squares on F^2
Data / restraints / parameters	3315 / 1 / 231
Goodness-of-fit on F^2	1.068
Final R indices [I>2sigma(I)]	R1 = 0.0516, wR2 = 0.1264
R indices (all data)	R1 = 0.0594, wR2 = 0.1320
Absolute structure parameter	0.02(14)
Extinction coefficient	n/a
Largest diff. peak and hole	0.457 and -0.323 e.$Å^{-3}$

Table A2.3.3. *Atomic coordinates (x 10^4) and equivalent isotropic displacement parameters ($Å^2$x 10^3) for compound* ***33***. *U(eq) is defined as one third of the trace of the orthogonalized U^{ij} tensor.*

	x	y	z	U(eq)
O(1)	2960(4)	4788(2)	8897(1)	25(1)
O(2)	1892(4)	6270(2)	8370(1)	27(1)
C(1)	2981(6)	5314(2)	8307(2)	21(1)
C(2)	1690(5)	4607(2)	7847(2)	19(1)
O(3)	633(4)	5051(2)	7295(1)	23(1)
C(3)	2389(5)	4301(2)	7184(2)	19(1)
C(4)	4363(5)	4811(2)	6862(2)	20(1)
O(4)	5136(5)	5596(2)	7076(1)	30(1)
C(5)	5223(5)	4335(2)	6245(2)	23(1)
C(6)	3506(6)	3683(2)	5891(2)	22(1)
C(16)	1575(6)	4278(3)	5608(2)	23(1)
C(17)	1223(6)	5275(3)	5695(2)	29(1)
C(18)	80(7)	3656(3)	5173(2)	33(1)
C(7)	2766(6)	2818(2)	6349(2)	22(1)
C(8)	1674(5)	3218(2)	6976(2)	18(1)
C(9)	2147(5)	2494(2)	7547(2)	18(1)
C(10)	4520(5)	2638(2)	7789(2)	19(1)
O(5)	4575(4)	2656(2)	8443(1)	23(1)
O(6)	6185(4)	2784(2)	7481(1)	23(1)
C(11)	2371(6)	2430(2)	8699(2)	24(1)
C(12)	1785(6)	3126(3)	9261(2)	27(1)

C(13)	1006(6)	4139(2)	8956(2)	24(1)
C(19)	-769(7)	4696(3)	9340(2)	31(1)
C(14)	314(5)	3881(2)	8254(2)	20(1)
C(15)	800(5)	2712(2)	8150(2)	20(1)

Table A2.3.4 *Bond lengths [Å] and angles [°] for compound* ***33***.

O(1)-C(1)	1.403(4)
O(1)-C(13)	1.452(4)
O(2)-C(1)	1.410(4)
O(2)-H(2O)	0.85(3)
C(1)-C(2)	1.536(5)
C(1)-H(1)	1.0000
C(2)-O(3)	1.432(4)
C(2)-C(3)	1.492(5)
C(2)-C(14)	1.513(4)
O(3)-C(3)	1.456(4)
C(3)-C(4)	1.516(4)
C(3)-C(8)	1.533(4)
C(4)-O(4)	1.206(4)
C(4)-C(5)	1.512(5)
C(5)-C(6)	1.525(5)
C(5)-H(5A)	0.9900
C(5)-H(5B)	0.9900
C(6)-C(16)	1.514(5)
C(6)-C(7)	1.538(4)
C(6)-H(6)	1.0000
C(16)-C(17)	1.325(5)
C(16)-C(18)	1.510(5)
C(17)-H(17A)	0.9500
C(17)-H(17B)	0.9500
C(18)-H(18A)	0.9800
C(18)-H(18B)	0.9800
C(18)-H(18C)	0.9800
C(7)-C(8)	1.547(5)

C(7)-H(7A)	0.9900
C(7)-H(7B)	0.9900
C(8)-C(9)	1.540(4)
C(8)-H(8)	1.0000
C(9)-C(15)	1.518(5)
C(9)-C(10)	1.525(4)
C(9)-H(9)	1.0000
C(10)-O(6)	1.203(4)
C(10)-O(5)	1.358(4)
O(5)-C(11)	1.458(4)
C(11)-C(12)	1.519(5)
C(11)-C(15)	1.524(5)
C(11)-H(11)	1.0000
C(12)-C(13)	1.534(5)
C(12)-H(12A)	0.9900
C(12)-H(12B)	0.9900
C(13)-C(19)	1.516(5)
C(13)-C(14)	1.552(5)
C(19)-H(19A)	0.9800
C(19)-H(19B)	0.9800
C(19)-H(19C)	0.9800
C(14)-C(15)	1.563(4)
C(14)-H(14)	1.0000
C(15)-H(15)	1.0000
C(1)-O(1)-C(13)	111.3(3)
C(1)-O(2)-H(2O)	116(4)
O(1)-C(1)-O(2)	110.1(3)
O(1)-C(1)-C(2)	104.3(2)
O(2)-C(1)-C(2)	110.5(3)
O(1)-C(1)-H(1)	110.6
O(2)-C(1)-H(1)	110.6
C(2)-C(1)-H(1)	110.6
O(3)-C(2)-C(3)	59.7(2)
O(3)-C(2)-C(14)	117.1(3)
C(3)-C(2)-C(14)	120.2(3)
O(3)-C(2)-C(1)	118.7(2)

C(3)-C(2)-C(1)	126.1(3)
C(14)-C(2)-C(1)	107.6(3)
C(2)-O(3)-C(3)	62.2(2)
O(3)-C(3)-C(2)	58.11(19)
O(3)-C(3)-C(4)	110.2(2)
C(2)-C(3)-C(4)	120.8(3)
O(3)-C(3)-C(8)	117.1(3)
C(2)-C(3)-C(8)	115.2(3)
C(4)-C(3)-C(8)	119.8(3)
O(4)-C(4)-C(5)	121.8(3)
O(4)-C(4)-C(3)	120.6(3)
C(5)-C(4)-C(3)	117.6(3)
C(4)-C(5)-C(6)	113.8(3)
C(4)-C(5)-H(5A)	108.8
C(6)-C(5)-H(5A)	108.8
C(4)-C(5)-H(5B)	108.8
C(6)-C(5)-H(5B)	108.8
H(5A)-C(5)-H(5B)	107.7
C(16)-C(6)-C(5)	115.0(3)
C(16)-C(6)-C(7)	113.0(3)
C(5)-C(6)-C(7)	107.7(3)
C(16)-C(6)-H(6)	106.9
C(5)-C(6)-H(6)	106.9
C(7)-C(6)-H(6)	106.9
C(17)-C(16)-C(18)	120.7(3)
C(17)-C(16)-C(6)	124.7(3)
C(18)-C(16)-C(6)	114.6(3)
C(16)-C(17)-H(17A)	120.0
C(16)-C(17)-H(17B)	120.0
H(17A)-C(17)-H(17B)	120.0
C(16)-C(18)-H(18A)	109.5
C(16)-C(18)-H(18B)	109.5
H(18A)-C(18)-H(18B)	109.5
C(16)-C(18)-H(18C)	109.5
H(18A)-C(18)-H(18C)	109.5
H(18B)-C(18)-H(18C)	109.5

C(6)-C(7)-C(8)	113.4(2)
C(6)-C(7)-H(7A)	108.9
C(8)-C(7)-H(7A)	108.9
C(6)-C(7)-H(7B)	108.9
C(8)-C(7)-H(7B)	108.9
H(7A)-C(7)-H(7B)	107.7
C(3)-C(8)-C(9)	107.0(2)
C(3)-C(8)-C(7)	115.2(3)
C(9)-C(8)-C(7)	111.3(2)
C(3)-C(8)-H(8)	107.7
C(9)-C(8)-H(8)	107.7
C(7)-C(8)-H(8)	107.7
C(15)-C(9)-C(10)	101.9(3)
C(15)-C(9)-C(8)	115.0(2)
C(10)-C(9)-C(8)	110.6(3)
C(15)-C(9)-H(9)	109.7
C(10)-C(9)-H(9)	109.7
C(8)-C(9)-H(9)	109.7
O(6)-C(10)-O(5)	120.5(3)
O(6)-C(10)-C(9)	128.6(3)
O(5)-C(10)-C(9)	110.7(3)
C(10)-O(5)-C(11)	109.7(3)
O(5)-C(11)-C(12)	111.7(3)
O(5)-C(11)-C(15)	104.2(3)
C(12)-C(11)-C(15)	106.7(3)
O(5)-C(11)-H(11)	111.3
C(12)-C(11)-H(11)	111.3
C(15)-C(11)-H(11)	111.3
C(11)-C(12)-C(13)	105.3(3)
C(11)-C(12)-H(12A)	110.7
C(13)-C(12)-H(12A)	110.7
C(11)-C(12)-H(12B)	110.7
C(13)-C(12)-H(12B)	110.7
H(12A)-C(12)-H(12B)	108.8
O(1)-C(13)-C(19)	109.7(3)
O(1)-C(13)-C(12)	106.6(3)

C(19)-C(13)-C(12)	114.1(3)
O(1)-C(13)-C(14)	105.3(3)
C(19)-C(13)-C(14)	114.0(3)
C(12)-C(13)-C(14)	106.5(3)
C(13)-C(19)-H(19A)	109.5
C(13)-C(19)-H(19B)	109.5
H(19A)-C(19)-H(19B)	109.5
C(13)-C(19)-H(19C)	109.5
H(19A)-C(19)-H(19C)	109.5
H(19B)-C(19)-H(19C)	109.5
C(2)-C(14)-C(13)	104.1(3)
C(2)-C(14)-C(15)	115.3(3)
C(13)-C(14)-C(15)	106.8(3)
C(2)-C(14)-H(14)	110.1
C(13)-C(14)-H(14)	110.1
C(15)-C(14)-H(14)	110.1
C(9)-C(15)-C(11)	103.8(3)
C(9)-C(15)-C(14)	113.3(3)
C(11)-C(15)-C(14)	104.3(3)
C(9)-C(15)-H(15)	111.6
C(11)-C(15)-H(15)	111.6
C(14)-C(15)-H(15)	111.6

Symmetry transformations used to generate equivalent atoms:

Table A.2.3.5 *Anisotropic displacement parameters ($Å^2$x 10^3) for V22369. The anisotropic displacement factor exponent takes the form: $-2p^2[h^2\ a^{*2}U^{11} + \ldots + 2\ h\ k\ a^*\ b^*\ U^{12}]$.*

	U^{11}	U^{22}	U^{33}	U^{23}	U^{13}	U^{12}
O(1)	22(1)	23(1)	31(1)	0(1)	-3(1)	-1(1)
O(2)	29(1)	15(1)	37(1)	-2(1)	5(1)	1(1)
C(1)	20(2)	16(1)	28(2)	1(1)	2(1)	-1(1)
C(2)	14(1)	14(1)	28(2)	0(1)	-2(1)	2(1)
O(3)	21(1)	15(1)	31(1)	2(1)	-2(1)	5(1)

C(3)	16(1)	14(1)	26(2)	-1(1)	-1(1)	4(1)
C(4)	19(1)	11(1)	30(2)	0(1)	0(1)	1(1)
O(4)	33(1)	20(1)	37(1)	-2(1)	4(1)	-11(1)
C(5)	17(2)	21(1)	30(2)	-2(1)	2(1)	-2(1)
C(6)	21(2)	17(1)	28(2)	-2(1)	1(1)	2(1)
C(16)	20(2)	23(2)	27(2)	3(1)	0(1)	0(1)
C(17)	28(2)	23(2)	35(2)	3(1)	-1(2)	5(1)
C(18)	28(2)	31(2)	41(2)	-2(2)	-10(2)	1(2)
C(7)	20(2)	15(1)	30(2)	-3(1)	-2(1)	1(1)
C(8)	13(1)	12(1)	29(2)	1(1)	-4(1)	0(1)
C(9)	13(1)	11(1)	30(2)	0(1)	-2(1)	0(1)
C(10)	18(2)	11(1)	29(2)	0(1)	-4(1)	1(1)
O(5)	16(1)	25(1)	29(1)	1(1)	-4(1)	2(1)
O(6)	14(1)	21(1)	35(1)	0(1)	-2(1)	1(1)
C(11)	20(2)	19(1)	32(2)	4(1)	1(1)	2(1)
C(12)	24(2)	27(2)	30(2)	2(1)	0(1)	5(1)
C(13)	17(2)	23(2)	32(2)	-1(1)	-1(1)	-1(1)
C(19)	29(2)	30(2)	34(2)	-1(1)	4(2)	4(2)
C(14)	14(1)	17(1)	29(2)	-1(1)	0(1)	2(1)
C(15)	14(1)	15(1)	32(2)	2(1)	-1(1)	0(1)

Table A.2.3.6 *Hydrogen coordinates (x 10^4) and isotropic displacement parameters (Å^{2}x 10^3) for compound* ***33***.

	x	y	z	U(eq)
H(2O)	2370(80)	6750(30)	8130(20)	40
H(1)	4540	5413	8152	26
H(5A)	6525	3900	6348	27
H(5B)	5732	4892	5955	27
H(6)	4294	3346	5523	26
H(17A)	18	5605	5483	34
H(17B)	2174	5660	5970	34
H(18A)	-1046	4107	4981	50

H(18B)	-653	3115	5424	50
H(18C)	968	3340	4830	50
H(7A)	4076	2395	6463	26
H(7B)	1696	2369	6121	26
H(8)	30	3230	6906	22
H(9)	1920	1763	7411	22
H(11)	2228	1687	8818	28
H(12A)	3099	3242	9539	32
H(12B)	587	2817	9525	32
H(19A)	-202	4850	9772	46
H(19B)	-2089	4258	9375	46
H(19C)	-1163	5338	9121	46
H(14)	-1304	4024	8191	24
H(15)	-594	2293	8164	24

Table A2.3.7 *Torsion angles [°] for compound* ***33***.

C(13)-O(1)-C(1)-O(2)	90.2(3)
C(13)-O(1)-C(1)-C(2)	-28.4(3)
O(1)-C(1)-C(2)-O(3)	155.4(3)
O(2)-C(1)-C(2)-O(3)	37.1(4)
O(1)-C(1)-C(2)-C(3)	-132.8(3)
O(2)-C(1)-C(2)-C(3)	108.9(3)
O(1)-C(1)-C(2)-C(14)	19.5(3)
O(2)-C(1)-C(2)-C(14)	-98.8(3)
C(14)-C(2)-O(3)-C(3)	-110.9(3)
C(1)-C(2)-O(3)-C(3)	117.3(3)
C(2)-O(3)-C(3)-C(4)	-114.4(3)
C(2)-O(3)-C(3)-C(8)	104.2(3)
C(14)-C(2)-C(3)-O(3)	105.6(3)
C(1)-C(2)-C(3)-O(3)	-105.2(3)
O(3)-C(2)-C(3)-C(4)	95.9(3)
C(14)-C(2)-C(3)-C(4)	-158.5(3)
C(1)-C(2)-C(3)-C(4)	-9.3(4)
O(3)-C(2)-C(3)-C(8)	-107.4(3)

C(14)-C(2)-C(3)-C(8)	-1.8(4)
C(1)-C(2)-C(3)-C(8)	147.3(3)
O(3)-C(3)-C(4)-O(4)	50.0(4)
C(2)-C(3)-C(4)-O(4)	-14.2(5)
C(8)-C(3)-C(4)-O(4)	-169.8(3)
O(3)-C(3)-C(4)-C(5)	-126.5(3)
C(2)-C(3)-C(4)-C(5)	169.3(3)
C(8)-C(3)-C(4)-C(5)	13.7(4)
O(4)-C(4)-C(5)-C(6)	-153.6(3)
C(3)-C(4)-C(5)-C(6)	22.9(4)
C(4)-C(5)-C(6)-C(16)	67.8(4)
C(4)-C(5)-C(6)-C(7)	-59.2(3)
C(5)-C(6)-C(16)-C(17)	-5.8(5)
C(7)-C(6)-C(16)-C(17)	118.4(4)
C(5)-C(6)-C(16)-C(18)	171.0(3)
C(7)-C(6)-C(16)-C(18)	-64.8(4)
C(16)-C(6)-C(7)-C(8)	-67.3(3)
C(5)-C(6)-C(7)-C(8)	60.9(3)
O(3)-C(3)-C(8)-C(9)	-109.9(3)
C(2)-C(3)-C(8)-C(9)	-44.4(3)
C(4)-C(3)-C(8)-C(9)	112.5(3)
O(3)-C(3)-C(8)-C(7)	125.8(3)
C(2)-C(3)-C(8)-C(7)	-168.7(3)
C(4)-C(3)-C(8)-C(7)	-11.8(4)
C(6)-C(7)-C(8)-C(3)	-25.9(4)
C(6)-C(7)-C(8)-C(9)	-147.9(3)
C(3)-C(8)-C(9)-C(15)	64.2(3)
C(7)-C(8)-C(9)-C(15)	-169.1(2)
C(3)-C(8)-C(9)-C(10)	-50.4(3)
C(7)-C(8)-C(9)-C(10)	76.2(3)
C(15)-C(9)-C(10)-O(6)	-161.4(3)
C(8)-C(9)-C(10)-O(6)	-38.7(4)
C(15)-C(9)-C(10)-O(5)	14.2(3)
C(8)-C(9)-C(10)-O(5)	136.8(3)
O(6)-C(10)-O(5)-C(11)	-178.4(3)
C(9)-C(10)-O(5)-C(11)	5.6(3)

C(10)-O(5)-C(11)-C(12)	-137.9(3)
C(10)-O(5)-C(11)-C(15)	-23.1(3)
O(5)-C(11)-C(12)-C(13)	80.8(3)
C(15)-C(11)-C(12)-C(13)	-32.4(3)
C(1)-O(1)-C(13)-C(19)	-97.2(3)
C(1)-O(1)-C(13)-C(12)	138.8(3)
C(1)-O(1)-C(13)-C(14)	25.9(3)
C(11)-C(12)-C(13)-O(1)	-91.1(3)
C(11)-C(12)-C(13)-C(19)	147.7(3)
C(11)-C(12)-C(13)-C(14)	20.9(3)
O(3)-C(2)-C(14)-C(13)	-141.2(3)
C(3)-C(2)-C(14)-C(13)	149.8(3)
C(1)-C(2)-C(14)-C(13)	-4.4(3)
O(3)-C(2)-C(14)-C(15)	102.3(3)
C(3)-C(2)-C(14)-C(15)	33.2(4)
C(1)-C(2)-C(14)-C(15)	-121.0(3)
O(1)-C(13)-C(14)-C(2)	-11.7(3)
C(19)-C(13)-C(14)-C(2)	108.6(3)
C(12)-C(13)-C(14)-C(2)	-124.6(3)
O(1)-C(13)-C(14)-C(15)	110.7(3)
C(19)-C(13)-C(14)-C(15)	-129.0(3)
C(12)-C(13)-C(14)-C(15)	-2.3(3)
C(10)-C(9)-C(15)-C(11)	-27.0(3)
C(8)-C(9)-C(15)-C(11)	-146.6(3)
C(10)-C(9)-C(15)-C(14)	85.5(3)
C(8)-C(9)-C(15)-C(14)	-34.1(4)
O(5)-C(11)-C(15)-C(9)	31.1(3)
C(12)-C(11)-C(15)-C(9)	149.4(3)
O(5)-C(11)-C(15)-C(14)	-87.8(3)
C(12)-C(11)-C(15)-C(14)	30.6(3)
C(2)-C(14)-C(15)-C(9)	-14.2(4)
C(13)-C(14)-C(15)-C(9)	-129.3(3)
C(2)-C(14)-C(15)-C(11)	98.0(3)
C(13)-C(14)-C(15)-C(11)	-17.1(3)

Table A2.3.8 *Hydrogen bonds for compound* ***33*** *[Å and °].*

D-H...A	d(D-H)	d(H...A)	d(D...A)	<(DHA)
O(2)-H(2O)...O(6)#1	0.85(3)	2.04(3)	2.887(3)	173(5)
C(1)-H(1)...O(4)	1.00	2.27	2.887(4)	118.5
C(9)-H(9)...O(4)#2	1.00	2.56	3.060(4)	110.5
C(14)-H(14)...O(6)#3	1.00	2.65	3.283(4)	121.0
C(15)-H(15)...O(6)#3	1.00	2.48	3.106(4)	119.9

Symmetry transformations used to generate equivalent atoms:

#1 -x+1,y+1/2,-z+3/2 #2 -x+1,y-1/2,-z+3/2 #3 x-1,y,z

A2.4 X-RAY CRYSTAL STRUCTURE OF COMPOUND 1

Figure A2.4.1 *X-ray crystal structure of compound* ***1***.

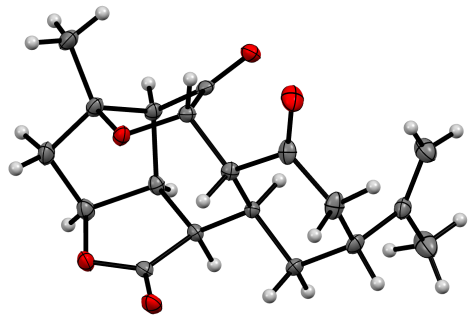


Table A2.4.2 *Crystal data and structure refinement for compound* ***1***.

Empirical formula	$C_{19}H_{22}O_5$	
Formula weight	330.36	
Temperature	100(2) K	
Wavelength	1.54178 Å	
Crystal system	Orthorhombic	
Space group	$P2_12_12_1$	
Unit cell dimensions	a = 10.5762(8) Å	a= 90°.
	b = 10.7831(11) Å	b= 90°.
	c = 13.8667(15) Å	g = 90°.
Volume	1581.4(3) $Å^3$	
Z	4	
Density (calculated)	1.388 Mg/m^3	
Absorption coefficient	0.820 mm^{-1}	
F(000)	704	
Crystal size	0.300 x 0.150 x 0.100 mm^3	
Theta range for data collection	5.196 to 74.559°.	
Index ranges	-13<=h<=13, -13<=k<=13, -17<=l<=17	
Reflections collected	25211	
Independent reflections	3240 [R(int) = 0.0504]	
Completeness to theta = 67.679°	100.0 %	
Absorption correction	Semi-empirical from equivalents	
Max. and min. transmission	0.7538 and 0.6138	
Refinement method	Full-matrix least-squares on F^2	

Data / restraints / parameters	3240 / 0 / 219
Goodness-of-fit on F^2	1.045
Final R indices [I>2sigma(I)]	R1 = 0.0306, wR2 = 0.0791
R indices (all data)	R1 = 0.0324, wR2 = 0.0803
Absolute structure parameter	-0.02(5)
Extinction coefficient	n/a
Largest diff. peak and hole	0.756 and -0.188 e.$Å^{-3}$

Table A.2.4.3 *Atomic coordinates (x 10^4) and equivalent isotropic displacement parameters ($Å^2$x 10^3) for compound* ***1****. U(eq) is defined as one third of the trace of the orthogonalized U^{ij} tensor.*

	x	y	z	U(eq)
C(1)	5052(2)	2908(2)	4104(1)	15(1)
O(1)	4757(1)	1706(1)	4235(1)	18(1)
O(2)	4325(1)	3602(1)	3709(1)	20(1)
C(2)	6325(2)	3210(2)	4553(1)	13(1)
C(3)	6950(2)	1924(2)	4738(1)	15(1)
C(4)	5836(2)	997(2)	4568(1)	19(1)
C(5)	6253(2)	118(2)	3766(2)	22(1)
C(6)	7333(2)	769(2)	3257(2)	18(1)
C(16)	8121(2)	-69(2)	2615(2)	23(1)
O(3)	6826(1)	1824(1)	2717(1)	16(1)
C(7)	8042(2)	1445(2)	4071(1)	16(1)
C(8)	8704(2)	2428(2)	3493(1)	14(1)
O(4)	9762(1)	2839(1)	3584(1)	18(1)
C(9)	7777(2)	2781(2)	2698(1)	14(1)
C(10)	7158(2)	4030(2)	2932(1)	14(1)
C(11)	7806(2)	5120(2)	2425(1)	18(1)
O(5)	8613(2)	4967(2)	1815(1)	27(1)
C(12)	7301(2)	6387(2)	2684(2)	23(1)
C(13)	7166(2)	6591(2)	3779(1)	18(1)
C(17)	8417(2)	6814(2)	4290(1)	18(1)
C(18)	9522(2)	6846(2)	3848(2)	26(1)
C(19)	8333(2)	7048(3)	5360(2)	31(1)

C(14)	6397(2)	5522(2)	4216(1)	17(1)
C(15)	7033(2)	4260(2)	4032(1)	12(1)

Table A2.4.4 *Bond lengths [Å] and angles [°] for compound* ***1***.

C(1)-O(2)	1.205(2)
C(1)-O(1)	1.345(2)
C(1)-C(2)	1.519(2)
O(1)-C(4)	1.450(2)
C(2)-C(15)	1.538(2)
C(2)-C(3)	1.558(2)
C(2)-H(2)	1.0000
C(3)-C(4)	1.562(2)
C(3)-C(7)	1.567(2)
C(3)-H(3)	1.0000
C(4)-C(5)	1.526(3)
C(4)-H(4)	1.0000
C(5)-C(6)	1.514(3)
C(5)-H(5A)	0.9900
C(5)-H(5B)	0.9900
C(6)-O(3)	1.464(2)
C(6)-C(16)	1.519(3)
C(6)-C(7)	1.538(2)
C(16)-H(16A)	0.9800
C(16)-H(16B)	0.9800
C(16)-H(16C)	0.9800
O(3)-C(9)	1.440(2)
C(7)-C(8)	1.502(3)
C(7)-H(7)	1.0000
C(8)-O(4)	1.210(2)
C(8)-C(9)	1.524(2)
C(9)-C(10)	1.532(2)
C(9)-H(9)	1.0000
C(10)-C(11)	1.532(3)
C(10)-C(15)	1.552(2)

C(10)-H(10)	1.0000
C(11)-O(5)	1.213(3)
C(11)-C(12)	1.510(3)
C(12)-C(13)	1.540(3)
C(12)-H(12A)	0.9900
C(12)-H(12B)	0.9900
C(13)-C(17)	1.521(3)
C(13)-C(14)	1.536(2)
C(13)-H(13)	1.0000
C(17)-C(18)	1.320(3)
C(17)-C(19)	1.507(3)
C(18)-H(18A)	0.9500
C(18)-H(18B)	0.9500
C(19)-H(19A)	0.9800
C(19)-H(19B)	0.9800
C(19)-H(19C)	0.9800
C(14)-C(15)	1.539(2)
C(14)-H(14A)	0.9900
C(14)-H(14B)	0.9900
C(15)-H(15)	1.0000

O(2)-C(1)-O(1)	120.78(16)
O(2)-C(1)-C(2)	128.23(17)
O(1)-C(1)-C(2)	110.92(15)
C(1)-O(1)-C(4)	111.62(14)
C(1)-C(2)-C(15)	113.41(14)
C(1)-C(2)-C(3)	104.63(14)
C(15)-C(2)-C(3)	121.73(15)
C(1)-C(2)-H(2)	105.2
C(15)-C(2)-H(2)	105.2
C(3)-C(2)-H(2)	105.2
C(2)-C(3)-C(4)	102.99(14)
C(2)-C(3)-C(7)	120.57(14)
C(4)-C(3)-C(7)	104.81(14)
C(2)-C(3)-H(3)	109.3
C(4)-C(3)-H(3)	109.3

C(7)-C(3)-H(3)	109.3
O(1)-C(4)-C(5)	108.84(16)
O(1)-C(4)-C(3)	107.71(15)
C(5)-C(4)-C(3)	106.80(15)
O(1)-C(4)-H(4)	111.1
C(5)-C(4)-H(4)	111.1
C(3)-C(4)-H(4)	111.1
C(6)-C(5)-C(4)	105.65(15)
C(6)-C(5)-H(5A)	110.6
C(4)-C(5)-H(5A)	110.6
C(6)-C(5)-H(5B)	110.6
C(4)-C(5)-H(5B)	110.6
H(5A)-C(5)-H(5B)	108.7
O(3)-C(6)-C(5)	108.81(15)
O(3)-C(6)-C(16)	111.30(17)
C(5)-C(6)-C(16)	114.30(16)
O(3)-C(6)-C(7)	100.67(14)
C(5)-C(6)-C(7)	104.23(16)
C(16)-C(6)-C(7)	116.41(15)
C(6)-C(16)-H(16A)	109.5
C(6)-C(16)-H(16B)	109.5
H(16A)-C(16)-H(16B)	109.5
C(6)-C(16)-H(16C)	109.5
H(16A)-C(16)-H(16C)	109.5
H(16B)-C(16)-H(16C)	109.5
C(9)-O(3)-C(6)	108.09(13)
C(8)-C(7)-C(6)	99.87(14)
C(8)-C(7)-C(3)	115.22(14)
C(6)-C(7)-C(3)	103.31(14)
C(8)-C(7)-H(7)	112.5
C(6)-C(7)-H(7)	112.5
C(3)-C(7)-H(7)	112.5
O(4)-C(8)-C(7)	129.37(16)
O(4)-C(8)-C(9)	125.40(17)
C(7)-C(8)-C(9)	105.15(15)
O(3)-C(9)-C(8)	104.91(14)

O(3)-C(9)-C(10)	109.12(14)
C(8)-C(9)-C(10)	109.92(14)
O(3)-C(9)-H(9)	110.9
C(8)-C(9)-H(9)	110.9
C(10)-C(9)-H(9)	110.9
C(11)-C(10)-C(9)	112.76(15)
C(11)-C(10)-C(15)	111.51(14)
C(9)-C(10)-C(15)	112.63(14)
C(11)-C(10)-H(10)	106.5
C(9)-C(10)-H(10)	106.5
C(15)-C(10)-H(10)	106.5
O(5)-C(11)-C(12)	122.55(18)
O(5)-C(11)-C(10)	122.04(18)
C(12)-C(11)-C(10)	115.25(16)
C(11)-C(12)-C(13)	113.38(15)
C(11)-C(12)-H(12A)	108.9
C(13)-C(12)-H(12A)	108.9
C(11)-C(12)-H(12B)	108.9
C(13)-C(12)-H(12B)	108.9
H(12A)-C(12)-H(12B)	107.7
C(17)-C(13)-C(14)	113.26(15)
C(17)-C(13)-C(12)	113.68(16)
C(14)-C(13)-C(12)	109.33(16)
C(17)-C(13)-H(13)	106.7
C(14)-C(13)-H(13)	106.7
C(12)-C(13)-H(13)	106.7
C(18)-C(17)-C(19)	120.33(19)
C(18)-C(17)-C(13)	123.89(17)
C(19)-C(17)-C(13)	115.75(17)
C(17)-C(18)-H(18A)	120.0
C(17)-C(18)-H(18B)	120.0
H(18A)-C(18)-H(18B)	120.0
C(17)-C(19)-H(19A)	109.5
C(17)-C(19)-H(19B)	109.5
H(19A)-C(19)-H(19B)	109.5
C(17)-C(19)-H(19C)	109.5

H(19A)-C(19)-H(19C)	109.5
H(19B)-C(19)-H(19C)	109.5
C(13)-C(14)-C(15)	111.50(14)
C(13)-C(14)-H(14A)	109.3
C(15)-C(14)-H(14A)	109.3
C(13)-C(14)-H(14B)	109.3
C(15)-C(14)-H(14B)	109.3
H(14A)-C(14)-H(14B)	108.0
C(2)-C(15)-C(14)	111.08(14)
C(2)-C(15)-C(10)	112.70(14)
C(14)-C(15)-C(10)	109.96(14)
C(2)-C(15)-H(15)	107.6
C(14)-C(15)-H(15)	107.6
C(10)-C(15)-H(15)	107.6

Symmetry transformations used to generate equivalent atoms:

Table A2.4.5 *Anisotropic displacement parameters ($Å^2 x\ 10^3$) for compound **1**. The anisotropic displacement factor exponent takes the form: $-2p^2[h^2\ a^{*2}U^{11} + ... + 2hka^*\ b^*\ U^{12}]$*

	U^{11}	U^{22}	U^{33}	U^{23}	U^{13}	U^{12}
C(1)	12(1)	16(1)	16(1)	-1(1)	2(1)	-1(1)
O(1)	14(1)	17(1)	24(1)	1(1)	-2(1)	-3(1)
O(2)	13(1)	21(1)	25(1)	2(1)	-2(1)	0(1)
C(2)	11(1)	14(1)	14(1)	-1(1)	0(1)	-1(1)
C(3)	15(1)	14(1)	15(1)	3(1)	-2(1)	-2(1)
C(4)	17(1)	15(1)	23(1)	3(1)	-1(1)	-3(1)
C(5)	22(1)	12(1)	31(1)	-1(1)	-2(1)	-3(1)
C(6)	17(1)	13(1)	23(1)	-2(1)	-4(1)	2(1)
C(16)	22(1)	17(1)	30(1)	-8(1)	-2(1)	4(1)
O(3)	16(1)	14(1)	20(1)	-2(1)	-4(1)	1(1)
C(7)	15(1)	12(1)	20(1)	0(1)	-3(1)	2(1)
C(8)	13(1)	15(1)	15(1)	-4(1)	1(1)	3(1)
O(4)	13(1)	21(1)	21(1)	-1(1)	1(1)	0(1)

C(9)	13(1)	15(1)	15(1)	-1(1)	1(1)	1(1)
C(10)	15(1)	14(1)	14(1)	1(1)	-2(1)	1(1)
C(11)	23(1)	18(1)	14(1)	1(1)	-6(1)	-4(1)
O(5)	34(1)	28(1)	19(1)	1(1)	6(1)	-9(1)
C(12)	31(1)	15(1)	22(1)	4(1)	-7(1)	-1(1)
C(13)	20(1)	10(1)	22(1)	0(1)	-1(1)	2(1)
C(17)	23(1)	13(1)	19(1)	-1(1)	1(1)	-4(1)
C(18)	23(1)	32(1)	22(1)	-1(1)	2(1)	-7(1)
C(19)	30(1)	43(1)	20(1)	-7(1)	4(1)	-13(1)
C(14)	15(1)	12(1)	24(1)	-2(1)	2(1)	1(1)
C(15)	12(1)	10(1)	15(1)	0(1)	1(1)	-1(1)

Table A2.4.6 *Hydrogen coordinates (x 10^4) and isotropic displacement parameters ($Å^2$x 10^3) for compound* ***1***.

	x	y	z	U(eq)
H(2)	6125	3546	5208	16
H(3)	7227	1873	5426	18
H(4)	5630	530	5171	22
H(5A)	6539	-683	4038	26
H(5B)	5548	-40	3313	26
H(16A)	7579	-441	2120	35
H(16B)	8505	-726	3006	35
H(16C)	8789	419	2304	35
H(7)	8646	890	4419	19
H(9)	8209	2808	2057	17
H(10)	6278	3990	2671	17
H(12A)	6463	6498	2377	27
H(12B)	7875	7026	2419	27
H(13)	6650	7361	3865	21
H(18A)	10269	7018	4204	31
H(18B)	9569	6697	3174	31
H(19A)	9168	7282	5606	47

H(19B)	8045	6293	5686	47
H(19C)	7732	7721	5482	47
H(14A)	5539	5518	3931	20
H(14B)	6309	5653	4920	20
H(15)	7907	4300	4307	15

Table A2.4.7 *Torsion angles [°] for compound* ***1***.

O(2)-C(1)-O(1)-C(4)	170.04(17)
C(2)-C(1)-O(1)-C(4)	-12.7(2)
O(2)-C(1)-C(2)-C(15)	-32.8(3)
O(1)-C(1)-C(2)-C(15)	150.19(15)
O(2)-C(1)-C(2)-C(3)	-167.69(18)
O(1)-C(1)-C(2)-C(3)	15.34(18)
C(1)-C(2)-C(3)-C(4)	-11.45(17)
C(15)-C(2)-C(3)-C(4)	-141.55(16)
C(1)-C(2)-C(3)-C(7)	104.72(17)
C(15)-C(2)-C(3)-C(7)	-25.4(2)
C(1)-O(1)-C(4)-C(5)	-110.86(17)
C(1)-O(1)-C(4)-C(3)	4.6(2)
C(2)-C(3)-C(4)-O(1)	4.94(18)
C(7)-C(3)-C(4)-O(1)	-122.00(15)
C(2)-C(3)-C(4)-C(5)	121.72(16)
C(7)-C(3)-C(4)-C(5)	-5.22(19)
O(1)-C(4)-C(5)-C(6)	97.19(17)
C(3)-C(4)-C(5)-C(6)	-18.8(2)
C(4)-C(5)-C(6)-O(3)	-70.65(19)
C(4)-C(5)-C(6)-C(16)	164.26(16)
C(4)-C(5)-C(6)-C(7)	36.09(19)
C(5)-C(6)-O(3)-C(9)	148.40(15)
C(16)-C(6)-O(3)-C(9)	-84.77(18)
C(7)-C(6)-O(3)-C(9)	39.23(17)
O(3)-C(6)-C(7)-C(8)	-45.18(16)
C(5)-C(6)-C(7)-C(8)	-157.91(14)
C(16)-C(6)-C(7)-C(8)	75.23(19)

O(3)-C(6)-C(7)-C(3)	73.87(16)
C(5)-C(6)-C(7)-C(3)	-38.85(17)
C(16)-C(6)-C(7)-C(3)	-165.72(16)
C(2)-C(3)-C(7)-C(8)	19.3(2)
C(4)-C(3)-C(7)-C(8)	134.58(16)
C(2)-C(3)-C(7)-C(6)	-88.48(18)
C(4)-C(3)-C(7)-C(6)	26.75(18)
C(6)-C(7)-C(8)-O(4)	-140.98(19)
C(3)-C(7)-C(8)-O(4)	109.1(2)
C(6)-C(7)-C(8)-C(9)	35.84(17)
C(3)-C(7)-C(8)-C(9)	-74.05(17)
C(6)-O(3)-C(9)-C(8)	-16.76(18)
C(6)-O(3)-C(9)-C(10)	-134.50(15)
O(4)-C(8)-C(9)-O(3)	163.79(17)
C(7)-C(8)-C(9)-O(3)	-13.19(18)
O(4)-C(8)-C(9)-C(10)	-79.0(2)
C(7)-C(8)-C(9)-C(10)	104.00(16)
O(3)-C(9)-C(10)-C(11)	-148.60(14)
C(8)-C(9)-C(10)-C(11)	96.86(17)
O(3)-C(9)-C(10)-C(15)	84.12(17)
C(8)-C(9)-C(10)-C(15)	-30.4(2)
C(9)-C(10)-C(11)-O(5)	8.8(2)
C(15)-C(10)-C(11)-O(5)	136.61(18)
C(9)-C(10)-C(11)-C(12)	-175.67(15)
C(15)-C(10)-C(11)-C(12)	-47.8(2)
O(5)-C(11)-C(12)-C(13)	-136.2(2)
C(10)-C(11)-C(12)-C(13)	48.2(2)
C(11)-C(12)-C(13)-C(17)	75.3(2)
C(11)-C(12)-C(13)-C(14)	-52.4(2)
C(14)-C(13)-C(17)-C(18)	126.3(2)
C(12)-C(13)-C(17)-C(18)	0.7(3)
C(14)-C(13)-C(17)-C(19)	-55.8(2)
C(12)-C(13)-C(17)-C(19)	178.63(18)
C(17)-C(13)-C(14)-C(15)	-68.85(19)
C(12)-C(13)-C(14)-C(15)	59.0(2)
C(1)-C(2)-C(15)-C(14)	71.42(19)

C(3)-C(2)-C(15)-C(14)	-162.34(15)
C(1)-C(2)-C(15)-C(10)	-52.49(19)
C(3)-C(2)-C(15)-C(10)	73.76(19)
C(13)-C(14)-C(15)-C(2)	174.67(15)
C(13)-C(14)-C(15)-C(10)	-59.88(18)
C(11)-C(10)-C(15)-C(2)	177.06(14)
C(9)-C(10)-C(15)-C(2)	-55.01(19)
C(11)-C(10)-C(15)-C(14)	52.53(18)
C(9)-C(10)-C(15)-C(14)	-179.54(14)

CHAPTER 2

Total Synthesis of Lycojapomine A & B †

2.1 INTRODUCTION

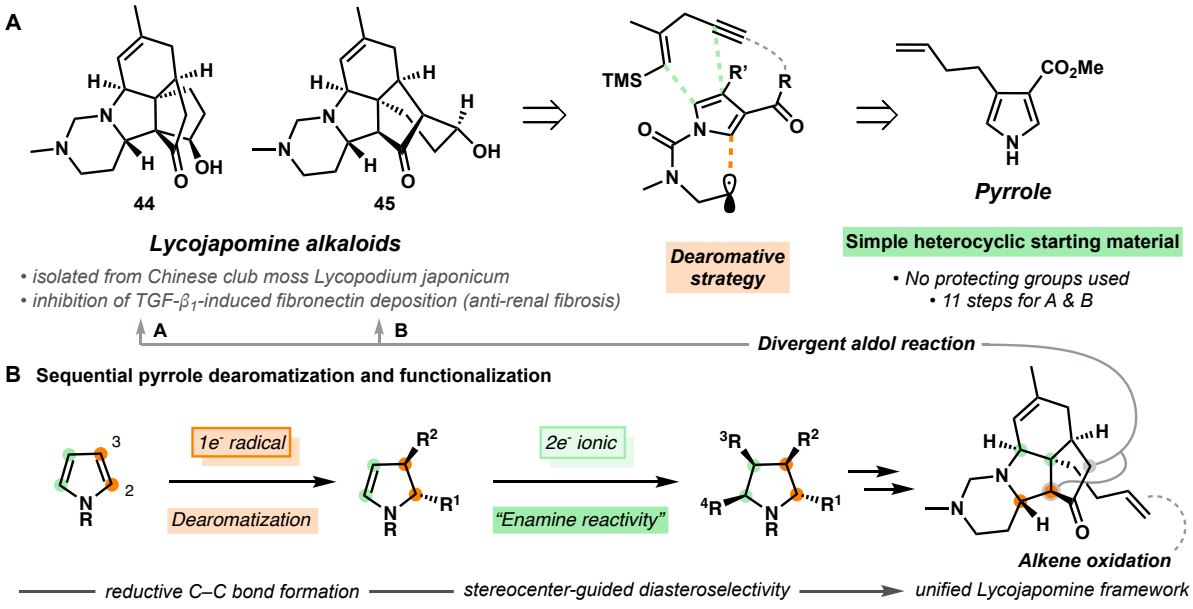
The synthesis of alkaloids has been an ongoing area of research and innovation in organic chemistry over the past century.[1,2] Dating back to landmark studies, such as Robinson's highly efficient synthesis of tropinone in 1917,[3,4] chemists have enabled access to these natural products by providing new and concise strategies for their synthesis. This is not only due to their intriguing and abundant chemical structures, but more importantly their biological activity and use in medicine.[5] Among them, the *Lycopodium* alkaloids represent one of the largest alkaloid families, possessing anti-inflammatory and neuroprotective effects.[6] Two unusual members of this class, Lycojapomine A (**44**) and Lycojapomine B (**45**) were recently isolated from the club-moss *Lycopodium japonicum*, the extracts of which are used in traditional Chinese medicine (Figure 2.2.1, A).[7,8] Ongoing research into the medicinal efficacy of these extracts and the low abundance of **44** and **45** (0.000017 - 0.000018% isolation yield) necessitates the synthesis of these key chemical components to enable further biological investigations. From a structural perspective, both **44** and **45** possess unprecedented molecular frameworks, with Lycojapomine A (**44**) bearing an unusual aza[3.3.3]propellane motif and Lycojapomine B (**45**) having an isomeric structural relationship.

† Portions of this chapter have been reproduced and modified with permission from Gross, B. M.; Stoltz, B. M. *J. Am. Chem. Soc.* **2025**, *147*, 20200–20204. © 2025 American Chemical Society.

2.2 RETROSYNTHETIC STRATEGY: PYRROLE DEAROMATIZATION

Due to the aliphatic nature of these caged ring systems, they are often traced back to saturated starting materials. This retrosynthetic logic has been well established, however necessitates the synthesis of complicated sp^3-rich precursors.[9] These often include complex stereochemical information and necessitate protection of reactive functional groups, inflating the step-count and decreasing synthetic efficiency. Instead, we sought to design a route for **44** and **45** from a simple sp^2-hybridized aromatic heterocycle, streamlining the synthesis and avoiding unnecessary protecting groups.[10]

Figure 2.2.1 *(A) Structure of Lycojapomine A (**44**) and B (**45**) and proposed retrosynthetic elements. (B) Concept of reductive functionalization of a pyrrole.*



Retrosynthetically, we identified the central pyrrolidine ring of **44** and **45** as a linchpin that could be derived from a heterocyclic pyrrole precursor. While dearomatization of other nitrogen-containing heterocycles (i.e. pyridines, quinolines, isoquinolines) is well established through hydrogenation methodologies,[11] controlled dearomatization of electron-

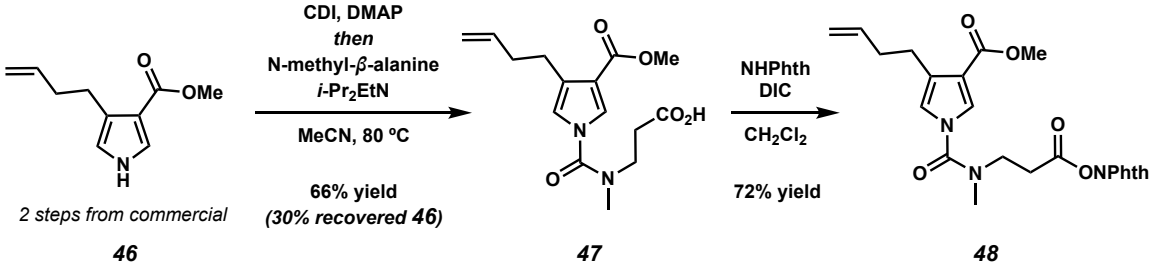
rich pyrroles represents an underdeveloped challenge.[12,13] Additionally, execution of this strategy would require not only saturation, but also introduction of additional substituents to build the fully substituted pyrrolidine and surrounding three-dimensional nitrogen and carbon framework. To begin our synthetic approach, we planned a radical addition to initially break the aromaticity of the pyrrole (Figure 2.2.1, B). Upon successful addition, the first two stereocenters are generated, revealing a dihydropyrrole. The chiral information would then be transferred to establish the remaining five stereocenters with the correct relative configuration. We identified the intermediate as having a reactive functional group, similar to an enamine, and envisioned leveraging it for an ionic two-electron annulation. Upon successfully setting the stereocenters around the pyrrolidine ring system, we imagined divergent aldol reactions to access both **44** and **45**, controlling bond formation and stereoselectivity to access the two alkaloids.

2.3 PHOTOCATALYTIC RADICAL ADDITION

The substituted pyrrole **46** was prepared in two steps from commercial materials in 74% yield (Figure 2.3.1).[14] Aminal formation with **46** under acidic conditions proved challenging, preferentially alkylating at the C2 carbon. We instead proceeded using carbonyl diimidazole and commercially available N-methyl-β-alanine to form urea **47** in 66% yield. We imagined that the urea motif would additionally aid in providing electron-withdrawing character to facilitate radical addition and provide the necessary stabilization of the product as the resulting enamide. While carboxylic acid **47** could be envisioned as a primary radical precursor in its own right, we elected to convert it to the N-hydroxy

phthalimide ester **48** in 72% yield, completing the synthesis of two potential radical precursors.

Figure 2.3.1 *Synthesis of starting material* ***48****.*

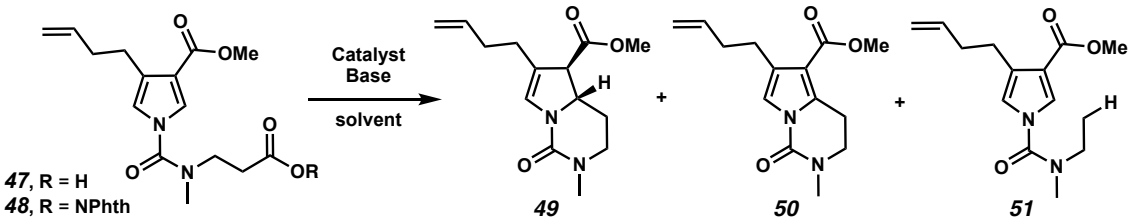


Building on reports published by Wang and co-workers, we proceeded to investigate radical formation from the carboxylic acid **47** and reductive addition to generate **49** (Table 2.3.2).[15] We were quickly faced with the challenge of generating the primary radical, which is significantly high in energy and short-lived. Upon irradiation of the carboxylic acid **47** with an Iridium-photocatalyst and K_2HPO_4, we isolated trace amounts of **50**, which conceptually proved that radical addition is feasible (Entry 1).[16] Upon employing Iron-catalyzed Ligand-to-Metal charge transfer,[17] we were able to observe increased radical formation, and isolation of **50**, along with decarboxylated product **51** in 50% overall yield (Entry 2). While decarboxylation was successful, we were unable to access dearomatized product **49**. This led us to investigate the redox active N-hydroxy phthalimide ester **48**, which can be activated at much lower reduction potentials, possibly circumventing the undesired oxidation and rearomatization to pyrrole **50**. Irradiation with photocatalyst Eosin Y,[18] as well transition-metal induced decarboxylation initially failed to yield any improvement[19] (Entry 3-4).

The first successful reactivity was observed using $Ru(bpy)_3$ and Hantzsch Ester (HE) as reductant to isolate product **49** in 11% yield (Entry 5).[20] Increasing the equivalents of HE

did not improve these results, instead resulting in premature reduction of the primary radical to give increased yields of **51**. Upon evaluating solvents, we observed that the formation of **6** preferentially occurred in polar solvents, such as DMSO or NMP. While Et_3N did not yield any improvement, we hypothesized that the redox potential of the photocatalyst determined the reaction pathway, potentially contributing to oxidation of the generated radical and rearomatization to **50**.[21] We therefore opted to investigate $Ir(ppy)_3$, which possesses one of the lower oxidation potentials of commercially known photocatalysts. As put forth, irradiation with $Ir(ppy)_3$ increased the yield substantially (Entry 17). While dimethyl sulfoxide proved to be poorly miscible with iPr_2EtN, we proceeded with NMP, delivering the product **49** in 81% yield (Entry 18).

Table 2.3.2 *Optimization of dearomative intramolecular radical addition.*



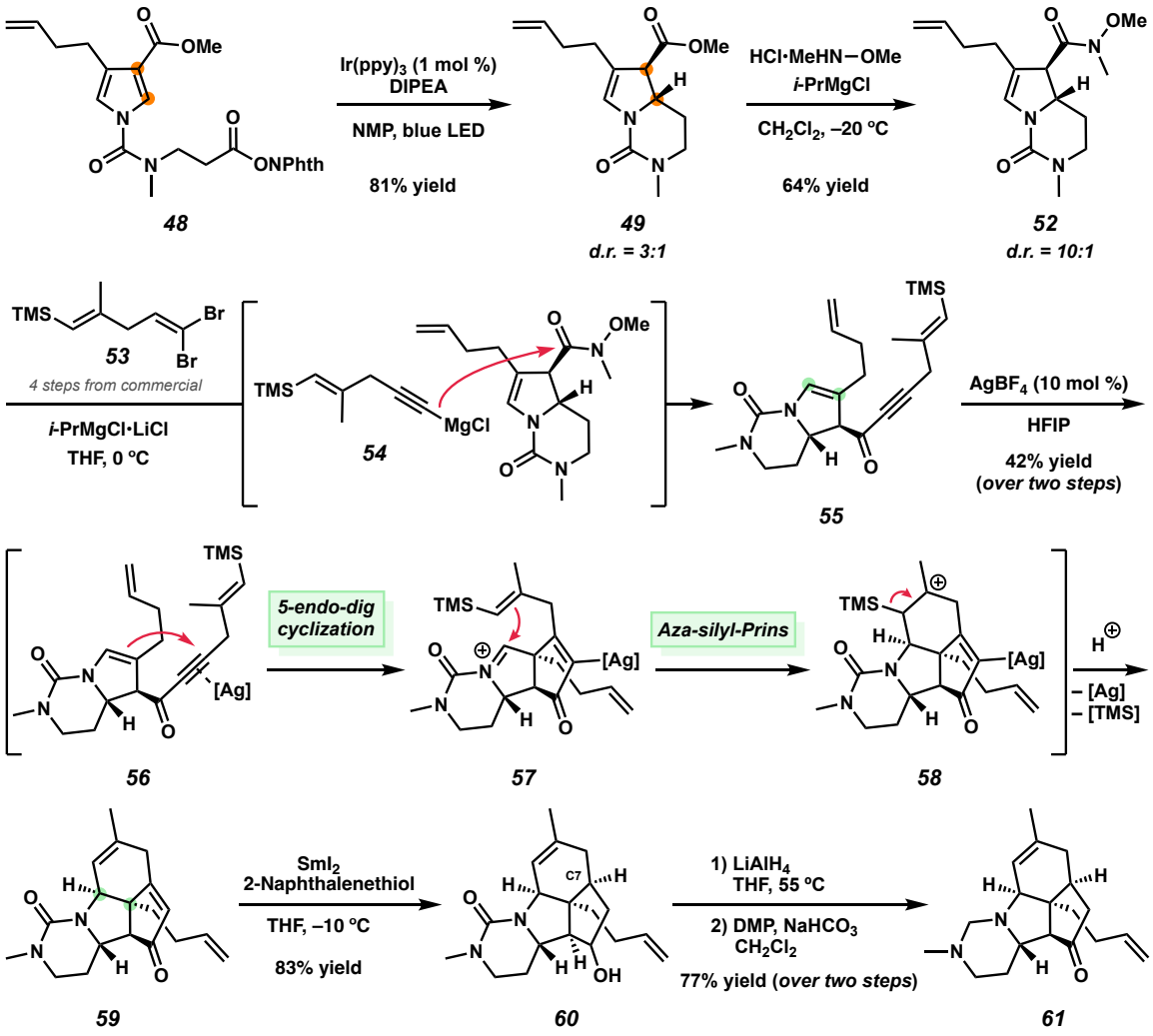
Entry	Catalyst	Additive	Solvent	*49* [e]	*50* [e]	*51* [e]
1 (R=H)	$Ir[dF(CF_3)ppy)]_2(dtbbpy)PF_6$	K_2HPO_4	DMF	-	5	-
2[a]	$Fe(NO_3)_3 \cdot 9\ H_2O$ (5 mol %) di(2-picolyl)amine (5.1 mol %)	TRIP disulfide (5 mol%), Na_2CO_3 (0.1 equiv)	DCE: H_2O (1:1)	-	25	25
3[b] (R=NPhth)	Eosin Y (10 mol %)	DIPEA (2.5 equiv)	CH_2Cl_2	-	10	-
4[c]	$Ni(acac)_2$ (2.0 equiv)	Zn (50 equiv), LiCl (20 equiv), 50°C	DMF	-	-	-
5[c]	$Ru(bpy)_3(PF_6)_2$	HE (1.5 equiv), DIPEA (2.0 equiv)	CH_2Cl_2	11	6	15
6[c]	$Ru(bpy)_3(PF_6)_2$	HE (1.5 equiv)	CH_2Cl_2	1	8	22
7[c]	$Ru(bpy)_3(PF_6)_2$	DIPEA (2.0 equiv)	CH_2Cl_2	10	7	11
8[c]	$Ru(bpy)_3(PF_6)_2$	DIPEA (2.0 equiv)	MeCN	8	12	10
9[c]	$Ru(bpy)_3(PF_6)_2$	DIPEA (2.0 equiv)	DMF	-	-	-
10[c]	$Ru(bpy)_3(PF_6)_2$	DIPEA (2.0 equiv)	DMA	11	24	12
11[c]	$Ru(bpy)_3(PF_6)_2$	DIPEA (2.0 equiv)	DMSO	18	32	11
12[c]	$Ru(bpy)_3(PF_6)_2$	DIPEA (2.0 equiv)	NMP	15	23	13
13[c]	$Ru(bpy)_3(PF_6)_2$	Et_3N (2.0 equiv)	DMSO	10	17	5
14[c]	$Ru(bpy)_3(PF_6)_2$	Et_3N (10.0 equiv)	DMSO	14	24	8
15[c]	$Ir(dtbbpy)(ppy)_2PF_6$	Et_3N (5.0 equiv)	DMSO	25	20	5
16[c]	$Ir(dtbbpy)(ppy)_2PF_6$	DIPEA (10.0 equiv)	DMSO	42[d]	35	4
17[c]	$Ir(ppy)_3$	DIPEA (10.0 equiv)	DMSO	53[d]	33	2
18[c]	$Ir(ppy)_3$	DIPEA (10.0 equiv)	NMP	81	10	3

Reactions were performed with 10 mg of starting material. Yield determined by ^{1}H-NMR with internal standard. [a]Irradiated with purple LED (390 nm); [b]Irradiated with CFL; [c]1 mol % catalyst used, irradiated with blue LED (450 nm); [d]200 mg scale, isolated yield, d.r. = 3:1; [e]Yield given in %.

2.4 ANNULATION CASCADE TO FORM THE CORE STRUCTURE

With the optimized conditions in hand, we could access dihydropyrrole **49** in high yield, setting the first two stereocenters of our synthesis (Scheme 2.4.1).

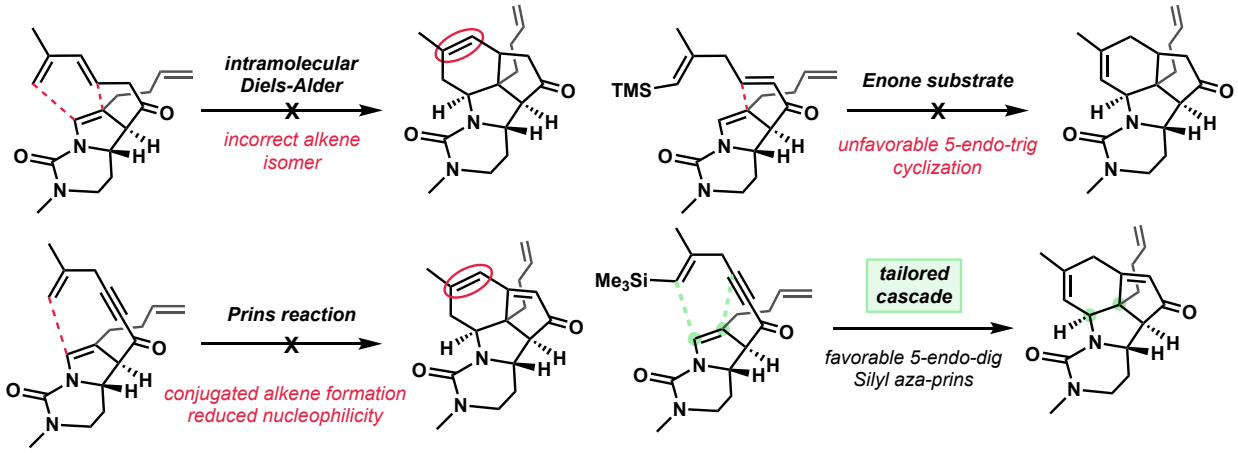
Scheme 2.4.1 *Synthetic sequence to access the Lycojapomine core structure.*



We observed preferential formation of the desired *trans* product (3:1 d.r.), which could be enriched upon isomerization under basic conditions. This proved to be inconsequential as Weinreb amide formation with *i*-PrMgCl formed **52** with a greater than 10:1 d.r. in 64% yield. With a functional electrophile for 1,2-addition (i.e. Weinreb amide **52**), we

envisioned introducing the alkyl chain to construct the cyclohexene moiety via an intramolecular annulation. While several different pathways could be imagined to construct the cyclohexene present in **59**, we were faced with several constraints (Figure 2.4.2). Mainly, Diels-Alder reaction would likely provide the wrong double bond isomer, and cyclization of the enamide onto an enone would require an unfavorable *5-endo-trig* cyclization.

Figure 2.4.2 *Potential pathways and considerations for cascade ring annulation.*



We therefore devised a tailored cascade, that would begin with constructing intermediate ynone **55** (Scheme 2.4.1). To do so, we utilized dibromide **53** as an alkyne precursor, which we accessed in four steps from commercial materials.[22,23] Dibromide **53** could successfully undergo Fritsch-Buttenberg-Wiechell rearrangement, to generate the metalated acetylide in-situ. We then introduced Weinreb amide **52** in the same step leading to nucleophilic addition and production of ynone **55**. With the use of *n*-BuLi, we observed diminished yields of product formation, likely due to the high basicity of the lithium acetylide. Isolating the alkyne before addition proved problematic, as rapid decomposition was observed. The use of the less basic turbo-Grignard (*i*PrMgCl·LiCl) significantly improved

the reaction profile,[24] as 1,2-shift was smoothly induced and addition of the acetylide **54** to form **55** proceeded without the formation of any significant side products. The ynone **55** was unstable upon purification on silica gel, which led to its direct use in the annulation cascade.

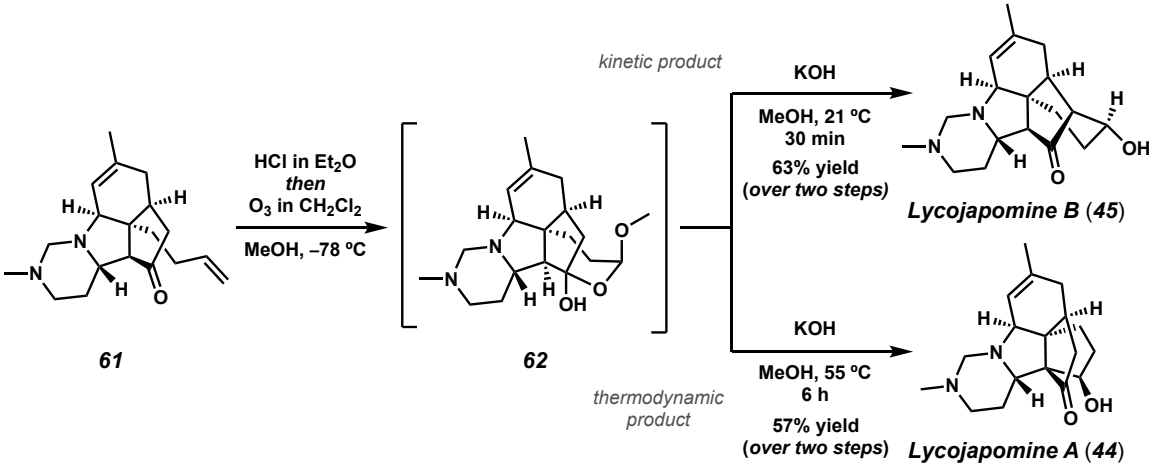
Having the alkyne preinstalled, we envisioned selective activation with metal π-acids.[25] While the use of gold catalysts did not provide any appreciable results, silver salts proved competent in the reaction with ynone **55**. Upon employing catalytic $AgBF_4$, the alkyne in **56** can be primed for *5-endo-dig* cyclization of the enamide, to reveal iminium ion **57**. The formation of the first 5/5 ring fusion is favored as the *cis* over the strained *trans* fused 5/5 system, directing the annulation to occur from the top-face of the molecule. Thus, the predominant formation of **57** leads to intramolecular Aza-Prins reaction with the vinyl silane from the same face. With carbocationic intermediate **58** being stabilized by the *β*-silicon effect, desilylation directs double bond formation to afford **59** with the alkene installed at the desired position. Forging three carbon-carbon bonds and two stereocenters, we isolate **59** as a single diastereomer in an appreciable yield of 42% over two steps from amide **52**. The use of hexafluroisopropanol (HFIP) proved essential to facilitate the cascade, acting as a proton source to turn over the catalyst and likely contributing to the stabilization of cationic intermediates.

With the tetracyclic core in hand, SmI_2 facilitated complete reduction of the cyclopentenone moiety to give **60** in 83% yield,[26] delivering the proton at C7 from the desired convex face with excellent diastereoselectivity. Reduction of the urea proceeded with lithium aluminum hydride and oxidation of the cyclopentanol delivered tetracyclic ketone **61** in 77% yield over two steps.

2.5 DIVERGENT ALDOL REACTION AND COMPLETION OF THE SYNTHESIS

With the pendant terminal alkene present in **61**, we envisioned chemoselective oxidative cleavage and subsequent aldol reaction, proposing to access both isomers (Lycojapomine A and B) by control of enolate formation. Careful reaction control enabled selective oxidation of the terminal (over the tri-substituted) alkene, but revealed significant instability of the expected aldehyde, which rapidly decomposed. Due to the potential susceptibility of the hexahydro pyrimidine to oxidation, we decided to protonate it as an HCl salt that could be used directly in the subsequent oxidation. Dihydroxylation with OsO_4 proceeded to generate the corresponding diol, however concurrent oxidative cleavage only resulted in decomposition. We ultimately succeeded by trapping out the unstable aldehyde as the methanol adduct following ozonolysis, yielding an isolable product, the structure of which is proposed to be **62** (Scheme 2.5.1). By titrating a saturated solution of ozone into the reaction at cryogenic temperatures, we could achieve excellent selectivity to access the oxidized intermediate in high yield.[27]

Scheme 2.5.1 *Oxidative cleavage and divergent aldol reaction to access* ***44*** *and* ***45****.*



To complete the synthesis, we attempted a range of aldol reactions of **62**. Initially, treatment of **62** with various mild bases (i.e. DBU, Et_3N, K_2CO_3, Cs_2CO_3 etc.) led to non-specific decomposition. Alternatively, exposing **62** to acid resulted in recovery of starting material. Interestingly, upon exposure to methanolic potassium hydroxide, we can direct clean and selective collapse of **62** to Lycojapomine B (**45**) in 63% yield over two steps, without observing **44**. While different conditions did not lead to the formation of Lycojapomine A (**44**), we found that simply heating the solution of **62** in KOH/MeOH for an extended period exclusively delivered **44** in 57% yield over two steps, likely proceeding through an aldol/retro-aldol mechanism. In a control experiment, heating a solution of **45** in KOH/MeOH cleanly converted the natural product to its isomer **44**. We achieved precise control, funneling aldol product formation to either the kinetic or thermodynamic product, attributing this selectivity to the lower ground-state energy of **44**. Overall, we can successfully access both natural products **44** and **45** in excellent yields, highlighting the power of late stage divergency in our retrosynthesis.

2.6 CONCLUSION

Previous syntheses of complex alkaloids and related natural products have often relied on aliphatic precursors, that can be tedious to prepare and often necessitate protecting groups to mask reactive functional groups. The retrosynthetic approach that is disclosed instead begins with a sp^2-hybridized aromatic nitrogen heterocycle. This strategy is enabled by a photo-induced radical cyclization to selectively dearomatize a pyrrole, manipulating its inherent reactivity. Utilizing the generated enamine, we achieve a silver-catalyzed cyclization cascade to annulate two rings and assemble the core carbon framework in a

single step. By controlling divergent product formation of a late-stage aldol reaction, we can access both Lycojapomine A and B in 13 steps from commercial starting materials. We believe this concept of sequential pyrrole functionalization can be applied in different settings and enables a new retrosynthetic tool for the synthesis of different members of the Lycopodium alkaloids.

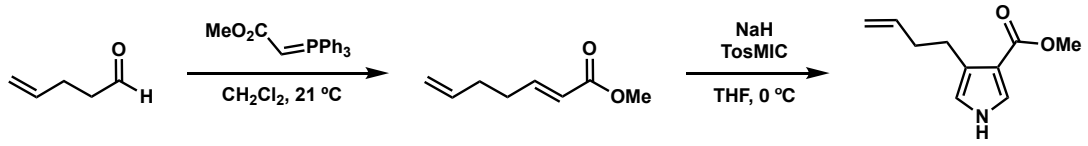
2.7 EXPERIMENTAL SECTION

2.7.1 MATERIALS AND METHODS

Unless otherwise stated, reactions were performed in flame-dried glassware under an argon or nitrogen atmosphere using dry, deoxygenated solvents. Solvents were dried by passage through an activated alumina column under argon.[28] Reaction progress was monitored by thin-layer chromatography (TLC). TLC was performed using E. Merck silica gel 60 F254 precoated glass plates (0.25 mm) and visualized by UV fluorescence quenching, p-anisaldehyde, or $KMnO_4$ staining. Silicycle SiliaFlash® P60 Academic Silica gel (particle size 40–63 μm) was used for flash chromatography. ^{1}H NMR spectra were recorded on Varian Inova 500 MHz and 600 MHz and Bruker 400 MHz spectrometers and are reported relative to residual $CHCl_3$ (δ 7.26 ppm), C_6D_6 (δ 7.16 ppm) or CD3OD (δ 3.31 ppm). ^{13}C NMR spectra were recorded on a Varian Inova 500 MHz spectrometer (125 MHz) and Bruker 400 MHz spectrometers (100 MHz) and are reported relative to $CHCl_3$ (δ 77.16 ppm), C_6D_6 (δ 128.06 ppm) or CD_3OD (δ 49.01 ppm). Data for ^{1}H NMR are reported as follows: chemical shift (δ ppm) (multiplicity, coupling constant (Hz), integration). Multiplicities are reported as follows: s = singlet, d = doublet, t = triplet, q = quartet, p = pentet, sept = septuplet, m = multiplet, br s = broad singlet, br d = broad doublet. Data for

^{13}C NMR are reported in terms of chemical shifts (δ ppm). IR spectra were obtained by use of a Perkin Elmer Spectrum BXII spectrometer or Nicolet 6700 FTIR spectrometer using thin films deposited on NaCl plates and reported in frequency of absorption (cm^{-1}). Optical rotations were measured with a Jasco P-2000 polarimeter operating on the sodium D-line (589 nm), using a 100 mm path- length cell. High resolution mass spectra (HRMS) were obtained using an Agilent 6200 Series TOF with an Agilent G1978A Multimode source in electrospray ionization (ESI+) mode.

2.7.2 EXPERIMENTAL PROCEDURES

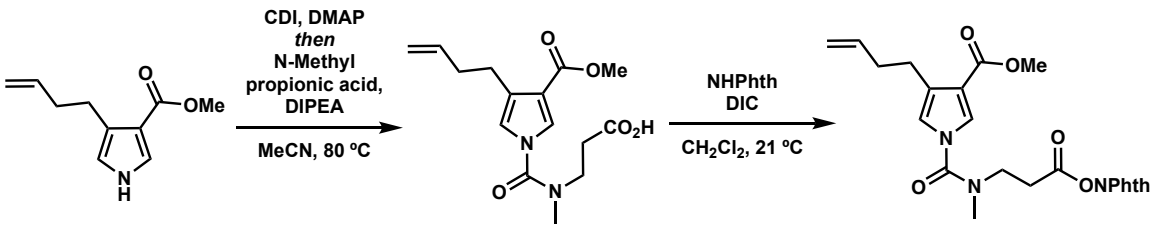


63 ***64*** ***46***

Ester 64: In a round-bottom flask, Aldehyde **63** (24.4 g, 0.29 mol, 1.0 equiv) was dissolved in CH_2Cl_2 (1.1 L, 0.25 M) and Methyl(triphenylphosphoranylidene)acetate (106 g, 0.32 mol, 1.1 equiv) was added portionwise. The reaction was stirred for 15 h, after which no more starting material was present as determined by TLC analysis. A mixture of Et_2O and hexanes (1:1, 500 mL) was added, upon which a white solid crashed out ($O=PPh_3$). The mixture was filtered, and the filtrate concentrated under reduced pressure. The crude oil was purified by flash column chromatography on silica gel (10% Et_2O/hexanes) to yield Ester **64** (38 g, 0.27 mol, 93% yield) as a colorless oil. *The spectroscopic data was in accordance with the values previously reported in the literature*;[29] ^1H NMR (500 MHz, $CDCl_3$) δ 6.98 (dt, *J* = 16.0 Hz, 6.5 Hz, 1H), 5.84 (d, *J* = 16.0 Hz, 1H), 5.79 (ddt, *J* = 16.5

Hz, 10.0 Hz, 6.5 Hz, 1H), 5.05 (dd, J = 16.5 Hz, 2.0 Hz, 1H), 5.00 (dd, J = 10.0 Hz, 2.0 Hz, 1H), 3.72 (s, 3H), 2.31 – 2.29 (m, 2H), 2.24 – 2.21 (m, 2H).

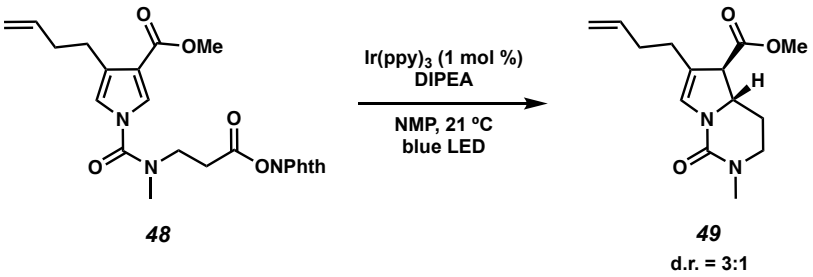
Pyrrole 46: In a flame dried round-bottom flask under N_2, NaH (60% in mineral oil, 2.86 g, 71.4 mmol, 2.0 equiv) was dissolved in THF (35.7 mL, 1M). The reaction mixture was cooled to 0 °C in an ice bath, and a solution of Ester **64** (5.0 g, 35.7 mmol, 1.0 equiv) and TosMIC (7.3 g, 37.5 mmol, 1.05 equiv) in THF (37.5 mL, 1M) was added semi-dropwise. Upon completion of addition, the reaction was stirred for 30 min and the ice bath removed. After 13 h, the starting material was consumed as determined by TLC analysis and saturated aqueous $NaHCO_3$ was added. The aqueous layer was extracted with EtOAc (3x), the combined organic extracts dried over Na_2SO_4 and concentrated under reduced pressure. The crude product was purified by flash column chromatography on silica gel (30% EtOAc/hexanes) and the product **46** (5.1 g, 28.6 mmol, 80% yield) isolated as a pale-yellow solid; ^{1}H NMR (400 MHz, $CDCl_3$) δ 8.45 (brs, 1H), 7.38 (dd, J = 3.2, 2.2 Hz, 1H), 6.56 (s, 1H), 5.89 (ddt, J = 16.9, 10.3, 6.6 Hz, 1H), 5.20 – 4.90 (m, 1H), 3.80 (s, 3H), 2.87 – 2.80 (m, 2H), 2.36 (tdt, J = 7.8, 6.4, 1.4 Hz, 2H); ^{13}C NMR (101 MHz, $CDCl_3$) δ 165.9, 139.0, 125.7, 124.7, 117.0, 114.5, 114.1, 50.9, 34.5, 25.7; IR (neat film, NaCl) 3272, 2916, 1686, 1436, 1398, 1338, 1236, 1160, 1090, 918, 743 cm^{-1}; HRMS (ESI+): m/z calc'd for $C_{10}H_{14}NO_2$ $[M+H]^+$: 180.1019, found 180.1020.



Carboxylic acid 47: A round-bottom flask equipped with a reflux condenser was flushed with Argon, and charged with pyrrole **46** (4.82 g, 26.8 mmol, 1.0 equiv). Acetonitrile (107 mL, 0.25 M) was added, followed by CDI (6.54 g, 40.2 mmol, 1.5 equiv) and DMAP (326 mg, 0.1 mmol, 0.1 equiv). The reaction flask was heated to 80 °C for 3 h, after which it was cooled to ambient temperature. N-Methyl propionic acid (5.38 g, 53.6 mmol, 2.0 equiv) and *i*Pr_2EtN (4.65 mL, 80.3 mmol, 3.0 equiv) were added and the flask heated to 80 °C for 12 h. The reaction mixture was cooled to ambient temperature, quenched with 1M aqueous HCl and the aqueous layer extracted with EtOAc (3x). The combined organic extracts were dried over Na_2SO_4 and concentrated under reduced pressure. The crude product was separated from left-over starting material **46** (1.4 g, 8.0 mmol, 30% yield) by flash column chromatography on silica gel (30% EtOAc/hexanes → 1% AcOH/10% MeOH/CH_2Cl_2) to provide carboxylic acid **47** (5.4 g, 17.5 mmol, 66% yield) which was used in the next step without further purification. *The yield for **47** was calculated based on an 80% purity of the crude product as determined by quantitative 1H-NMR with 1,3,5-trimethoxybenzene as an internal standard*.

N-Hydroxy phthalimide ester 48: Crude carboxylic acid **47** (5.9 g, *~80% purity*) was placed in a round-bottom flask and dissolved in CH_2Cl_2 (87 mL, 0.2 M). N-Hydroxy phthalimide (3.1 g, 19.3 mmol, 1.1 equiv) and DMAP (106 mg, 0.87 mmol, 0.05 equiv) were added, after which DIC (3.56 mL, 22.8 mmol, 1.3 equiv) was added semi-dropwise. Upon addition was finished, the reaction mixture was stirred for 15 min, after which it was directly loaded onto a flash column with silica gel for purification (33% EtOAc/hexanes). The N-Hydroxy phthalimide ester **48** (5.7 g, 12.6 mmol, 72% yield) was isolated as a white solid. *It is noteworthy to point out that prolonged reaction time led to significant*

*decomposition and lower isolated yields of the product **48**;* ^{1}H NMR (400 MHz, $CDCl_3$) δ^{1}H NMR (400 MHz, $CDCl_3$) δ 7.89 (dd, *J* = 5.6, 3.0 Hz, 2H), 7.82 – 7.79 (m, 2H), 7.66 (d, *J* = 2.4 Hz, 1H), 6.86 (dt, *J* = 2.1, 1.0 Hz, 1H), 5.87 (ddt, *J* = 16.9, 10.2, 6.6 Hz, 1H), 5.04 (dd, *J* = 17.1, 1.9 Hz, 1H), 4.97 – 4.93 (m, 1H), 3.86 (t, *J* = 6.5 Hz, 2H), 3.79 (s, 3H), 3.19 (s, 3H), 3.08 (t, *J* = 6.5 Hz, 2H), 2.80 (td, *J* = 7.5, 1.0 Hz, 2H), 2.36 (dd, *J* = 7.7, 1.4 Hz, 2H); ^{13}C NMR (101 MHz, $CDCl_3$) δ 168.1, 164.9, 161.8, 153.7, 138.6, 135.0, 128.9, 127.0, 126.6, 124.2, 119.3, 116.6, 114.8, 51.1, 46.4, 38.9, 33.9, 29.6, 25.6; IR (neat film, NaCl) 2947, 1814, 1787, 1745, 1708, 1520, 1486, 1399, 1371, 1243, 1186, 1150, 1081, 973, 698 cm^{-1}; HRMS (ESI+): m/z calc'd for $C_{23}H_{24}N_3O_7$ $[M+H]^+$: 454.1614, found 454.1645.



48 ***49***

d.r. = 3:1

Dihydropyrrole 49: A 50 mL eggplant-shaped flask was charged with a magnetic stir bar, **48** (200 mg, 0.44 mmol, 1.0 equiv) and $Ir(ppy_3)$ (2.9 mg, 0.004 mmol, 1 mol %) and sealed with a rubber septum. The flask was evacuated and backfilled with N_2 (3x), after which the solids were dissolved in NMP (8.8 mL, 0.05 M). The solution was degassed by placing the flask under vacuum for 15 min and backfilled with N_2. Freshly distilled *i*Pr_2EtN (0.77 mL, 4.4 mmol, 10 equiv) was added and the septum secured and covered with electrical tape. The reaction flask was fastened in a Penn PhD Photoreactor M2 with copper wire (~1.5 cm above the light source) and irradiated with blue LEDs for 10h (450 nm, 1000 rpm, 6870

fan, 100% LED intensity). The flask was removed from the photoreactor and the solvent removed under reduced pressure. The crude product was purified by flash column chromatography on silica gel (33% acetone/hexanes) to deliver the product **49** (94 mg, 0.36 mmol, 81% yield) in a diastereomeric ratio of 3:1 (trans:cis) as a yellow oil. *The diastereomers were separated on preparative HPLC (Agilent Zorbax Eclipse XDB-C18 column, 5 μm, 32% MeCN/H_2O + 1% AcOH) and assigned based on the NOE as observed by 2D-NOESY NMR analysis*.

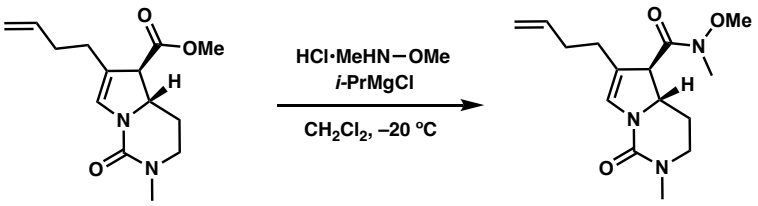
Major diastereomer of **49** (*trans*):

^{1}H NMR (600 MHz, $CDCl_3$) δ 6.58 (d, *J* = 2.0 Hz, 1H), 5.86 – 5.69 (m, 1H), 5.02 (dd, *J* = 17.2, 1.7 Hz, 1H), 4.96 (ddd, *J* = 10.2, 1.7, 1.1 Hz, 1H), 4.40 (ddd, *J* = 11.8, 9.6, 3.4 Hz, 1H), 3.75 (s, 3H), 3.66 – 3.57 (m, 1H), 3.40 (td, *J* = 12.3, 4.2 Hz, 1H), 3.18 (ddd, *J* = 12.0, 5.3, 1.8 Hz, 1H), 2.94 (s, 3H), 2.30 – 2.14 (m, 3H), 2.13 – 2.04 (m, 2H), 1.88 (qd, *J* = 12.5, 5.4 Hz, 1H); ^{13}C NMR (101 MHz, $CDCl_3$) δ 172.5, 151.9, 138.0, 127.0, 116.8, 115.2, 59.7, 57.3, 52.4, 47.4, 34.9, 31.7, 27.9, 26.6; IR (neat film, NaCl) 3346, 2937, 1732, 1536, 1510, 1443, 1405, 1335, 1236, 914, 740 cm^{-1}; HRMS (ESI+): m/z calc'd for $C_{14}H_{21}N_2O_3$ $[M+H]^+$: 265.1552, 265.1551 found.

Minor diastereomer of **49** (*cis*):

^{1}H NMR (400 MHz, $CDCl_3$) δ 6.67 (d, *J* = 1.8 Hz, 1H), 5.98 – 5.62 (m, 1H), 5.02 (dd, *J* = 17.1, 1.6 Hz, 1H), 4.96 (d, *J* = 10.5 Hz, 1H), 4.25 (ddd, *J* = 12.2, 10.5, 3.5 Hz, 1H), 3.69 (s, 3H), 3.62 (d, *J* = 10.4 Hz, 1H), 3.35 (td, *J* = 12.2, 4.2 Hz, 1H), 3.20 (ddd, *J* = 12.1, 5.3, 2.0 Hz, 1H), 2.92 (s, 3H), 2.28 – 2.13 (m, 3H), 2.08 (dd, *J* = 12.0, 6.4 Hz, 1H), 2.01 (d, *J* = 12.8 Hz, 1H), 1.87 (qd, *J* = 12.4, 5.3 Hz, 1H); ^{13}C NMR (101 MHz, $CDCl_3$) δ 171.3, 151.9, 138.0, 127.9, 117.7, 115.2, 58.6, 54.7, 52.0, 47.5, 34.8, 32.0, 26.9, 24.2; IR (neat

film, NaCl) 3339, 2922, 1689, 1505, 1452, 1406, 1330, 1249, 1082, 996, 913, 743 cm^{-1}; HRMS (ESI+): m/z calc'd for $C_{14}H_{21}N_2O_3$ $[M+H]^+$: 265.1552, 265.1548 found.

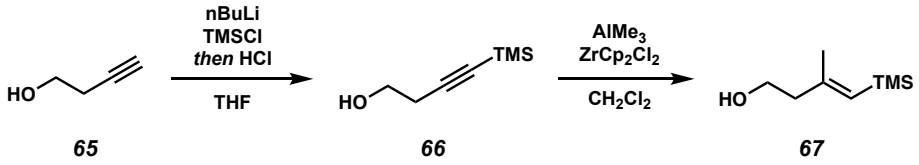


49
d.r. = 3:1

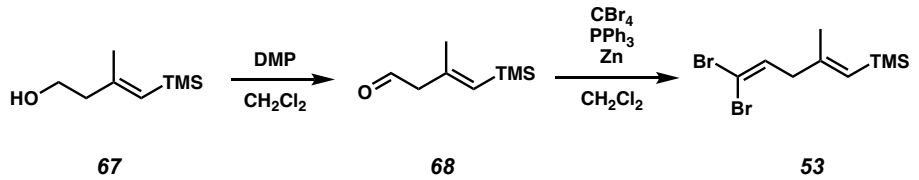
52
d.r. = 10:1

Amide 52: A flame-dried vial under N_2 was charged with ester **49** (278 mg, 1.05 mmol, 1.0 equiv) and HN(Me)OMe·HCl (153 mg, 1.58 mmol, 1.5 equiv). The reactants were dissolved in THF (3.5 mL, 0.3 M) and the vial cooled to –35 °C in an acetonitrile/dry ice bath. A solution of *i*-PrMgCl (2M in THF, 2.1 mL, 4.2 mmol, 4.0 equiv) was added dropwise and the reaction mixture stirred for 1.5 h. After this time the cooling bath had reached a temperature of –10 °C and the starting material was consumed as determined by TLC analysis. The reaction was quenched by addition of saturated aqueous NH_4Cl (0.5 mL), filtered through a plug of Na_2SO_4 and loaded directly onto a flash column with silica gel for purification (60% acetone/hexanes). The amide **52** (196 mg, 0.67mmol, 64% yield) was isolated as a white film; ^1H NMR (400 MHz, C_6D_6) δ 6.99 (s, 1H), 5.80 – 5.65 (m, 1H), 5.00 (dd, *J* = 17.1, 1.9 Hz, 1H), 4.96 – 4.91 (m, 1H), 4.40 (ddd, *J* = 11.6, 9.9, 3.8 Hz, 1H), 3.86 (d, *J* = 10.1 Hz, 1H), 2.97 (s, 3H), 2.86 (s, 3H), 2.76 (s, 3H), 2.52 (td, *J* = 12.0, 4.4 Hz, 1H), 2.34 (ddd, *J* = 11.8, 5.1, 2.0 Hz, 1H), 2.18 – 2.04 (m, 4H), 1.40 – 1.34 (m, 1H), 1.30 (td, *J* = 12.1, 5.2 Hz, 1H); ^{13}C NMR (101 MHz, C_6D_6) δ 173.1, 151.6, 138.5, 118.3, 117.2, 115.0, 60.9, 60.8, 58.6, 54.7, 47.0, 34.6, 32.1, 27.7, 27.0; IR (neat film, NaCl)

2926, 1647, 1504, 1453, 1398, 1078 cm^{-1}; HRMS (ESI+): m/z calc'd for $C_{15}H_{24}N_3O_3$ $[M+H]^+$: 294.1818, found 294.1823.

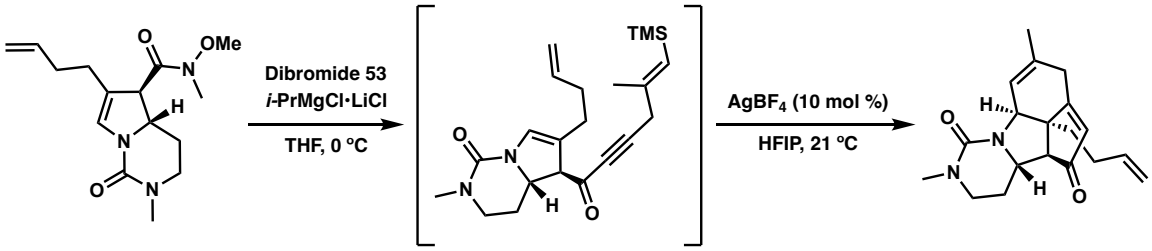


Vinylsilane 67: Vinylsilane **67** was prepared according to literature procedures in two steps from 3-Butin-1-ol **65**.[30,31] *The spectroscopic data for **67** was in accordance with the values previously reported in the literature*; ^1H NMR (500 MHz, $CDCl_3$) δ 5.30 (s, 1H), 3.71 (t, *J* = 7.2 Hz, 2H), 2.35 (t, *J* = 7.2 Hz, 2H), 1.80 (s, 3H), 1.60 (bs, 1H), 0.12 (s, 9H).



Aldehyde 68: A round-bottom flask was charged with alcohol **67** (948 mg, 6 mmol, 1.0 equiv) and CH_2Cl_2 (60 mL, 0.1 M). Dess-Martin periodinane (2.8 g, 6.6 mmol, 1.1 equiv) was added portion wise and the reaction stirred for 45 min until the starting material was consumed as determined by TLC analysis. The reaction was concentrated to near dryness under reduced pressure and the crude product filtered over a plug of silica gel eluting with pentane. The solvent was evaporated to near dryness under reduced pressure and the solution of aldehyde **68** was directly used in the next step without further purification. *Aldehyde **68** proved to be inherently volatile and was therefore only concentrated under slightly reduced pressure to avoid diminished yields.*

Dibromide 53: A flame-dried round-bottom flask under N_2 was charged with Zn powder (780 mg, 12 mmol, 2.0 equiv), carbon tetrabromide (3.97 g, 12 mmol, 2.0 equiv) and PPh_3 (3.14 g, 12 mmol, 2.0 equiv). The contents were dissolved in CH_2Cl_2 (17 mL, 0.35 M) and vigorously stirred for 16 h, upon which the reaction mixture had turned to a pastel light pink color. The aldehyde **68** was added as a solution with CH_2Cl_2 and the reaction stirred for 2 hours. After the starting material was consumed as determined by TLC analysis, the reaction mixture was diluted with pentanes and flushed over a plug of celite. The solvent was removed under reduced pressure and the crude product purified by flash column chromatography on silica gel (pentane). The dibromide **53** (1.0 g, 3.3 mmol, 55% yield over two steps) was isolated as a colorless oil. *Dibromide **53** proved to be volatile under high vacuum and unstable upon extended storage at –20 °C. It was therefore used in the following reaction on the same day*; ^{1}H NMR (400 MHz, $CDCl_3$) δ 6.42 (t, *J* = 7.4 Hz, 1H), 5.25 (q, *J* = 1.1 Hz, 1H), 2.85 (dd, *J* = 7.4, 1.3 Hz, 2H), 1.79 (d, *J* = 1.0 Hz, 3H), 0.11 (s, 9H); ^{13}C NMR (101 MHz, $CDCl_3$) δ 149.9, 136.6, 125.9, 90.0, 45.7, 21.9, 0.1; IR (neat film, NaCl) 2953, 1700, 1427, 1249, 844, 780 cm^{-1}; HRMS (ESI+): m/z calc'd for $C_9H_{17}Br_2Si$ $[M+H]^+$: 310.9466, found 310.9462.

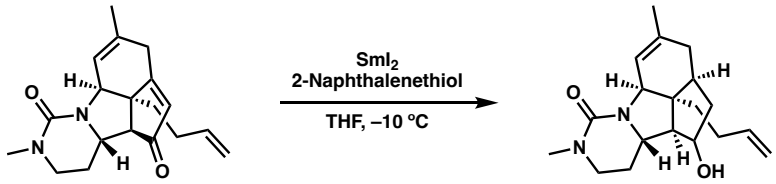


Tetracycle 59: A flame-dried vial under N_2 was charged with dibromide **53** (231 mg, 0.74 mmol, 1.5 equiv) and THF (1.65 mL, 0.3 M). The vial was placed in an ice bath at 0 °C

and a solution of *i*PrMgCl·LiCl (1.3 M in THF, 1.52 mL, 1.98 mmol, 4.0 equiv) was added dropwise. The reaction was stirred for 1 h, after which a solution of starting material **52** (145 mg, 0.49 mmol, 1.0 equiv) in THF (1.5 mL) was added semi-dropwise. The reaction was stirred for an additional hour at 0 °C, after which it was quenched with saturated aqueous NH_4Cl (0.5 mL) and warmed to ambient temperature. The reaction mixture was diluted with EtOAc, filtered over a plug of Na_2SO_4 and celite, and the solvent evaporated under reduced pressure. The crude product **55** was obtained as a brown oil and directly used in the next step without further purification.

The intermediate **55** was transferred into a vial and moved into a glovebox under N_2. $AgBF_4$ (9.6 mg, 0.049 mmol, 0.1 equiv) was added and the reactants dissolved in HFIP (9.9 mL, 0.05 M). The reaction was transferred outside the glovebox and stirred for an additional 30 min. Upon full consumption of the starting material as determined by LC-MS, the reaction was diluted with saturated aqueous NH_4Cl and the aqueous layer extracted with EtOAc (4x). The combined organic extracts were dried over Na_2SO_4 and the solvent evaporated under reduced pressure. The crude product was purified by flash chromatography on silica gel (33% acetone/hexanes) to yield the product **59** (65.5 mg, 0.21 mmol, 42% yield) as an off-white solid; ^{1}H NMR (400 MHz, $CDCl_3$) δ 5.98 (ddt, *J* = 3.8, 3.0, 1.5 Hz, 1H), 5.80 (s, 1H), 5.72 (ddt, *J* = 17.2, 10.3, 5.9 Hz, 1H), 5.02 – 4.89 (m, 2H), 4.38 (s, 1H), 3.46 (ddd, *J* = 11.6, 8.1, 3.9 Hz, 1H), 3.26 (td, *J* = 12.3, 3.4 Hz, 1H), 3.13 (ddd, *J* = 12.1, 4.9, 2.2 Hz, 1H), 3.01 – 2.96 (m, 2H), 2.91 (s, 3H), 2.50 (d, *J* = 7.9 Hz, 1H), 2.24 (dtd, *J* = 12.9, 3.6, 2.2 Hz, 1H), 1.88 – 1.83 (m, 4H), 1.82 (s, 3H), 1.78 – 1.68 (m, 1H); ^{13}C NMR (101 MHz, $CDCl_3$) δ 206.3, 179.4, 154.6, 137.1, 132.4, 125.0, 122.6, 115.7, 62.9, 62.5, 58.5, 55.6, 47.2, 35.9, 35.1, 32.3, 29.7, 28.4, 23.6; IR (neat film, NaCl) 2922, 1695, 1634, 1503, 1446

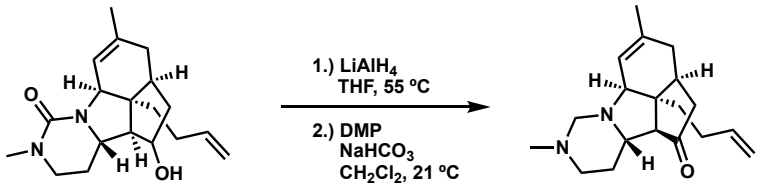
cm^{-1}; HRMS (ESI+): m/z calc'd for $C_{19}H_{25}N_2O_2$ $[M+H]^+$: 313.1916, found 313.1950.



59 ***60***

Alcohol 60: A vial under N_2 was charged with enone **59** (37 mg, 0.12 mmol, 1.0 equiv) and 2-Naphthalenethiol (381 mg, 2.4 mmol, 20.0 equiv) and the reactants dissolved in THF (2.4 mL, 0.05 M). The vial was cooled to –10 °C in a brine/ice bath and a solution of SmI_2 in THF (0.1 M, 11.9 mL, 1.19 mmol, 10.0 equiv) was added dropwise over the course of 1 h via syringe pump. Upon completion of addition, the ice bath was removed and the reaction stirred for an additional 30 minutes at ambient temperature. The reaction was quenched with a 1:1 mixture of aqueous saturated $Na_2S_2O_3$ and hexanes, the aqueous layer extracted with EtOAc (3x), the combined organic extracts dried over Na_2SO_4 and concentrated under reduced pressure. The crude product was purified by flash column chromatography on silica gel (50% acetone/hexanes) to yield the alcohol **60** (31.3 mg, 0.099 mmol, 83% yield) as a colorless foam; ^{1}H NMR (400 MHz, $CDCl_3$) δ 5.75 (ddt, *J* = 16.8, 10.2, 6.5 Hz, 1H), 5.57 – 5.46 (m, 1H), 4.98 (dd, *J* = 17.1, 1.7 Hz, 1H), 4.91 (dd, *J* = 10.2, 1.7 Hz, 1H), 4.25 (s, 1H), 4.24 – 4.12 (m, 1H), 3.60 (ddd, *J* = 10.8, 8.5, 3.9 Hz, 1H), 3.31 (td, *J* = 12.3, 3.8 Hz, 1H), 3.07 (ddd, *J* = 11.9, 5.0, 2.1 Hz, 1H), 2.91 (s, 3H), 2.44 (brs, 1H), 2.27 – 2.12 (m, 2H), 2.11 – 1.87 (m, 5H), 1.84 – 1.73 (m, 2H), 1.69 (s, 3H), 1.67 – 1.60 (m, 1H), 1.55 (dd, *J* = 9.5, 7.3 Hz, 2H); ^{13}C NMR (101 MHz, $CDCl_3$) δ 155.0, 138.6, 133.8, 122.9, 114.6, 71.5, 62.4, 59.8, 55.9, 51.3, 47.5, 42.6, 39.7, 37.7, 34.9, 30.6, 29.9,

29.6, 24.2; IR (neat film, NaCl) 2920, 2852, 1734, 1636, 1506, 1444, 1073, 802 cm^{-1}; HRMS (ESI+): m/z calc'd for $C_{19}H_{29}N_2O_2$ $[M+H]^+$: 317.2224, found 317.2107.

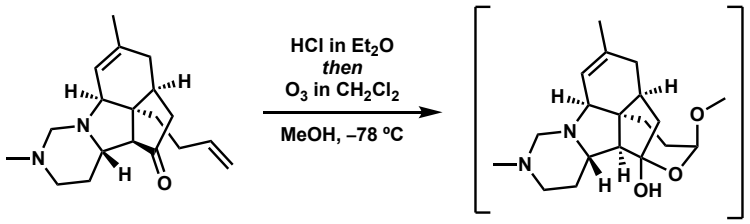


60 ***61***

Ketone 61: A vial under N_2 was charged with starting material **60** (31.3 mg, 0.099 mmol, 1.0 equiv) and THF (3.3 mL, 0.03 M). $LiAlH_4$ (22.5 mg, 0.59 mmol, 6.0 equiv) was added in one portion, the reaction vial sealed and placed in a heating block at 55 °C. After 2 h, the starting material had been consumed as determined by LC-MS analysis and the reaction cooled to 0 °C. The reaction was quenched with saturated aqueous $NaHCO_3$ (0.3 mL) and diluted with CH_2Cl_2. The contents were filtered over a plug of Na_2SO_4 and celite and the solvent evaporated under reduced pressure. The crude product was used in the next step without further purification.

The intermediate was dissolved in CH_2Cl_2 (2 mL, 0.05 M) and $NaHCO_3$ (25 mg, 0.297 mmol, 3.0 equiv) and Dess-Martin periodinane (45 mg, 0.129 mmol, 1.3 equiv) were added sequentially. After 1 h, full consumption of starting material was observed by LC-MS analysis and the reaction mixture directly loaded onto a flash column packed with silica gel for purification (3-5% MeOH/CH_2Cl_2 + 0.1% NH_4OH). The product **61** (23 mg, 0.077 mmol, 77% yield over two steps) was isolated as a pale yellow solid; ^1H NMR (600 MHz, CD_3OD) δ 5.84 (ddt, *J* = 16.8, 10.1, 6.5 Hz, 1H), 5.73 – 5.65 (m, 1H), 5.04 (dd, *J* = 17.1, 1.8 Hz, 1H), 4.95 (dd, *J* = 10.2, 1.7 Hz, 1H), 3.97 (dd, *J* = 12.1, 2.0 Hz, 1H), 3.65 (d, *J* =

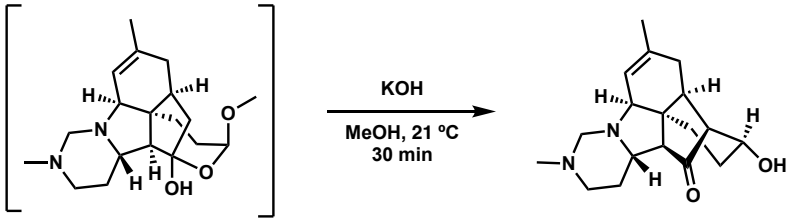
4.1 Hz, 1H), 3.28 (dd, *J* = 12.4, 3.9 Hz, 1H), 3.17 (d, *J* = 12.2 Hz, 1H), 3.05 (d, *J* = 11.4 Hz, 1H), 2.50 – 2.41 (m, 1H), 2.37 – 2.24 (m, 5H), 2.22 (s, 3H), 2.19 – 2.09 (m, 2H), 2.05 – 1.97 (m, 1H), 1.95 (dd, *J* = 13.1, 4.1 Hz, 1H), 1.87 – 1.79 (m, 2H), 1.77 (s, 3H), 1.51 (dq, *J* = 13.5, 3.0 Hz, 1H); ^{13}C NMR (101 MHz, CD_3OD) δ 221.8, 139.8, 135.5, 120.1, 115.1, 70.5, 64.0, 62.3, 61.8, 55.9, 50.8, 46.0, 42.5, 41.6, 36.9, 32.0, 30.7, 27.3, 24.2; IR (neat film, NaCl) 3382, 2921, 1694, 1632, 1503, 1450, 1309, 1092 cm^{-1}; HRMS (ESI+): m/z calc'd for $C_{19}H_{29}N_2O$ $[M+H]^+$: 301.2280, found 301.2353.



61 ***62***

Compound 62: In a vial, starting material **61** (10 mg, 0.033 mmol, 1.0 equiv) was dissolved in CH_2Cl_2 (0.5 mL) and HCl (1M in Et_2O, 0.04 mL, 1.2 equiv) was added dropwise. The solvent was evaporated under reduced pressure, leaving behind a white salt. The contents were dissolved in MeOH (0.66 mL, 0.05 M) and the vial flushed and equipped with an argon balloon (*This step was done to avoid excess condensation of water during the reaction*). The vial was cooled at –78 °C in a dry ice/acetone bath. Simultaneously, ozone was bubbled through a test tube filled with CH_2Cl_2 at –78 °C for 3 min, to create a saturated solution, as indicated by the blue color. The saturated solution of ozone in CH_2Cl_2 (~1.5 mL) was added to the reaction mixture portion wise (0.1–0.5 mL). The reaction was carefully monitored by TLC analysis (10% MeOH/CH_2Cl_2 + 1% Et_3N) every 5 minutes after addition, until the starting material had been completely consumed. $P(OMe)_3$ (0.3 mL)

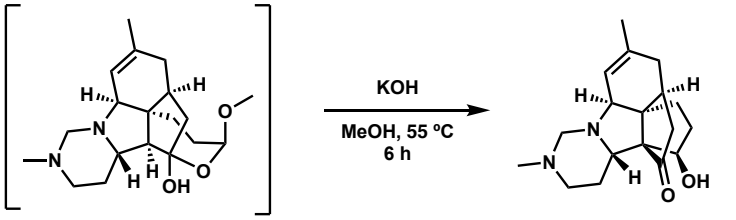
and Et_3N (0.5 mL) were added, the reaction warmed to ambient temperature and stirred for 2 h. The volatiles were removed under reduced pressure and the residue purified by flash column chromatography on silica gel (10% MeOH/CH_2Cl_2 + 1% Et_3N) to give crude intermediate **62** (7.7 mg) as a colorless film. *Intermediate **62** proved to be unstable and decomposed upon extended storage. It was therefore used on the same day in the following reaction*.



62 ***Lycojapomine B (45)***

Lycojapomine B: A vial was charged with starting material **62** (4.0 mg, 0.01 mmol, 1.0 equiv), which was dissolved in MeOH (0.5 mL, 0.02 M). A solution of KOH (11.2 mg) in MeOH (0.14 mL) was added and the reaction stirred at ambient temperature for 30 min. The reaction was adjusted to pH ~9-10 with aqueous saturated NH_4Cl, diluted with CH_2Cl_2 and flushed over a plug of Na_2SO_4 and silica gel. The solvent was removed under reduced pressure and the crude product purified by preparatory HPLC (Agilent Zorbax Eclipse XDB-C18 column, 5 μm, 25% MeCN/H_2O + 0.2% Et_2NH, flowrate: 5 mL/min, monitor wavelength = 209 nm, retention time = 7.5 min) to give Lycojapomine B (**45**, 2.7 mg, 0.009 mmol, 63% yield over two steps) as a white solid; ^1H NMR (600 MHz, CD_3OD) δ 5.50 (dt, *J* = 5.0, 1.9 Hz, 1H), 3.98 (ddd, *J* = 10.8, 6.5, 4.3 Hz, 1H), 3.69 (d, *J* = 8.7 Hz, 1H), 3.44 (d, *J* = 5.0 Hz, 1H), 2.83 (brd, *J* = 11.9 Hz, 1H), 2.76 (d, *J* = 8.7 Hz, 1H), 2.55 (d, *J* = 4.2 Hz, 1H), 2.32 (td, *J* = 9.9, 2.9 Hz, 1H), 2.28 (d, *J* = 9.6 Hz, 1H), 2.24 (s, 3H), 2.18 (dt, *J* =

13.7, 6.2 Hz, 1H), 2.03 – 1.91 (m, 3H), 1.91 – 1.82 (m, 2H), 1.78 (s, 3H), 1.74 – 1.70 (m, 2H), 1.64 – 1.50 (m, 2H); ^{13}C NMR (101 MHz, CD_3OD) δ 217.7, 140.1, 122.5, 73.6, 72.0, 67.5, 63.1, 62.0, 61.7, 54.4, 50.4, 45.2, 42.7, 37.5, 34.1, 32.0, 31.0, 23.9; IR (neat film, NaCl) 3349, 2930, 1729, 1445, 1131 cm^{-1}; HRMS (ESI+): m/z calc'd for $C_{18}H_{27}N_2O_2$ $[M+H]^+$: 303.2067, found 303.2070.



62 ***Lycojapomine A (44)***

Lycojapomine A: A vial was charged with starting material **62** (2.2 mg, 0.007 mmol, 1.0 equiv), which was dissolved in MeOH (0.36 mL, 0.02 M). A solution of KOH (8.0 mg) in MeOH (0.1 mL) was added and the reaction stirred at 55 °C for 6 h. The reaction was adjusted to pH ~9-10 with aqueous saturated NH_4Cl, diluted with CH_2Cl_2 and flushed over a plug of Na_2SO_4 and silica gel. The solvent was removed under reduced pressure and the crude product purified by preparatory HPLC (Agilent Zorbax Eclipse XDB-C18 column, 5 μm, 25% MeCN/H_2O + 0.2% Et_2NH, flowrate: 5 mL/min, monitor wavelength = 209 nm, retention time = 9.0 min) to give Lycojapomine A (**44**, 1.7 mg, 0.0057 mmol, 57% yield over two steps) as a white solid; ^{1}H NMR (600 MHz, CD_3OD) δ 5.65 (brs, 1H), 4.27 (dd, *J* = 5.8, 4.5 Hz, 1H), 3.78 (dd, *J* = 11.6, 2.0 Hz, 1H), 3.57 (brs, 1H), 3.21 (dd, *J* = 12.4, 3.8 Hz, 1H), 2.99 (d, *J* = 11.7 Hz, 1H), 2.94 (d, *J* = 11.6 Hz, 1H), 2.47 (dd, *J* = 17.5, 8.4 Hz, 1H), 2.40 – 2.34 (m, 1H), 2.26 – 2.20 (m, 2H), 2.17 (dd, *J* = 17.5, 9.5 Hz, 1H), 2.13 (s, 3H), 2.10 – 1.93 (m, 4H), 1.79 – 1.75 (m, 1H), 1.77 (s, 3H), 1.76 – 1.67 (m, 1H), 1.45

(dddd, J = 12.9, 3.9, 2.8, 2.4 Hz, 1H); ^{13}C NMR (101 MHz, CD_3OD) δ 222.8, 136.9, 120.1, 75.9, 75.1, 70.9, 64.4, 63.2, 61.8, 56.1, 47.4, 42.9, 39.3, 38.6, 38.5, 31.8, 25.1, 24.3; IR (neat film, NaCl) 3340, 2931, 1729, 1445, 1121, 1055, 867, 805 cm^{-1}; HRMS (ESI+): m/z calc'd for $C_{18}H_{27}N_2O_2$ $[M+H]^+$: 303.2073, found 303.2060.

2.8 REFERENCES AND NOTES

(1) *Alkaloids: Biochemistry, Ecology, and Medicinal Applications* (eds. Roberts, M.F.; Wink, M.); Springer US, Boston, MA, 1998. doi:10.1007/978-1-4757-2905-4.

(2) Heinrich, M.; Mah, J.; Amirkia, V. Alkaloids Used as Medicines: Structural Phytochemistry Meets Biodiversity—An Update and Forward Look. *Molecules* **2021**, *26*, 1836.

(3) Robinson, R. LXIII.—A synthesis of tropinone. *J. Chem. Soc., Trans.* **1917**, *111*, 762–768.

(4) Medley, J. W.; Movassaghi, M. Robinson's landmark synthesis of tropinone. *Chem. Commun.* **2013**, *49*, 10775–10777.

(5) Pereira, A. G. *et al.* Plant Alkaloids: Production, Extraction, and Potential Therapeutic Properties. In *Natural Secondary Metabolites: From Nature, Through Science, to Industry* (eds. Carocho, M.; Heleno, S. A.; Barros, L.); Springer International Publishing, Cham, 2023; pp 157–200. doi: 10.1007/978-3-031-18587-8_6.

(6) *For reviews on Lycopodium alkaloids see*: (a) Ma, X.; Gang, D. R. The Lycopodium alkaloids. *Nat. Prod. Rep.* **2004**, *21*, 752–772. (b) Zhang, Z.-J.; Jiang, S.; Zhao, Q.-S. The Chemistry and Biology of Lycopodium Alkaloids. *Chemistry & Biodiversity* **2024**, *21* e202400954.

(7) Xia, D. *et al.* Lycojapomines A–E: Lycopodium Alkaloids with Anti-Renal Fibrosis Potential from Lycopodium japonicum. *Org. Lett.* **2022**, *24*, 4684–4688.

(8) Olafsdóttir, E. S.; Halldorsdottir, E. S.; Pich, N. M.; Omarsdottir, S. Lycopodium Alkaloids: Pharmacology. In *Natural Products: Phytochemistry, Botany and*

Metabolism of Alkaloids, Phenolics and Terpenes (eds. Ramawat, K. G.; Mérillon, J.-M.); Springer, Berlin, Heidelberg, 2013; pp 1239–1262. doi:10.1007/978-3-642-22144-6_42.

(9) *For recent examples of Lycopodium alkaloid syntheses see*: (a) Zhao, X.-H. *et al.* Total Synthesis of (±)-Lycojaponicumin D and Lycodoline-Type Lycopodium Alkaloids. *J. Am. Chem. Soc.* **2017**, *139*, 7095–7103. (b) Wang, F.-X. *et al.* Total Synthesis of Lycopodium Alkaloids Palhinine A and Palhinine D. *J. Am. Chem. Soc.* **2017**, *139*, 4282–4285. (c) Zhang, J. *et al.* Diversity-oriented synthesis of Lycopodium alkaloids inspired by the hidden functional group pairing pattern. *Nat Commun* **2014**, *5*, 4614. (d) Williams, B. M.; Trauner, D. Expedient Synthesis of (+)-Lycopalhine A. *Angew. Chem. Int. Ed.* **2016**, *55*, 2191–2194. (e) Kurose, T.; Tsukano, C.; Nanjo, T.; Takemoto, Y. Total Synthesis of Lyconesidine B, a Lycopodium Alkaloid with an Oxygenated, Amine-Type Fawcettimine Core. *Org. Lett.* **2021**, *23*, 676–681.

(10) Huck, C. J.; Sarlah, D. Shaping Molecular Landscapes: Recent Advances, Opportunities, and Challenges in Dearomatization. *Chem* **2020**, *6*, 1589–1603.

(11) (a) Escolano, M. *et al.* Recent Strategies in the Nucleophilic Dearomatization of Pyridines, Quinolines, and Isoquinolines. *Chem. Rev.* **124**, 1122–1246 (2024). *For recent selected examples in synthesis see*: (b) Landwehr, E. M. *et al.* Concise syntheses of GB22, GB13, and himgaline by cross-coupling and complete reduction. *Science* **2022**, *375*, 1270–1274. (c) Welin, E. R. *et al.* Concise total syntheses of (-)-jorunnamycin A and (-)-jorumycin enabled by asymmetric catalysis. *Science* **2019**, *363*, 270–275.

(12) *For a recent review see*: (a) Olivier, W. J.; Smith, J. A.; Bissember, A. C. Synthesis of Pyrrolidine- and γ-Lactam-Containing Natural Products and Related Compounds from Pyrrole Scaffolds. *The Chemical Record* **2022**, *22*, e202100277. *For a recent selected example in synthesis see*: (b) Parr, B. T.; Economou, C.; Herzon, S. B. A concise synthesis of (+)-batzelladine B from simple pyrrole-based starting materials. *Nature* **2015**, *525*, 507–510.

(13) *For reviews on dearomatization strategies in synthesis see:* (a) Roche, S. P.; Porco, J. A. Dearomatization Strategies in the Synthesis of Complex Natural Products. *Angew. Chem. Int. Ed.* **2011**, *55*, 4068–4093. (b) Huck, C. J.; Boyko, Y. D.; Sarlah, D. Dearomative logic in natural product total synthesis. *Nat. Prod. Rep.* **2022**, *39*, 2231–2291.

(14) Pavri, N. P.; Trudell, M. L. An Efficient Method for the Synthesis of 3-Arylpyrroles. *J. Org. Chem.* **1997**, *62*, 2649–2651.

(15) (a) Zhang, Y. *et al.* Photoredox Asymmetric Nucleophilic Dearomatization of Indoles with Neutral Radicals. *ACS Catal.* **2021**, *11*, 998–1007; Zhang, Y. *et al.* Organophotocatalytic dearomatization of indoles, pyrroles and benzo(thio)furans via a Giese-type transformation. *Commun Chem* **2021**, *4*, 1–13.

(16) Prier, C. K.; Rankic, D. A.; MacMillan, D. W. C. Visible Light Photoredox Catalysis with Transition Metal Complexes: Applications in Organic Synthesis. *Chem. Rev.* **2013**, *113*, 5322–5363.

(17) Lu, Y.-C.; West, J. G. Chemoselective Decarboxylative Protonation Enabled by Cooperative Earth-Abundant Element Catalysis. *Angew. Chem. Int. Ed.* **2023**, *23*, e202213055.

(18) Yin, H. *et al.* Stereoselective and Divergent Construction of β-Thiolated/Selenolated Amino Acids via Photoredox-Catalyzed Asymmetric Giese Reaction. *J. Am. Chem. Soc.* **2020**, *142*, 14201–14209.

(19) Qin, T. *et al.* Nickel-Catalyzed Barton Decarboxylation and Giese Reactions: A Practical Take on Classic Transforms. *Angew. Chem. Int. Ed.* **2017**, *56*, 260–265.

(20) Lackner, G. L.; Quasdorf, K. W.; Overman, L. E. Direct Construction of Quaternary Carbons from Tertiary Alcohols via Photoredox-Catalyzed Fragmentation of tert-Alkyl N-Phthalimidoyl Oxalates. *J. Am. Chem. Soc.* **2013**, *135*, 15342–15345.

(21) Alpers, D.; Brasholz, M.; Rehbein, J. Photoredox-Induced Radical 6-exo-trig Cyclizations onto the Indole Nucleus: Aromative versus Dearomative Pathways. *European Journal of Organic Chemistry* **2017**, *2017*, 2186–2193.

(22) Ma, S.; Negishi, E. Anti-Carbometalation of Homopropargyl Alcohols and Their Higher Homologues via Non-Chelation-Controlled Syn-Carbometalation and Chelation-Controlled Isomerization. *J. Org. Chem.* **1997**, *62*, 784–785.

(23) Suzuki, K.; Tomooka, K.; Katayama, E.; Matsumoto, T.; Tsuchihashi, G. Stereocontrolled asymmetric total synthesis of protomycinolide IV. *J. Am. Chem. Soc.* **1986**, *108*, 5221–5229.

(24) Krasovskiy, A.; Knochel, P. A LiCl-Mediated Br/Mg Exchange Reaction for the Preparation of Functionalized Aryl- and Heteroarylmagnesium Compounds from Organic Bromides. *Angew. Chem. Int. Ed.* **2004**, *43*, 3333–3336.

(25) Liddon, J. T. R. *et al.* Catalyst-Driven Scaffold Diversity: Selective Synthesis of Spirocycles, Carbazoles and Quinolines from Indolyl Ynones. *Chemistry – A European Journal* **2016**, *22*, 8777–8780.

(26) Nakayama, Y. *et al.* Total Synthesis of Ritterazine B. *J. Am. Chem. Soc.* **2021**, *143*, 4187–4192.

(27) Holton, R. A. *et al.* First total synthesis of taxol. 2. Completion of the C and D rings. *J. Am. Chem. Soc.* **1994**, *116*, 1599–1600.

(28) Pangborn, A. M.; Giardello, M. A.; Grubbs, R. H.; Rosen, R. K.; Timmers, F. J. Safe and Convenient Procedure for Solvent Purification. *Organometallics* **1996**, *15*, 1518–1520.

(29) Tsimelzon, A.; Braslau, R. Radical [*n* + 1] Annulations with Sulfur Dioxide, *J. Org. Chem.* **2005**, *70*, 10854–10859.

(30) Davies, J. A. *et al*; Total Synthesis of Kalimantacin A, *Org. Lett.* **2020**, *22*, 6349–6353.

(31) Ma, S.; Negishi, E.; *Anti*-Carbometalation of Homopropargyl Alcohols and Their Higher Homologues via Non-Chelation-Controlled *Syn*-Carbometalation and Chelation-Controlled Isomerization, *J. Org. Chem.* **1997**, *62*, 784–785.

APPENDIX 3

Spectra Relevant to Chapter 2:

Total Synthesis of Lycojapomine A & B

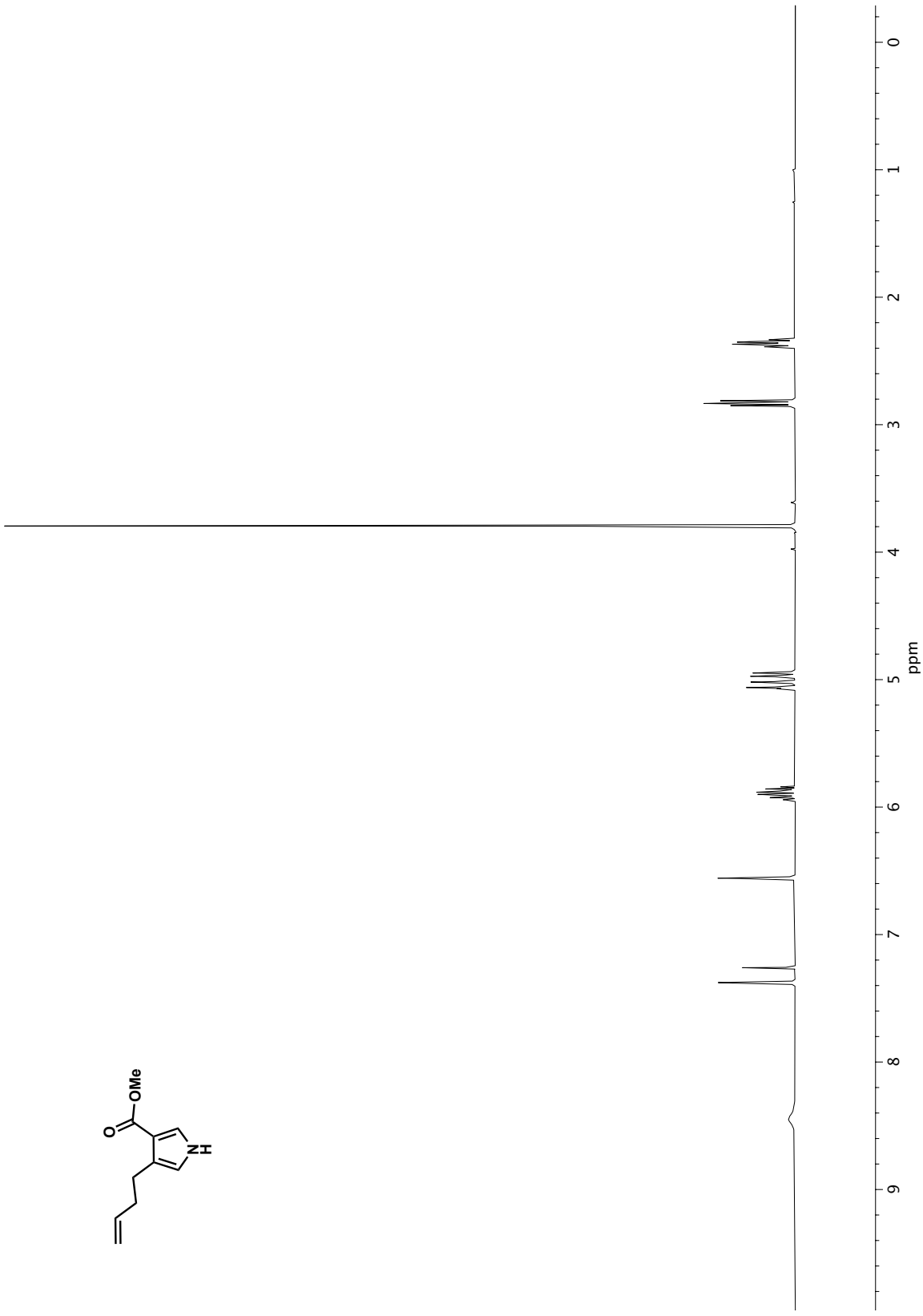


Figure A3.1. ^{1}H NMR (400 MHz, $CDCl_3$) of compound **46**.

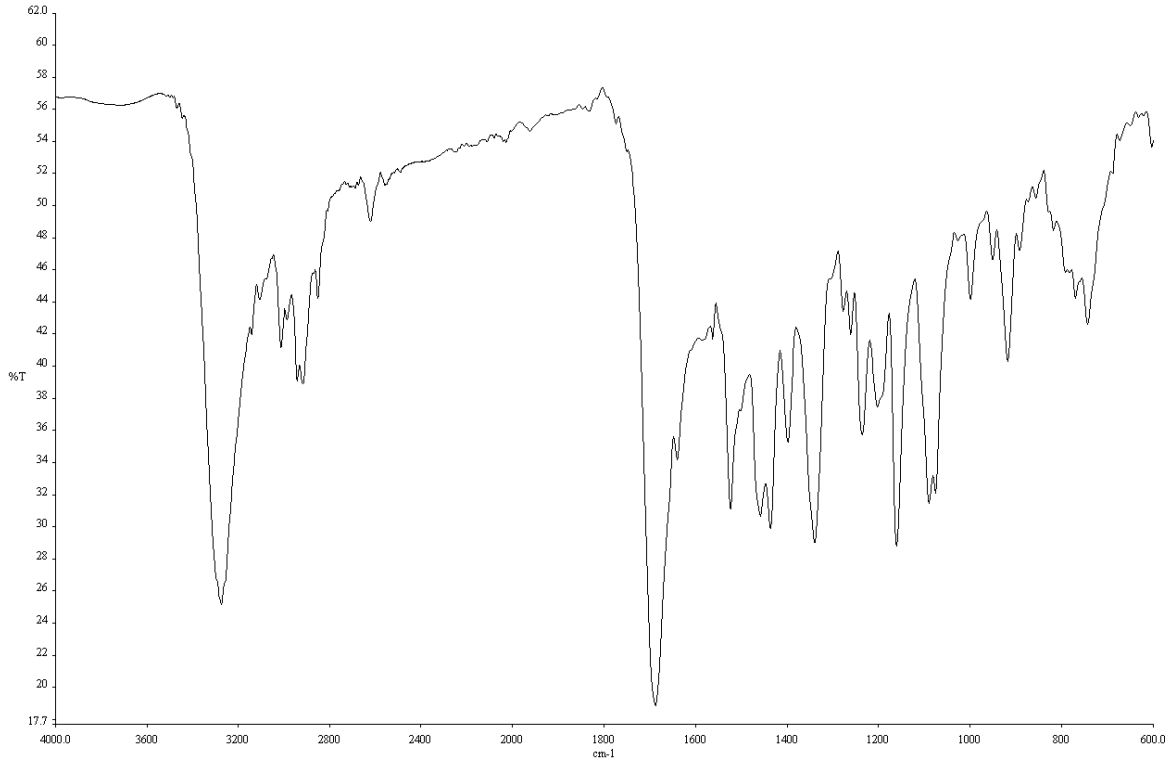


Figure A3.2. Infrared spectrum (Thin Film, NaCl) of compound **46**.

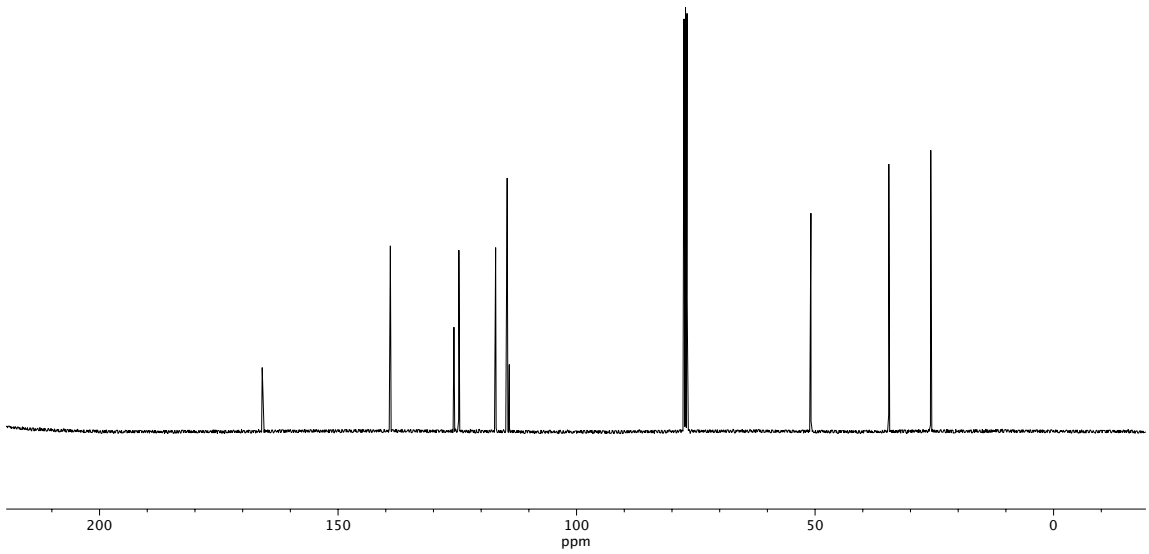


Figure A3.3. ^{13}C NMR (101 MHz, $CDCl_3$) of compound **46**.

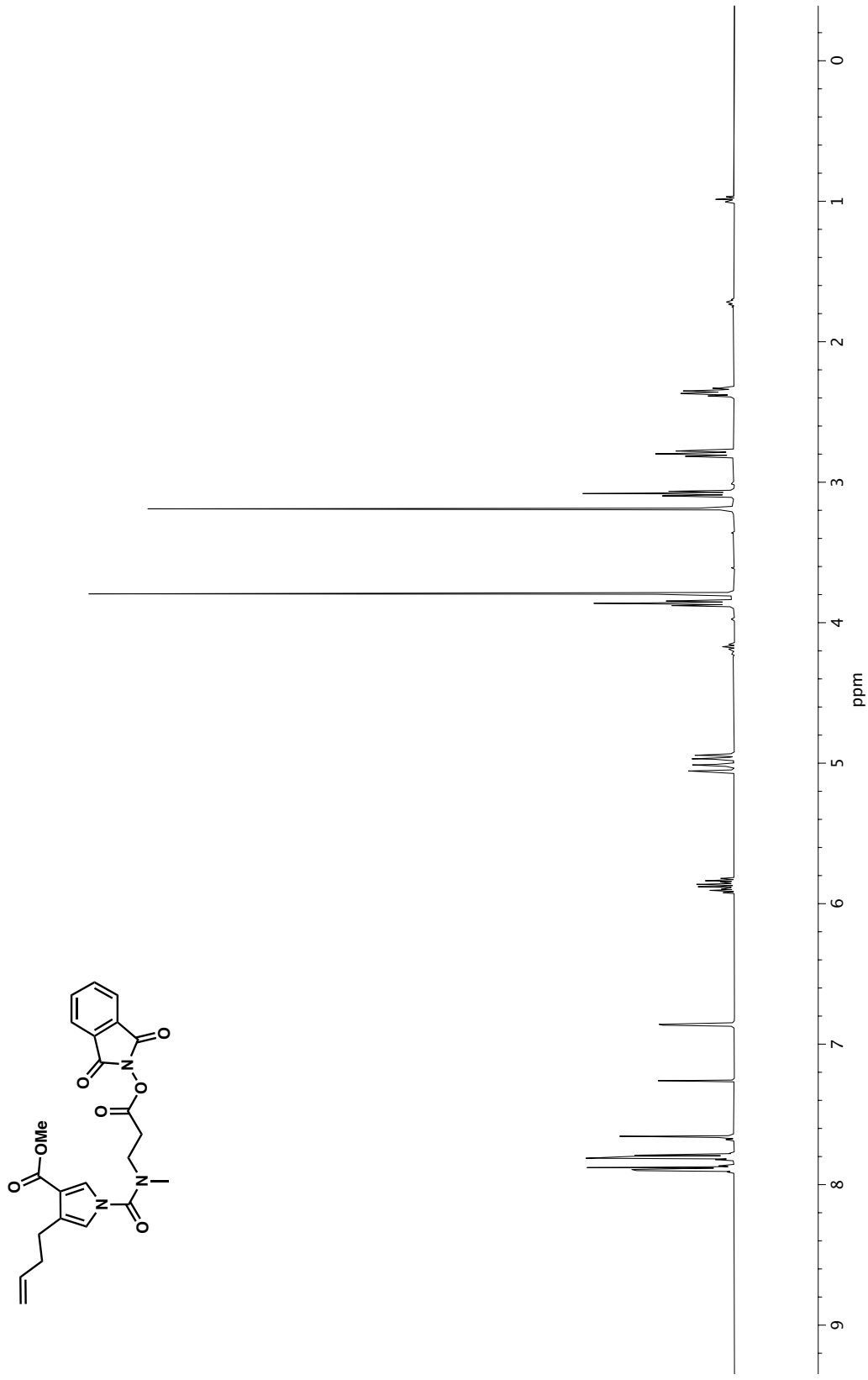


Figure A3.4. ^{1}H NMR (400 MHz, $CDCl_3$) of compound **48**.

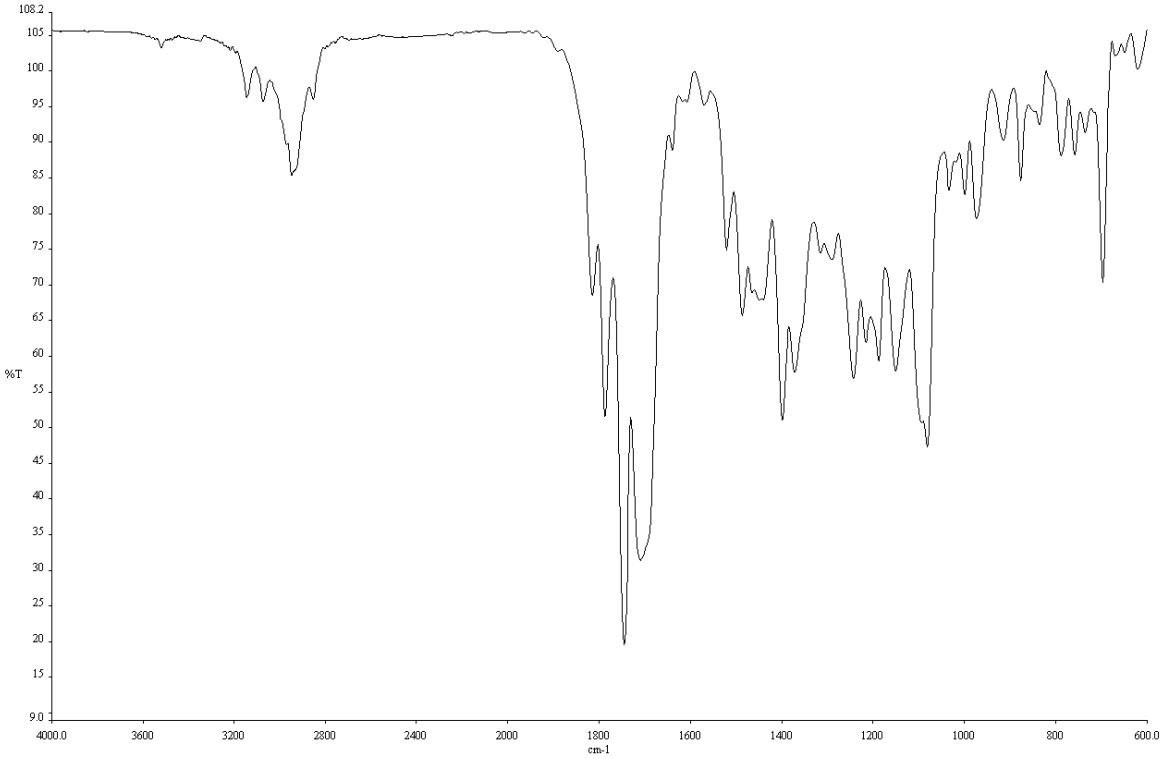


Figure A3.5. Infrared spectrum (Thin Film, NaCl) of compound **48**.

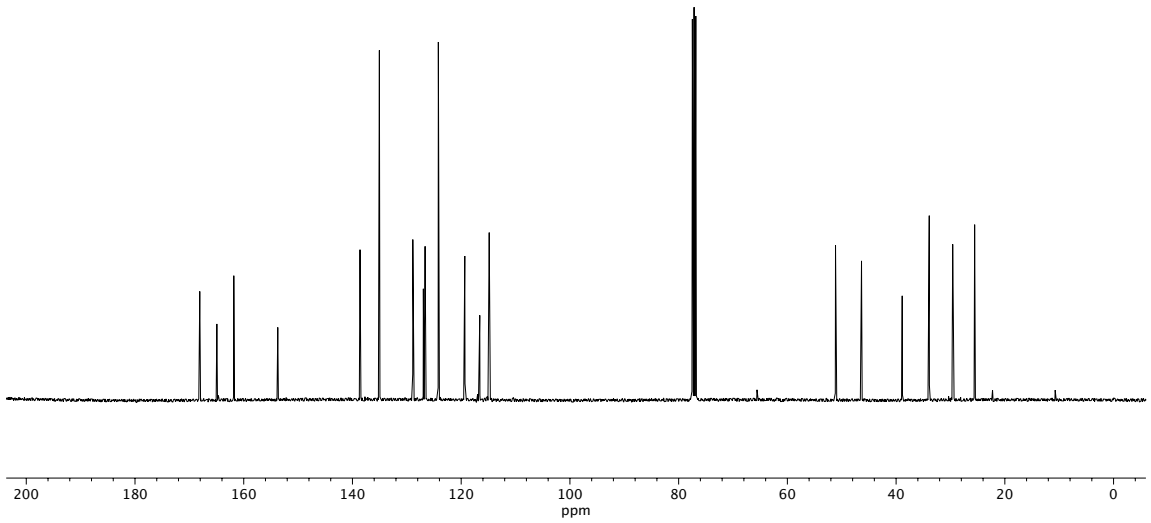


Figure A3.6. ^{13}C NMR (101 MHz, $CDCl_3$) of compound **48**.

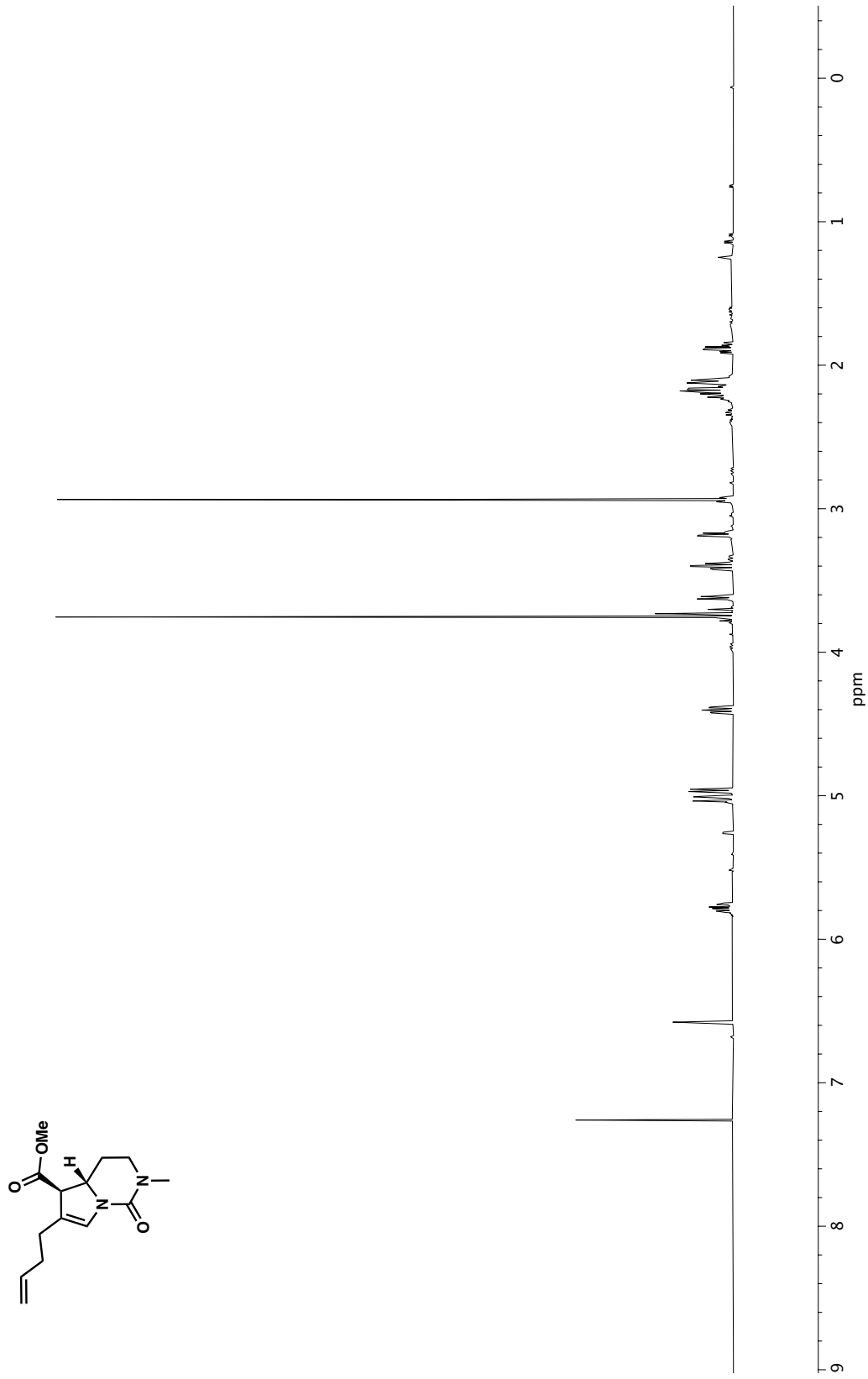


Figure A3.7. ^{1}H NMR (600 MHz, $CDCl_3$) of compound **49** (*trans*).

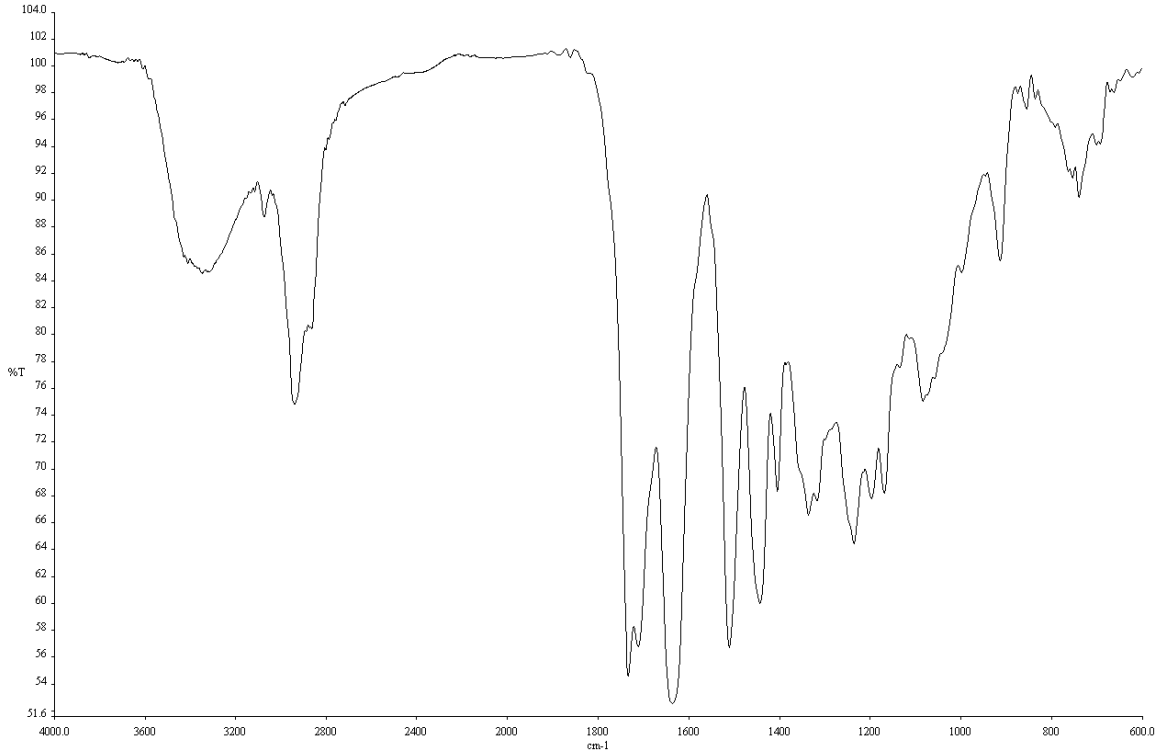


Figure A3.8. Infrared spectrum (Thin Film, NaCl) of compound **49** (*trans*).

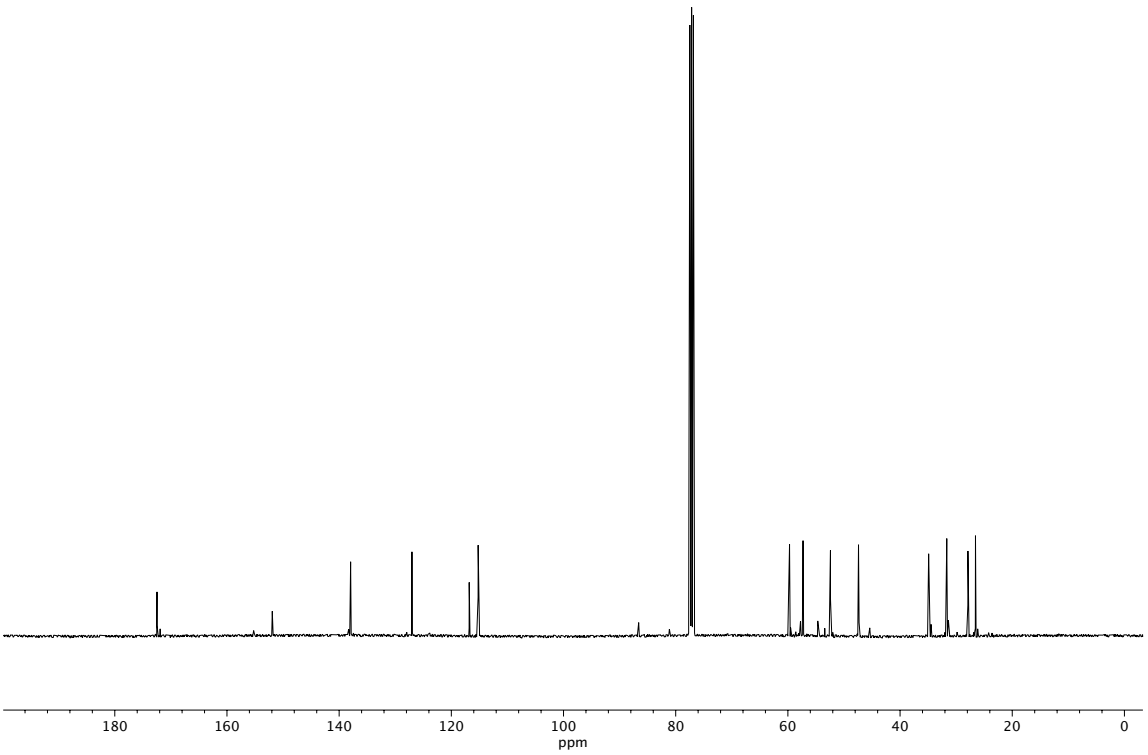


Figure A3.9. ^{13}C NMR (101 MHz, $CDCl_3$) of compound **49** (*trans*).

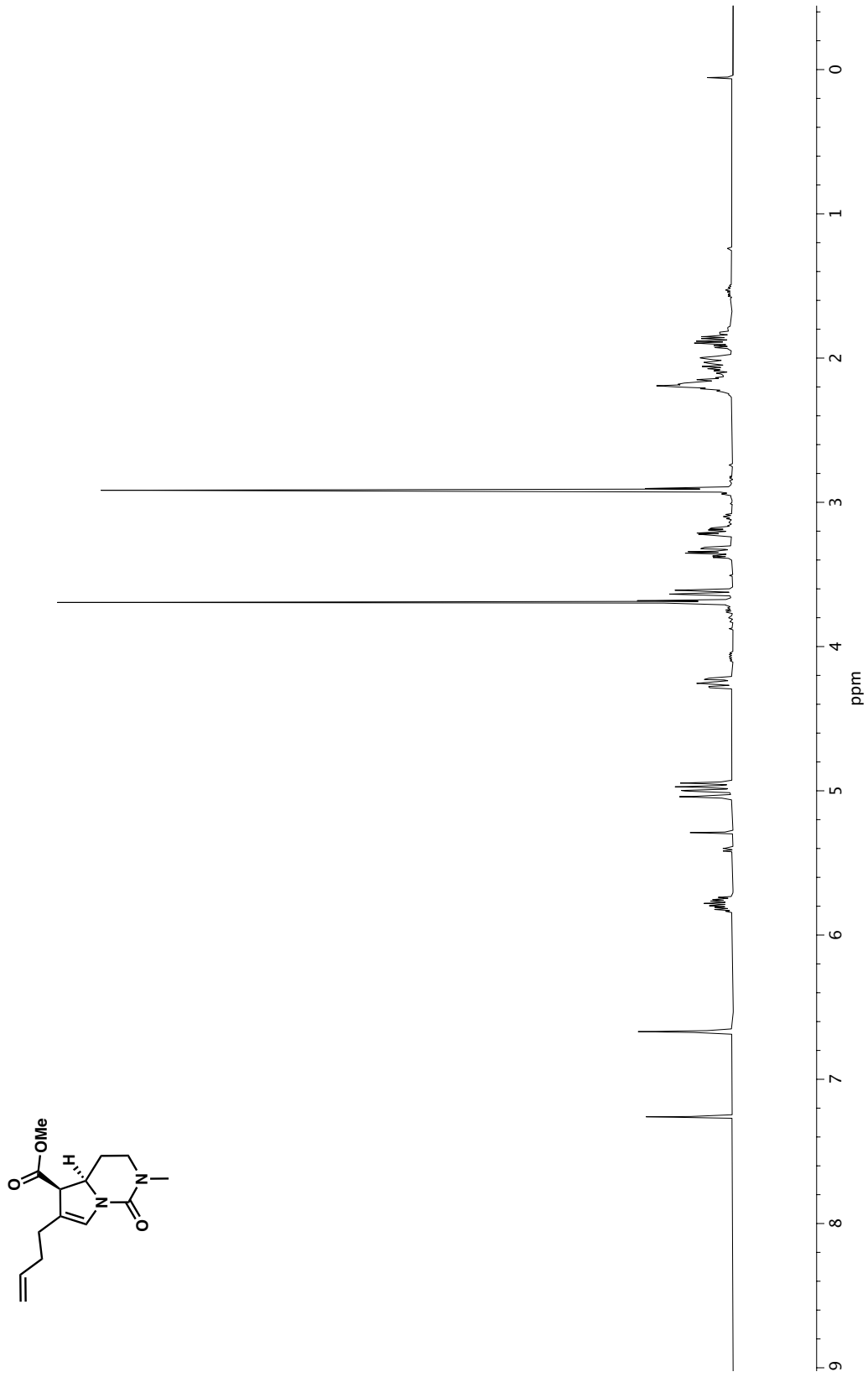


Figure A3.10. ^{1}H NMR (400 MHz, $CDCl_3$) of compound **49** (*cis*).

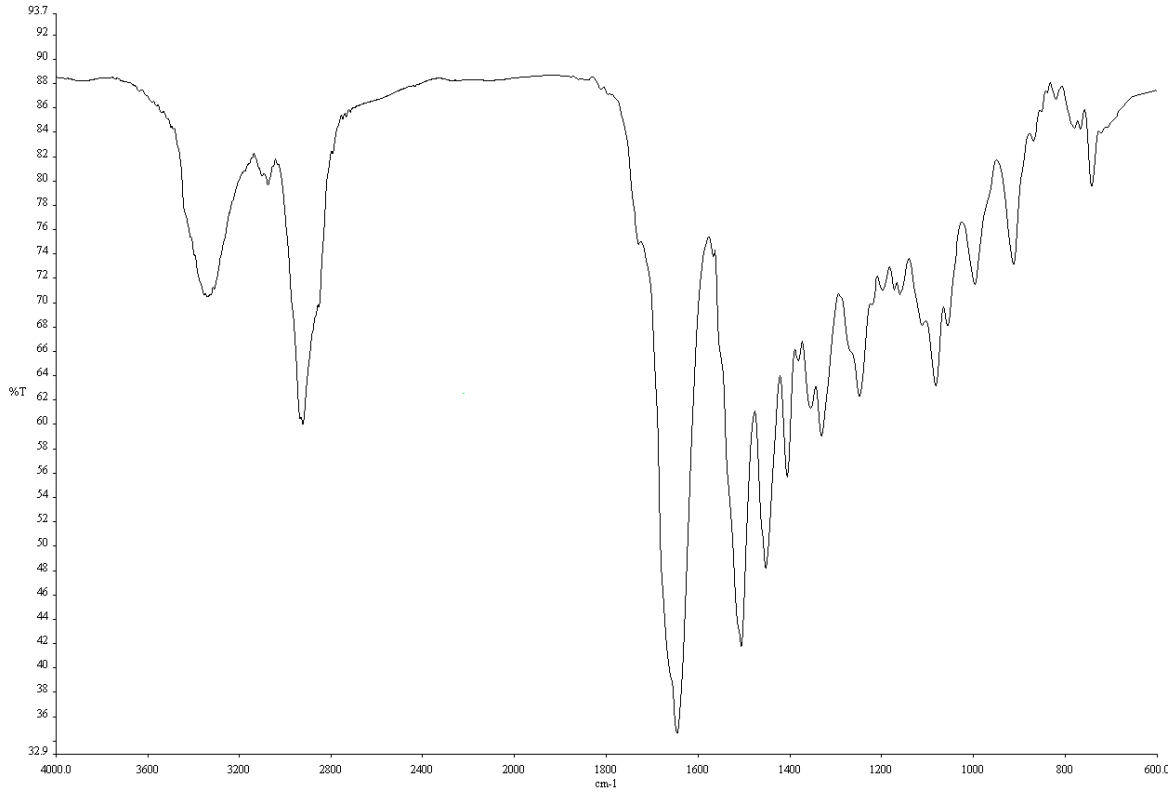


Figure A3.11. Infrared spectrum (Thin Film, NaCl) of compound **49** (*cis*).

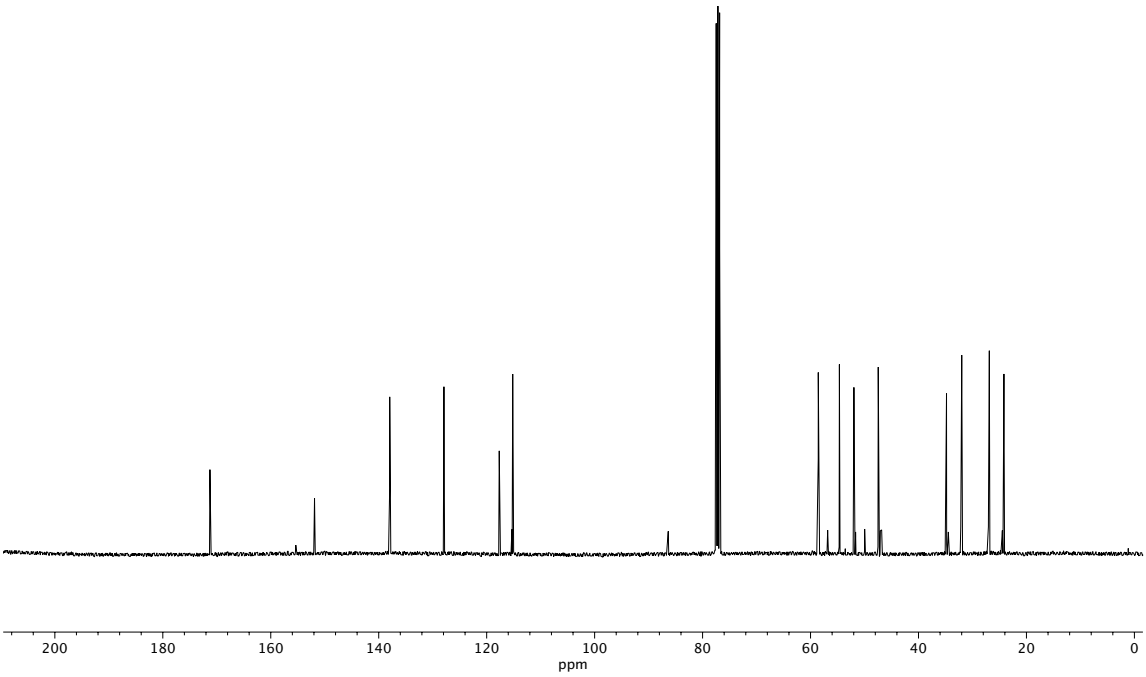


Figure A3.12. ^{13}C NMR (101 MHz, $CDCl_3$) of compound **49** (*cis*).

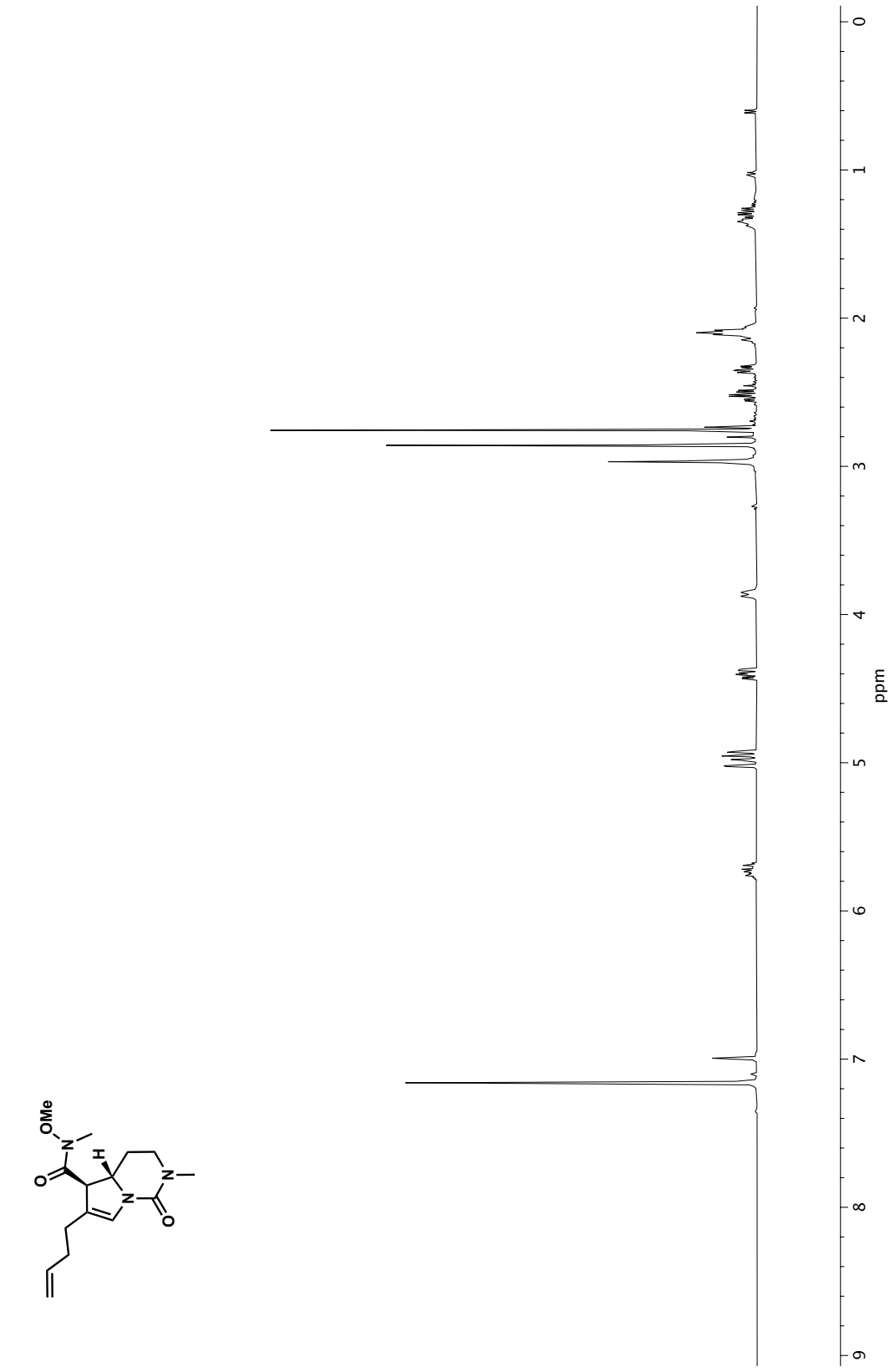


Figure A3.13. ^{1}H NMR (400 MHz, C_6D_6) of compound **52**.

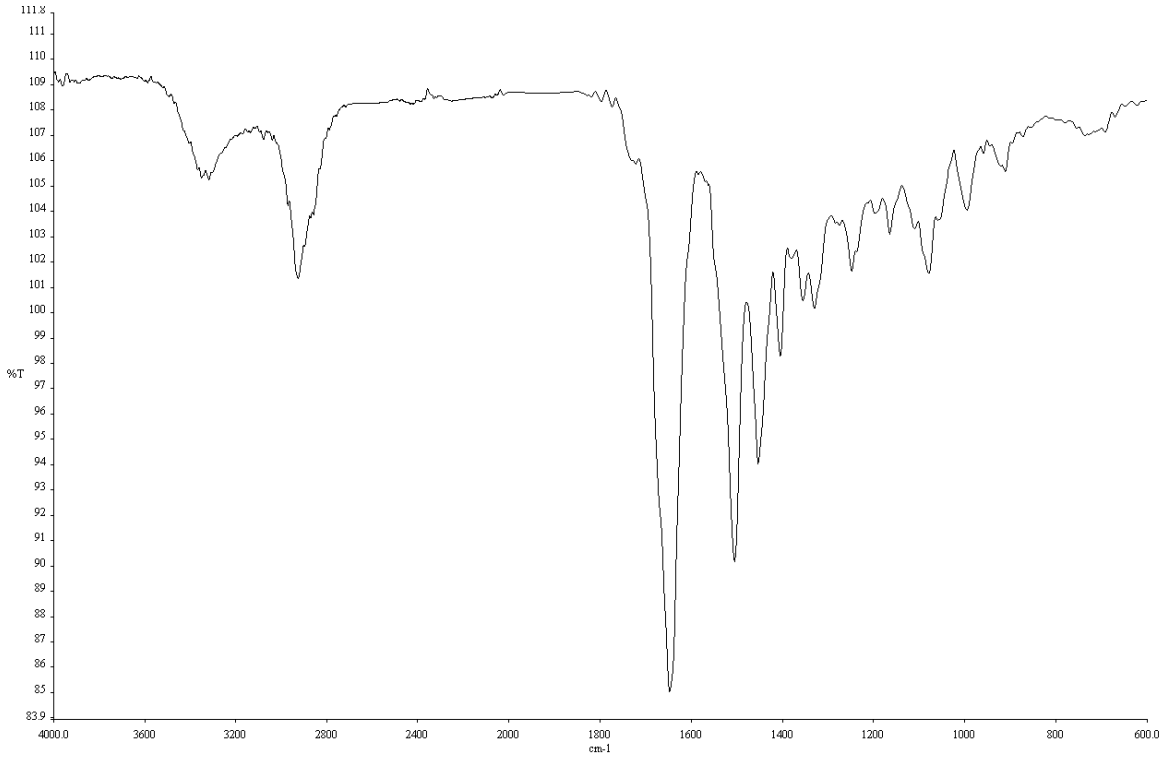


Figure A3.14. Infrared spectrum (Thin Film, NaCl) of compound **52**.

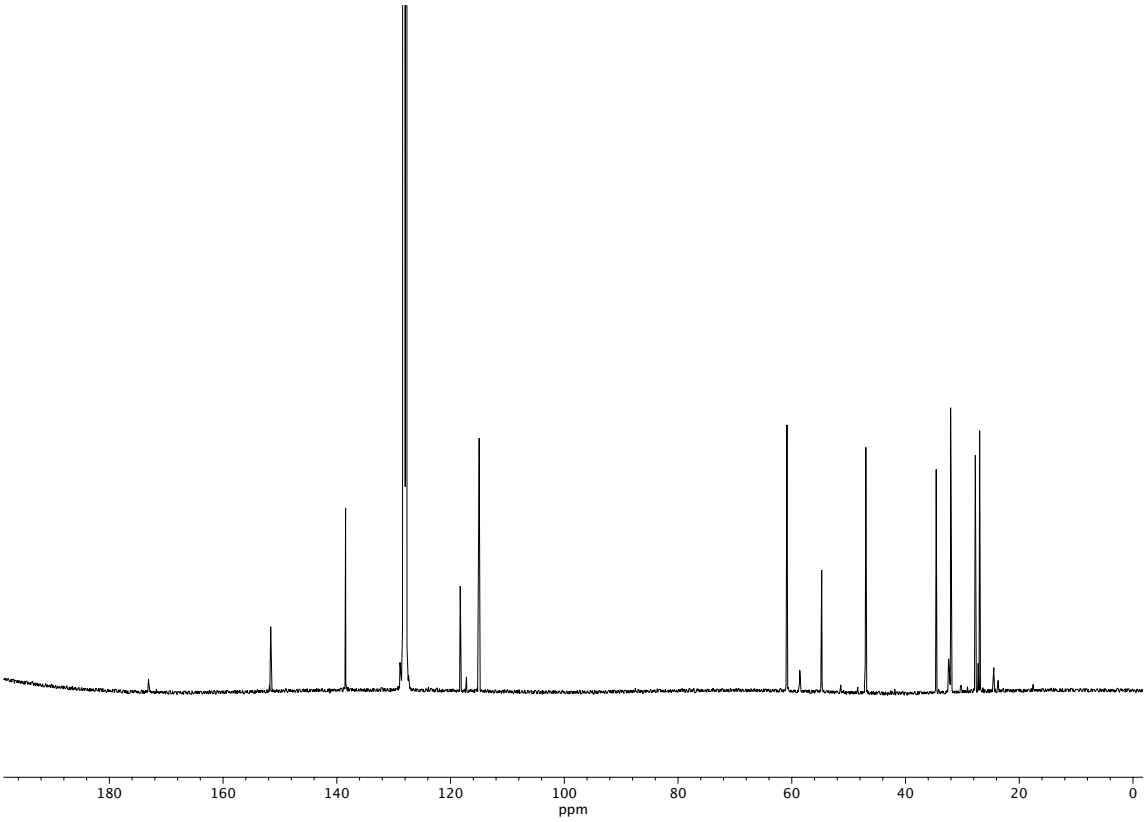


Figure A3.15. ^{13}C NMR (101 MHz, C_6D_6) of compound **52**.

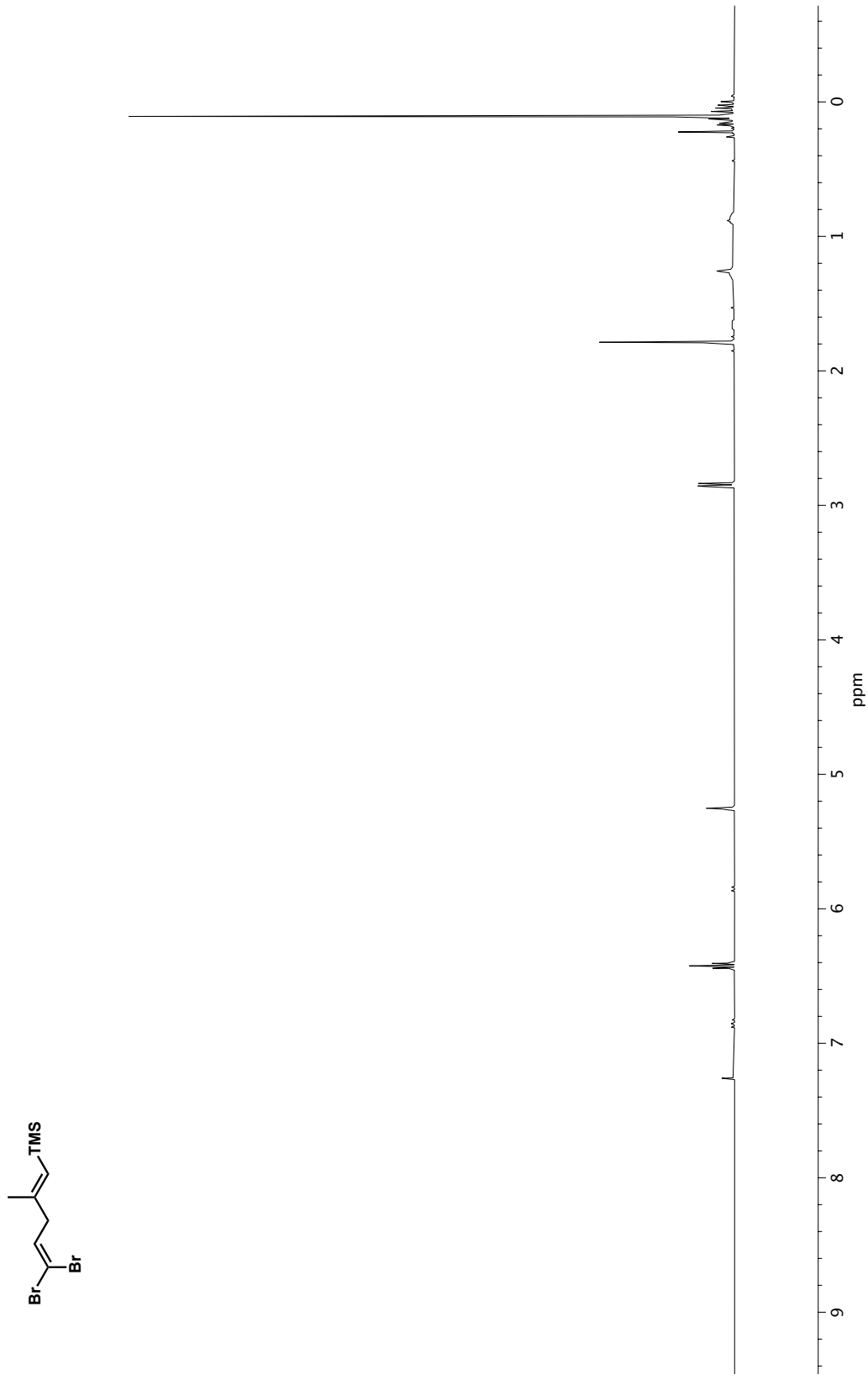


Figure A3.16. ^{1}H NMR (400 MHz, $CDCl_3$) of compound **53**.

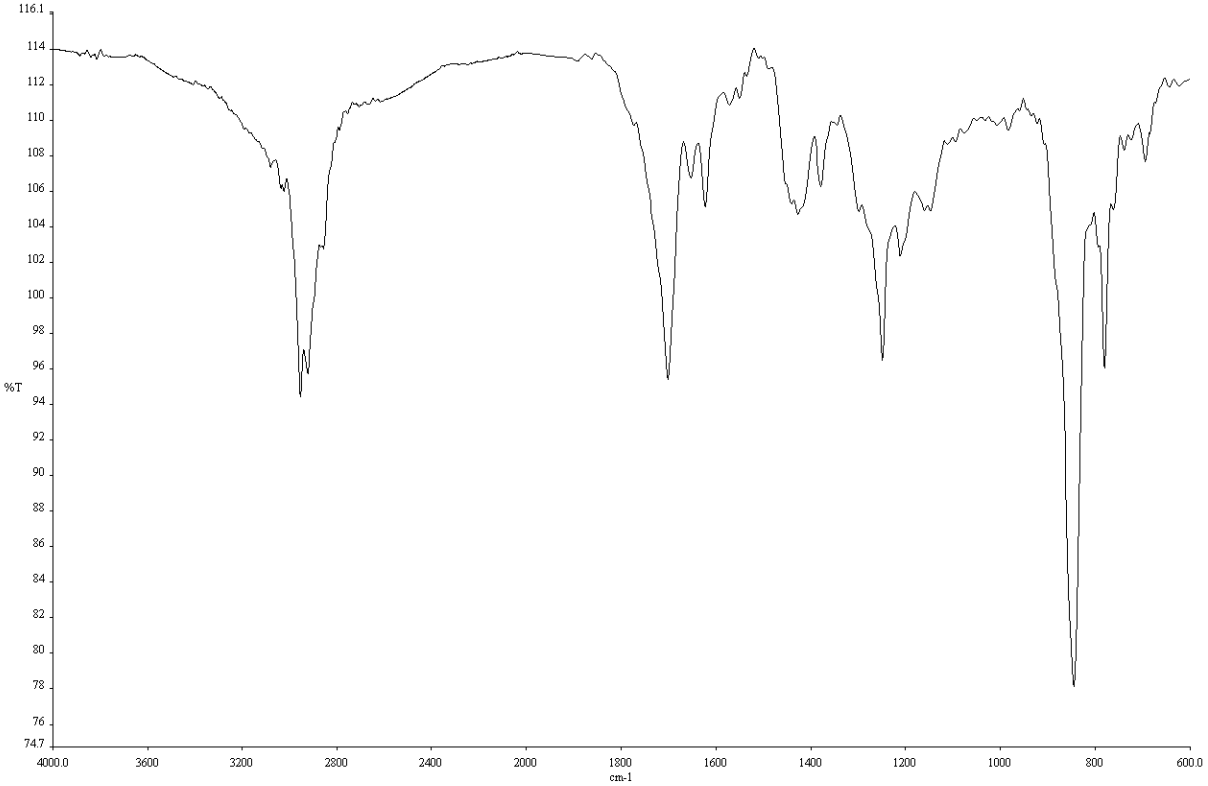


Figure A3.17. Infrared spectrum (Thin Film, NaCl) of compound **53**.

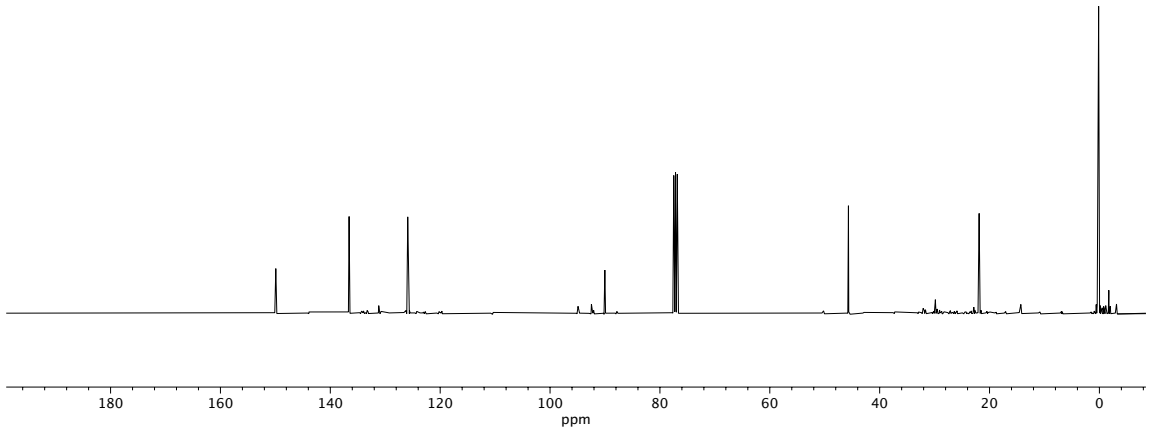


Figure A3.18. ^{13}C NMR (101 MHz, $CDCl_3$) of compound **53**.

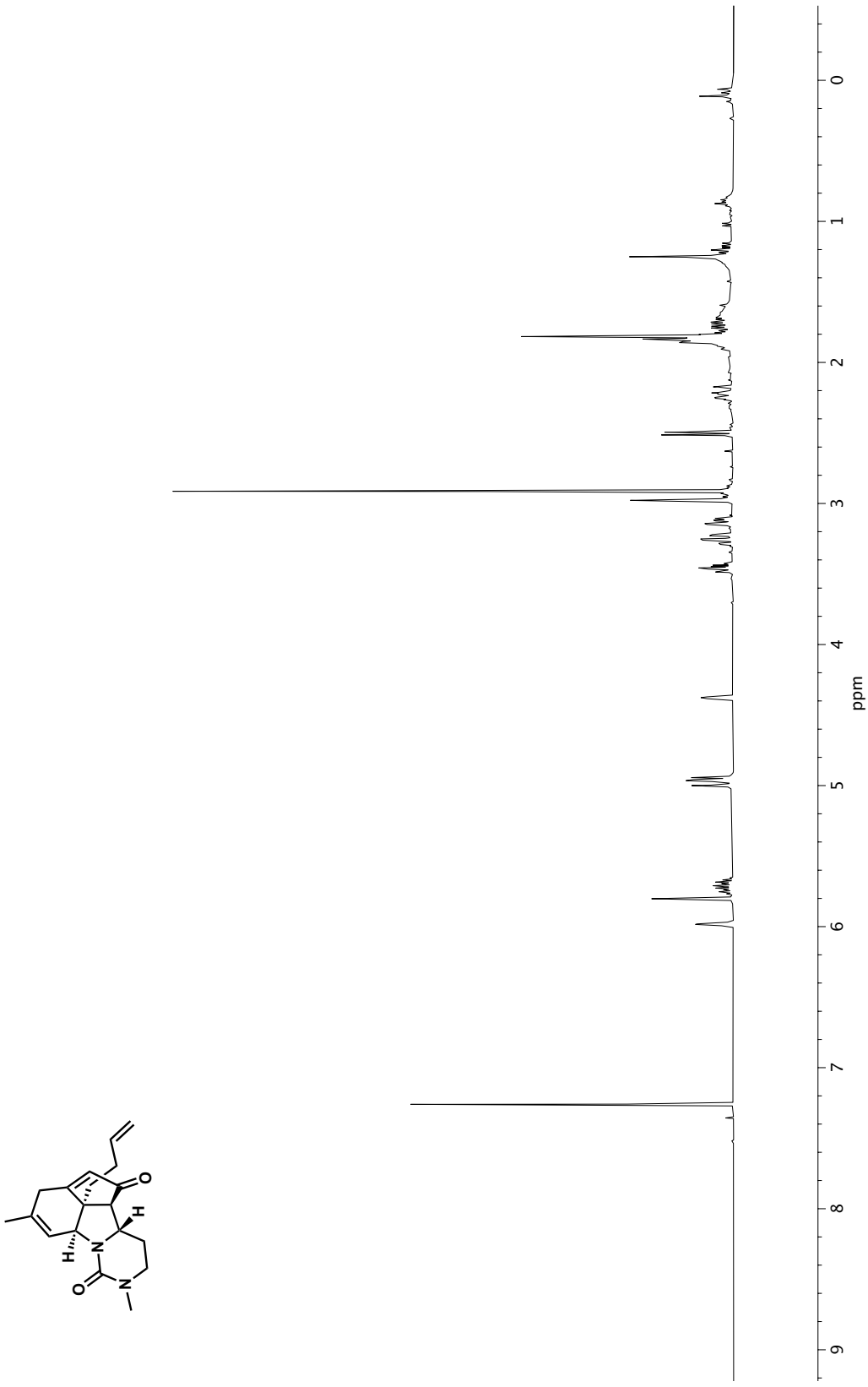


Figure A3.19. ^{1}H NMR (400 MHz, $CDCl_3$) of compound **59**.

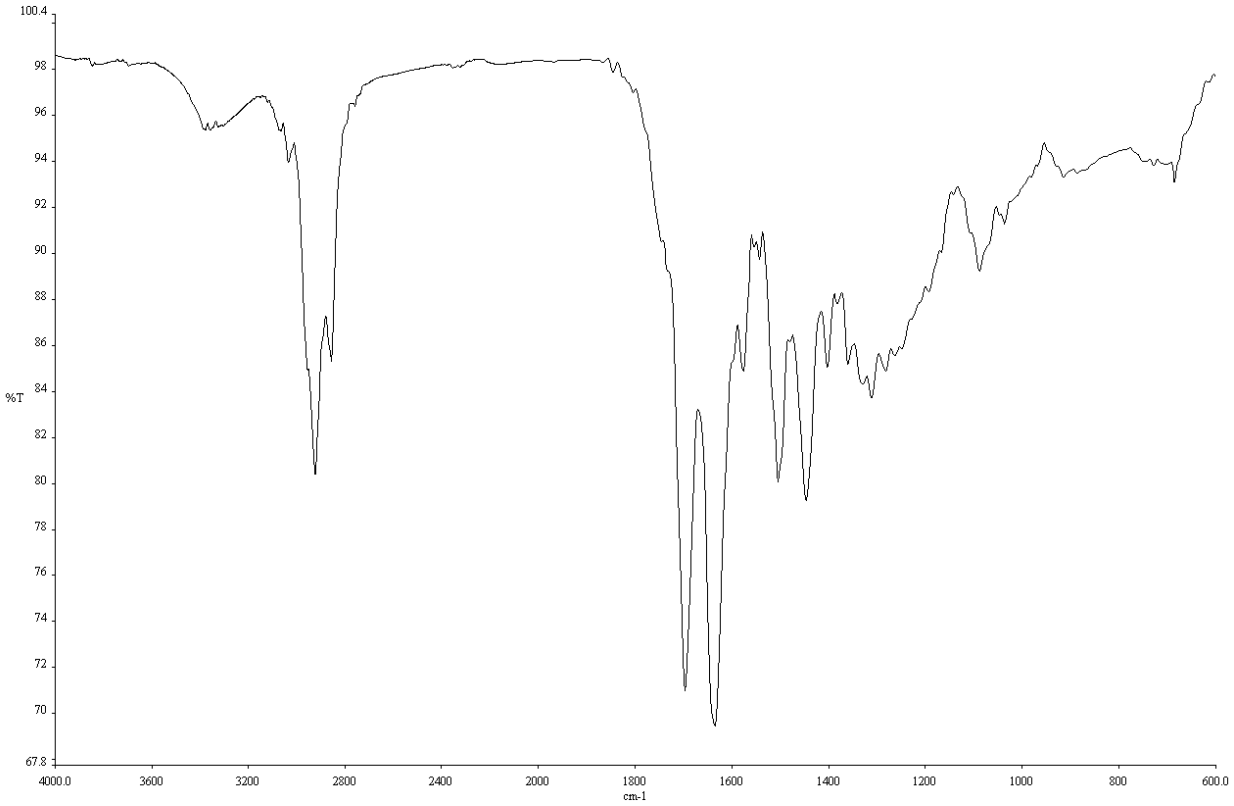


Figure A3.20. Infrared spectrum (Thin Film, NaCl) of compound **59**.

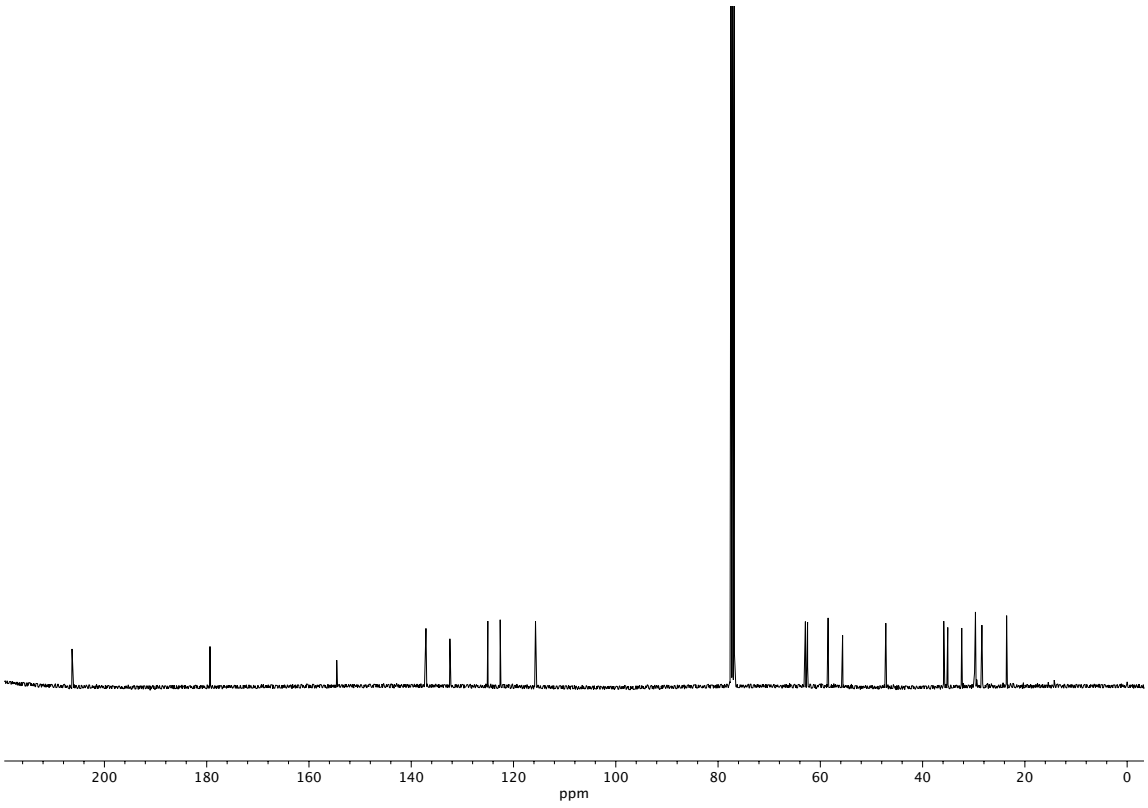


Figure A3.21. ^{13}C NMR (101 MHz, $CDCl_3$) of compound **59**.

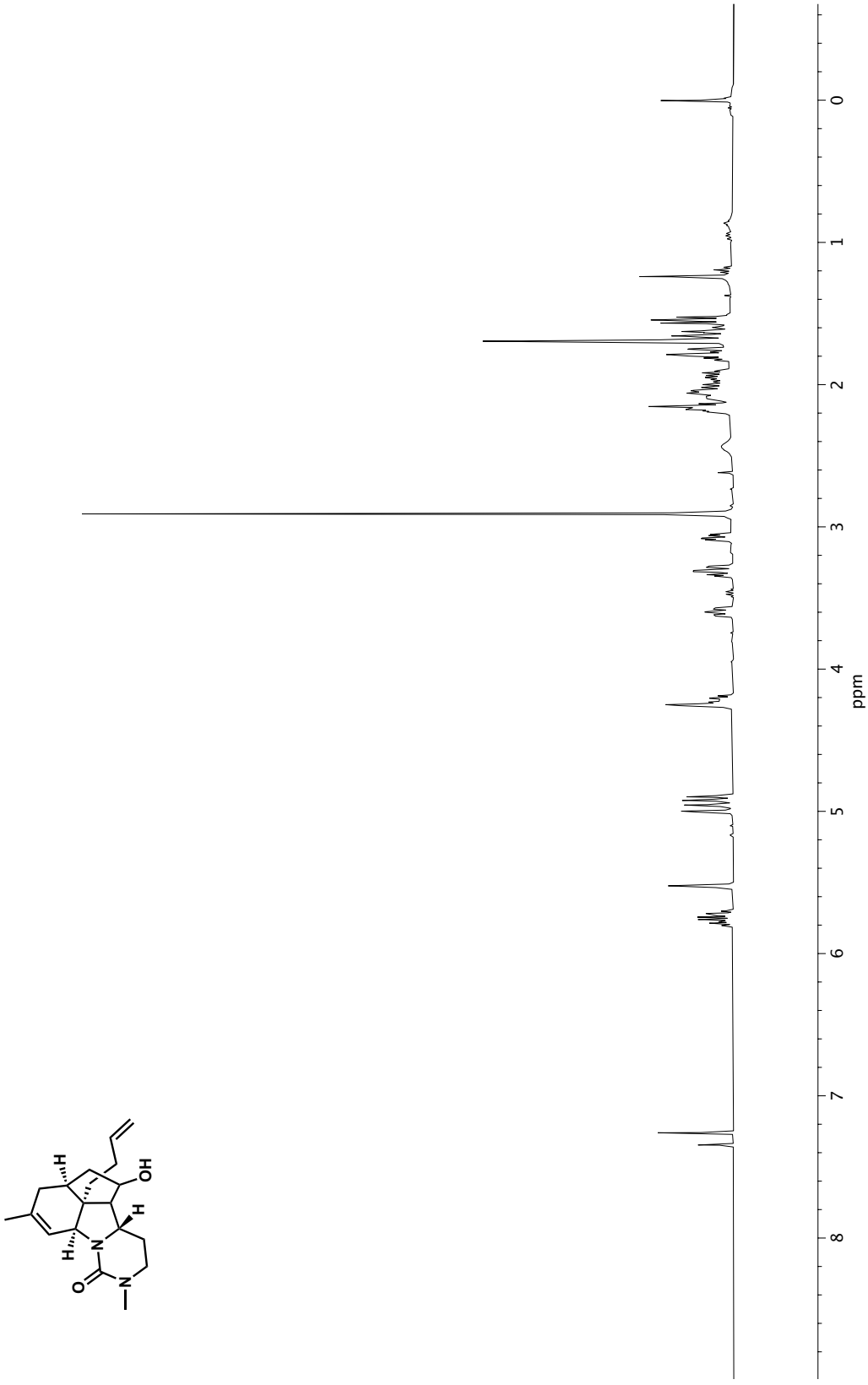


Figure A3.22. ^{1}H NMR (400 MHz, $CDCl_3$) of compound **60**.

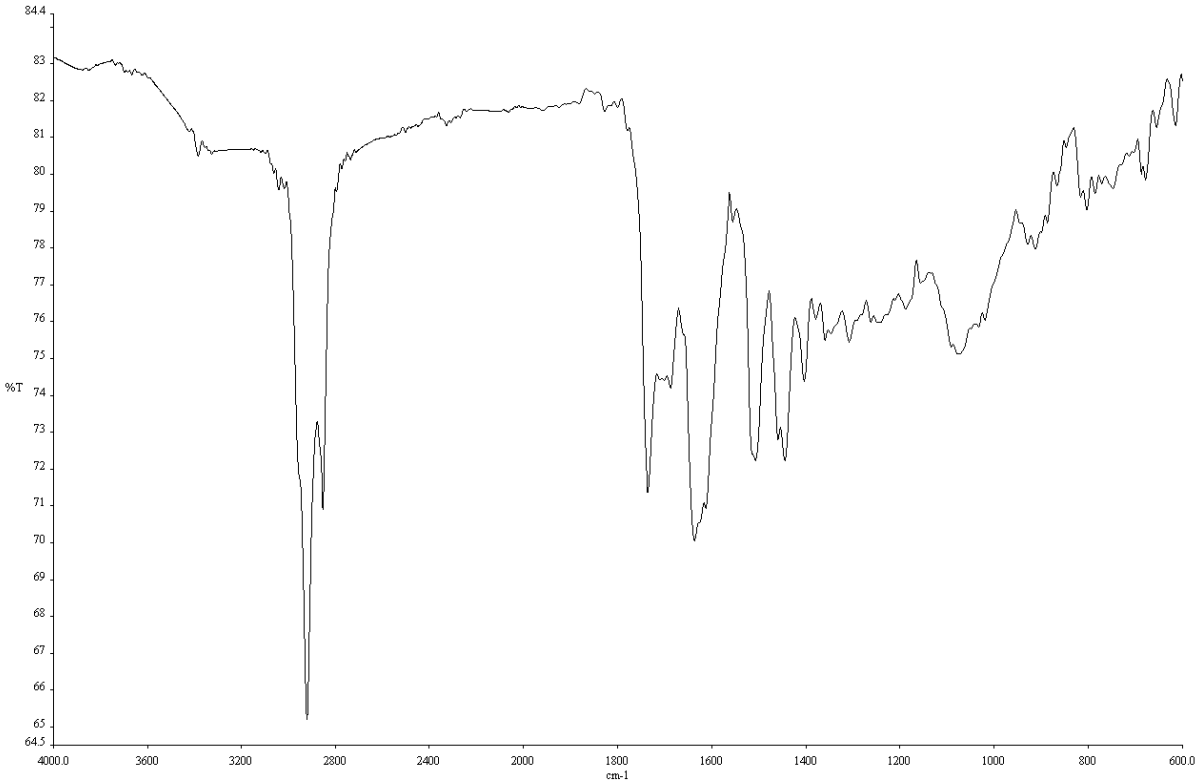


Figure A3.23. Infrared spectrum (Thin Film, NaCl) of compound **60**.

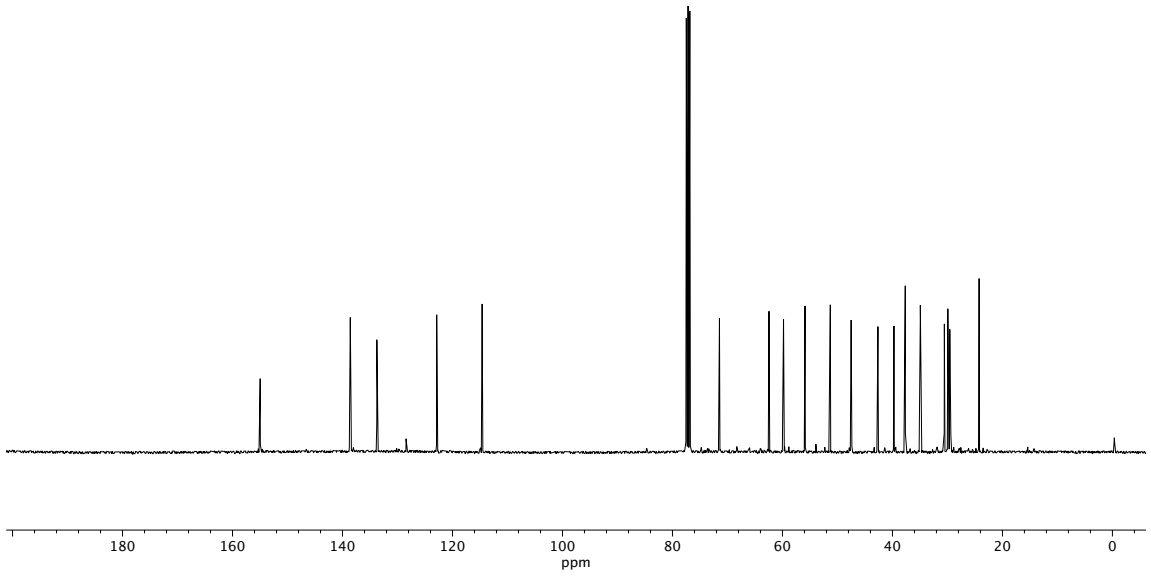


Figure A3.24. ^{13}C NMR (101 MHz, $CDCl_3$) of compound **60**.

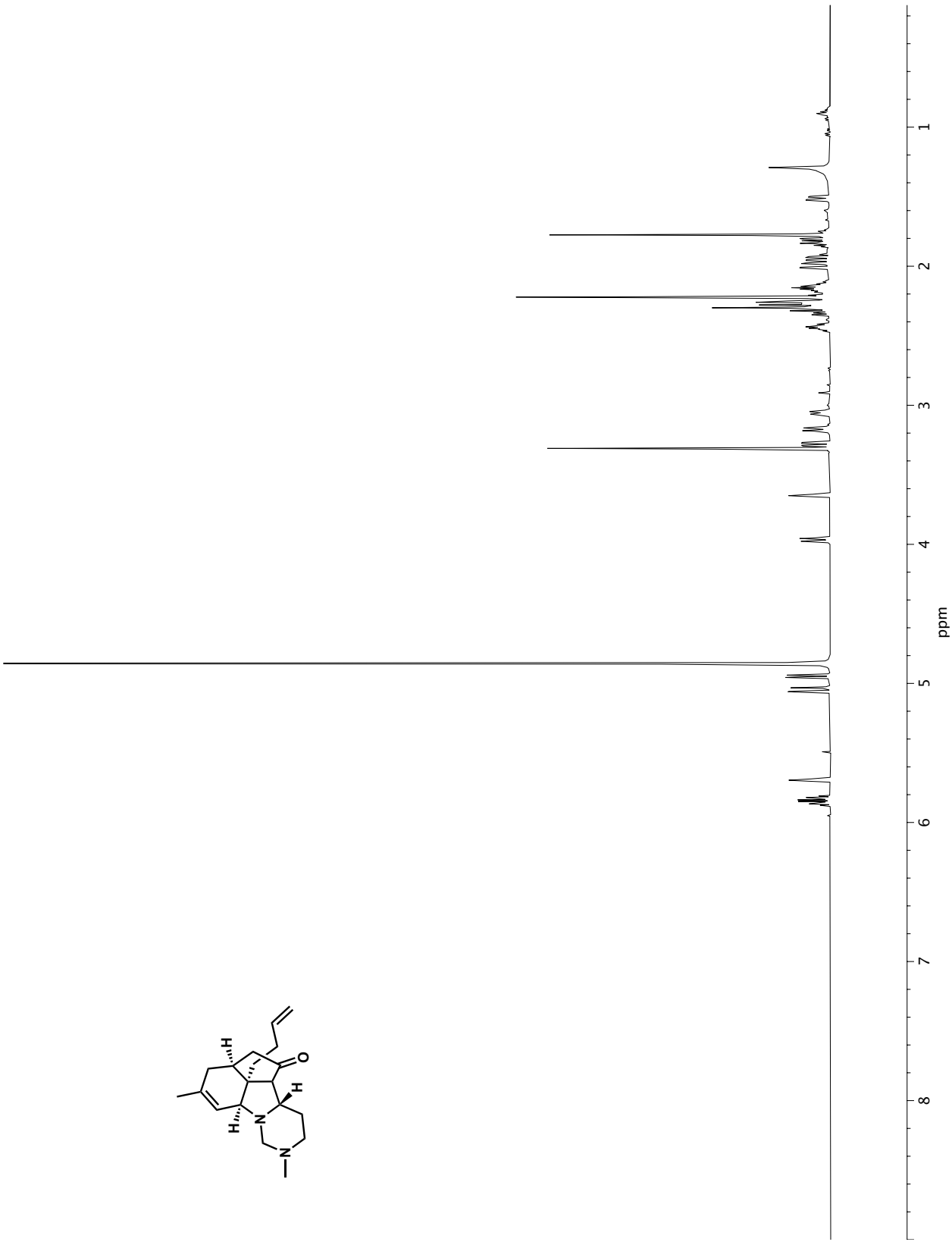


Figure A3.25. ^{1}H NMR (600 MHz, CD_3OD) of compound **61**.

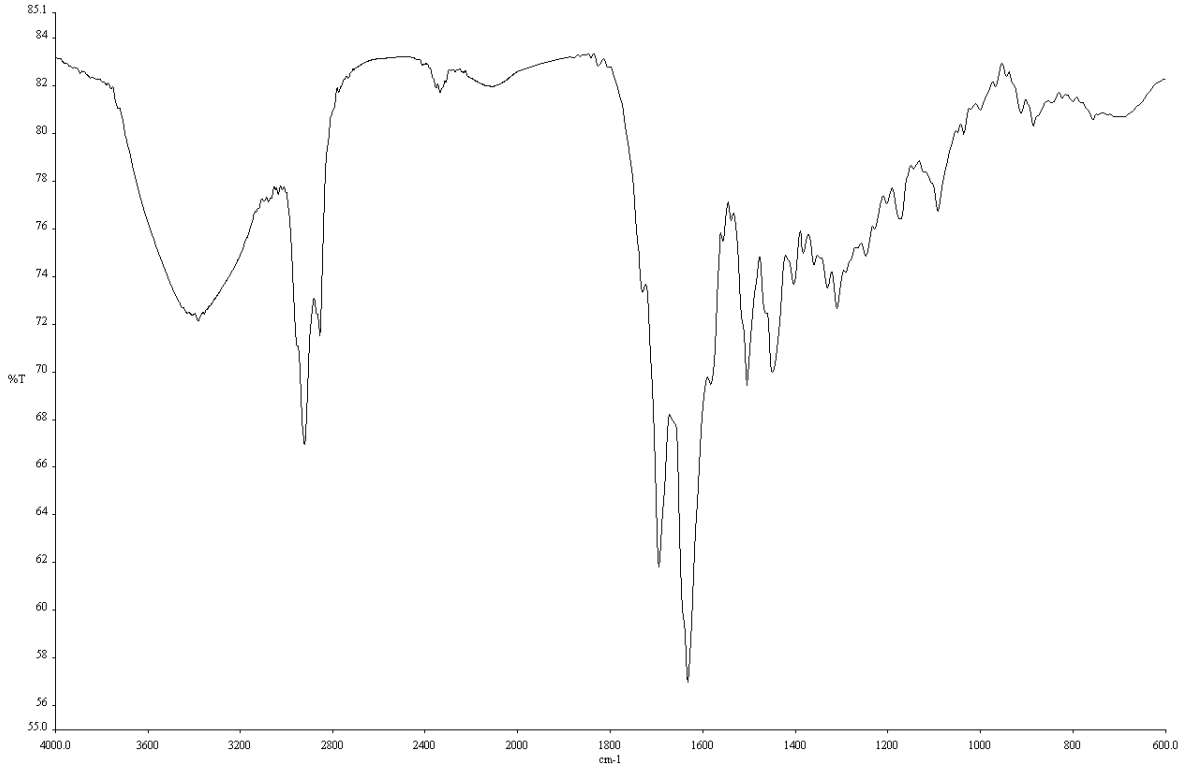


Figure A3.26. Infrared spectrum (Thin Film, NaCl) of compound **61**.

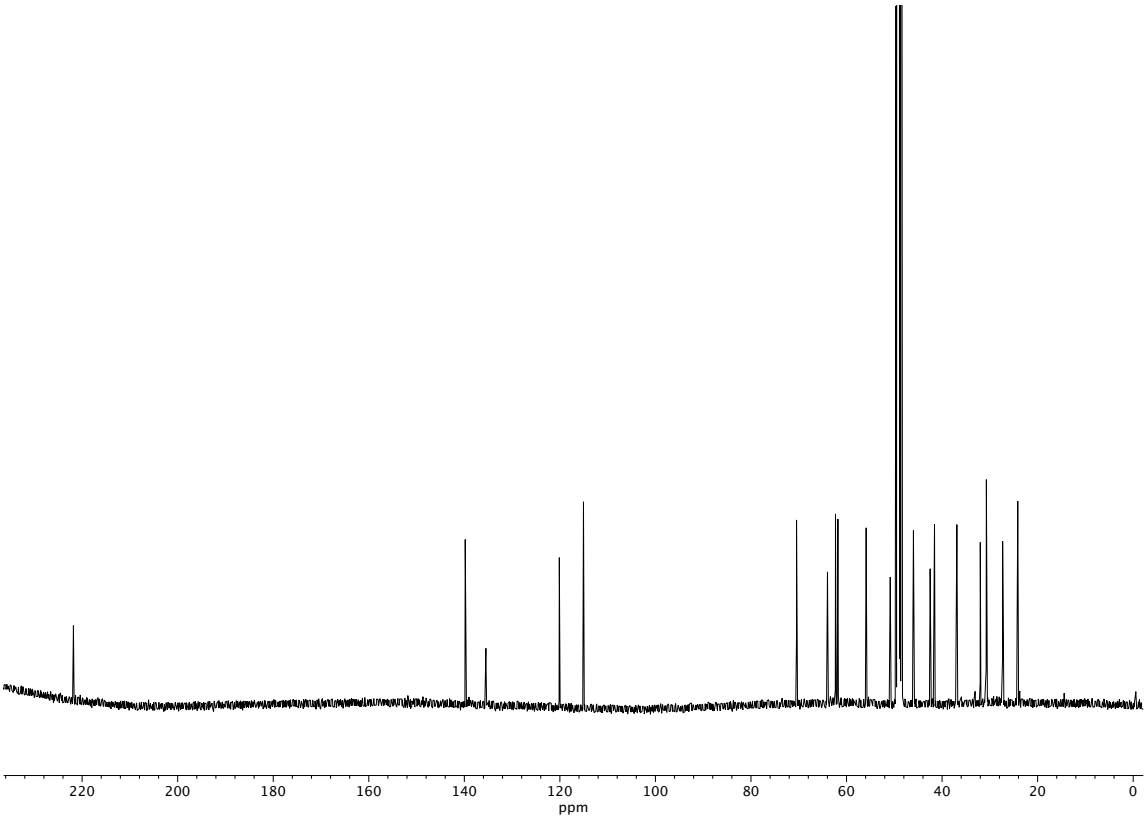


Figure A3.27. ^{13}C NMR (101 MHz, CD_3OD) of compound **61**.

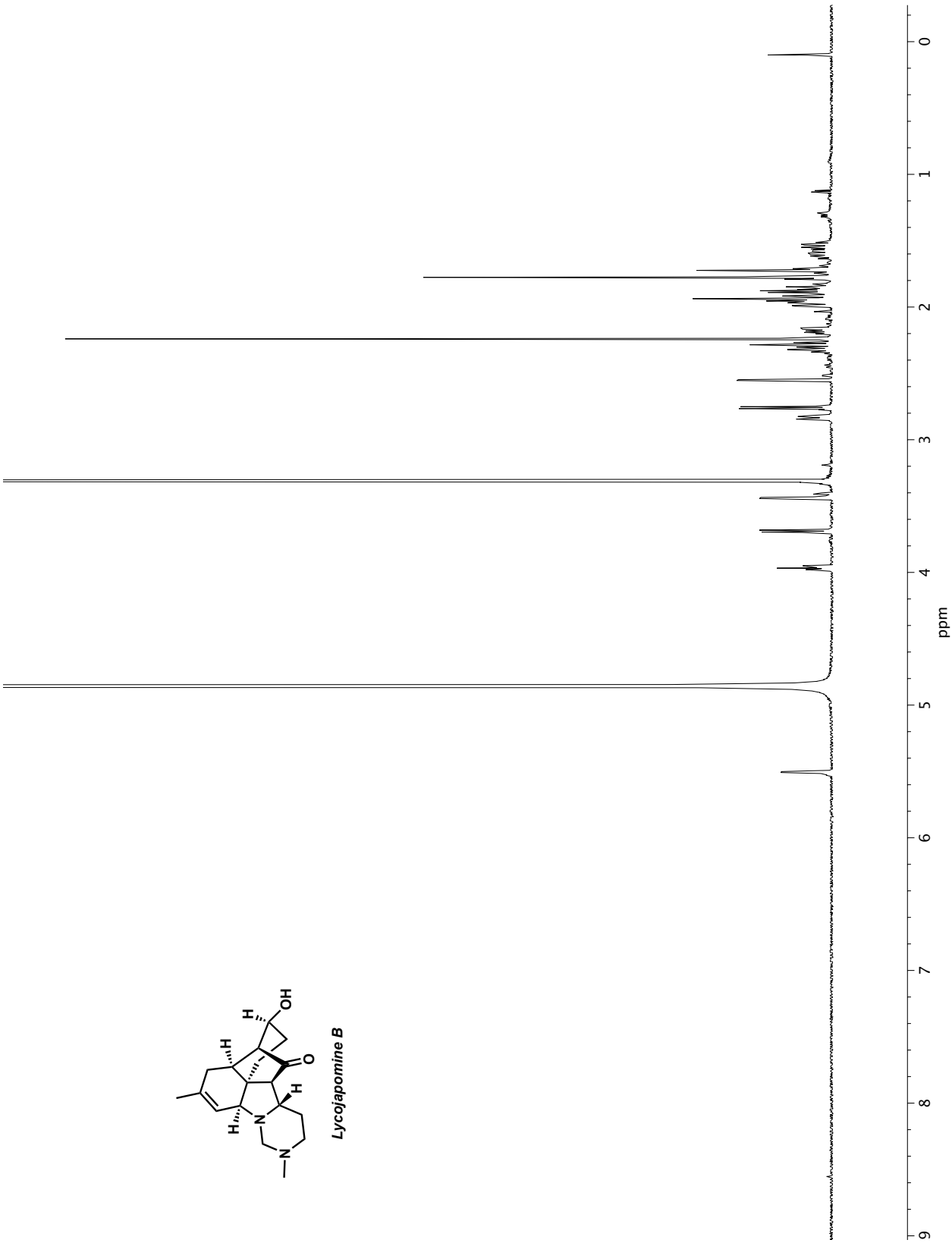


Figure A3.28. ^{1}H NMR (600 MHz, CD_3OD) of compound **45**.

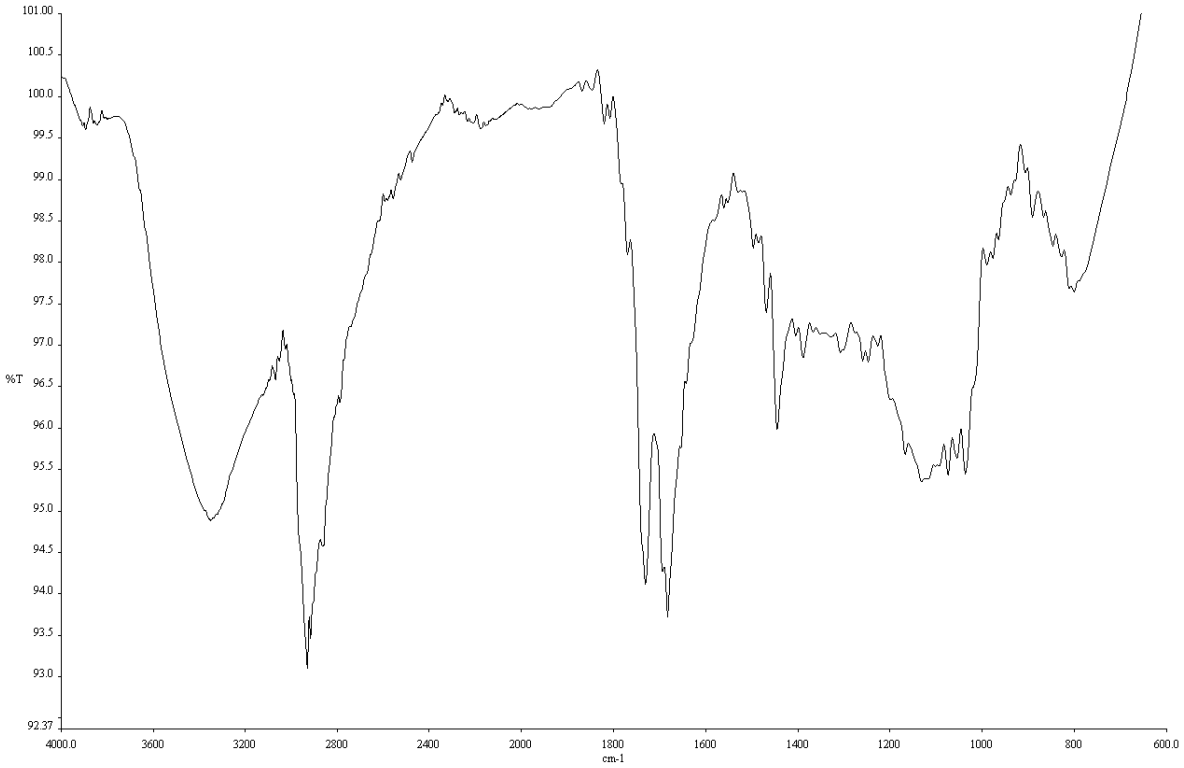


Figure A3.29. Infrared spectrum (Thin Film, NaCl) of compound **45**.

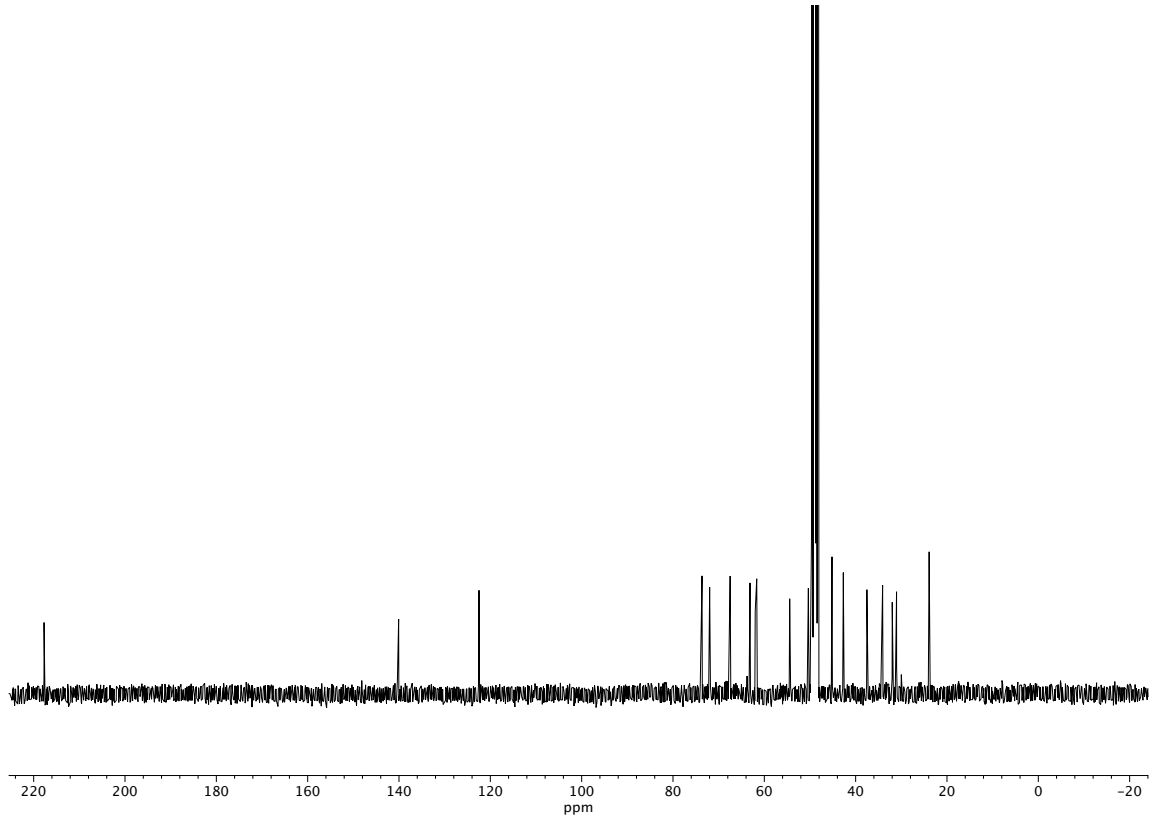


Figure A3.30. ^{13}C NMR (101 MHz, CD_3OD) of compound **45**.

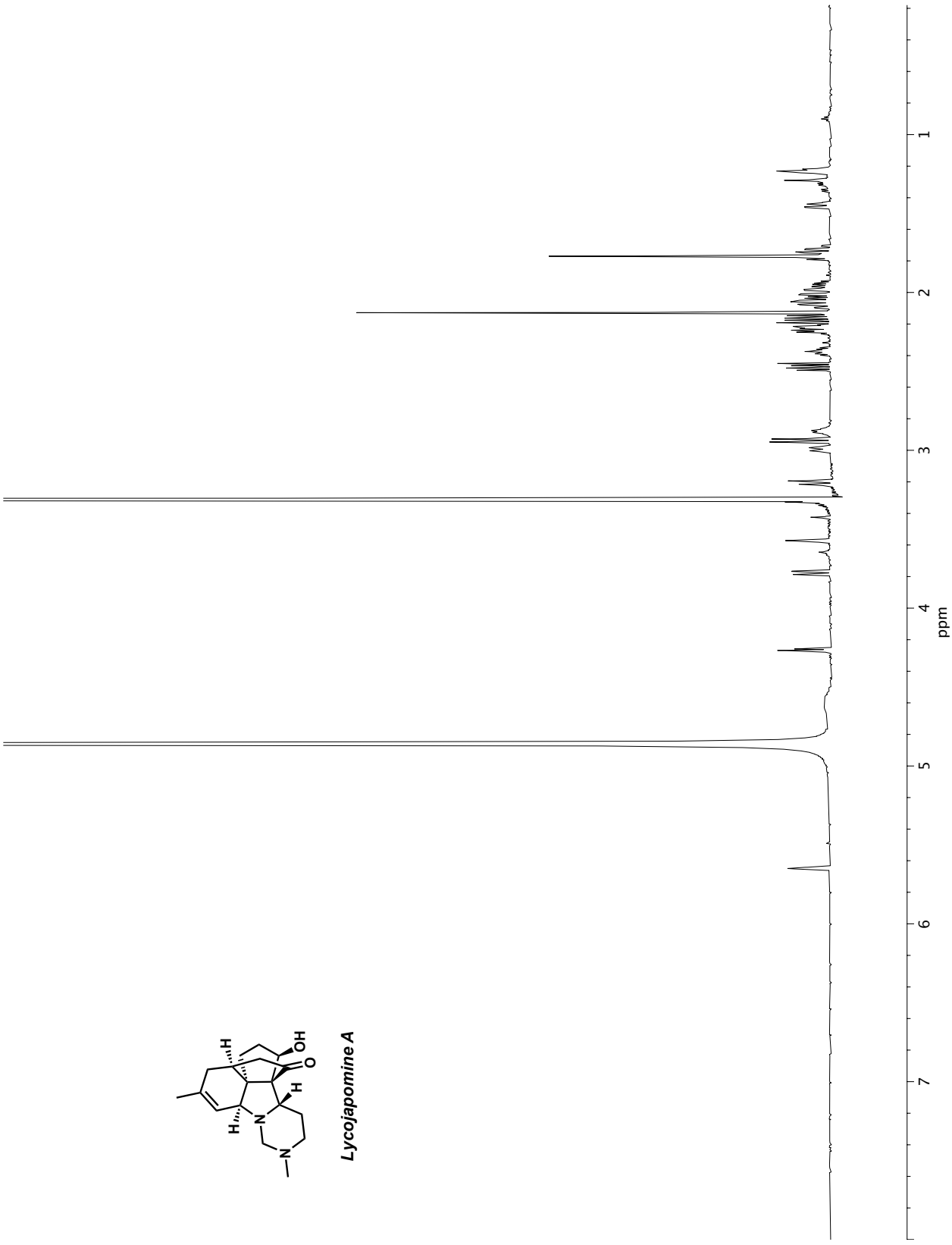


Figure A3.31. ^{1}H NMR (600 MHz, CD_3OD) of compound **44**.

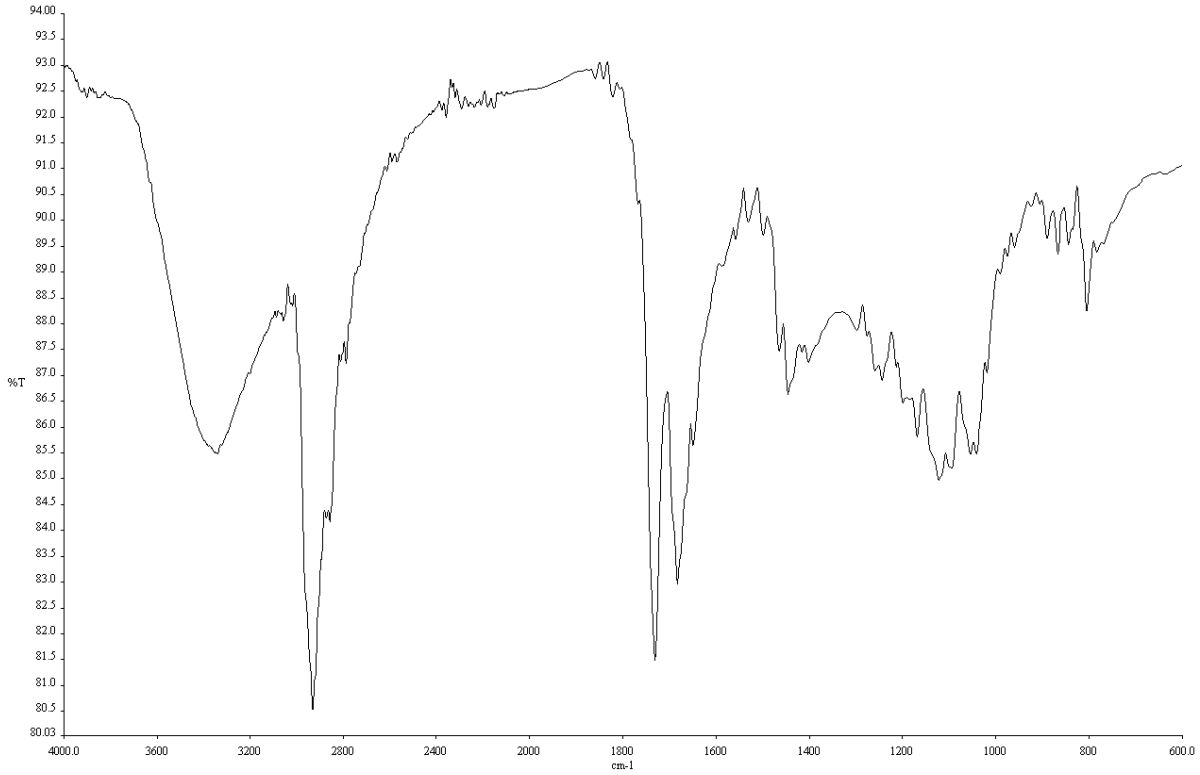


Figure A3.32. Infrared spectrum (Thin Film, NaCl) of compound **44**.

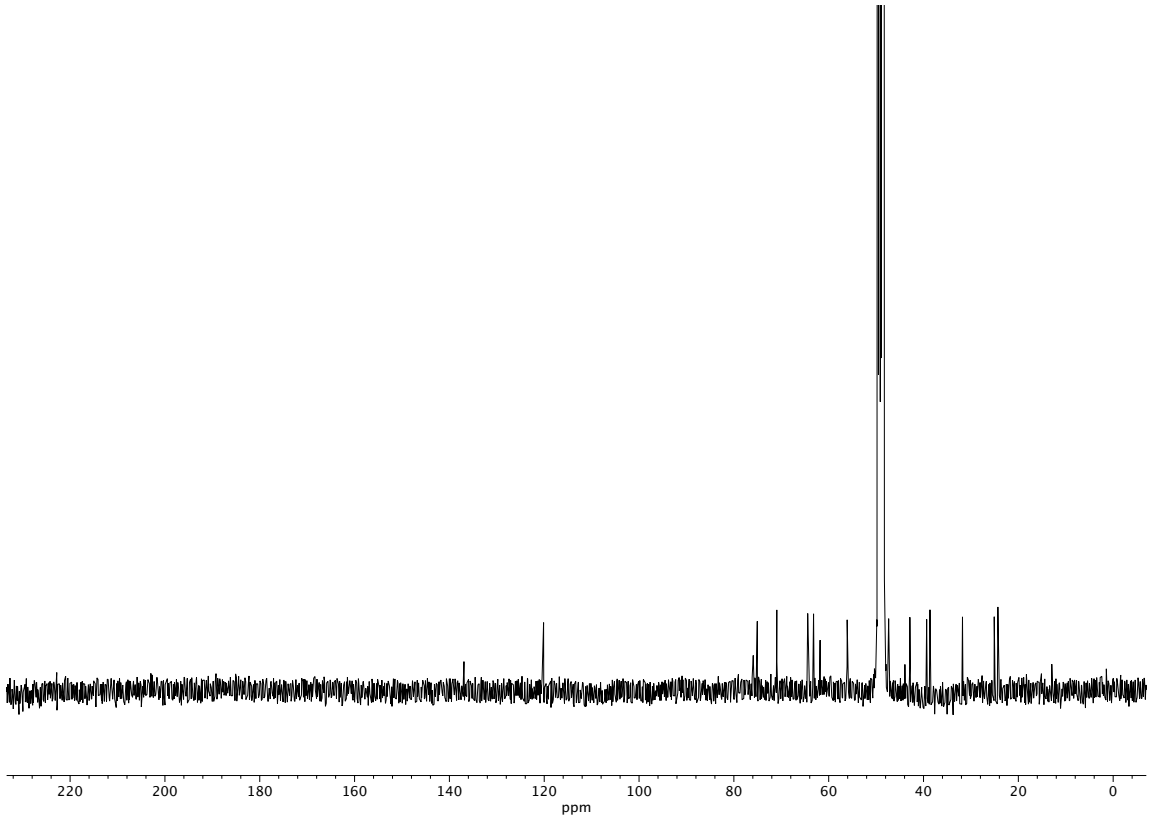


Figure A3.33. ^{13}C NMR (101 MHz, CD_3OD) of compound **44**.

CHAPTER 3

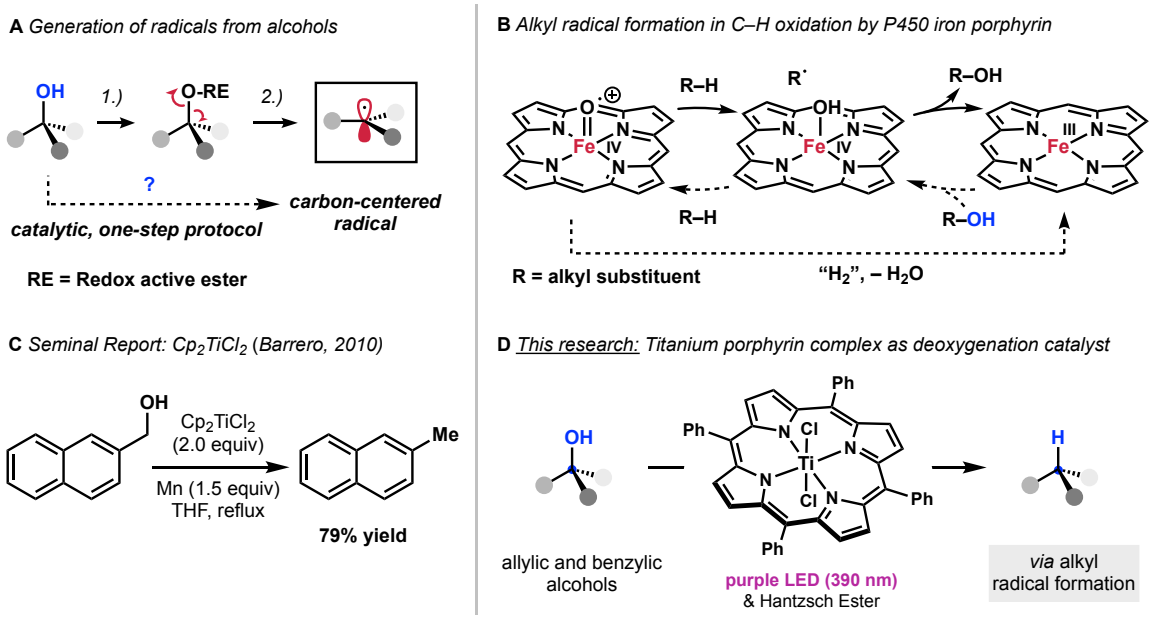
Radical Deoxygenation of Alcohols by a Titanium Porphyrin Catalyst

3.1 INTRODUCTION

The use of radical intermediates in synthetic organic chemistry has seen an increased rise in popularity over the last decade.[1,2] Due to the development of new reaction methodology, carbon-centered radicals have become valuable synthetic intermediates that give way to a variety of downstream manipulations (Figure 3.1.1, A).[2] These have led to a certain generality in single-electron logic, with reactions such as hydrogen-atom transfer, Giese additions or metal-mediated cross-couplings being well-established. Their complementary nature to ionic transformations has opened doors for new chemical reactivity, making them popular in industrial and academic settings alike. To gain accessibility to these reactions however, selective generation of the carbon-centered radical from ubiquitous precursors is necessary. One of the longer standing challenges in this area has been the radical deoxygenation of alcohols, by generation of the corresponding alkyl radical.[3] Due to the strong nature of the C–O bond and lack of driving force for homolytic bond cleavage, traditional methods rely on a two-step protocol, via preactivation of the alcohol. This is exemplified by the original protocol in the Barton deoxygenation, forming the xanthate ester before being able to induce radical C–O bond cleavage.[4] Many groups

have evolved this logic through the introduction of more easily accessible redox active esters that can be preformed or generated in-situ and employed for radical formation.[5] To address this challenge, we sought to identify a new catalyst that provides convenient entry to the generation of carbon-centered radicals directly from the alcohol. This would provide the blueprint for a catalytic, one-step protocol, making the direct radical deoxygenation of alcohols more accessible.

Figure 3.1.1 *Evolution of a titanium porphyrin catalyst for deoxygenation.*



Trying to identify a possible transition-metal catalyst for deoxygenation, we were inspired by the intriguing reactivity of the iron porphyrin active site found in P450 enzymes (Figure 3.1.1, B).[6] Looking closer at the mechanism, the iron metal center undergoes oxygen rebound chemistry and generates a carbon-centered radical in the process.[7] The enzyme essentially performs the opposite reaction to our desired process, selectively oxidizing inert C–H bonds. An iron(IV)-oxo radical cation abstracts an H atom from the substrate to generate the alkyl radical intermediate. This radical rebounds with the iron(IV)-oxo

complex, which is reduced to iron(III) in the process, and releases the alcohol. Within the laws of microscopic reversibility, we envisioned adapting this mechanism to perform the opposite reaction. This would involve coordination of the alcohol to a metal(III) center, which now must be reducing, to cleave the C–O bond, generate a metal (IV)-oxo complex and release the alkyl radical. Our catalyst would have to be turned over by an equivalent of H_2, to release water and regenerate the active metal(III) complex. To overturn the reactivity of the oxidizing heme, we deemed to switch out the iron metal for an alternate transition metal that can be reducing in its nature.

A seminal report by Barrero and co-workers in 2010 introduced the ability of Nugent's reagent (Cp_2TiCl_2) to directly deoxygenate various alcohols (Figure 3.1.1, C).[8] While its ability to reductively open epoxides had been well established, the authors were able to demonstrate direct C–O bond cleavage of an alcohol by the reagent for the first time. Interestingly, they observed the necessity to employ two equivalents of titanium metal to give full conversion of starting material. Believed to first undergo reduction to Ti(III) by excess manganese, the metal binds to the alcohol, undergoing oxidation to a Ti(IV)-oxo species and releasing the carbon-centered radical. However, excess Ti(III) can recombine with the alkyl radical to give a semi-stable carbon-Ti(IV) bond. This species is formed after deoxygenation and is later hydrolyzed during work-up, showcasing the challenge of achieving catalytic turnover for a titanium catalyst. In an impressive preliminary result, the group was able to succeed in the use of catalytic Cp_2TiCl_2 (0.3 equiv), turning over the catalyst with excess manganese (8.0 equiv) and TMSCl (4.0 equiv).[8] This system was later adapted by Shu and co-workers for activation of tertiary alcohols for Giese addition.[9] Following their reports, several studies have been presented that employ titanium metal

complexes in similar fashion for deoxygenation reactions.[10] These seminal findings and reports led us to further investigate titanium as a deoxygenation catalyst.

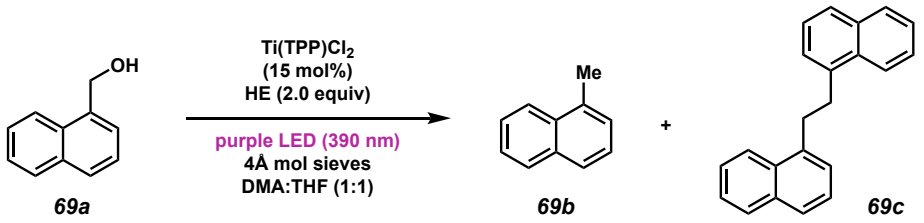
3.2 REACTION OPTIMIZATION

We proposed synthesizing a titanium porphyrin complex, analogous to the iron porphyrin complex present in P450 enzymes. The porphyrin framework provides a stable ligand with potential photoabsorbance for activation and reduction. To our benefit, the group of Woo et al. has reported the synthesis and characterization of various transition-metal porphyrin complexes, including titanium analogs.[11] Based on their literature precedent, we were able to successfully prepare the phenyl-substituted titanium porphyrin complex Ti(TPP)Cl_2 (Table 3.2.1). The complex would serve as our Ti(IV) precatalyst, which could undergo initial reduction to the active Ti(III) species. While metal reductants can realize this transformation, we wanted to circumvent the use of excess reagents, such as silyl chlorides, to turn over the catalyst. Gänsauer and co-workers showed the successful implementation of photochemistry for reduction, by excitation of Cp_2TiCl_2 in the presence of *i*Pr_2EtN with green light.[12] However, the short lifetime of the photoexcited species and slow decomposition of Cp_2TiCl_2 render the catalyst problematic for direct photoexcitation. The photoabsorbance of porphyrins is well established, and we sought to realize direct photoexcitation of our catalyst with visible light. If successful, it could undergo the desired Ti(IV) to Ti(III) redox cycle.

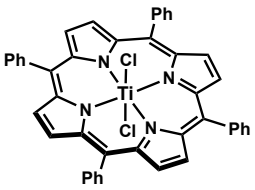
To facilitate reduction with an electron donor, we investigated different wavelengths for photoexcitation in the presence of Hantzsch Ester (HE). We chose substrate **69a** as a practical model substrate for deoxygenation (Table 3.2.1). To our delight, upon irradiation

of the reaction mixture with purple LEDs (390 nm) in DMA as solvent, we observed deoxygenation to product **69b** in 45% yield (Entry 2).

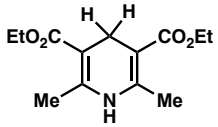
Table 3.2.1 *Optimization of reaction conditions.*



entry	deviation from standard conditions	yield of *69a*	yield of *69c*
1	*none*	**84%**	trace
2	DMA	45%	-
3	THF	-	90%
4	CH_2Cl_2	-	89%
5	HE (4.0 equiv)	64%	trace
6	10 mol% Ti-catalyst	61%	trace
7	blue LED (450 nm)	5%	-
8	no Ti-catalyst	-	-
9	no purple LED	-	-
10	no HE	-	-
11	no 4Å mol sieves	-	-



$Ti(TPP)Cl_2$



Hantzsch Ester (HE)

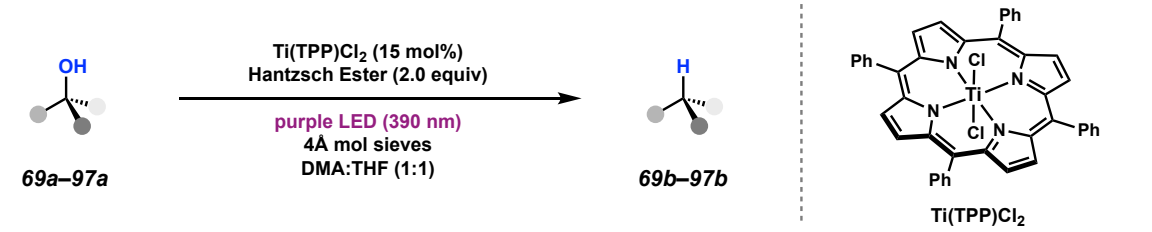
Most of the left-over mass balance was unreacted starting material **69a**. Irradiation with blue LEDs resulted in zero to minimal turnover (Entry 7). When switching solvents to dichloromethane or THF, the reaction was pushed to full conversion and delivered a clean reaction profile (Entry 3 & 4). In these cases, however, we observed sole formation of the dimeric product **69c**. This result can potentially be attributed to different aggregation of catalyst transition states or the rate of hydrogen atom transfer. When employing a 1:1 mixture of DMA and THF, we preserved full consumption of starting material and observed only trace amount of dimer formation, isolating the desired product **69b** in 84% yield. Alternating the equivalents of Hantzsch ester or catalyst loading did not produce an

improvement (Entry 5 & 6). In control reactions, omitting any of the additives, including molecular sieves, resulted in no conversion and shutdown of reactivity (Entry 8-11).

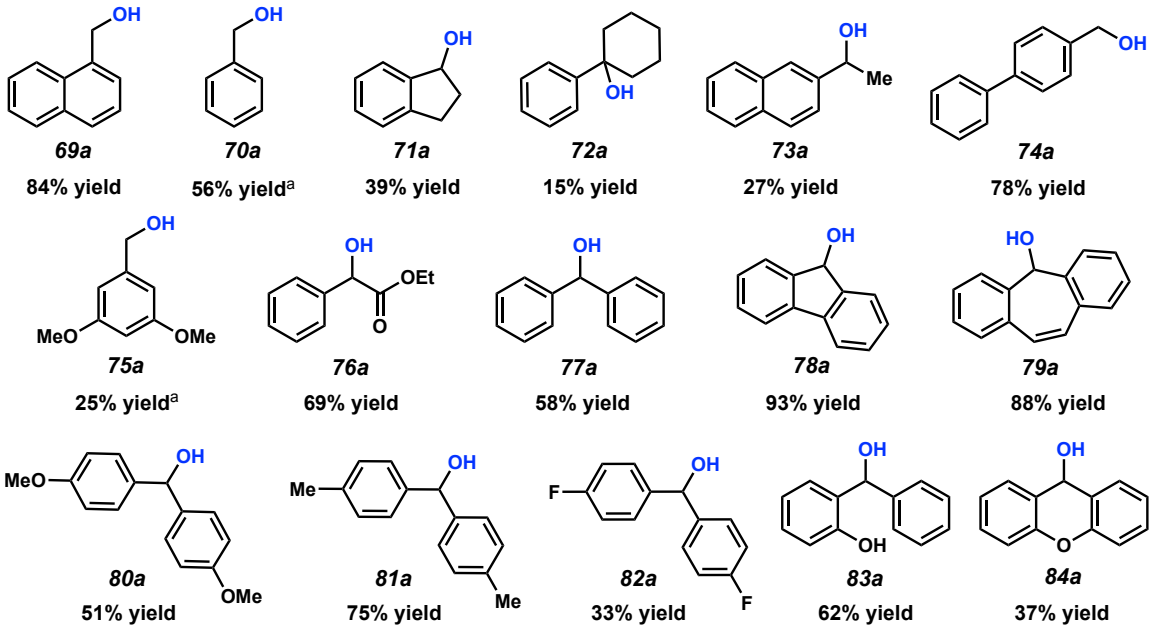
3.3 EVALUATION OF SUBSTRATE GENERALITY

With these results in hand, we set out to investigate the functional group tolerance of the catalytic system and ability to deoxygenate various substrates (Figure 3.3.1). Expanding on benzylic alcohols, we observed good conversion of benzyl alcohol **70a**, and slightly lower conversion going to secondary (**71a**) and tertiary (**72a**) benzylic alcohols. Biphenyl **74a** gave excellent conversion, isolating the product in 78% yield. Interestingly, the ethyl naphthalene substrate **73a** gave lower conversion than the model substrate **69a**, suggesting the presence of β-alkyl substituents to hinder turnover of the catalyst. When switching to diarylmethanes, we observed more general activation on a variety of substrates (**77a**-**84a**). Substituents such as methoxy, methyl, fluorine or phenols (**83a**) were widely compatible. Interestingly, we observed lower yield due to partial dimer formation in some cases, likely depending on the specific electronics of the system. Esters also proved to be well tolerated, isolating the deoxygenated product of mandelic acid ethyl ester **76a** in 69% yield. Expanding on the scope, we sought out to test allylic systems. We were pleased to observe full conversion of cinnamyl alcohol **85a**. Our catalyst achieved the deoxygenation on a wide range of cinnamyl alcohols, showing little side reaction to dimerized byproducts in most cases. Electron-withdrawing groups in the halogen series (**86a**-**88a**) were well tolerated, as were electron-donating groups, such as unprotected phenol substrate **89a**, and the dimethoxy-substituted substrate **90a**.

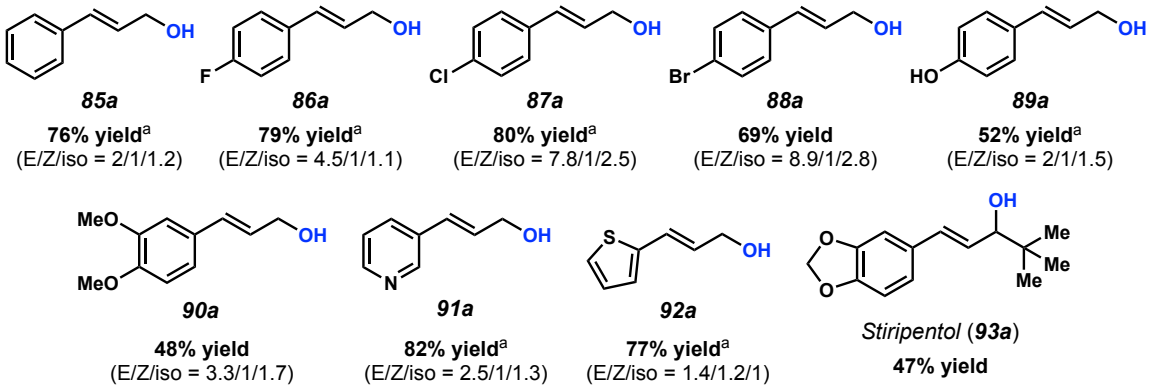
Figure 3.3.1 *Substrate scope for radical deoxygenation.*



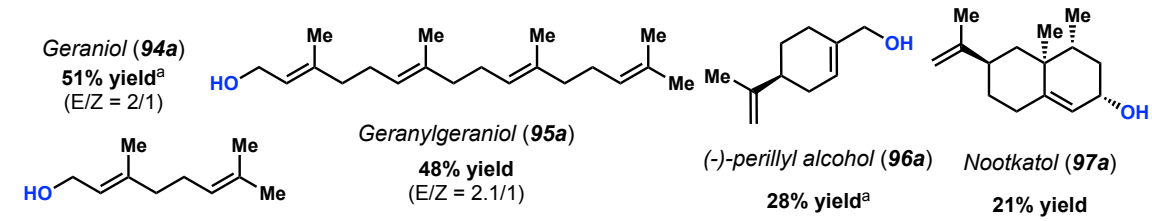
benzylic alcohols



cinnamyl alcohols



natural products (allylic alcohols)



[a] Yield determined by quantitative ^{1}H-NMR with 1,3,5-trimethoxybenzene as internal standard.

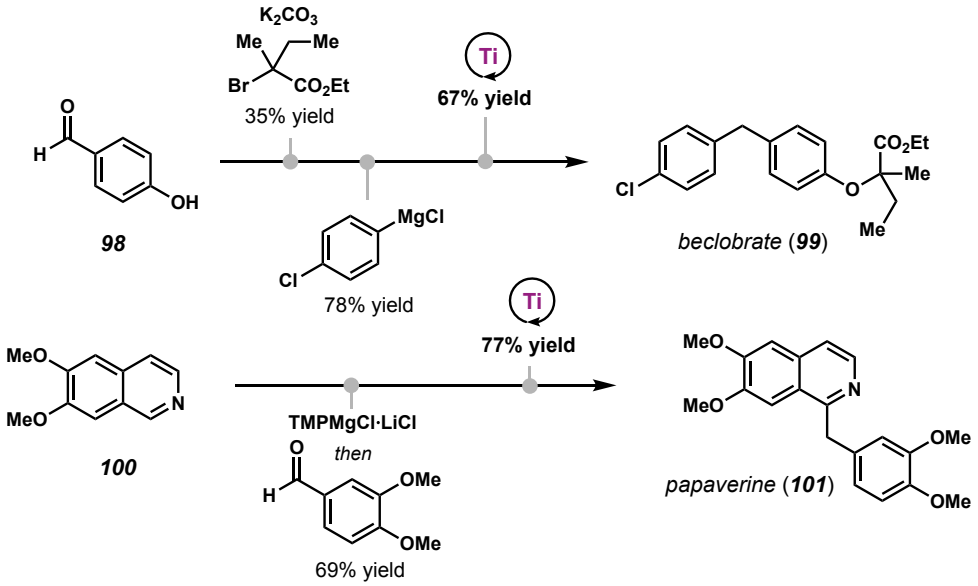
In most cases we observed a mixture of olefin isomers, namely the *E*/*Z* styrene, and the migration of the double bond to the allylic substituted benzene. We generally noted preferential formation of the (*E*)-isomer in most derivates, yet substrate control seems to play a crucial part in determining product distribution. To our delight, even heterocycles such as pyridine or thiophene (**91a** and **92a**) were well tolerated and gave high yields of product. The neopentylic, secondary alcohol in the anticonvulsant medication *Stiripentol* (**93a**) could be activated by our catalytic system as well, giving the deoxygenated derivative in decent yield. Lastly, we asked the question if non-conjugated allylic alcohols could be utilized as well.

Testing the deoxygenation on geraniol and geranylgeraniol (**94a** & **95a**), we were pleased to find good turnover and isolation of the product in 51% and 48% yield respectively. Further advancements on different terpenes, such as perillyl alcohol (**96a**) and secondary alcohol nootkatol (**97a**), gave deoxygenated product in both cases, yet in modest yields. In preliminary findings, we observed trace amounts of product formation on tertiary, secondary or primary alcohols, highlighting the potential of this catalytic system to expand on more general aliphatic alcohols.

With the substrate scope evaluated, we identified an opportunity to showcase the new method in synthetic scenarios. Observing generally good reactivity on the diarylmethane derivates, these motifs are found in a variety of pharmaceutical and natural products.[13] Retrosynthetically, we sought out addition of a Grignard or metalated starting material to the corresponding aldehyde and subsequently directly deoxygenating the resulting alcohol using our titanium catalyst (Figure 3.3.2). Targeting the lipoprotein regulator *beclobrate* (**99**), we alkylated 4-hydroxybenzaldehyde **98**, following addition of 4-chloro-

phenylmagnesium chloride in good yield. The intermediate was well tolerated in our catalytic system, giving the deoxygenated target **99** in 67% yield, completing the three-step sequence.

Figure 3.3.2 *Implementation of deoxygenation method in synthesis.*

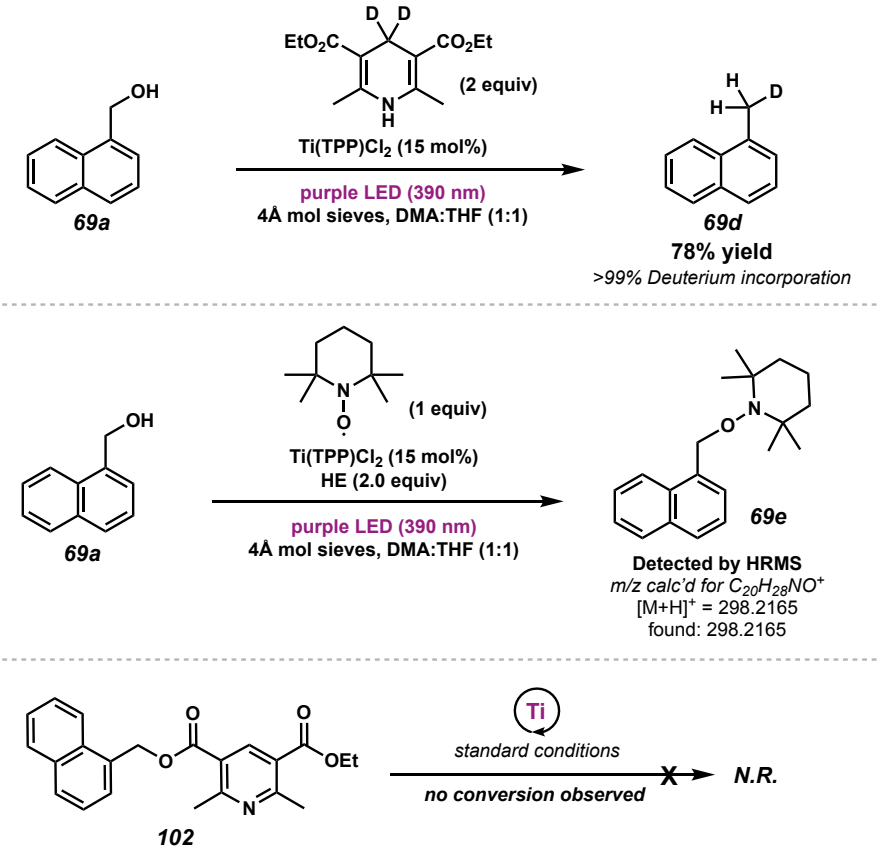


Synthesis of the opium alkaloid and antispasmodic drug *papaverine* (**101**) commenced from commercial isoquinoline **100**. Metalation with turbo-Hauser base and addition into veratraldehyde gave an intermediate secondary alcohol in 69% yield.[14] Our standard deoxygenation conditions proceeded, displaying the natural product **101** in 77% yield. With Grignard and metal additions being robust and straightforward transformations, our system displays convenient utility for the synthesis of diarylmethane motifs. As exemplified in these cases, our deoxygenation method may present enhanced chemoselectivity and functional group tolerance, compared to analogous deoxygenations with hydrosilanes or heterogeneous hydrogenations.

3.4 MECHANISTIC INVESTIGATIONS

To gain further insight into our catalytic method, we conducted several preliminary mechanistic experiments (Figure 3.4.1). To rule out any solvent, such as DMA, water or other reagents participating as H atom source, we synthesized a deuterated Hantzsch ester derivative.[15] Employing it in our standard reaction conditions with substrate **69a**, we isolated deuterated product **69d** in 78% yield, suggesting Hantzsch ester as the exclusive H atom source.

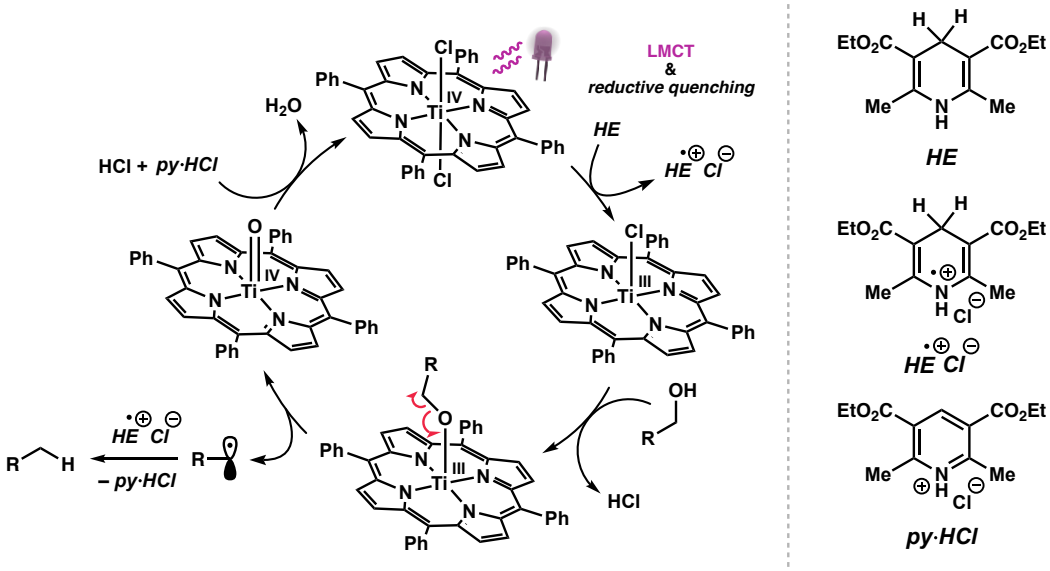
Figure 3.4.1 *Mechanistic control experiments.*



To support our hypothesis of a radical intermediate, we added TEMPO as a radical trap to our standard conditions. The reaction shut down, and we only observed trace dimer formation. Subjecting the mixture to HRMS analysis, we detected the adduct **69e**, with a match on its exact mass (see Experimental Section). Lastly, we wanted to rule out any

potential in-situ activation of our alcohol by the Hantzsch ester, as observed by Sato, Morisaki, and co-workers.[16] We therefore synthesized the adduct **102** and subjected it to our reaction conditions. We observed no conversion of the substrate, cleanly isolating unreacted starting material. Given these results, we propose a potential catalytic cycle, starting from our Ti(IV) precatalyst (Figure 3.4.2). As shown in literature precedent, the Ti(IV) species can easily be reduced to Ti(III). In our case, we propose photoexcitation of the porphyrin framework by purple LEDs through ligand to metal charge transfer (LMCT), making the titanium center viable for reductive quenching by the Hantzsch ester.[17,18] The reduced Ti(III) species can coordinate the alcohol starting material, initiating homolytic C–O bond cleavage. This results in generation of the alkyl radical intermediate, which can undergo H atom transfer with the Hantzsch ester radical cation. The Ti(IV)-oxo species can be turned over with the two equivalents of HCl generated in the course of the reaction, producing water as a byproduct, and closing the catalytic cycle with regeneration of our precatalyst.[19]

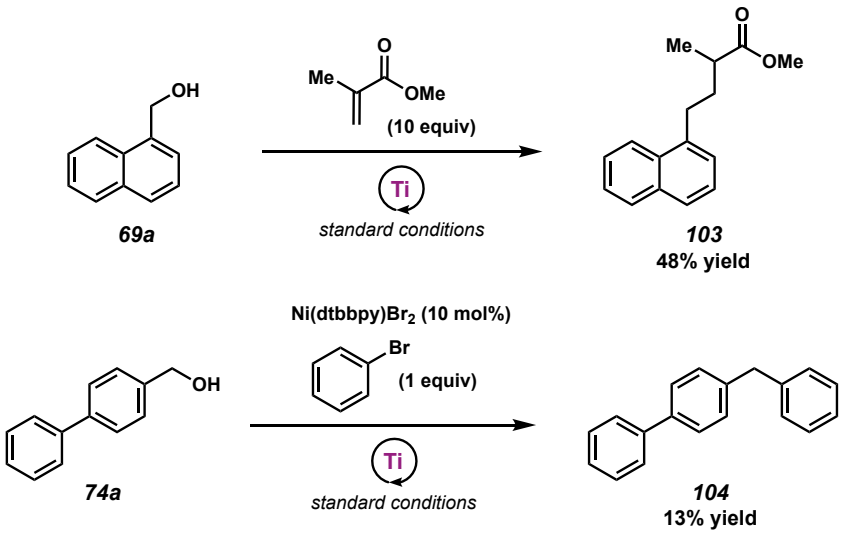
Figure 3.4.2 *Preliminary mechanistic proposal.*



3.5 USE IN GIESE ADDITION AND CROSS-COUPLING

Building on the value of the carbon-centered radical, we tested interception of the intermediate for downstream functionalization (Figure 3.5.1). When adding an excess of methyl methacrylate to the reaction, we could isolate the Giese addition product **103** in 48% yield. Furthermore, when adding one equivalent of phenyl bromide and 10 mol% of nickel catalyst to substrate **74a**, we were delighted to observe formation of the cross-coupled product **104** in 13% yield.[20,21] These results further validate our radical mechanism and present the generality of this system to be employed in radical transformations, greatly increasing its synthetic value.

Figure 3.5.1 *Interception of radical for Giese addition and Nickel cross-coupling.*



3.6 CONCLUSION

In summary, we present the unique catalytic activity of a titanium porphyrin complex and its ability to activate C–O bonds, presumed by generation of an alkyl radical. While usually a two-step process, we present a novel catalytic system that achieves the direct

transformation with minimal additives. Unlike other titanium deoxygenations, we harness the photoabsorption of a porphyrin framework to photoexcite the catalyst, using Hantzsch ester as mild reductant. This creates reaction conditions with high functional group tolerance, excluding the addition of metal reductants or chlorosilanes to turn over the catalyst. We demonstrated our reaction on a variety of substrates, showcasing the synthetic utility for diarylmethanes, cinnamyl alcohols, as well as allylic alcohols. In preliminary investigations we intercept the radical intermediate, employing it successfully for Giese addition and nickel-catalyzed cross coupling. This demonstrates the compatibility of the method for general entry into radical chemistry directly from alcohols. With the ability to manipulate the porphyrin framework and conduct further in-depth mechanistic interrogations, the potential of the titanium catalyst is extensive, with future studies aimed at the activation of aliphatic alcohols as well.

3.7 EXPERIMENTAL SECTION

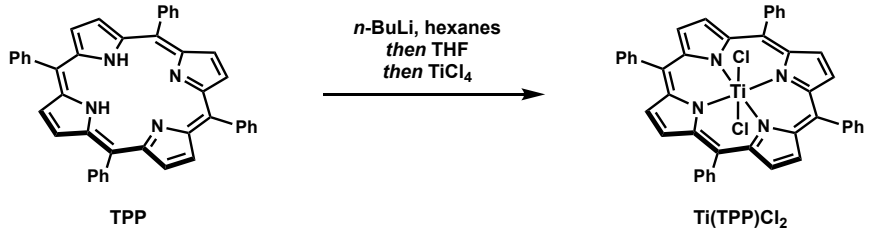
3.7.1 MATERIALS AND METHODS

Unless otherwise stated, reactions were performed in flame-dried glassware under an argon or nitrogen atmosphere using dry, deoxygenated solvents. Solvents were dried by passage through an activated alumina column under argon.[22] Reaction progress was monitored by thin-layer chromatography (TLC). TLC was performed using E. Merck silica gel 60 F254 precoated glass plates (0.25 mm) and visualized by UV fluorescence quenching, p-anisaldehyde, or $KMnO_4$ staining. Silicycle SiliaFlash® P60 Academic Silica gel (particle size 40–63 μm) was used for flash chromatography. ^1H NMR spectra were recorded on Varian Inova 500 MHz and 600 MHz and Bruker 400 MHz spectrometers and are reported

relative to residual $CHCl_3$ (δ 7.26 ppm), C_6D_6 (δ 7.16 ppm) or CD3OD (δ 3.31 ppm). ^{13}C NMR spectra were recorded on a Varian Inova 500 MHz spectrometer (125 MHz) and Bruker 400 MHz spectrometers (101 MHz) and are reported relative to $CHCl_3$ (δ 77.16 ppm), C_6D_6 (δ 128.06 ppm) or CD_3OD (δ 49.01 ppm). Data for ^1H NMR are reported as follows: chemical shift (δ ppm) (multiplicity, coupling constant (Hz), integration). Multiplicities are reported as follows: s = singlet, d = doublet, t = triplet, q = quartet, p = pentet, sept = septuplet, m = multiplet, br s = broad singlet, br d = broad doublet. Data for ^{13}C NMR are reported in terms of chemical shifts (δ ppm). IR spectra were obtained by use of a Perkin Elmer Spectrum BXII spectrometer or Nicolet 6700 FTIR spectrometer using thin films deposited on NaCl plates and reported in frequency of absorption (cm^{-1}). UV-Vis spectra were obtained by use of a Doube Beam Thermo Fisher Evolution 201 UV-Vis Spectrophotometer and reported in absorbance over wavelength (nm). High resolution mass spectra (HRMS) were obtained using an Agilent 6200 Series TOF with an Agilent G1978A Multimode source in electrospray ionization (ESI+) mode or a JOEL JMS-T2000 AccuTOF GC-Alpha high resolution mass spectrometer using field desorption (FD+) ionization, or field ionization (FI+).

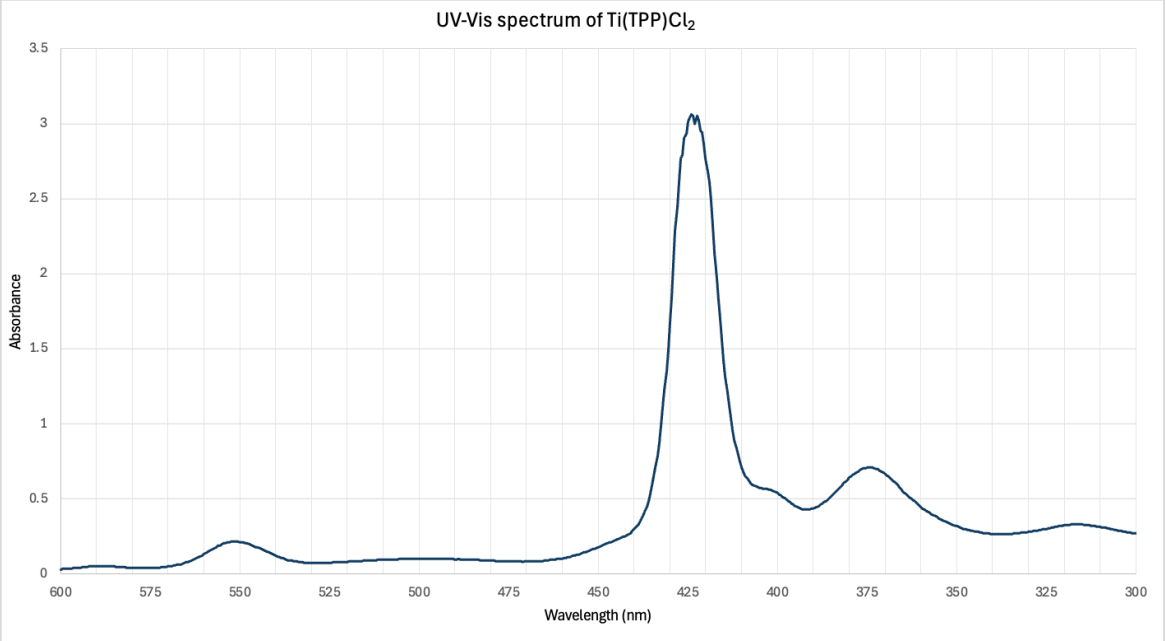
3.7.2 EXPERIMENTAL PROCEDURES

3.7.2.1 Synthesis of Ti(TPP)Cl_2:



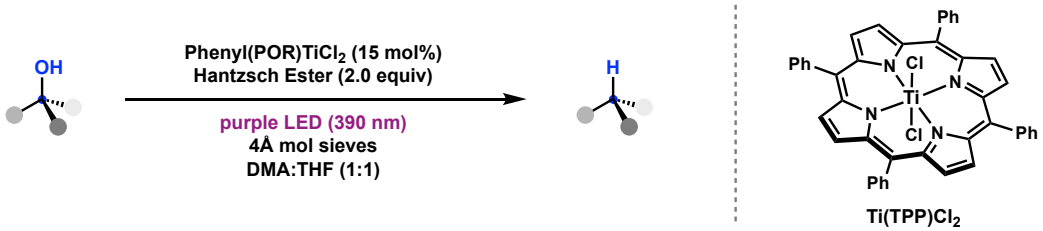
Ti(TPP)Cl_2: A Schlenk flask was flame-dried under vacuum and charged with TPP (1 g, 1.6 mmol, 1.0 equiv), which had previously been suspended with benzene (2x), the solvent evaporated under reduced pressure and dried under high-vacuum. The starting material was suspended in toluene (40 mL), which had previously been degassed using the freeze-pump-thaw method (3x). A solution of *n*-BuLi (2.5 M in hexanes, 1.3 mL, 3.28 mmol, 2.05 equiv) was added dropwise at room temperature, upon which the solution turned bright "forest green". After stirring for 10 min, $TiCl_4$ (0.7 mL, 6.4 mmol, 4.0 equiv) was added dropwise, the reaction mixture heated to 50 ºC in an oil bath and stirred for an additional 2 h. The reaction mixture was cooled to room temperature and the solvent evaporated to near dryness under reduced pressure. The residue was redissolved in a minimal amount of methylene chloride and layered with a surplus of hexanes. After diffusion over 72 h, a dark solid had crystallized, which was filtered off in a glovebox under inert atmosphere. The crystals were washed with hexanes to yield the product **Ti(TPP)Cl_2** (0.84 g, 1.15 mmol, 72% yield) as a dark-green solid. UV-Vis (CH_2Cl_2): 315, 374, 400, 424 (Soret), 552 nm; ^{1}H NMR (600 MHz, C_6D_6) δ 8.91 (s, 8H), 7.91 (d, J = 7.6 Hz, 8H), 7.45 (t, J = 7.7 Hz, 4H), 7.37 (t, J = 7.6 Hz, 8H); HRMS (FD+): m/z calc'd for $C_{44}H_{28}Cl_2N_4Ti$ $[M]^{+\bullet}$: 730.1165, found 730.1158.

***Figure 3.7.2.1.1**: UV-Vis spectrum of Ti(TPP)Cl₂.*



Data collected at room temperature (21 ºC). Sample prepared under inert atmosphere in a 4mm quartz cuvette in CH_2Cl_2.

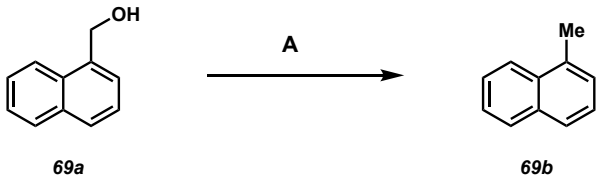
3.7.2.2 GENERAL REACTION PROCEDURE A:



A 5mL microwave-vial was charged with a magnetic stir bar, the starting material alcohol (0.05 mmol, 1.0 equiv) and Hantzsch ester (25.6 mg, 0.1 mmol, 2.0 equiv) and transferred into a glovebox under N_2. The titanium catalyst **Ti(TPP)Cl₂** (5.6 mg, 0.0075 mmol, 15 mol %) was weighed out, transferred into the reaction vial and the contents dissolved using a solvent mixture of THF:DMA (1:1, 1.0 mL, 0.05 M). Previously activated mol sieves (4Å, 300 mg, 6g/mmol) were added and the vial sealed with an aluminum cap using the appropriate crimper. The sealed reaction vial was transferred out of the glovebox and

fastened above a Kessil lamp (PR160L-390nm), approximately 2-3 cm above the light source. The lamp was equipped with a reflective mirror and stirred using a magnetic stir plate set at 800 rpm. The reaction mixture was irradiated for 12-16h, under ventilation with two fans and a fume hood exhaust. Upon completion, the internal temperature of the reaction mixture had reached between 35-40 ºC. The vial was transferred to a fume hood, the reaction quenched with an aqueous solution of LiCl (10% w/v, 2 mL) and extracted with organic solvent. The extract was directly analyzed by quantitative ^{1}H-NMR or concentrated under reduced pressure and purified using flash chromatography on silica gel.

3.7.2.3 SUBSTRATES FOR DEOXYGENATION

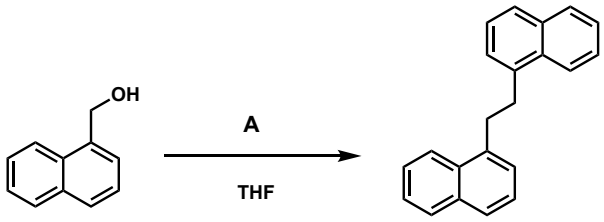


69a ***69b***

Reaction performed according to **General Procedure A**, using starting material **69a** (7.9 mg, 0.05 mmol). The aqueous layer was extracted with ethyl acetate (3 x 1.5 mL), dried over Na_2SO_4 and the solvent evaporated under reduced pressure. The crude product was purified by flash chromatography on silica gel (hexanes), to give product **69b** (6.0 mg, 0.042 mmol, 84% yield) as a colorless oil.

^{1}H NMR (400 MHz, $CDCl_3$) δ 8.18 – 7.97 (m, 1H), 7.92 – 7.83 (m, 1H), 7.72 (d, J = 8.1 Hz, 1H), 7.62 – 7.45 (m, 2H), 7.44 – 7.30 (m, 2H), 2.72 (s, 3H).

The spectroscopic data is in agreement with the values previously reported.[23]

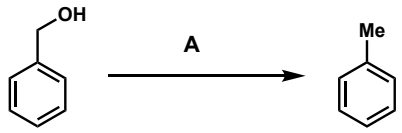


69a ***69c***

Reaction performed according to **General Procedure A**, using starting material **69a** (7.9 mg, 0.05 mmol) and THF (1.0 mL) as solvent. The aqueous layer was extracted with ethyl acetate (3 x 1.5 mL), dried over Na_2SO_4 and the solvent evaporated under reduced pressure. The crude product was purified by flash chromatography on silica gel (hexanes), to give product **69c** (6.3 mg, 0.023 mmol, 90% yield) as a colorless solid.

^{1}H NMR (400 MHz, $CDCl_3$) δ 8.13 (d, J = 7.9 Hz, 2H), 7.93 – 7.87 (m, 2H), 7.76 (d, J = 8.1 Hz, 2H), 7.62 – 7.46 (m, 4H), 7.45 – 7.33 (m, 4H), 3.52 (s, 4H).

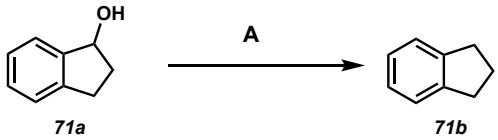
The spectroscopic data is in agreement with the values previously reported.[24]



70a ***70b***

Reaction performed according to **General Procedure A**, using starting material **70a** (5.4 mg, 0.05 mmol). The aqueous layer was extracted with $CDCl_3$ (2 x 0.5 mL) and the combined organic layers spiked with 1,3,5-trimethoxy benzene (1.0 equiv). An aliquot (0.5 mL) was directly transferred into an NMR tube and the yield of **70b** (0.028 mmol, 56% yield) determined by quantitative ^{1}H-NMR with 1,3,5-trimethoxy benzene as an internal standard.

The spectroscopic data aligned with the values previously reported.[25]

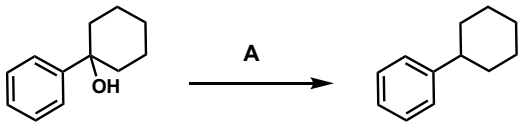


71a ***71b***

Reaction performed according to **General Procedure A**, using starting material **71a** (6.7 mg, 0.05 mmol). The aqueous layer was extracted with ethyl acetate (3 x 1.5 mL), dried over Na_2SO_4 and the solvent evaporated under reduced pressure. The crude product was purified by flash chromatography on silica gel (hexanes), to give product **71b** (2.3 mg, 0.02 mmol, 39% yield) as a colorless oil.

^{1}H NMR (400 MHz, $CDCl_3$) δ 7.24 (dt, *J* = 7.2, 3.6 Hz, 2H), 7.17 – 7.12 (m, 2H), 2.93 (t, *J* = 7.4 Hz, 4H), 2.08 (p, *J* = 7.4 Hz, 2H).

The spectroscopic data is in agreement with the values previously reported.[26]

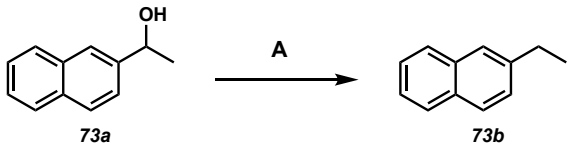


72a ***72b***

Reaction performed according to **General Procedure A**, using starting material **72a** (8.8 mg, 0.05 mmol). The aqueous layer was extracted with ethyl acetate (3 x 1.5 mL), dried over Na_2SO_4 and the solvent evaporated under reduced pressure. The crude product was purified by flash chromatography on silica gel (hexanes), to give product **72b** (1.2 mg, 0.0075 mmol, 15% yield) as a colorless oil.

^{1}H NMR (400 MHz, $CDCl_3$) δ 7.33 – 7.27 (m, 2H), 7.23 – 7.14 (m, 3H), 2.56 – 2.45 (m, 1H), 1.86 (tddd, *J* = 11.0, 6.4, 3.1, 1.6 Hz, 4H), 1.75 (dtt, *J* = 12.5, 3.1, 1.5 Hz, 1H), 1.50 – 1.32 (m, 4H), 1.32 – 1.14 (m, 1H).

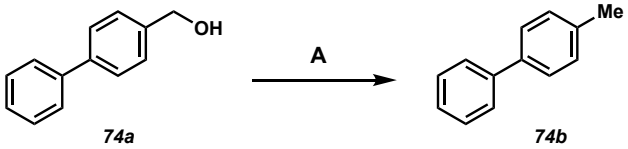
The spectroscopic data is in agreement with the values previously reported.[27]



Reaction performed according to **General Procedure A**, using starting material **73a** (8.6 mg, 0.05 mmol). The aqueous layer was extracted with ethyl acetate (3 x 1.5 mL), dried over Na_2SO_4 and the solvent evaporated under reduced pressure. The crude product was purified by flash chromatography on silica gel (hexanes), to give product **73b** (2.1 mg, 0.014 mmol, 27% yield) as a colorless oil.

^{1}H NMR (400 MHz, $CDCl_3$) δ 7.83 – 7.74 (m, 3H), 7.63 (s, 1H), 7.49 – 7.38 (m, 2H), 7.36 (dd, J = 8.4, 1.8 Hz, 1H), 2.82 (q, J = 7.6, 2H), 1.33 (t, J = 7.6 Hz, 3H).

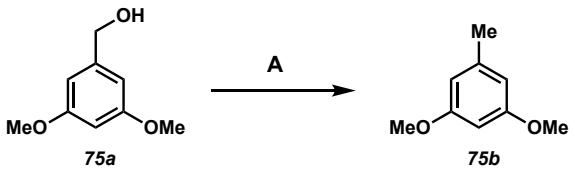
The spectroscopic data is in agreement with the values previously reported.[26]



Reaction performed according to **General Procedure A**, using starting material **74a** (9.2 mg, 0.05 mmol). The aqueous layer was extracted with ethyl acetate (3 x 1.5 mL), dried over Na_2SO_4 and the solvent evaporated under reduced pressure. The crude product was purified by flash chromatography on silica gel (hexanes), to give product **74b** (6.6 mg, 0.039 mmol, 78% yield) as a colorless oil.

^{1}H NMR (400 MHz, $CDCl_3$) δ 7.60 – 7.56 (m, 2H), 7.50 (d, J = 8.2 Hz, 2H), 7.43 (t, J = 7.6 Hz, 2H), 7.36 – 7.30 (m, 1H), 7.27 – 7.23 (m, 2H), 2.40 (s, 3H).

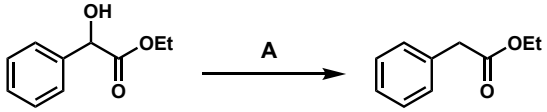
The spectroscopic data is in agreement with the values previously reported.[28]



75a *75b*

Reaction performed according to **General Procedure A**, using starting material **75a** (8.4 mg, 0.05 mmol). The aqueous layer was extracted with $CDCl_3$ (2 x 0.5 mL) and the combined organic layers spiked with 1,3,5-trimethoxy benzene (1.0 equiv). An aliquot (0.5 mL) was directly transferred into an NMR tube and the yield of **75b** (0.013 mmol, 25% yield) determined by quantitative ^{1}H-NMR with 1,3,5-trimethoxy benzene as an internal standard.

The spectroscopic data aligned with the values previously reported.[29]

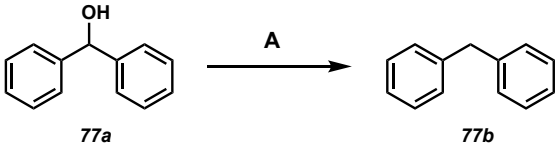


76a *76b*

Reaction performed according to **General Procedure A**, using starting material **76a** (9.0 mg, 0.05 mmol). The aqueous layer was extracted with ethyl acetate (3 x 1.5 mL), dried over Na_2SO_4 and the solvent evaporated under reduced pressure. The crude product was purified by flash chromatography on silica gel (hexanes/diethyl ether), to give product **76b** (5.7 mg, 0.035 mmol, 69% yield) as a colorless oil.

^{1}H NMR (400 MHz, $CDCl_3$) δ 7.35 – 7.24 (m, 5H), 4.15 (q, J = 7.1 Hz, 2H), 3.61 (s, 2H), 1.25 (t, J = 7.1 Hz, 3H).

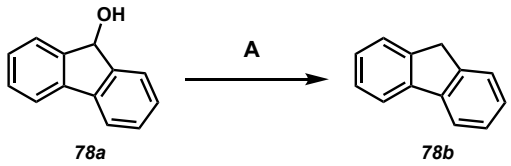
The spectroscopic data is in agreement with the values previously reported.[30]



Reaction performed according to **General Procedure A**, using starting material **77a** (9.2 mg, 0.05 mmol). The aqueous layer was extracted with ethyl acetate (3 x 1.5 mL), dried over Na_2SO_4 and the solvent evaporated under reduced pressure. The crude product was purified by flash chromatography on silica gel (hexanes), to give product **77b** (4.9 mg, 0.029 mmol, 58% yield) as a colorless oil.

^{1}H NMR (400 MHz, $CDCl_3$) δ 7.32 – 7.26 (m, 4H), 7.23 – 7.16 (m, 6H), 3.99 (s, 2H).

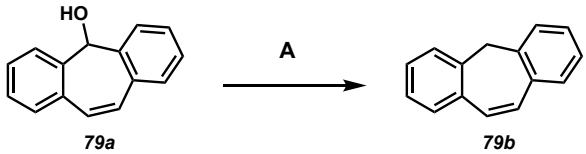
The spectroscopic data is in agreement with the values previously reported.[31]



Reaction performed according to **General Procedure A**, using starting material **78a** (9.1 mg, 0.05 mmol). The aqueous layer was extracted with ethyl acetate (3 x 1.5 mL), dried over Na_2SO_4 and the solvent evaporated under reduced pressure. The crude product was purified by flash chromatography on silica gel (hexanes), to give product **78b** (7.7 mg, 0.047 mmol, 93% yield) as a colorless oil.

^{1}H NMR (400 MHz, $CDCl_3$) δ 7.80 (d, J = 7.4 Hz, 2H), 7.55 (dt, J = 7.4, 1.0 Hz, 2H), 7.40 – 7.35 (m, 2H), 7.30 (td, J = 7.4, 1.2 Hz, 2H), 3.91 (s, 2H).

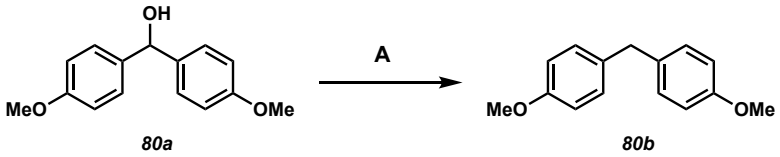
The spectroscopic data is in agreement with the values previously reported.[32]



Reaction performed according to **General Procedure A**, using starting material **79a** (10.4 mg, 0.05 mmol). The aqueous layer was extracted with ethyl acetate (3 x 1.5 mL), dried over Na_2SO_4 and the solvent evaporated under reduced pressure. The crude product was purified by flash chromatography on silica gel (hexanes), to give product **79b** (8.4 mg, 0.044 mmol, 88% yield) as a colorless oil.

^{1}H NMR (500 MHz, $CDCl_3$) δ 7.34 – 7.25 (m, 6H), 7.20 (td, *J* = 7.0, 1.8 Hz, 2H), 7.03 (s, 2H), 3.74 (s, 2H).

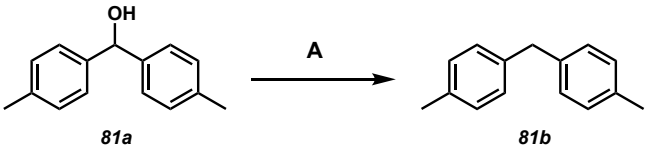
The spectroscopic data is in agreement with the values previously reported.[33]



Reaction performed according to **General Procedure A**, using starting material **80a** (12.2 mg, 0.05 mmol). The aqueous layer was extracted with ethyl acetate (3 x 1.5 mL), dried over Na_2SO_4 and the solvent evaporated under reduced pressure. The crude product was purified by flash chromatography on silica gel (hexanes/diethyl ether), to give product **80b** (5.8 mg, 0.025 mmol, 51% yield) as a colorless oil.

^{1}H NMR (600 MHz, $CDCl_3$) δ 7.09 (d, *J* = 8.6 Hz, 4H), 6.82 (d, *J* = 8.6 Hz, 4H), 3.87 (s, 2H), 3.78 (s, 6H).

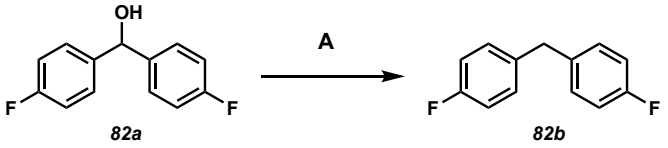
The spectroscopic data is in agreement with the values previously reported.[34]



Reaction performed according to **General Procedure A**, using starting material **81a** (10.6 mg, 0.05 mmol). The aqueous layer was extracted with ethyl acetate (3 x 1.5 mL), dried over Na_2SO_4 and the solvent evaporated under reduced pressure. The crude product was purified by flash chromatography on silica gel (hexanes), to give product **81b** (7.3 mg, 0.038 mmol, 75% yield) as a colorless oil.

^{1}H NMR (600 MHz, $CDCl_3$) δ 7.12 – 7.02 (m, 8H), 3.90 (s, 2H), 2.31 (s, 6H).

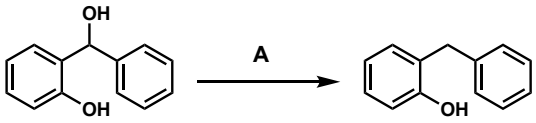
The spectroscopic data is in agreement with the values previously reported.[35]



Reaction performed according to **General Procedure A**, using starting material **82a** (11.0 mg, 0.05 mmol). The aqueous layer was extracted with ethyl acetate (3 x 1.5 mL), dried over Na_2SO_4 and the solvent evaporated under reduced pressure. The crude product was purified by flash chromatography on silica gel (hexanes), to give product **82b** (3.5 mg, 0.017 mmol, 33% yield) as a colorless oil.

^{1}H NMR (600 MHz, $CDCl_3$) δ 7.11 (dd, J = 8.6, 5.4 Hz, 4H), 6.97 (t, J = 8.7 Hz, 4H), 3.92 (s, 2H).

The spectroscopic data is in agreement with the values previously reported.[36]

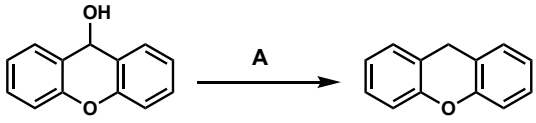


83a ***83b***

Reaction performed according to **General Procedure A**, using starting material **83a** (10.0 mg, 0.05 mmol). The aqueous layer was extracted with ethyl acetate (3 x 1.5 mL), dried over Na_2SO_4 and the solvent evaporated under reduced pressure. The crude product was purified by flash chromatography on silica gel (hexanes/ethyl acetate), to give product **83b** (5.7 mg, 0.031 mmol, 62% yield) as a colorless oil.

^{1}H NMR (600 MHz, $CDCl_3$) δ 7.32 – 7.27 (m, 2H), 7.25 – 7.18 (m, 3H), 7.15 – 7.10 (m, 2H), 6.89 (td, *J* = 7.4, 1.2 Hz, 1H), 6.79 (dd, *J* = 7.9, 1.2 Hz, 1H), 4.66 (brs, 1H), 4.00 (s, 2H).

The spectroscopic data is in agreement with the values previously reported.[37]

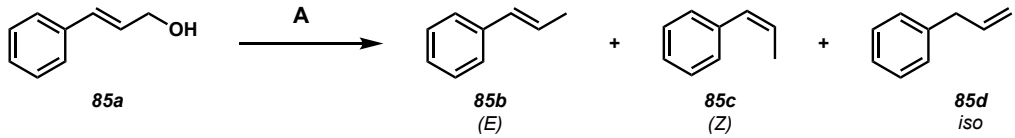


84a ***84b***

Reaction performed according to **General Procedure A**, using starting material **84a** (9.9 mg, 0.05 mmol). The aqueous layer was extracted with ethyl acetate (3 x 1.5 mL), dried over Na_2SO_4 and the solvent evaporated under reduced pressure. The crude product was purified by flash chromatography on silica gel (hexanes/diethyl ether), to give product **84b** (3.4 mg, 0.019 mmol, 37% yield) as a colorless oil.

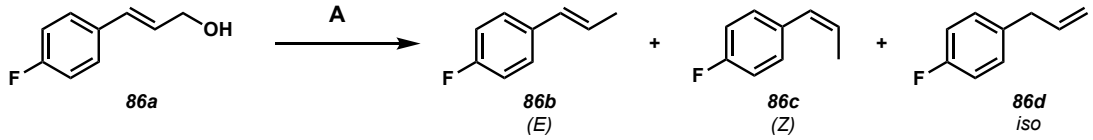
^{1}H NMR (400 MHz, $CDCl_3$) δ 7.22 – 7.13 (m, 4H), 7.06 – 6.97 (m, 4H), 4.06 (s, 2H).

The spectroscopic data is in agreement with the values previously reported.[38]



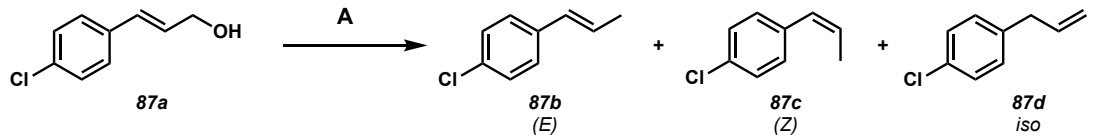
Reaction performed according to **General Procedure A**, using starting material **85a** (6.7 mg, 0.05 mmol). The aqueous layer was extracted with $CDCl_3$ (2 x 0.5 mL) and the combined organic layers spiked with 1,3,5-trimethoxy benzene (1.0 equiv). An aliquot (0.5 mL) was directly transferred into an NMR tube and the yield of **85b**:**85c**:**85d** (2:1:1.2, 0.038 mmol, 76% yield) determined by quantitative ^{1}H-NMR with 1,3,5-trimethoxy benzene as an internal standard.

The spectroscopic data aligned with the values previously reported.[39-41]



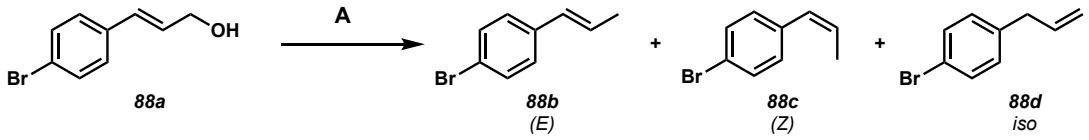
Reaction performed according to **General Procedure A**, using starting material **86a** (7.6 mg, 0.05 mmol). The aqueous layer was extracted with $CDCl_3$ (2 x 0.5 mL) and the combined organic layers spiked with 1,3,5-trimethoxy benzene (1.0 equiv). An aliquot (0.5 mL) was directly transferred into an NMR tube and the yield of **86b**:**86c**:**86d** (4.5:1:1.1, 0.04 mmol, 79% yield) determined by quantitative ^{1}H-NMR with 1,3,5-trimethoxy benzene as an internal standard.

The spectroscopic data aligned with the values previously reported.[42-44]



Reaction performed according to **General Procedure A**, using starting material **87a** (8.4 mg, 0.05 mmol). The aqueous layer was extracted with $CDCl_3$ (2 x 0.5 mL) and the combined organic layers spiked with 1,3,5-trimethoxy benzene (1.0 equiv). An aliquot (0.5 mL) was directly transferred into an NMR tube and the yield of **87b**:**87c**:**87d** (7.8:1:2.5, 0.04 mmol, 80% yield) determined by quantitative ^{1}H-NMR with 1,3,5-trimethoxy benzene as an internal standard.

The spectroscopic data aligned with the values previously reported.[45,46]



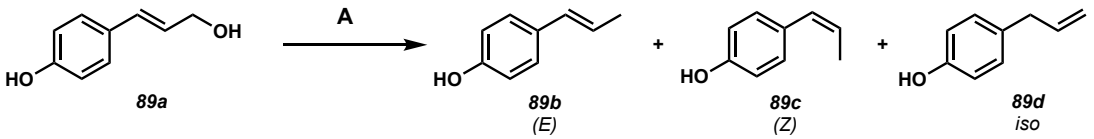
Reaction performed according to **General Procedure A**, using starting material **88a** (10.7 mg, 0.05 mmol). The aqueous layer was extracted with diethyl ether (3 x 1.5 mL), dried over Na_2SO_4 and the solvent evaporated under reduced pressure. The crude product was purified by flash chromatography on silica gel (hexanes), to give a mixture of products **88b**:**88c**:**88d** (8.9:1:2.8, 6.9 mg, 0.035 mmol, 69% yield) as a colorless oil.

88b, *(E)*: ^{1}H NMR (400 MHz, $CDCl_3$) δ 7.40 (d, *J* = 8.5 Hz, 2H), 7.18 (d, *J* = 8.5 Hz, 2H), 6.33 (dd, *J* = 15.8, 1.6 Hz, 1H), 6.23 (dq, *J* = 15.7, 6.3 Hz, 1H), 1.87 (dd, *J* = 6.4, 1.4 Hz, 3H).

88c, *(Z)*: ^{1}H NMR (400 MHz, $CDCl_3$) δ 7.45 (d, *J* = 8.5 Hz, 2H), 7.20 – 7.13 (m, 2H), 6.35 (dd, *J* = 11.7, 1.9 Hz, 1H), 5.82 (dq, *J* = 11.6, 7.2 Hz, 1H), 1.71 (d, *J* = 6.5 Hz, 3H).

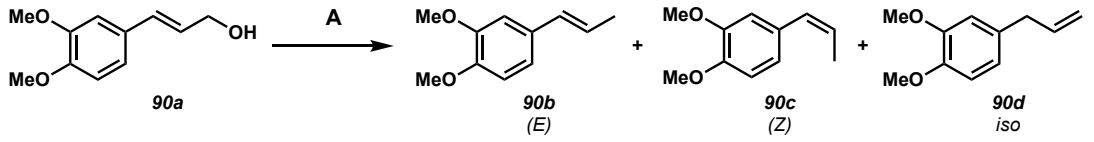
88d, *iso*: ^{1}H NMR (400 MHz, $CDCl_3$) δ 7.42 (m, 2H), 7.06 (d, *J* = 8.4 Hz, 2H), 5.93 (ddt, *J* = 17.0, 10.5, 6.6 Hz, 1H), 5.10 – 5.08 (m, 1H), 5.06 (dd, *J* = 8.8, 1.6 Hz, 1H), 3.34 (d, *J* = 6.7 Hz, 2H).

The spectroscopic data is in agreement with the values previously reported.[47-49]



Reaction performed according to **General Procedure A**, using starting material **89a** (7.5 mg, 0.05 mmol). The aqueous layer was extracted with $CDCl_3$ (2 x 0.5 mL) and the combined organic layers spiked with 1,3,5-trimethoxy benzene (1.0 equiv). An aliquot (0.5 mL) was directly transferred into an NMR tube and the yield of **89b**:**89c**:**89d** (2:1:1.5, 0.026 mmol, 52% yield) determined by quantitative ^{1}H-NMR with 1,3,5-trimethoxy benzene as an internal standard.

The spectroscopic data aligned with the values previously reported.[50-52]



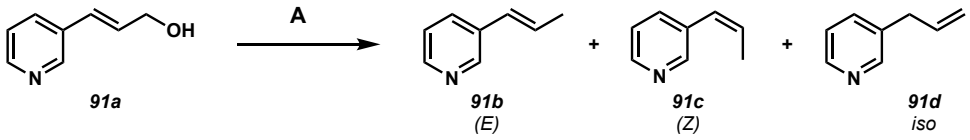
Reaction performed according to **General Procedure A**, using starting material **90a** (9.7 mg, 0.05 mmol). The aqueous layer was extracted with diethyl ether (3 x 1.5 mL), dried over Na_2SO_4 and the solvent evaporated under reduced pressure. The crude product was purified by flash chromatography on silica gel (hexanes/diethyl ether), to give a mixture of products **90b**:**90c**:**90d** (3.3:1:1.7, 4.3 mg, 0.024 mmol, 48% yield) as a colorless oil.

90b, *(E)*: ^{1}H NMR (600 MHz, $CDCl_3$) δ 6.91 – 6.82 (m, 2H), 6.80 (d, J = 8.2 Hz, 1H), 6.34 (dd, J = 15.6, 1.8 Hz, 1H), 6.11 (dq, J = 15.5, 6.6 Hz, 1H), 3.89 (s, 3H), 3.87 (s, 3H), 1.87 (dd, J = 6.6, 1.7 Hz, 3H).

90c, *(Z)*: ^{1}H NMR (600 MHz, $CDCl_3$) δ 6.91 – 6.82 (m, 2H), 6.80 (m, 1H), 6.39 – 6.36 (m, 1H), 5.72 (dq, *J* = 11.5, 7.2 Hz, 1H), 3.87 (s, 3H), 3.86 (s, 3H), 1.91 (dd, *J* = 7.2, 1.9 Hz, 3H).

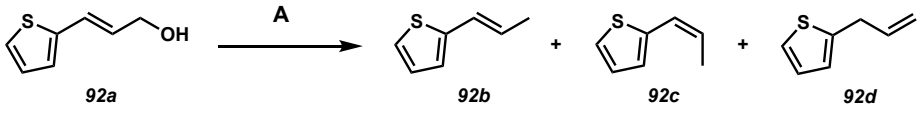
90d, *iso*: ^{1}H NMR (600 MHz, $CDCl_3$) δ 6.84 (m, 1H), 6.75 – 6.71 (m, 2H), 5.96 (ddt, *J* = 16.7, 9.9, 6.7 Hz, 1H), 5.11 – 5.00 (m, 2H), 3.89 (s, 3H), 3.88 (s, 3H), 3.34 (d, *J* = 6.7 Hz, 2H).

The spectroscopic data is in agreement with the values previously reported.[53-55]



Reaction performed according to **General Procedure A**, using starting material **91a** (6.8 mg, 0.05 mmol). The aqueous layer was extracted with $CDCl_3$ (2 x 0.5 mL) and the combined organic layers spiked with 1,3,5-trimethoxy benzene (1.0 equiv). An aliquot (0.5 mL) was directly transferred into an NMR tube and the yield of **91b**:**91c**:**91d** (2.5:1:1.3, 0.041 mmol, 82% yield) determined by quantitative ^{1}H-NMR with 1,3,5-trimethoxy benzene as an internal standard.

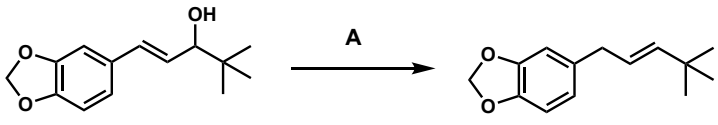
The spectroscopic data aligned with the values previously reported.[56,57]



Reaction performed according to **General Procedure A**, using starting material **92a** (7.0 mg, 0.05 mmol). The aqueous layer was extracted with $CDCl_3$ (2 x 0.5 mL) and the combined organic layers spiked with 1,3,5-trimethoxy benzene (1.0 equiv). An aliquot (0.5

mL) was directly transferred into an NMR tube and the yield of **92b**:**92c**:**92d** (1.4:1.2:1, 0.039 mmol, 77% yield) determined by quantitative ^{1}H-NMR with 1,3,5-trimethoxy benzene as an internal standard.

The spectroscopic data aligned with the values previously reported.[58-60]



Stiripentol (***93a***) ***93b***

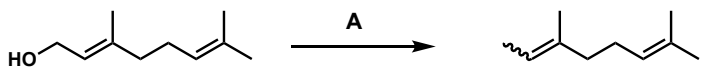
Reaction performed according to **General Procedure A**, using starting material **93a** (11.7 mg, 0.05 mmol). The aqueous layer was extracted with ethyl acetate (3 x 1.5 mL), dried over Na_2SO_4 and the solvent evaporated under reduced pressure. The crude product was purified by flash chromatography on silica gel (hexanes/diethyl ether), to give product **93b** (5.2 mg, 0.024 mmol, 47% yield) as a colorless solid.

^{1}H NMR (400 MHz, $CDCl_3$) δ 6.73 (d, *J* = 7.9 Hz, 1H), 6.69 – 6.56 (m, 2H), 5.92 (s, 2H), 5.54 (dt, *J* = 15.5, 1.3 Hz, 1H), 5.41 (dt, *J* = 15.4, 6.7 Hz, 1H), 3.23 (dq, *J* = 6.6, 0.6 Hz, 2H), 1.01 (s, 9H).

^{13}C NMR (101 MHz, $CDCl_3$) δ 147.7, 145.8, 143.3, 135.3, 123.6, 121.2, 109.1, 108.2, 100.9, 38.9, 33.1, 29.9.

IR (neat film, NaCl) 2954, 2927, 1503, 1487, 1361, 1245, 1095, 1040, 970, 940, 799 cm^{-1}.

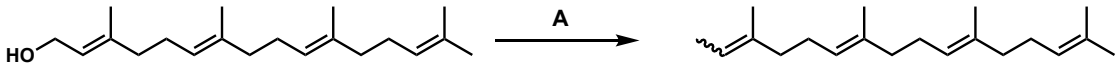
HRMS (FI+): m/z calc'd for $C_{14}H_{18}O_2$ $[M]^{+\bullet}$: 218.1301, found 218.1295.



Geraniol (***94a***) ***94b***

Reaction performed according to **General Procedure A**, using starting material **94a** (7.7 mg, 0.05 mmol). The aqueous layer was extracted with a mixture of pentane (0.3 mL) and $CDCl_3$ (0.5 mL) and the organic layer spiked with 1,3,5-trimethoxy benzene (1.0 equiv). An aliquot (0.5 mL) was directly transferred into an NMR tube and the yield of **94b** (E/Z = 2/1, 0.026 mmol, 51% yield) determined by quantitative ^{1}H-NMR with 1,3,5-trimethoxy benzene as an internal standard.

The spectroscopic data aligned with the values previously reported.[61]

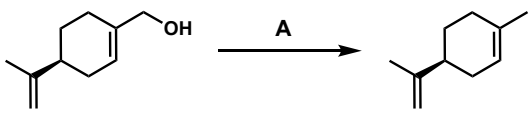


Geranylgeraniol (***95a***) ***95b***

Reaction performed according to **General Procedure A**, using starting material **95a** (14.5 mg, 0.05 mmol). The aqueous layer was extracted with ethyl acetate (3 x 1.5 mL), dried over Na_2SO_4 and the solvent evaporated under reduced pressure. The crude product was purified by flash chromatography on silica gel (hexanes), to give product **95b** (E/Z = 2.1/1, 6.6 mg, 0.024 mmol, 48% yield) as a colorless solid.

Major isomer of **3ba** (*E*): ^{1}H NMR (400 MHz, $CDCl_3$) δ 5.17 – 5.06 (m, 4H), 2.12 – 2.02 (m, 7H), 2.02 – 1.94 (m, 5H), 1.68 (s, 3H), 1.60 (s, 12H), 1.57 (d, *J* = 6.8, 3H).

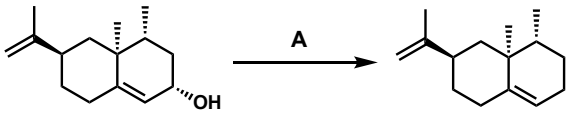
The spectroscopic data is in agreement with the values previously reported.[62]



(-)-perillyl alcohol (***96a***) ***96b***

Reaction performed according to **General Procedure A**, using starting material **96a** (7.6 mg, 0.05 mmol). The aqueous layer was extracted with a mixture of pentane (0.3 mL) and $CDCl_3$ (0.5 mL) and the organic layer spiked with 1,3,5-trimethoxy benzene (1.0 equiv). An aliquot (0.5 mL) was directly transferred into an NMR tube and the yield of **96b** (0.014 mmol, 28% yield) determined by quantitative ^{1}H-NMR with 1,3,5-trimethoxy benzene as an internal standard.

The spectroscopic data aligned with the values previously reported.[63]



Nootkatol (***97a***) ***97b***

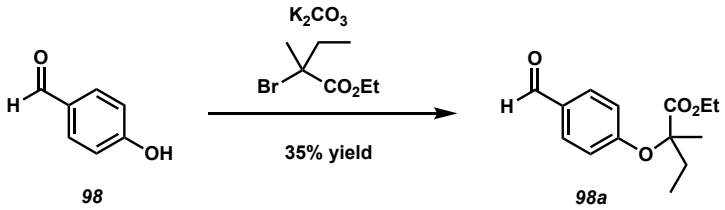
Reaction performed according to **General Procedure A**, using starting material **97a** (11 mg, 0.05 mmol). The aqueous layer was extracted with pentane (3 x 1.5 mL), dried over Na_2SO_4 and the solvent evaporated under reduced pressure. The crude product was purified by flash chromatography on silica gel (hexanes), to give product **97b** (2.1 mg, 0.01 mmol, 21% yield) as a colorless oil.

^{1}H NMR (400 MHz, $CDCl_3$) δ 5.37 – 5.29 (m, 1H), 4.68 (m, 2H), 2.38 – 2.15 (m, 2H), 2.08 (ddd, *J* = 13.9, 4.2, 2.6 Hz, 1H), 2.04 – 1.90 (m, 2H), 1.87 (dt, *J* = 12.8, 2.8 Hz, 1H), 1.76 (m, 2H), 1.71 (s, 3H), 1.44 – 1.37 (m, 3H), 1.19 (m, 1H), 0.95 (s, 3H), 0.88 (d, *J* = 6.3 Hz, 3H).

^{13}C NMR (101 MHz, $CDCl_3$) δ 150.9, 143.3, 120.3, 108.4, 45.1, 41.2, 41.1, 38.0, 33.3, 32.8, 27.3, 26.1, 21.0, 18.6, 15.8.

The spectroscopic data is in agreement with the values previously reported.[64]

3.7.2.4 SYNTHETIC DERIVATIVES



98 *98a*

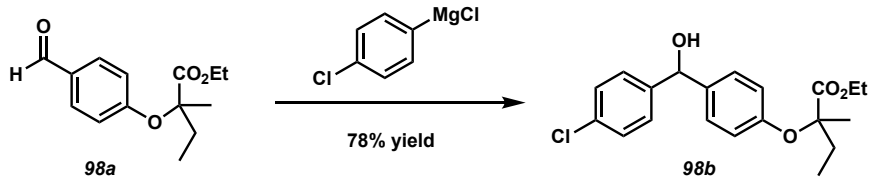
In a round-bottom flask equipped with a reflux condenser, aldehyde **98** (200 mg, 1.64 mmol, 1.0 equiv) was dissolved in acetonitrile (2.4 mL, 0.7M). K_2CO_3 (452 mg, 3.28 mmol, 2.0 equiv) and ethyl 2-bromo-2-methylbutanoate (514 mg, 2.46 mmol, 1.5 equiv) were added and the reaction mixture refluxed for 72 h. The reaction mixture was cooled to room temperature and quenched with a saturated aqueous solution of $NaHCO_3$. The aqueous layer was extracted with ethyl acetate (3x), the combined organic layers dried over Na_2SO_4, and the solvent evaporated under reduced pressure. The crude product was purified by flash chromatography on silica gel (10-20% ethyl acetate/hexanes) to give the product **98a** (143 mg, 0.57 mmol, 35% yield) as a colorless oil.

^{1}H NMR (400 MHz, $CDCl_3$) δ 9.87 (s, 1H), 7.78 (d, J = 8.8 Hz, 2H), 6.90 (d, J = 8.7 Hz, 2H), 4.23 (q, J = 7.2 Hz, 2H), 2.12 – 1.91 (m, 2H), 1.60 (s, 3H), 1.21 (t, J = 7.1 Hz, 3H), 0.99 (t, J = 7.5 Hz, 3H).

^{13}C NMR (101 MHz, $CDCl_3$) δ 190.9, 173.3, 161.2, 131.7, 130.4, 117.9, 82.4, 61.7, 32.9, 20.9, 14.2, 7.8.

IR (neat film, NaCl) 2979, 2943, 2737, 1731, 1694, 1599, 1578, 1504, 1463, 1379, 1309, 1238, 1156, 1126, 1016, 934, 838, 620 cm^{-1}.

HRMS (ESI+): m/z calc'd for $C_{14}H_{19}O_4^+$ $[M+H]^+$: 251.1278, found 251.1278.



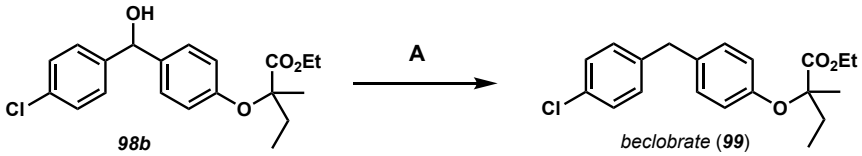
In a vial under inert atmosphere, 1-chloro-4-iodobenzene (48 mg, 0.2 mmol, 1.0 equiv) was dissolved in THF (1.3 mL, 0.15 M) and the solution cooled to –78 ºC. *i*PrMgCl•LiCl (1.3M in THF, 0.15 mL, 0.2 mmol, 1.0 equiv) was added dropwise and the reaction mixture stirred for 15 min. A solution of aldehyde **98a** (50 mg, 0.2 mmol, 1.0 equiv) in THF (0.25 mL) was added dropwise and the reaction warmed up to room temperature over the course of 16 h. The reaction mixture was quenched with a saturated aqueous solution of NH_4Cl, extracted with ethyl acetate (3x), the combined organic layers dried over Na_2SO_4, and the solvent evaporated under reduced pressure. The crude product was purified by flash chromatography on silica gel (20% ethyl acetate/hexanes) to give the product **98b** (56 mg, 0.16 mmol, 78% yield) as a yellow oil.

^{1}H NMR (400 MHz, $CDCl_3$) δ 7.29 (s, 4H), 7.18 (d, J = 8.6 Hz, 2H), 6.80 (d, J = 8.7 Hz, 2H), 5.74 (s, 1H), 4.22 (qd, J = 7.1, 1.5 Hz, 2H), 2.27 (brs, 1H), 1.96 (qd, J = 14.0, 7.5 Hz, 2H), 1.48 (s, 3H), 1.23 (t, J = 7.1 Hz, 3H), 0.97 (t, J = 7.5 Hz, 3H).

^{13}C NMR (101 MHz, $CDCl_3$) δ 174.0, 155.3, 142.4, 137.0, 133.3, 128.6, 127.9, 127.7, 119.1, 119.1, 82.1, 75.3, 61.4, 32.7, 20.9, 20.8, 14.3, 7.9.

IR (neat film, NaCl) 3444, 2978, 1729, 1608, 1504, 1228, 1168, 1126, 1013, 823 cm^{-1}.

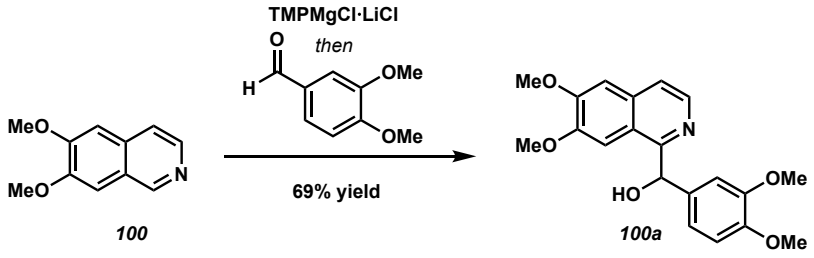
HRMS (ESI+): m/z calc'd for $C_{20}H_{22}ClO_3^+$ $[M–OH]^+$: 345.1252, found 345.1254.



Reaction performed according to **General Procedure A**, using starting material **98b** (18 mg, 0.05 mmol). The aqueous layer was extracted with ethyl acetate (3 x 1.5 mL), dried over Na_2SO_4 and the solvent evaporated under reduced pressure. The crude product was purified by flash chromatography on silica gel (hexanes/diethyl ether), to give beclobrate (**99**, 11.6 mg, 0.034 mmol, 67% yield) as a white solid.

^{1}H NMR (400 MHz, $CDCl_3$) δ 7.24 (d, J = 8.4 Hz, 2H), 7.08 (d, J = 8.4 Hz, 2H), 7.00 (d, J = 8.6 Hz, 2H), 6.77 (d, J = 8.6 Hz, 2H), 4.23 (q, J = 7.2 Hz, 2H), 3.87 (s, 2H), 2.06 – 1.86 (m, 2H), 1.47 (s, 3H), 1.25 (t, J = 7.1 Hz, 3H), 0.97 (t, J = 7.5 Hz, 3H).

The spectroscopic data is in agreement with the values previously reported.[65]

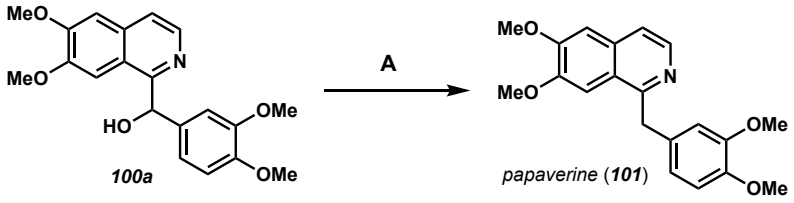


In a Schlenk flask under inert atmosphere, isoquinoline **100** (100 mg, 0.53 mmol, 1.0 equiv) was dissolved in THF (2.1 mL, 0.25 M) and a solution of TMPMgCl•LiCl (1.0 M in THF, 0.8 mL, 0.8 mmol, 1.5 equiv) was added dropwise. The reaction was stirred at room temperature for 4 h, after which it was cooled to 0 ºC and a solution of 3,4-dimethoxy benzaldehyde (133 mg, 0.8 mmol, 1.5 equiv) in THF (1 mL) was added dropwise. The

reaction mixture was stirred for 16 h at room temperature, after which a 1 M aqueous solution of HCl was added. The aqueous layer was extracted with ethyl acetate (3x), the combined organic layers dried over Na_2SO_4, and the solvent evaporated under reduced pressure. The crude product was purified by flash chromatography on silica gel (acetone/hexanes) to give the product **100a** (130 mg, 0.37 mmol, 69% yield) as a yellow solid.

^{1}H NMR (600 MHz, $CDCl_3$) δ 8.40 (d, *J* = 5.7 Hz, 1H), 7.52 (d, *J* = 5.6 Hz, 1H), 7.14 (s, 1H), 7.08 (s, 1H), 6.91 (dd, *J* = 8.2, 2.1 Hz, 1H), 6.83 (d, *J* = 2.0 Hz, 1H), 6.78 (d, *J* = 8.2 Hz, 1H), 6.17 (s, 1H), 3.99 (s, 3H), 3.82 (s, 3H), 3.81 (s, 3H), 3.76 (s, 3H).

The spectroscopic data is in agreement with the values previously reported.[66]

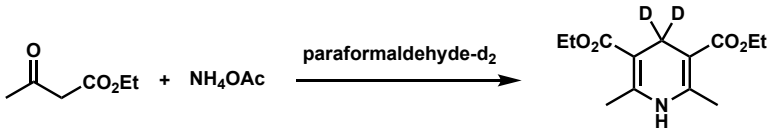


Reaction performed according to **General Procedure A**, using starting material **100a** (17.8 mg, 0.05 mmol). The aqueous layer was extracted with ethyl acetate (3 x 1.5 mL), dried over Na_2SO_4 and the solvent evaporated under reduced pressure. The crude product was purified by flash chromatography on silica gel (acetone/hexanes), to give papaverine (**101**, 13 mg, 0.039 mmol, 77% yield) as a white solid.

^{1}H NMR (600 MHz, $CDCl_3$) δ 8.37 (d, *J* = 5.7 Hz, 1H), 7.43 (d, *J* = 5.7 Hz, 1H), 7.35 (s, 1H), 7.05 (s, 1H), 6.84 – 6.78 (m, 2H), 6.76 (d, *J* = 8.5 Hz, 1H), 4.53 (s, 2H), 4.00 (s, 3H), 3.90 (s, 3H), 3.82 (s, 3H), 3.77 (s, 3H).

The spectroscopic data is in agreement with the values previously reported.[66]

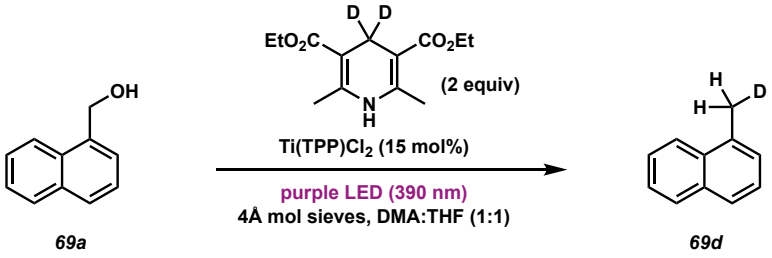
3.7.2.5 MECHANISTIC EXPERIMENTS



A round-bottom flask was charged with ethyl acetoacetate (2.6 g, 20 mmol, 4.0 equiv), paraformaldehyde-d_2 (162 mg, 5 mmol, 1.0 equiv) and NH_4OAc (771 mg, 10 mmol, 2.0 equiv). The contents were suspended in water (6 mL) and the reaction mixture heated at 90 ºC for 17 h. The heating source was removed and the reaction mixture left to slowly cool to ambient temperature. The resulting solid was filtered off and the crystals consecutively washed with H_2O and a minimal amount of ethanol to give the deuterated Hantzsch ester (701 mg, 2.75 mmol, 55% yield) as a yellow solid.

^{1}H NMR (600 MHz, $CDCl_3$) δ 5.12 (s, 1H), 4.17 (q, J = 7.1 Hz, 4H), 2.19 (s, 6H), 1.28 (t, J = 7.1 Hz, 6H).

The spectroscopic data is in agreement with the values previously reported.[67]

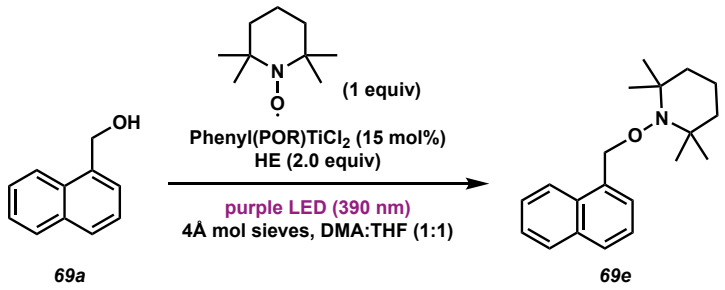


Reaction performed according to **General Procedure A**, using d_2-Hantzsch ester (25.5 mg, 0.1 mmol, 2.0 equiv) and starting material **69a** (7.9 mg, 0.05 mmol). The aqueous layer was extracted with ethyl acetate (3 x 1.5 mL), dried over Na_2SO_4 and the solvent evaporated under reduced pressure. The crude product was purified by flash

chromatography on silica gel (hexanes) to give deuterated product **69d** (5.6 mg, 0.039 mmol, 78% yield) as a white solid.

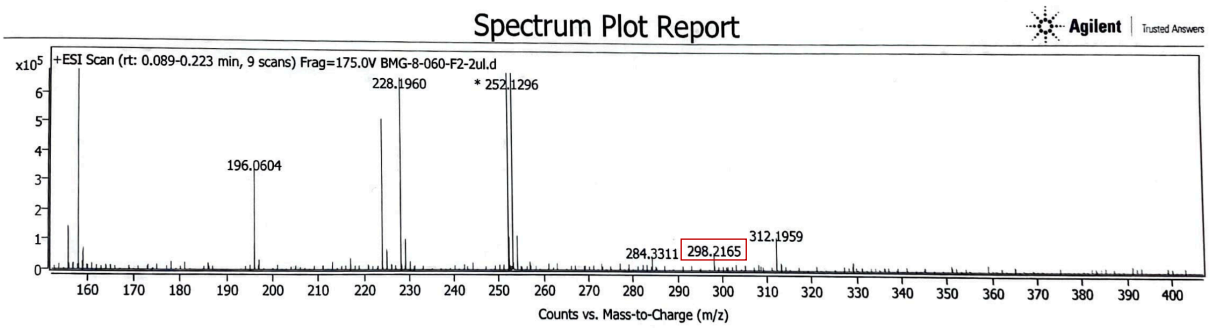
^{1}H NMR (400 MHz, $CDCl_3$) δ 8.04 – 7.98 (m, 1H), 7.88 – 7.83 (m, 1H), 7.71 (d, J = 8.1 Hz, 1H), 7.55 – 7.45 (m, 2H), 7.42 – 7.30 (m, 2H), 2.70 (s, 2H).

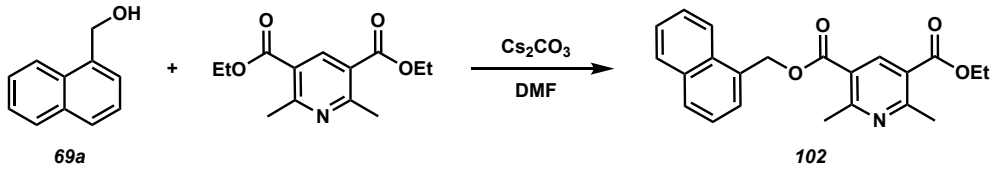
The spectroscopic data is in agreement with the values previously reported.[68]



Reaction performed according to **General Procedure A**, using starting material **69a** (7.9 mg, 0.05 mmol) with the addition of TEMPO (7.8 mg, 0.05 mmol, 1.0 equiv). The aqueous layer was extracted with ethyl acetate and the extract submitted for analysis of **69e** by mass spectrometry. HRMS (ESI+): m/z calc'd for $C_{20}H_{28}NO^+$ $[M+H]^+$: 298.2165, found 298.2165.

Figure 3.7.2.5.1*: Mass trace and analysis of adduct* ***69e****.*





69a *102*

In a reaction vial starting material **69a** (16 mg, 0.1 mmol, 1.0 equiv), oxidized Hantzsch ester (100 mg, 0.4 mmol, 4.0 equiv) and Cs_2CO_3 (130 mg, 0.4 mmol, 4.0 equiv) were suspended in DMF (1.0 mL) and the reaction mixture stirred for 15 h. An aqueous solution of LiCl (10% w/v) was added and the aqueous layer extracted with diethyl ether (3x). The combined organic layers were dried over Na_2SO_4, and the solvent evaporated under reduced pressure. The crude product was purified by flash chromatography on silica gel (5-10% diethyl ether/hexanes) to give the product **102** (19.2 mg, 0.053 mmol, 53% yield) as a white solid.

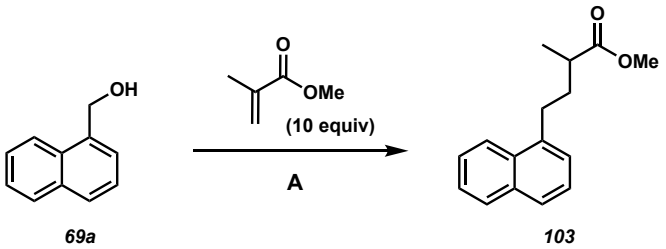
^{1}H NMR (400 MHz, $CDCl_3$) δ 8.66 (s, 1H), 8.12 (dt, *J* = 8.7, 1.0 Hz, 1H), 7.94 – 7.87 (m, 2H), 7.64 (dd, *J* = 7.0, 1.2 Hz, 1H), 7.62 – 7.45 (m, 3H), 5.83 (s, 2H), 4.33 (q, *J* = 7.1 Hz, 2H), 2.82 (d, *J* = 1.7 Hz, 6H), 1.34 (t, *J* = 7.1 Hz, 3H).

^{13}C NMR (101 MHz, $CDCl_3$) δ 165.9, 162.7, 162.5, 141.3, 133.9, 131.9, 131.2, 129.7, 129.0, 128.0, 126.8, 126.2, 125.4, 123.6, 123.2, 122.9, 65.7, 61.5, 25.2, 25.1, 14.3.

IR (neat film, NaCl) 2927, 1721, 1594, 1553, 1442, 1368, 1282, 1225, 1101, 1039, 770 cm^{-1}.

HRMS (ESI+): m/z calc'd for $C_{22}H_{22}NO_4^+$ $[M+H]^+$: 364.1543, found 364.1671.

3.7.2.6 GIESE ADDITON AND CROSS-COUPLING



69a ***103***

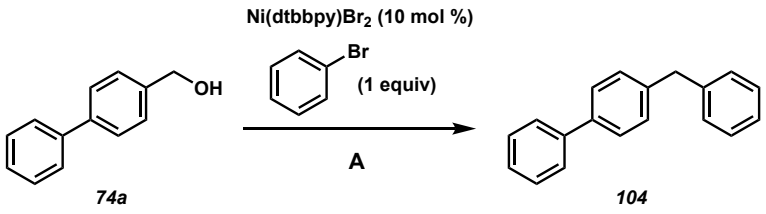
Reaction performed according to **General Procedure A**, using starting material **69a** (7.9 mg, 0.05 mmol) with addition of methyl methacrylate (50 mg, 0.5 mmol, 10.0 equiv). The aqueous layer was extracted with ethyl acetate (3 x 1.5 mL), dried over Na_2SO_4 and the solvent evaporated under reduced pressure. The crude product was purified by flash chromatography on silica gel (diethyl ether/hexanes) to give **103** (5.8 mg, 0.024 mmol, 48% yield) as a colorless oil.

^{1}H NMR (400 MHz, $CDCl_3$) δ 8.07 – 8.01 (m, 1H), 7.85 (dd, *J* = 7.7, 1.5 Hz, 1H), 7.72 (d, *J* = 8.2 Hz, 1H), 7.55 – 7.44 (m, 2H), 7.39 (dd, *J* = 8.2, 7.0 Hz, 1H), 7.32 (dd, *J* = 7.2, 1.3 Hz, 1H), 3.72 (s, 3H), 3.16 – 2.99 (m, 2H), 2.65 – 2.54 (m, 1H), 2.15 (dddd, *J* = 13.8, 10.2, 8.2, 5.8 Hz, 1H), 1.85 (ddt, *J* = 13.5, 10.2, 5.9 Hz, 1H), 1.25 (d, *J* = 7.0 Hz, 3H).

^{13}C NMR (101 MHz, $CDCl_3$) δ 177.2, 138.0, 134.0, 131.9, 128.9, 126.9, 126.2, 126.0, 125.7, 125.6, 123.9, 51.8, 39.6, 34.9, 30.9, 17.5.

IR (neat film, NaCl) 2928, 1731, 1459, 1360, 1202, 779, 745 cm^{-1}.

HRMS (FI+): m/z calc'd for $C_{16}H_{18}O_2$ $[M]^{+\bullet}$: 242.1301, found 242.1299.



74a ***104***

Reaction performed according to **General Procedure A**, using starting material **74a** (9.2 mg, 0.05 mmol) with the addition of bromobenzene (7.9 mg, 0.05 mmol, 1.0 equiv) and Ni(dtbbpy)Br_2 (2.4 mg, 0.005 mmol, 0.1 equiv). The aqueous layer was extracted with ethyl acetate (3 x 1.5 mL), dried over Na_2SO_4 and the solvent evaporated under reduced pressure. The crude product was purified by flash chromatography on silica gel (hexanes) to give **104** (1.6 mg, 0.0065 mmol, 13% yield) as a colorless film.

^{1}H NMR (600 MHz, $CDCl_3$) δ 7.59 – 7.55 (m, 2H), 7.52 (d, *J* = 8.1 Hz, 2H), 7.42 (t, *J* = 7.6 Hz, 2H), 7.34 – 7.28 (m, 3H), 7.27 – 7.26 (m, 2H), 7.25 – 7.19 (m, 3H), 4.03 (s, 2H).

The spectroscopic data is in agreement with the values previously reported.[69]

3.8 REFERENCES AND NOTES

(1) Zard, S. Z. *Radical Reactions in Organic Synthesis*; Oxford University Press, 2003.

(2) *For selected reviews see:* (a) Yan, M.; Lo, J. C.; Edwards, J. T.; Baran, P. S. Radicals: Reactive Intermediates with Translational Potential. *J. Am. Chem. Soc.* **2016**, *138* (39), 12692–12714. (b) Parsaee, F.; Senarathna, M. C.; Kannangara, P. B.; Alexander, S. N.; Arche, P. D. E.; Welin, E. R. Radical Philicity and Its Role in Selective Organic Transformations. *Nat. Rev. Chem.* **2021**, *5* (7), 486–499.

(3) Anwar, K.; Merkens, K.; Aguilar Troyano, F. J.; Gómez-Suárez, A. Radical Deoxyfunctionalisation Strategies. *Eur. J. Org. Chem.* **2022**, *2022* (26), e202200330.

(4) McCombie, S. W.; Motherwell, W. B.; Tozer, M. J. The Barton-McCombie Reaction. In *Organic Reactions*; John Wiley & Sons, Ltd, 2012; pp 161–432. https://doi.org/10.1002/0471264180.or077.02.

(5) *For selected seminal examples see:* (a) Barton, D. H. R.; McCombie, S. W. A New Method for the Deoxygenation of Secondary Alcohols. *J. Chem. Soc. Perkin 1* **1975**, No. 16, 1574–1585. (b) Dong, Z.; MacMillan, D. W. C. Metallaphotoredox-Enabled Deoxygenative Arylation of Alcohols. *Nature* **2021**, *598* (7881), 451–456. (c) Togo, H.; Matsubayashi, S.; Yamazaki, O.; Yokoyama, M. Deoxygenative Functionalization of Hydroxy Groups via Xanthates with Tetraphenyldisilane. *J. Org. Chem.* **2000**, *65* (9), 2816–2819. (d) Lackner, G. L.; Quasdorf, K. W.; Overman, L. E. Direct Construction of Quaternary Carbons from Tertiary Alcohols via Photoredox-Catalyzed Fragmentation of Tert-Alkyl N-Phthalimidoyl Oxalates. *J. Am. Chem. Soc.* **2013**, *135* (41), 15342–15345. (e) Nawrat, C. C.; Jamison, C. R.; Slutskyy, Y.; MacMillan, D. W. C.; Overman, L. E. Oxalates as Activating Groups

for Alcohols in Visible Light Photoredox Catalysis: Formation of Quaternary Centers by Redox-Neutral Fragment Coupling. *J. Am. Chem. Soc.* **2015**, *137* (35), 11270–11273. (f) Ye, Y.; Chen, H.; Sessler, J. L.; Gong, H. Zn-Mediated Fragmentation of Tertiary Alkyl Oxalates Enabling Formation of Alkylated and Arylated Quaternary Carbon Centers. *J. Am. Chem. Soc.* **2019**, *141* (2), 820–824. (g) Yu, L.; Li, S.; Ogawa, H.; Ma, Y.; Chen, Q.; Yamazaki, K.; Nagata, Y.; Nakamura, H. Fe-Electrocatalytic Deoxygenative Giese Reaction. *Nat. Commun.* **2025**, *16* (1), 8379. (h) Pan, Q.; Yu, R.; Cai, Z.; Chen, Y. Direct Deoxyarylation of Non-Activated Alcohols. *Angew. Chem. Int. Ed.* (n/a), e20148. https://doi.org/10.1002/anie.202520148.

(6) *Cytochrome P450*; Ortiz De Montellano, P. R., Ed.; Springer US: Boston, MA, 2005.

(7) Schlichting, I.; Berendzen, J.; Chu, K.; Stock, A. M.; Maves, S. A.; Benson, D. E.; Sweet, R. M.; Ringe, D.; Petsko, G. A.; Sligar, S. G. The Catalytic Pathway of Cytochrome P450cam at Atomic Resolution. *Science* **2000**, *287* (5458), 1615–1622. https://doi.org/10.1126/science.287.5458.1615.

(8) Diéguez, H. R.; López, A.; Domingo, V.; Arteaga, J. F.; Dobado, J. A.; Herrador, M. M.; Quílez del Moral, J. F.; Barrero, A. F. Weakening C−O Bonds: Ti(III), a New Reagent for Alcohol Deoxygenation and Carbonyl Coupling Olefination. *J. Am. Chem. Soc.* **2010**, *132* (1), 254–259. https://doi.org/10.1021/ja906083c.

(9) Xie, H.; Guo, J.; Wang, Y.-Q.; Wang, K.; Guo, P.; Su, P.-F.; Wang, X.; Shu, X.-Z. Radical Dehydroxylative Alkylation of Tertiary Alcohols by Ti Catalysis. *J. Am. Chem. Soc.* **2020**, *142* (39), 16787–16794. https://doi.org/10.1021/jacs.0c07492.

(10) *For selected examples employing titanium in deoxygenation of alcohols see*: (a) Sumiyama, K.; Toriumi, N.; Iwasawa, N. Use of Isopropyl Alcohol as a Reductant for Catalytic Dehydoxylative Dimerization of Benzylic Alcohols Utilizing Ti−O Bond Photohomolysis. *Eur. J. Org. Chem.* **2021**, *2021* (17), 2474–2478. (b) Lin, Q.; Tong, W.; Shu, X.-Z.; Chen, Y. Ti-Catalyzed Dehydroxylation of Tertiary Alcohols. *Org. Lett.* **2022**, *24* (46), 8459–8464. (c) Suga, T.; Takahashi, Y.; Miki, C.; Ukaji, Y. Direct and Unified Access to Carbon Radicals from Aliphatic Alcohols by Cost-Efficient Titanium-Mediated Homolytic C−OH Bond Cleavage. *Angew. Chem. Int. Ed.* **2022**, *61* (10), e202112533. (d) Suga, T.; Shimazu, S.; Ukaji, Y. Low-Valent Titanium-Mediated Radical Conjugate Addition Using Benzyl Alcohols as Benzyl Radical Sources. *Org. Lett.* **2018**, *20* (17), 5389–5392. (e) Căciuleanu, A.; Vöhringer, F.; Fleischer, I. Titanium-Catalysed Deoxygenation of Benzylic Alcohols and Lignin Model Compounds. *Org. Chem. Front.* **2023**, *10* (12), 2927–2935.

(11) Berreau, L. M.; Hays, J. A.; Young, V. G. Jr.; Woo, L. K. Synthesis of Early Transition Metal Porphyrin Halide Complexes: First Structural Characterization of a Vanadium(III) Porphyrin Complex. *Inorg. Chem.* **1994**, *33* (1), 105–108.

(12) Zhang, Z.; Hilche, T.; Slak, D.; Rietdijk, N. R.; Oloyede, U. N.; Flowers II, R. A.; Gansäuer, A. Titanocenes as Photoredox Catalysts Using Green-Light Irradiation. *Angew. Chem. Int. Ed.* **2020**, *59* (24), 9355–9359.

(13) Seki, M.; Tapkir, S. R.; Nadiveedhi, M. R.; Mulani, S. K.; Mashima, K. New Synthesis of Diarylmethanes, Key Building Blocks for SGLT2 Inhibitors. *ACS Omega* **2023**, *8* (19), 17288–17295. https://doi.org/10.1021/acsomega.3c01972.

(14) Melzer, B.; Bracher, F. A Divergent Approach to Benzylisoquinoline-Type and Oxoaporphine Alkaloids via Regioselective Direct Ring Metalation of Alkoxy Isoquinolines. *Org. Biomol. Chem.* **2015**, *13* (28), 7664–7672.

(15) Larraufie, M.-H.; Pellet, R.; Fensterbank, L.; Goddard, J.-P.; Lacôte, E.; Malacria, M.; Ollivier, C. Visible-Light-Induced Photoreductive Generation of Radicals from Epoxides and Aziridines. *Angew. Chem. Int. Ed.* **2011**, *50* (19), 4463–4466.

(16) Yagi, S.; Morisaki, K.; Sato, Y. Direct Site-Selective Deoxygenation of Benzylalcohol Derivatives. *Adv. Synth. Catal.* **2025**, *367* (14), e9590.

(17) Chaudhuri, A.; Denkler, L. M.; Zhuo, Q.; Mandal, A.; Bunescu, A. LMCT-Driven Iron Photocatalysis: Mechanistic Insights and Synthetic Applications. *Chem. – Eur. J.* **2025**, *31* (58), e02185.

(18) Büchner, R.; Fondell, M.; Haverkamp, R.; Pietzsch, A.; Cruz, V. V. da; Föhlisch, A. The Porphyrin Center as a Regulator for Metal–Ligand Covalency and π Hybridization in the Entire Molecule. *Phys. Chem. Chem. Phys.* **2021**, *23* (43), 24765–24772.

(19) Li, H.; Li, Y.; Yuan, W.; Qu, A.; Chen, K.; Zhu, Y. Photoredox/Ti Dual-Catalyzed Dehydroxylative Ring-Opening Giese Reaction of Cyclobutanone Oximes. *Green Synth. Catal.* **2024**, *5* (3), 159–164.

(20) Suga, T.; Ukaji, Y. Nickel-Catalyzed Cross-Electrophile Coupling between Benzyl Alcohols and Aryl Halides Assisted by Titanium Co-Reductant. *Org. Lett.* **2018**, *20* (24), 7846–7850.

(21) Chen, F.; Xu, X.-H.; Chu, L.; Qing, F.-L. Visible-Light-Induced Nickel-Catalyzed Radical Cross-Couplings to Access α-Aryl-α-Trifluoromethyl Alcohols. *Org. Lett.* **2022**, *24* (50), 9332–9336.

(22) Pangborn, A. B.; Giardello, M. A.; Grubbs, R. H.; Rosen, R. K.; Timmers, F. J. Safe and Convenient Procedure for Solvent Purification. *Organometallics* **1996**, *15* (5), 1518–1520.

(23) Molander, G. A.; Yun, C.-S.; Ribagorda, M.; Biolatto, B. B-Alkyl Suzuki−Miyaura Cross-Coupling Reactions with Air-Stable Potassium Alkyltrifluoroborates. *J. Org. Chem.* **2003**, *68* (14), 5534–5539.

(24) Sahoo, S. K. An Unprecedented Oxidative Intermolecular Homo Coupling Reaction between Two sp^3C–sp^3C Centers under Metal-Free Condition. *Tetrahedron Lett.* **2016**, *57* (31), 3476–3480.

(25) Fulmer, G. R.; Miller, A. J. M.; Sherden, N. H.; Gottlieb, H. E.; Nudelman, A.; Stoltz, B. M.; Bercaw, J. E.; Goldberg, K. I. NMR Chemical Shifts of Trace Impurities: Common Laboratory Solvents, Organics, and Gases in Deuterated Solvents Relevant to the Organometallic Chemist. *Organometallics* **2010**, *29* (9), 2176–2179.

(26) Saito, K.; Kondo, K.; Akiyama, T. B(C6F5)3-Catalyzed Hydrodesulfurization Using Hydrosilanes – Metal-Free Reduction of Sulfides. *Org. Lett.* **2015**, *17* (13), 3366–3369.

(27) Cahiez, G.; Chaboche, C.; Duplais, C.; Moyeux, A. A New Efficient Catalytic System for the Chemoselective Cobalt-Catalyzed Cross-Coupling of Aryl Grignard Reagents with Primary and Secondary Alkyl Bromides. *Org. Lett.* **2009**, *11* (2), 277–280.

(28) Karthikeyan, P.; Vanitha, A.; Radhika, P.; Suresh, K.; Sugumaran, A. Imidazolium Supported Palladium–Chloroglycine Complex: Recyclable Catalyst for Suzuki–Miyaura Coupling Reactions. *Tetrahedron Lett.* **2013**, *54* (52), 7193–7197.

(29) Koch, K.; Podlech, J.; Pfeiffer, E.; Metzler, M. Total Synthesis of Alternariol. *J. Org. Chem.* **2005**, *70* (8), 3275–3276.

(30) Xu, J.-X.; Wu, X.-F. Palladium-Catalyzed Decarboxylative Carbonylative Transformation of Benzyl Aryl Carbonates: Direct Synthesis of Aryl 2-Arylacetates. *Org. Lett.* **2018**, *20* (18), 5938–5941.

(31) Burns, M. J.; Fairlamb, I. J. S.; Kapdi, A. R.; Sehnal, P.; Taylor, R. J. K. Simple Palladium(II) Precatalyst for Suzuki−Miyaura Couplings: Efficient Reactions of Benzylic, Aryl, Heteroaryl, and Vinyl Coupling Partners. *Org. Lett.* **2007**, *9* (26), 5397–5400.

(32) Liu, T.-P.; Xing, C.-H.; Hu, Q.-S. Synthesis of Fluorene and Indenofluorene Compounds: Tandem Palladium-Catalyzed Suzuki Cross-Coupling and Cyclization. *Angew. Chem. Int. Ed.* **2010**, *49* (16), 2909–2912.

(33) Schmuck, C.; Wienand, W. The First Efficient Synthesis and Optical Resolution of Monosubstituted Cyclotribenzylenes. *Synthesis* **2002**, *2002* (05), 0655–0663.

(34) Suga, T.; Ukaji, Y. Nickel-Catalyzed Cross-Electrophile Coupling between Benzyl Alcohols and Aryl Halides Assisted by Titanium Co-Reductant. *Org. Lett.* **2018**, *20* (24), 7846–7850.

(35) Bedford, R. B.; Brenner, P. B.; Carter, E.; Clifton, J.; Cogswell, P. M.; Gower, N. J.; Haddow, M. F.; Harvey, J. N.; Kehl, J. A.; Murphy, D. M.; Neeve, E. C.; Neidig, M. L.; Nunn, J.; Snyder, B. E. R.; Taylor, J. Iron Phosphine Catalyzed Cross-Coupling

of Tetraorganoborates and Related Group 13 Nucleophiles with Alkyl Halides. *Organometallics* **2014**, *33* (20), 5767–5780.

(36) Tandiary, M. A.; Masui, Y.; Onaka, M. Deoxygenation of Tertiary and Secondary Benzylic Alcohols into Alkanes with Triethylsilane Catalyzed by Solid Acid Tin(IV) Ion-Exchanged Montmorillonite. *Tetrahedron Lett.* **2014**, *55* (30), 4160–4162.

(37) Maity, P.; Shacklady-McAtee, D. M.; Yap, G. P. A.; Sirianni, E. R.; Watson, M. P. Nickel-Catalyzed Cross Couplings of Benzylic Ammonium Salts and Boronic Acids: Stereospecific Formation of Diarylethanes via C–N Bond Activation. *J. Am. Chem. Soc.* **2013**, *135* (1), 280–285.

(38) Wang, Y.; McGonigal, P. R.; Herlé, B.; Besora, M.; Echavarren, A. M. Gold(I) Carbenes by Retro-Buchner Reaction: Generation and Fate. *J. Am. Chem. Soc.* **2014**, *136* (2), 801–809.

(39) Yu, J.; Zhou, Y.; Lin, Z.; Tong, R. Regioselective and Stereospecific Copper-Catalyzed Deoxygenation of Epoxides to Alkenes. *Org. Lett.* **2016**, *18* (18), 4734–4737.

(40) Singh, K.; Staig, S. J.; Weaver, J. D. Facile Synthesis of Z-Alkenes via Uphill Catalysis. *J. Am. Chem. Soc.* **2014**, *136* (14), 5275–5278.

(41) López-Pérez, A.; Adrio, J.; Carretero, J. C. Palladium-Catalyzed Cross-Coupling Reaction of Secondary Benzylic Bromides with Grignard Reagents. *Org. Lett.* **2009**, *11* (23), 5514–5517.

(42) Qin, L.; Sharique, M.; Tambar, U. K. Controllable, Sequential, and Stereoselective C–H Allylic Alkylation of Alkenes. *J. Am. Chem. Soc.* **2019**, *141* (43), 17305–17313.

(43) Yu, J.; Gaunt, M. J.; Spencer, J. B. Convenient Preparation of Trans-Arylalkenes via Palladium(II)-Catalyzed Isomerization of Cis-Arylalkenes. *J. Org. Chem.* **2002**, *67* (13), 4627–4629.

(44) Kim, H.; Choi, S. Y.; Shin, S. Asymmetric Synthesis of Dihydropyranones via Gold(I)-Catalyzed Intermolecular [4+2] Annulation of Propiolates and Alkenes. *Angew. Chem. Int. Ed.* **2018**, *57* (40), 13130–13134.

(45) McNulty, J.; Keskar, K. Stereoselective Wittig Olefination Reactions Employing a Novel *Ortho-P*-Aryl Alkoxide Effect. *Tetrahedron Lett.* **2008**, *49* (49), 7054–7057. https://doi.org/10.1016/j.tetlet.2008.09.150.

(46) Kohler, D. G.; Gockel, S. N.; Kennemur, J. L.; Waller, P. J.; Hull, K. L. Palladium-Catalysed Anti-Markovnikov Selective Oxidative Amination. *Nat. Chem.* **2018**, *10* (3), 333–340.

(47) Ek, F.; Axelsson, O.; Wistrand, L.-G.; Frejd, T. Aromatic Allylation via Diazotization: Metal-Free C−C Bond Formation. *J. Org. Chem.* **2002**, *67* (18), 6376–6381.

(48) Lu, X.-L.; Shannon, M.; Peng, X.-S.; Wong, H. N. C. Stereospecific Iron-Catalyzed Carbon(Sp2)–Carbon(Sp3) Cross-Coupling with Alkyllithium and Alkenyl Iodides. *Org. Lett.* **2019**, *21* (8), 2546–2549.

(49) Colomer, I.; Coura Barcelos, R.; Donohoe, T. J. Catalytic Hypervalent Iodine Promoters Lead to Styrene Dimerization and the Formation of Tri- and Tetrasubstituted Cyclobutanes. *Angew. Chem. Int. Ed.* **2016**, *55* (15), 4748–4752.

(50) Furuyama, T.; Yonehara, M.; Arimoto, S.; Kobayashi, M.; Matsumoto, Y.; Uchiyama, M. Development of Highly Chemoselective Bulky Zincate Complex,

tBu_4ZnLi_2: Design, Structure, and Practical Applications in Small-/Macromolecular Synthesis. *Chem. – Eur. J.* **2008**, *14* (33), 10348–10356.

(51) Angle, S. R.; Arnaiz, D. O. Synthesis of Dihydro-1H-Indenes via a Formal 3 + 2 Cycloaddition of Para-Quinone Methides and Styrenes. *J. Org. Chem.* **1990**, *55* (12), 3708–3710.

(52) Payer, S. E.; Pollak, H.; Schmidbauer, B.; Hamm, F.; Juričić, F.; Faber, K.; Glueck, S. M. Multienzyme One-Pot Cascade for the Stereoselective Hydroxyethyl Functionalization of Substituted Phenols. *Org. Lett.* **2018**, *20* (17), 5139–5143.

(53) Tlahuext-Aca, A.; Candish, L.; Garza-Sanchez, R. A.; Glorius, F. Decarboxylative Olefination of Activated Aliphatic Acids Enabled by Dual Organophotoredox/Copper Catalysis. *ACS Catal.* **2018**, *8* (3), 1715–1719.

(54) Movahhed, S.; Westphal, J.; Dindaroğlu, M.; Falk, A.; Schmalz, H.-G. Low-Pressure Cobalt-Catalyzed Enantioselective Hydrovinylation of Vinylarenes. *Chem. – Eur. J.* **2016**, *22* (22), 7381–7384.

(55) Nielsen, A. J.; Jenkins, H. A.; McNulty, J. Asymmetric Organocatalytic Stepwise [2+2] Entry to Tetra-Substituted Heterodimeric and Homochiral Cyclobutanes. *Chem. – Eur. J.* **2016**, *22* (27), 9111–9115.

(56) Mayer, M.; Czaplik, W. M.; Jacobi von Wangelin, A. Practical Iron-Catalyzed Allylations of Aryl Grignard Reagents. *Adv. Synth. Catal.* **2010**, *352* (13), 2147–2152.

(57) Tomita, R.; Yasu, Y.; Koike, T.; Akita, M. Combining Photoredox-Catalyzed Trifluoromethylation and Oxidation with DMSO: Facile Synthesis of α-

Trifluoromethylated Ketones from Aromatic Alkenes. *Angew. Chem. Int. Ed.* **2014**, *53* (28), 7144–7148.

(58) Race, N. J.; Bower, J. F. Palladium Catalyzed Cyclizations of Oxime Esters with 1,2-Disubstituted Alkenes: Synthesis of Dihydropyrroles. *Org. Lett.* **2013**, *15* (17), 4616–4619.

(59) Siddiki, S. M. A. H.; Touchy, A. S.; Kon, K.; Shimizu, K. Direct Olefination of Alcohols with Sulfones by Using Heterogeneous Platinum Catalysts. *Chem. – Eur. J.* **2016**, *22* (17), 6111–6119.

(60) Lara, M.; Mutti, F. G.; Glueck, S. M.; Kroutil, W. Biocatalytic Cleavage of Alkenes with O2 and Trametes Hirsuta G FCC 047. *Eur. J. Org. Chem.* **2008**, *2008* (21), 3668–3672.

(61) Matsushita, H.; Negishi, E. Palladium-Catalyzed Reactions of Allylic Electrophiles with Organometallic Reagents. A Regioselective 1,4-Elimination and a Regio- and Stereoselective Reduction of Allylic Derivatives. *J. Org. Chem.* **1982**, *47* (21), 4161–4165.

(62) Kim, H. J.; Su, L.; Jung, H.; Koo, S. Selective Deoxygenation of Allylic Alcohol: Stereocontrolled Synthesis of Lavandulol. *Org. Lett.* **2011**, *13* (10), 2682–2685.

(63) Nakamura, H.; Ishihara, K.; Yamamoto, H. Lewis Acid-Activated Chiral Leaving Group: Enantioselective Electrophilic Addition to Prochiral Olefins. *J. Org. Chem.* **2002**, *67* (15), 5124–5137.

(64) Sauer, A. M.; Crowe, W. E.; Henderson, G.; Laine, R. A. Hydrogenation Selectivity of the Bicyclo[4.4.0]Decane Ring System of Valencanes. *Synlett* **2010**, *2010* (03), 445–448.

(65) He, Z.; Song, F.; Sun, H.; Huang, Y. Transition-Metal-Free Suzuki-Type Cross-Coupling Reaction of Benzyl Halides and Boronic Acids via 1,2-Metalate Shift. *J. Am. Chem. Soc.* **2018**, *140* (7), 2693–2699.

(66) Melzer, B.; Bracher, F. A Divergent Approach to Benzylisoquinoline-Type and Oxoaporphine Alkaloids via Regioselective Direct Ring Metalation of Alkoxy Isoquinolines. *Org. Biomol. Chem.* **2015**, *13* (28), 7664–7672.

(67) Larraufie, M.-H.; Pellet, R.; Fensterbank, L.; Goddard, J.-P.; Lacôte, E.; Malacria, M.; Ollivier, C. Visible-Light-Induced Photoreductive Generation of Radicals from Epoxides and Aziridines. *Angew. Chem. Int. Ed.* **2011**, *50* (19), 4463–4466.

(68) Liu, Y.; Xiao, S.; Qi, Y.; Du, F. Reductive Homocoupling of Organohalides Using Nickel(II) Chloride and Samarium Metal. *Chem. – Asian J.* **2017**, *12* (6), 673–678.

(69) Keaveney, S. T.; Kundu, G.; Schoenebeck, F. Modular Functionalization of Arenes in a Triply Selective Sequence: Rapid C(Sp2) and C(Sp3) Coupling of C−Br, C−OTf, and C−Cl Bonds Enabled by a Single Palladium(I) Dimer. *Angew. Chem. Int. Ed.* **2018**, *57* (38), 12573–12577.

APPENDIX 4

Spectra Relevant to Chapter 3:

Radical Deoxygenation of Alcohols by a Titanium Porphyrin Catalyst

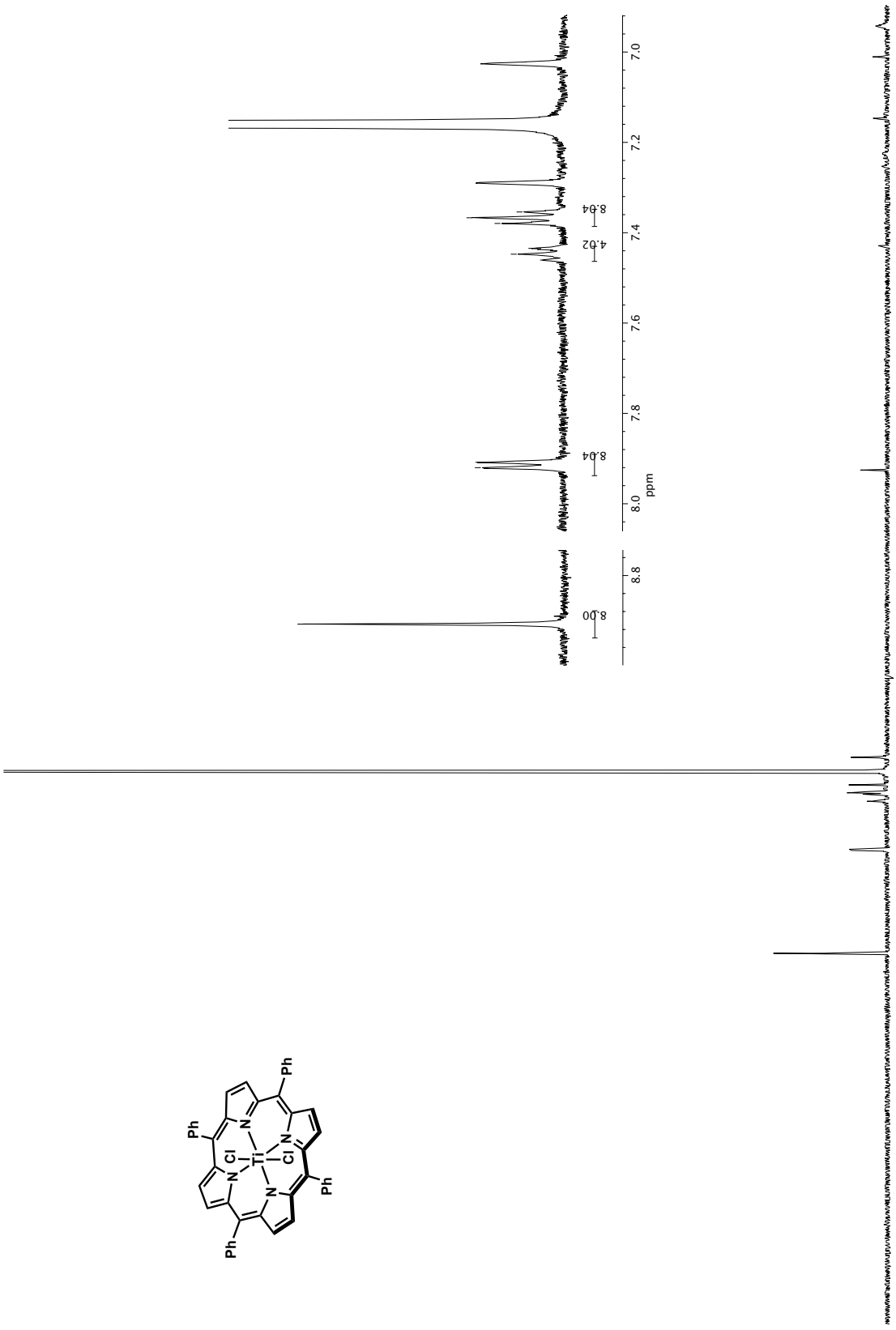


Figure A.4.1. ^{1}H NMR (600 MHz, C_6D_6) of **Ti(TPP)Cl$_2$.**

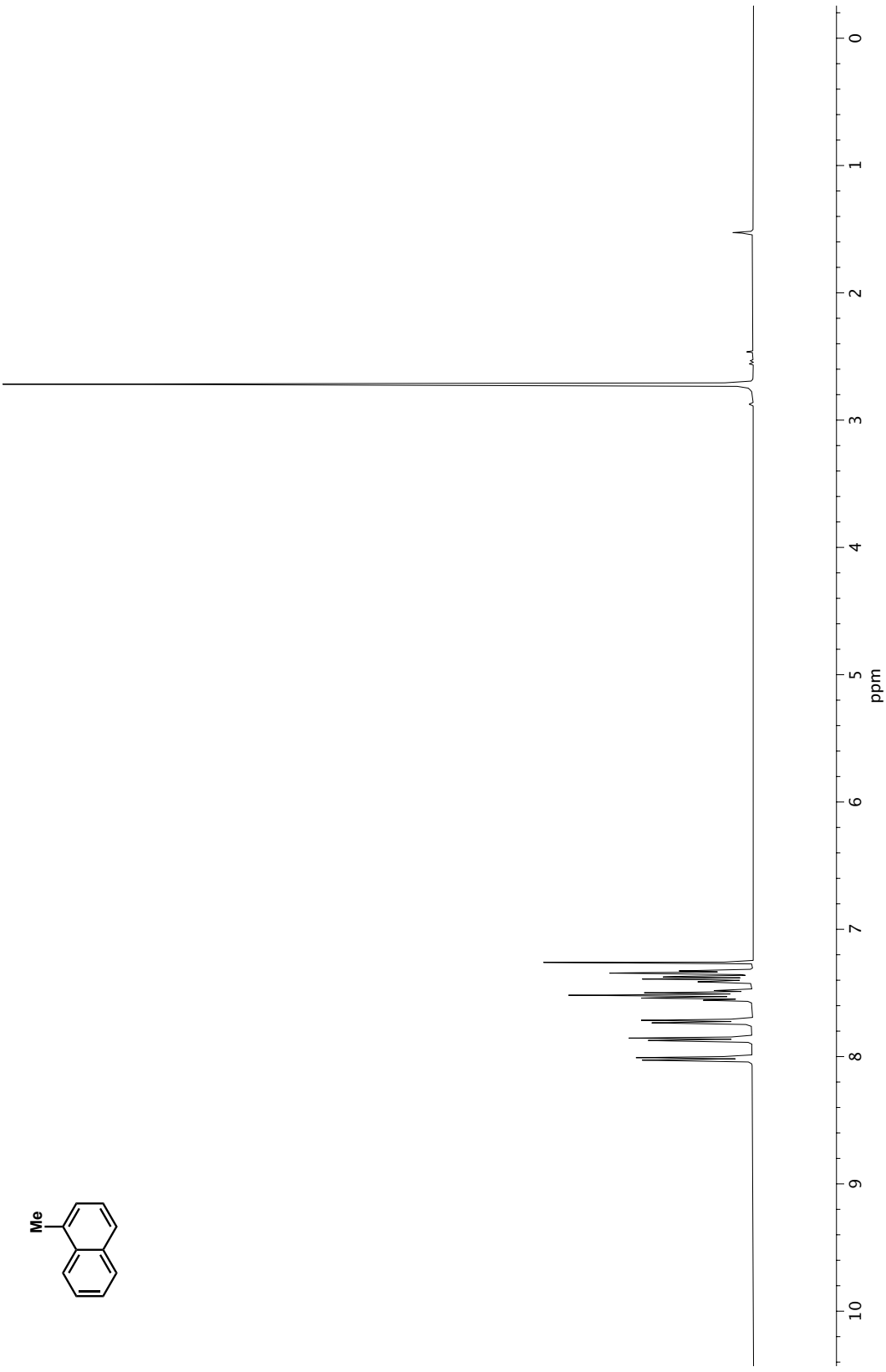


Figure A.4.2. ^{1}H NMR (400 MHz, $CDCl_3$) of compound **69b**.

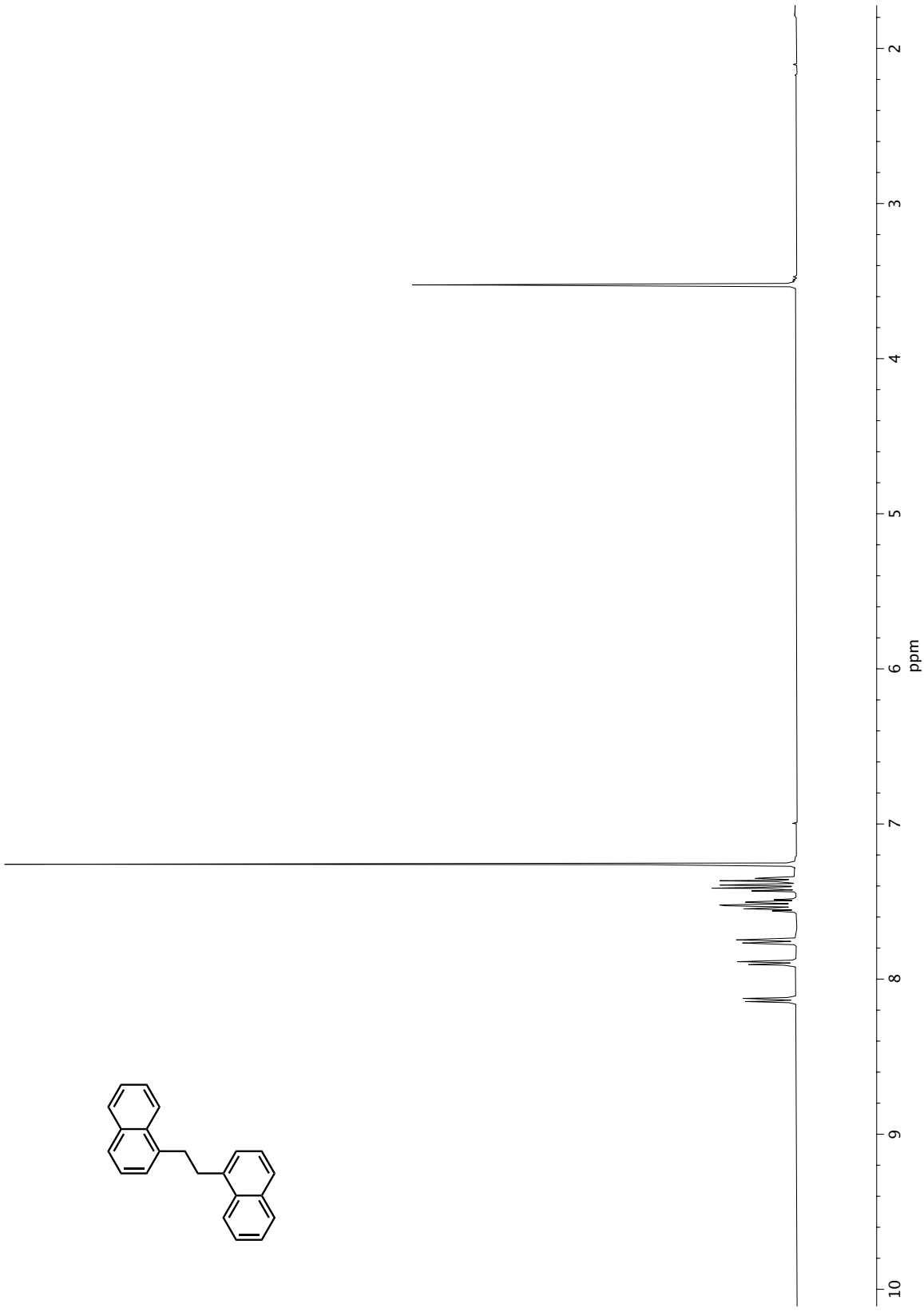


Figure A.4.3. ^{1}H NMR (400 MHz, $CDCl_3$) of compound **69c**.

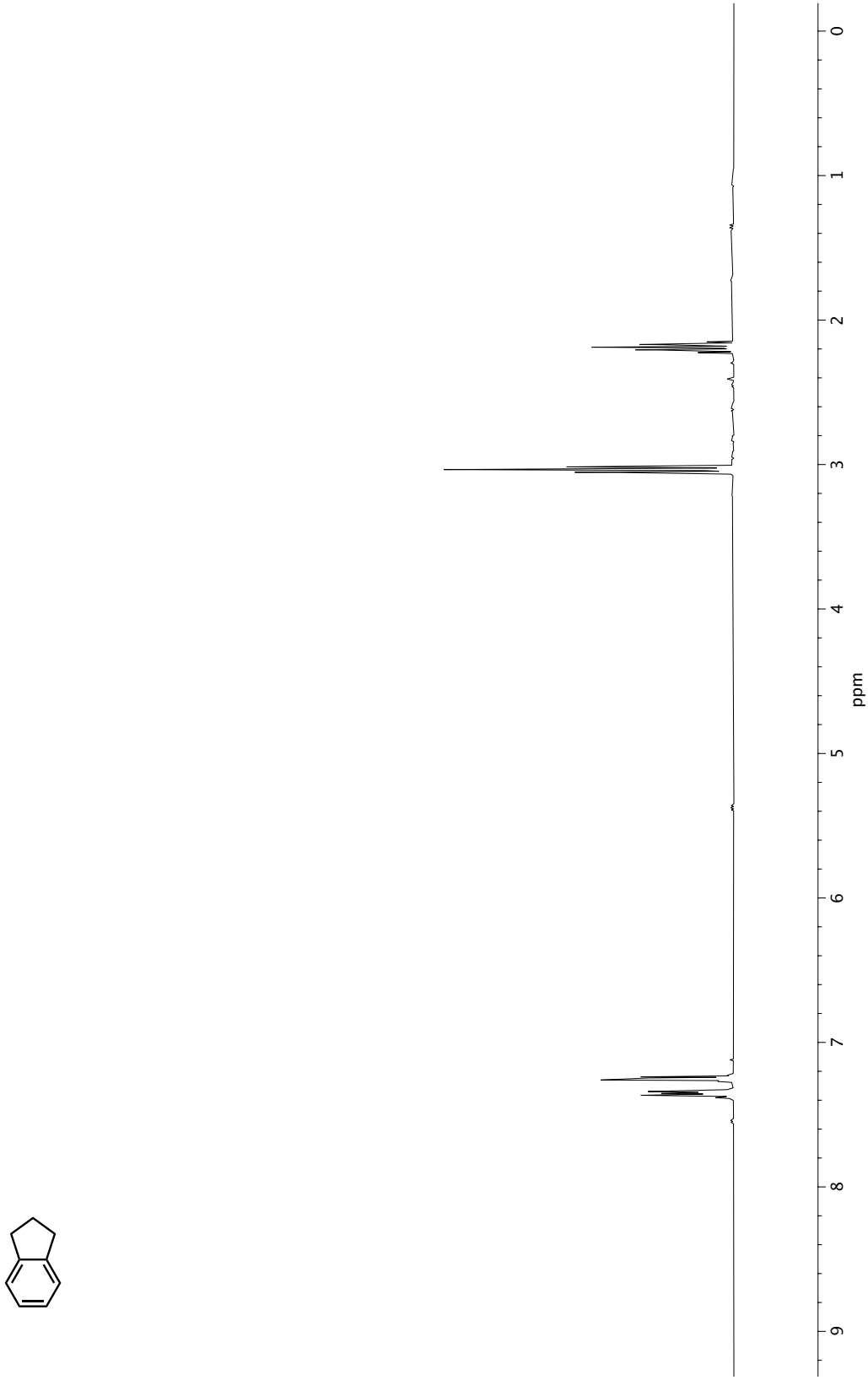


Figure A.4.4. ^{1}H NMR (400 MHz, $CDCl_3$) of compound **71b**.

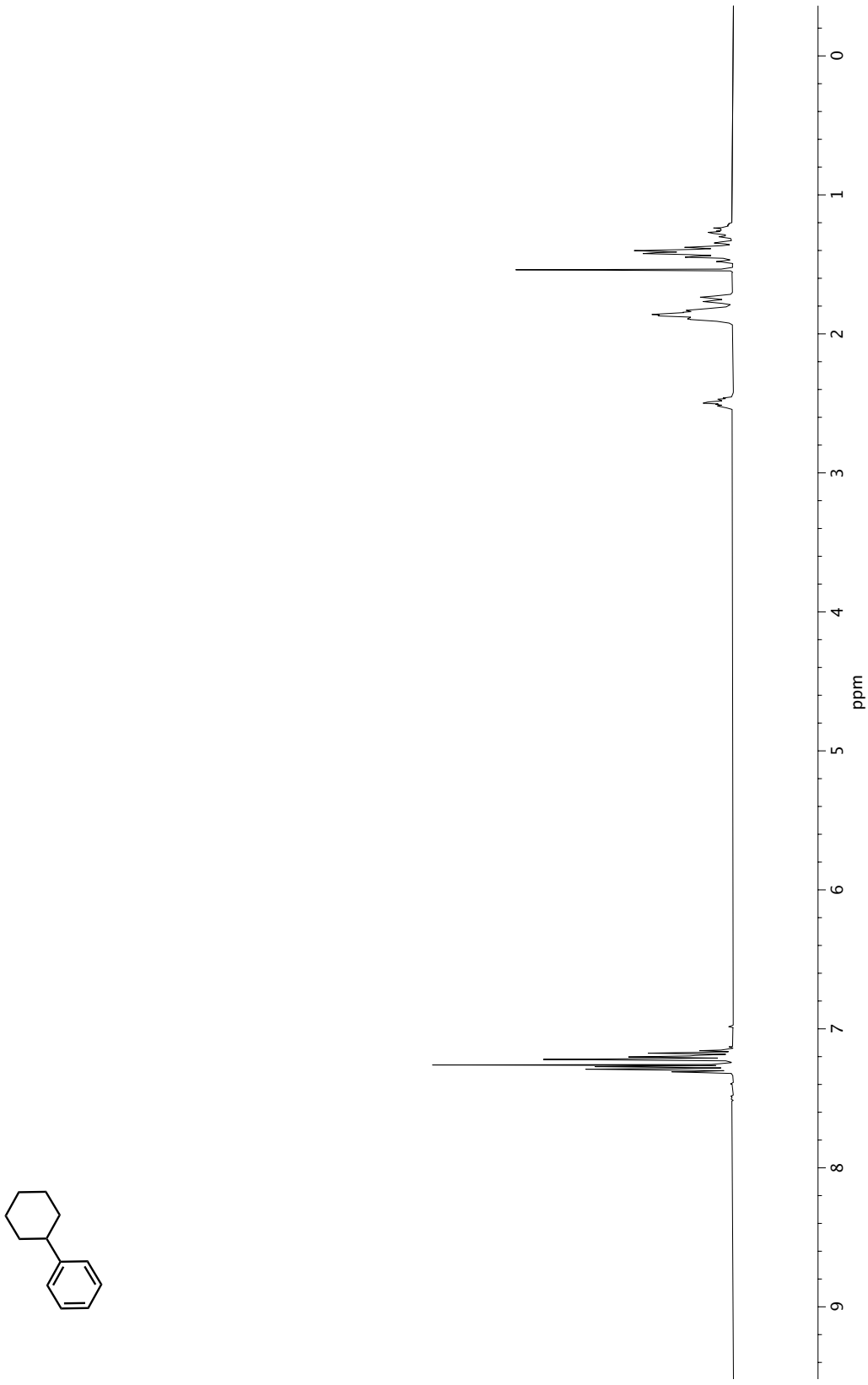


Figure A.4.5. ^{1}H NMR (400 MHz, $CDCl_3$) of compound **72b**.

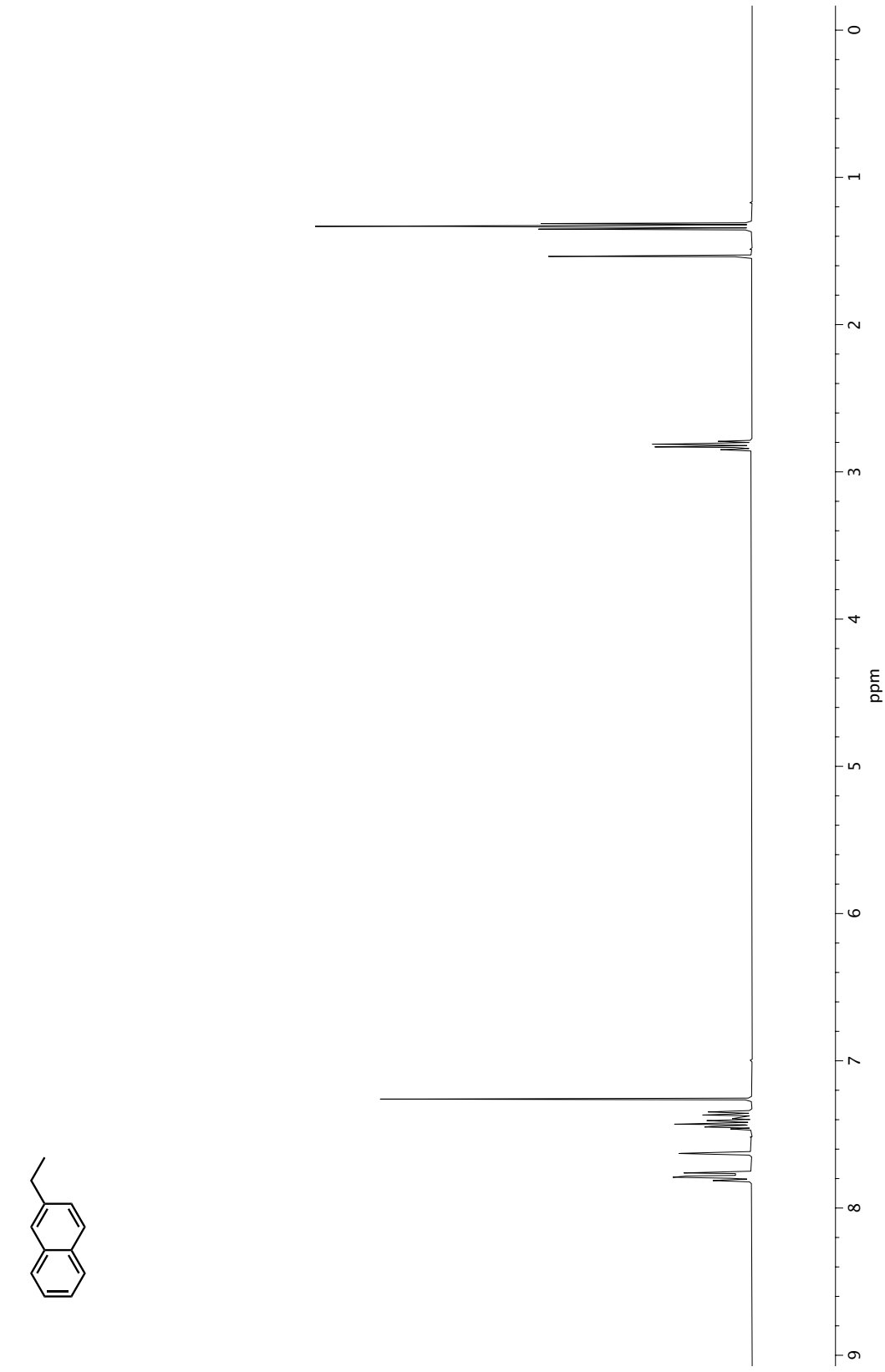


Figure A.4.6. ^{1}H NMR (400 MHz, $CDCl_3$) of compound **73b**.

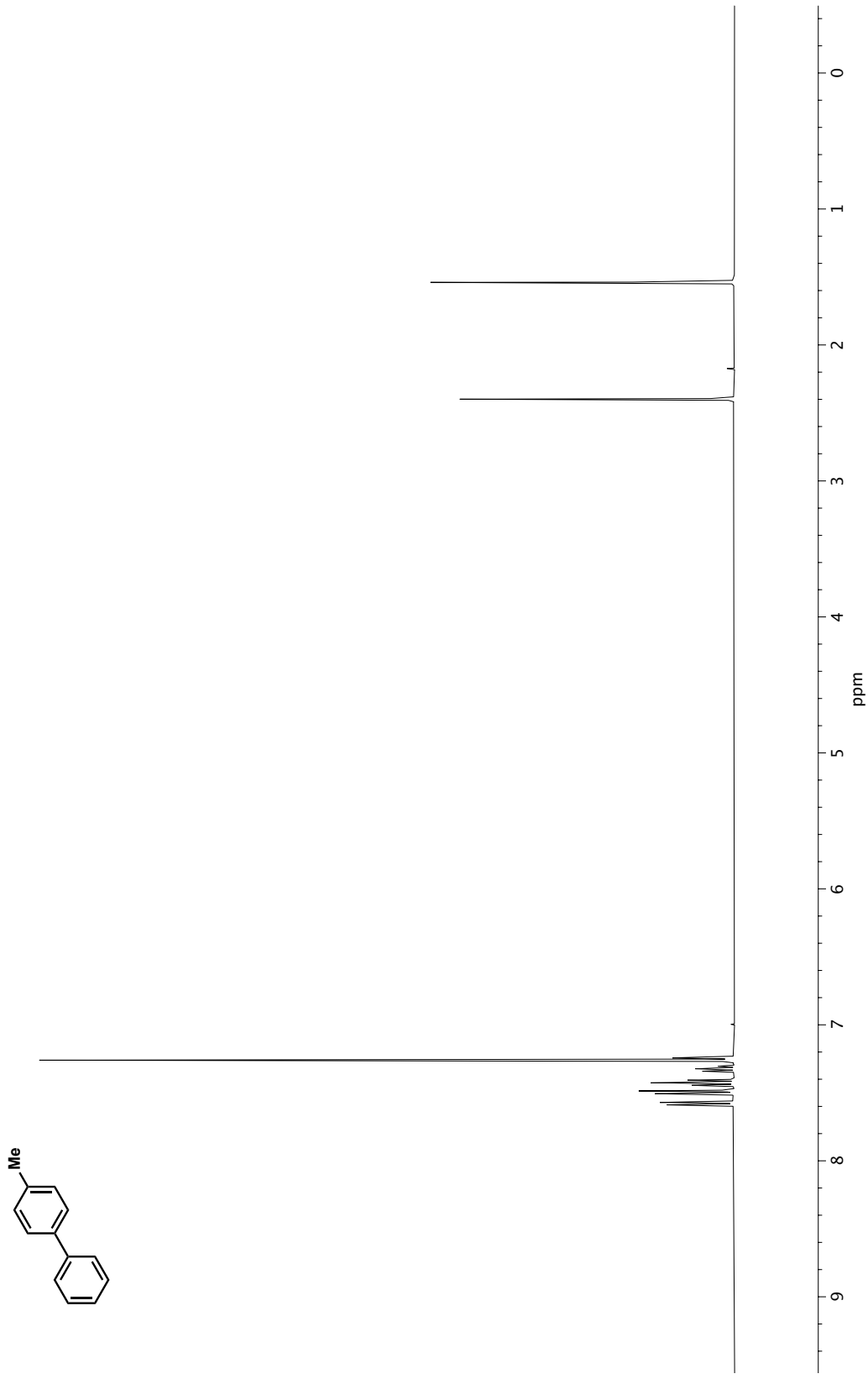


Figure A.4.7. ^{1}H NMR (400 MHz, $CDCl_3$) of compound **74b**.

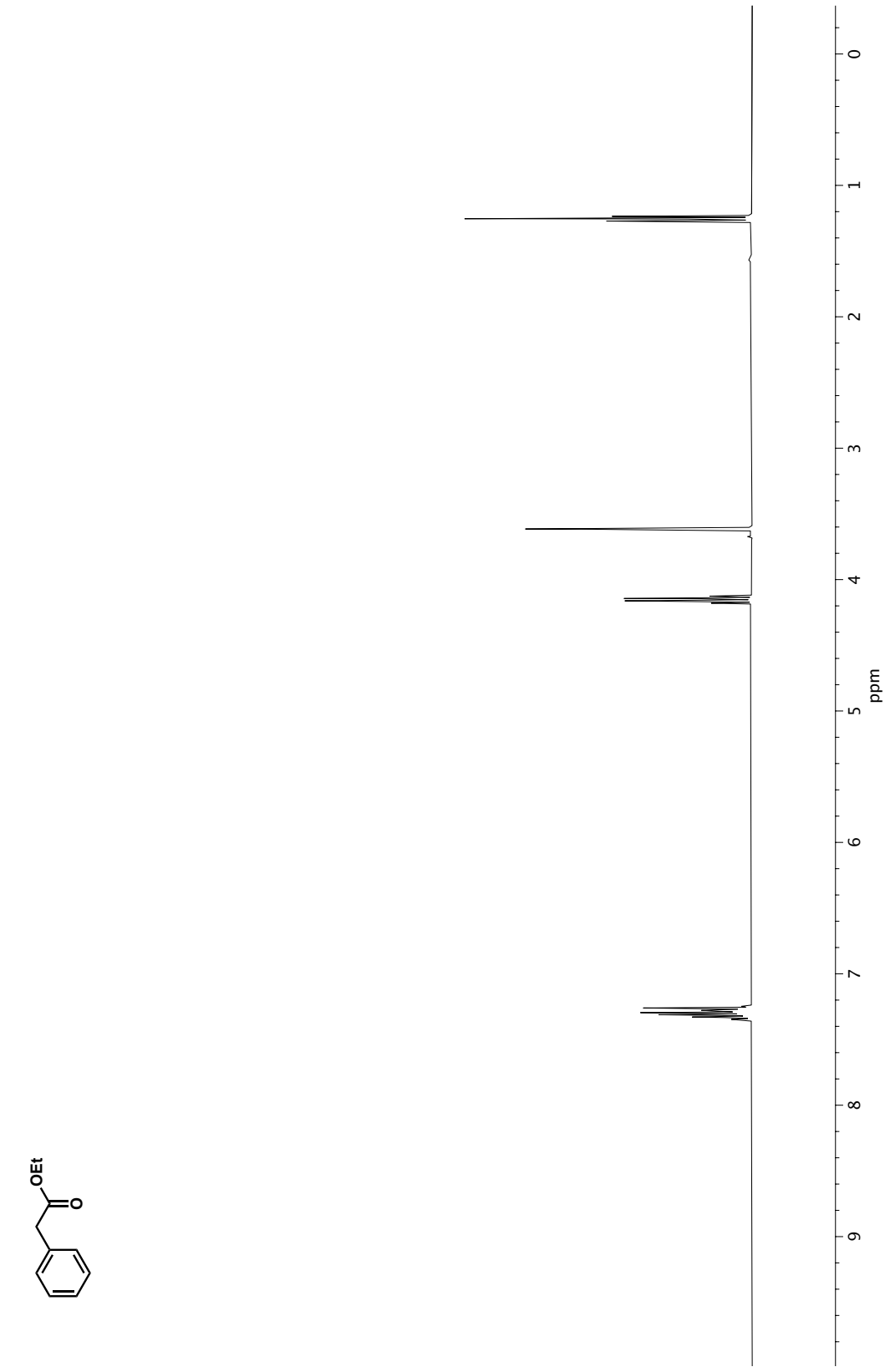


Figure A.4.8. ^{1}H NMR (400 MHz, $CDCl_3$) of compound **76b**.

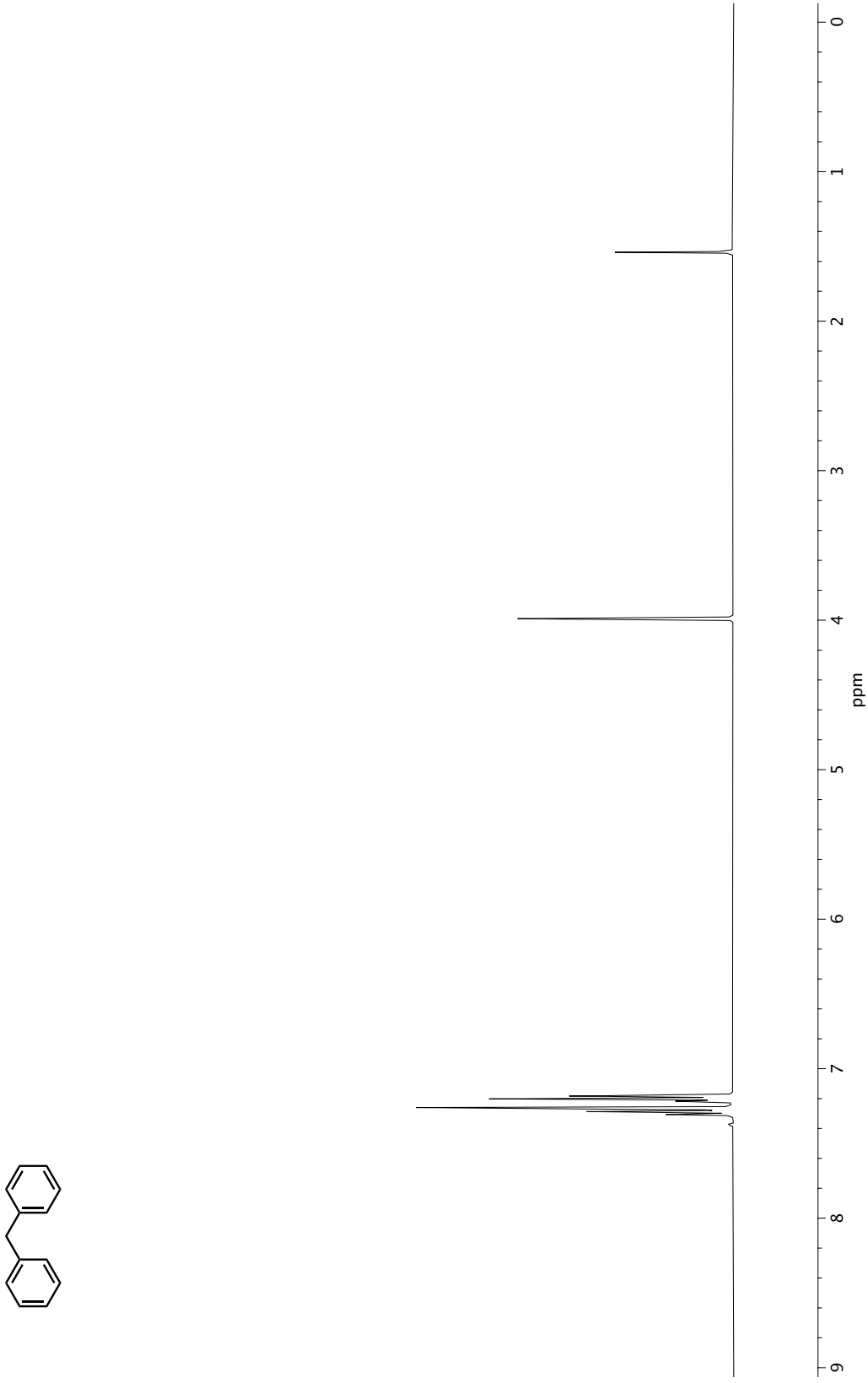


Figure A.4.9. ^{1}H NMR (400 MHz, $CDCl_3$) of compound **77b**.

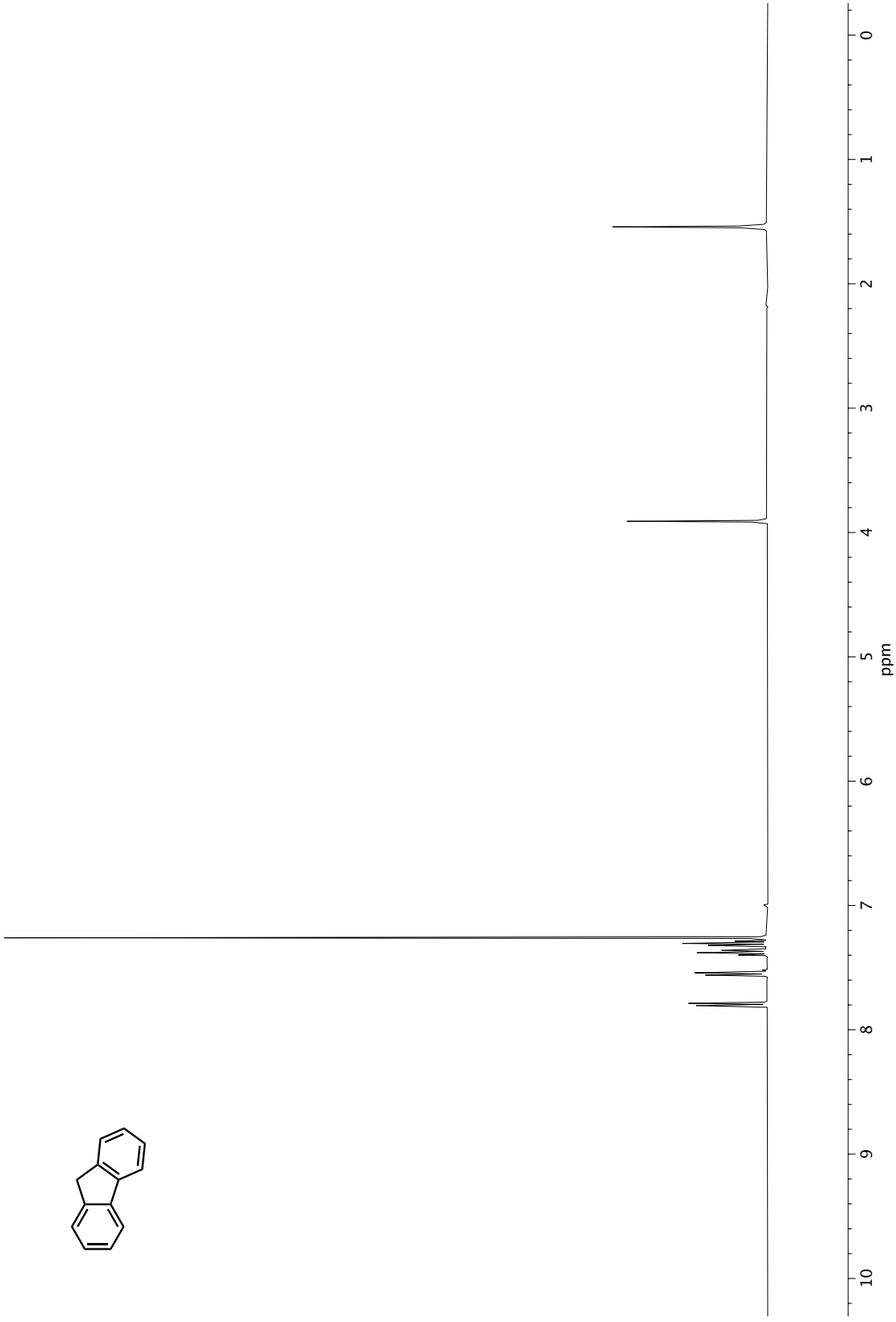
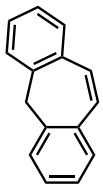


Figure A.4.10. ^{1}H NMR (400 MHz, $CDCl_3$) of **78b**.



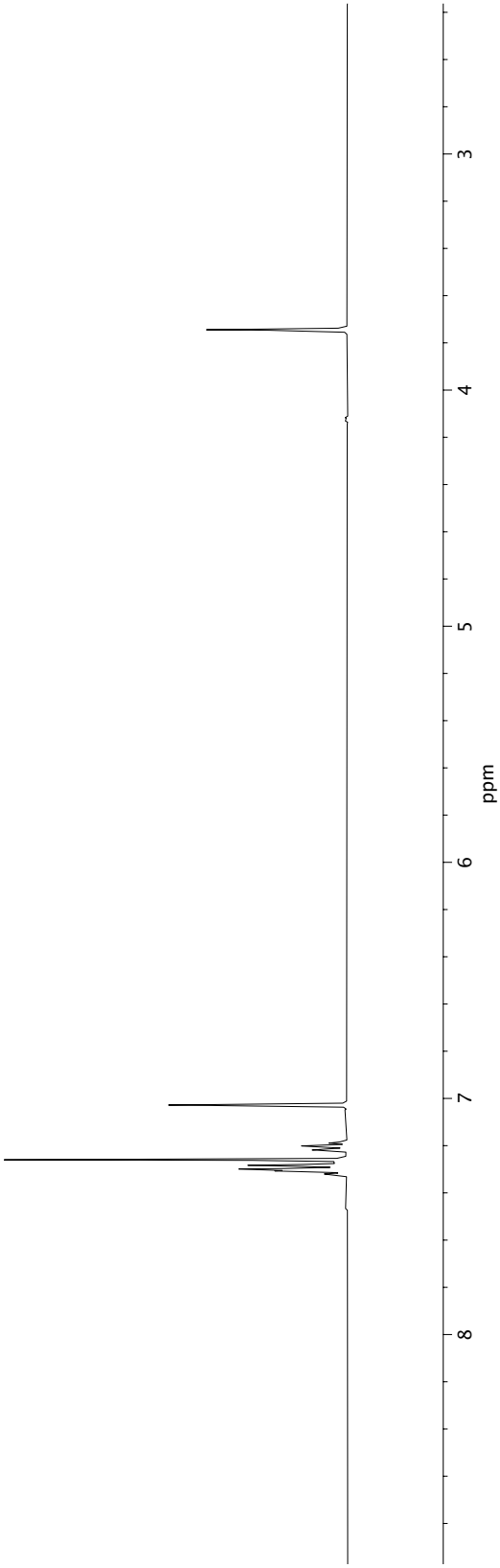


Figure A.4.11. ^{1}H NMR (500 MHz, $CDCl_3$) of **79b**.

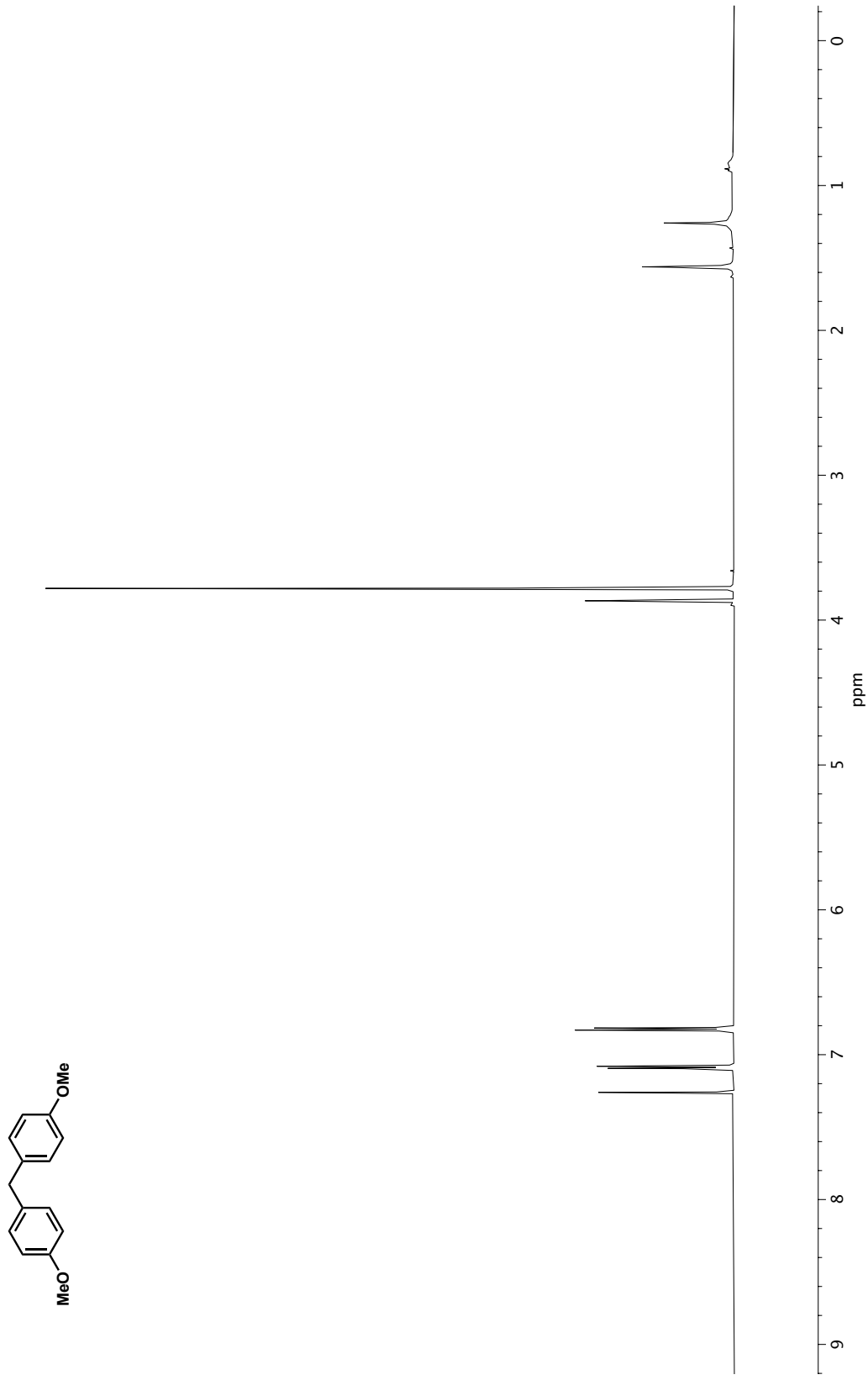


Figure A.4.12. ^{1}H NMR (600 MHz, $CDCl_3$) of **80b**.

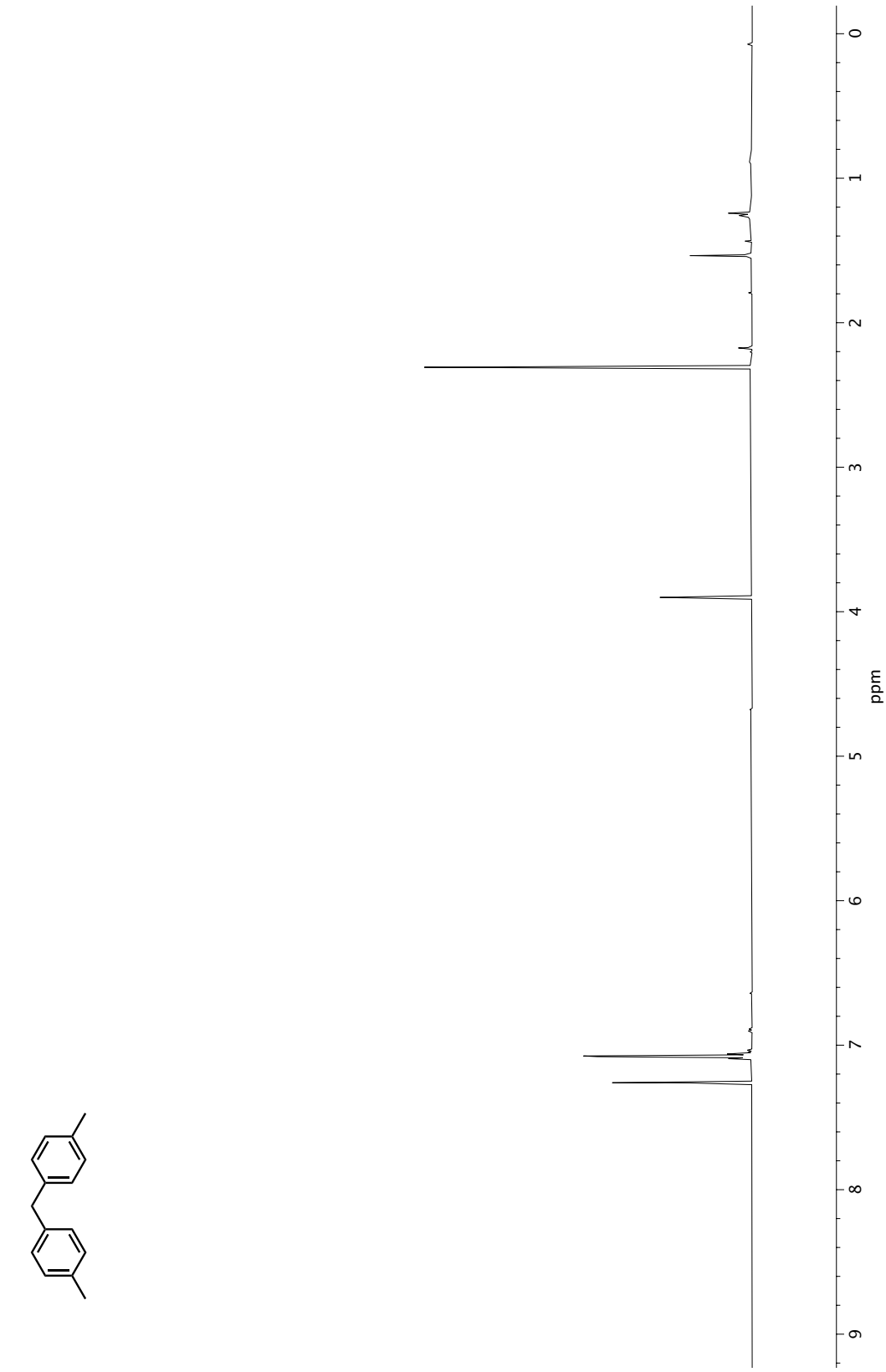


Figure A.4.13. ^{1}H NMR (600 MHz, $CDCl_3$) of **81b**.

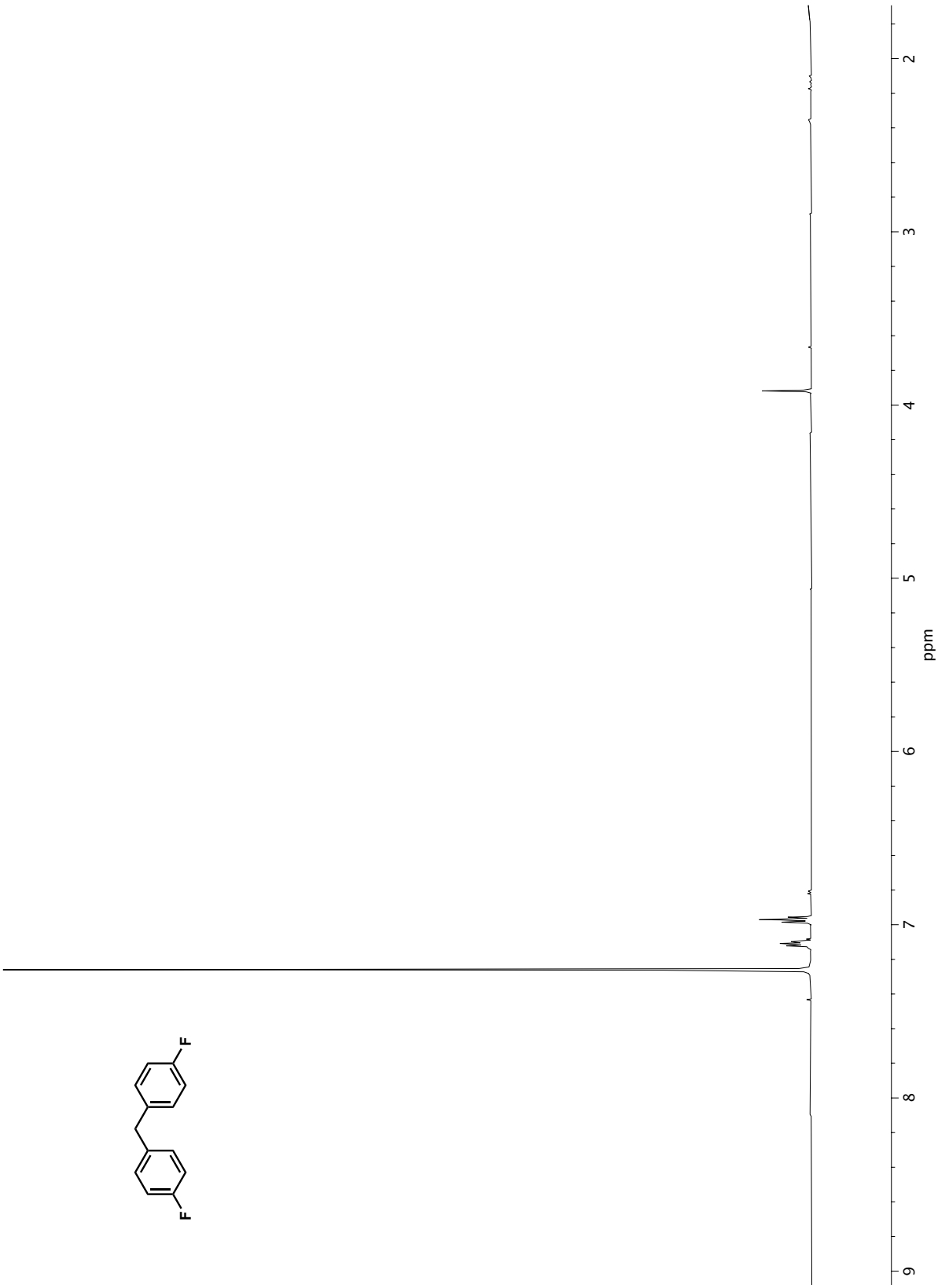


Figure A.4.14. ^{1}H NMR (600 MHz, $CDCl_3$) of **82b**.

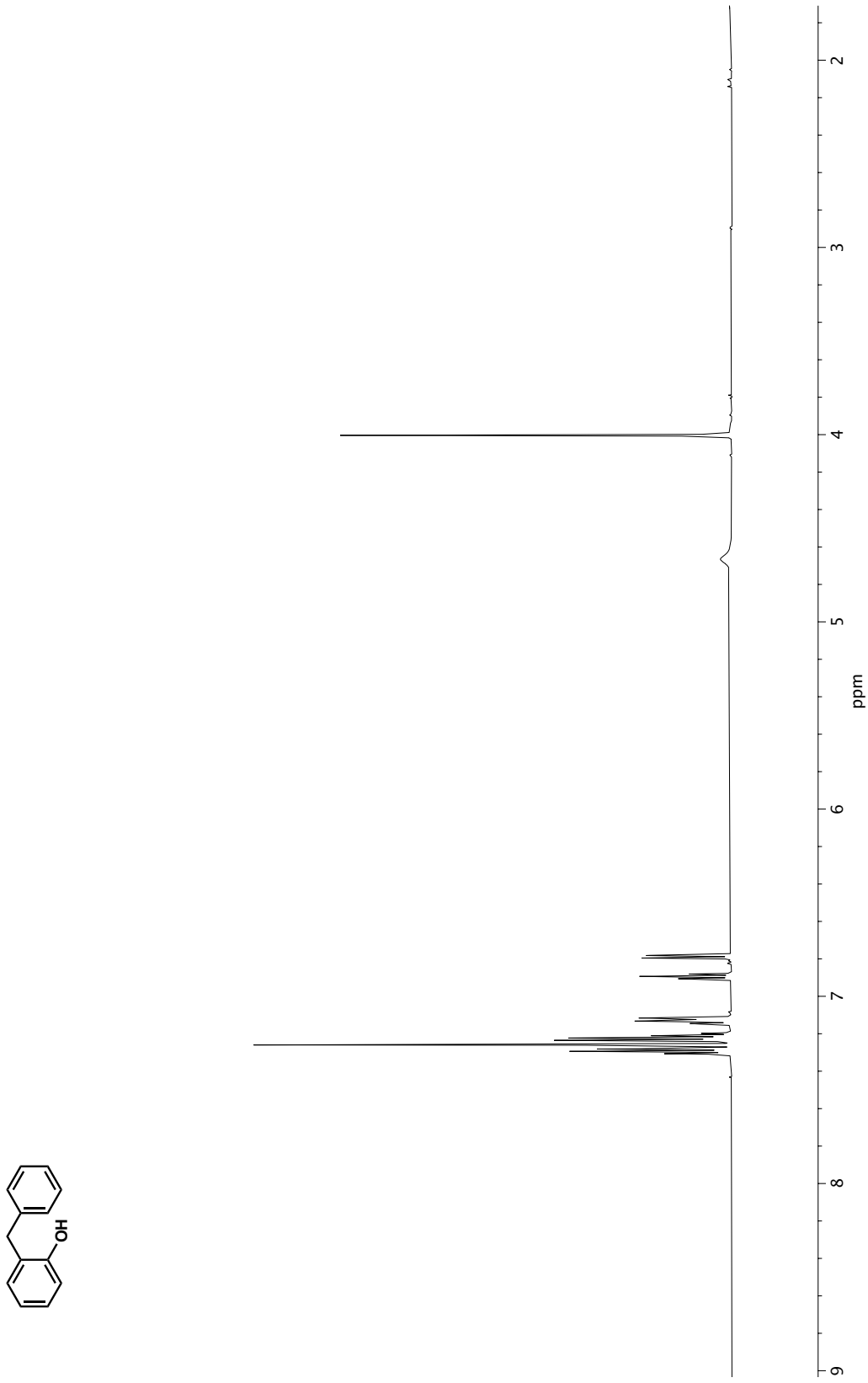


Figure A.4.15. ^{1}H NMR (600 MHz, $CDCl_3$) of **83b**.

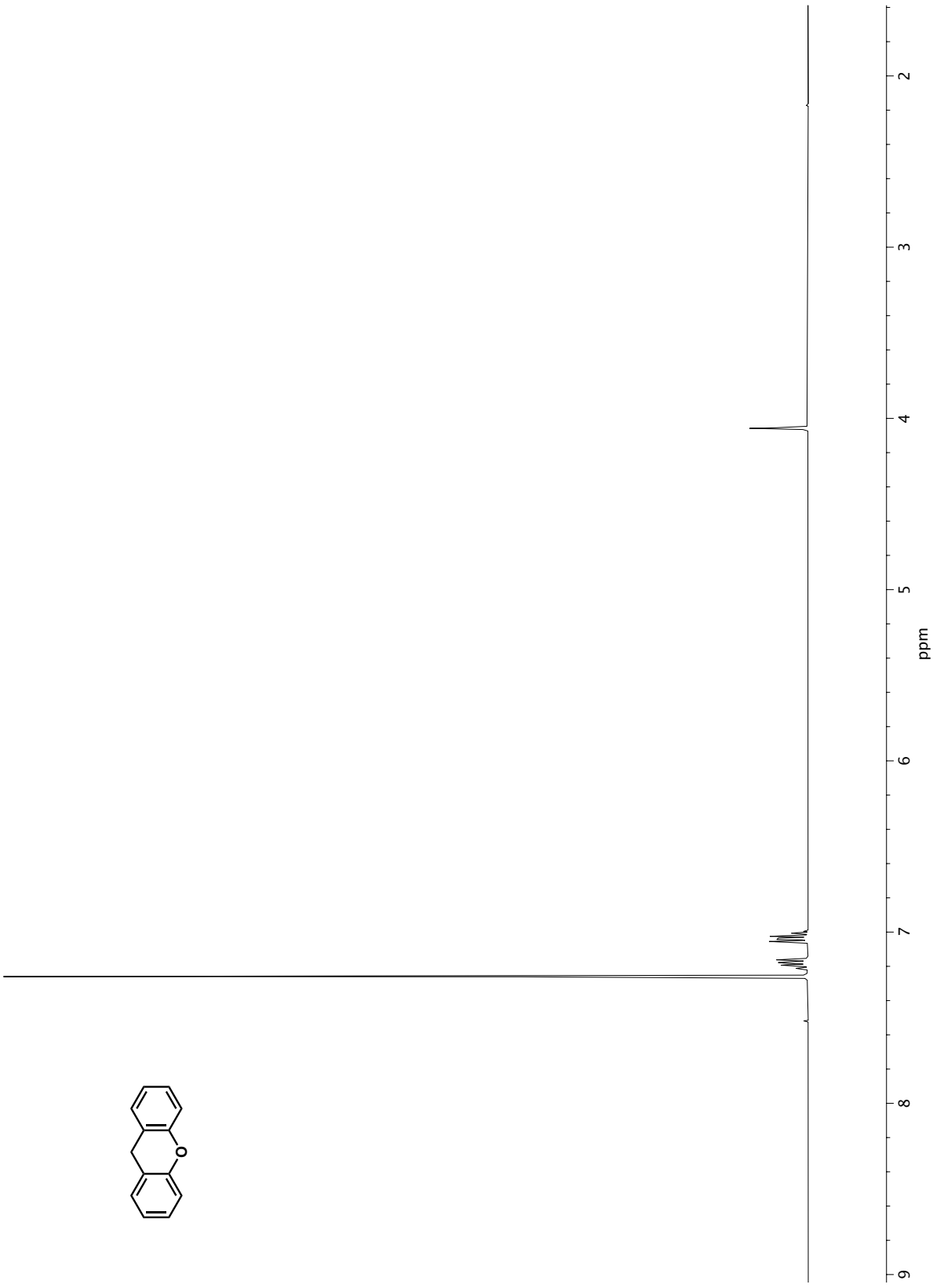


Figure A.4.16. ^{1}H NMR (400 MHz, $CDCl_3$) of **84b**.

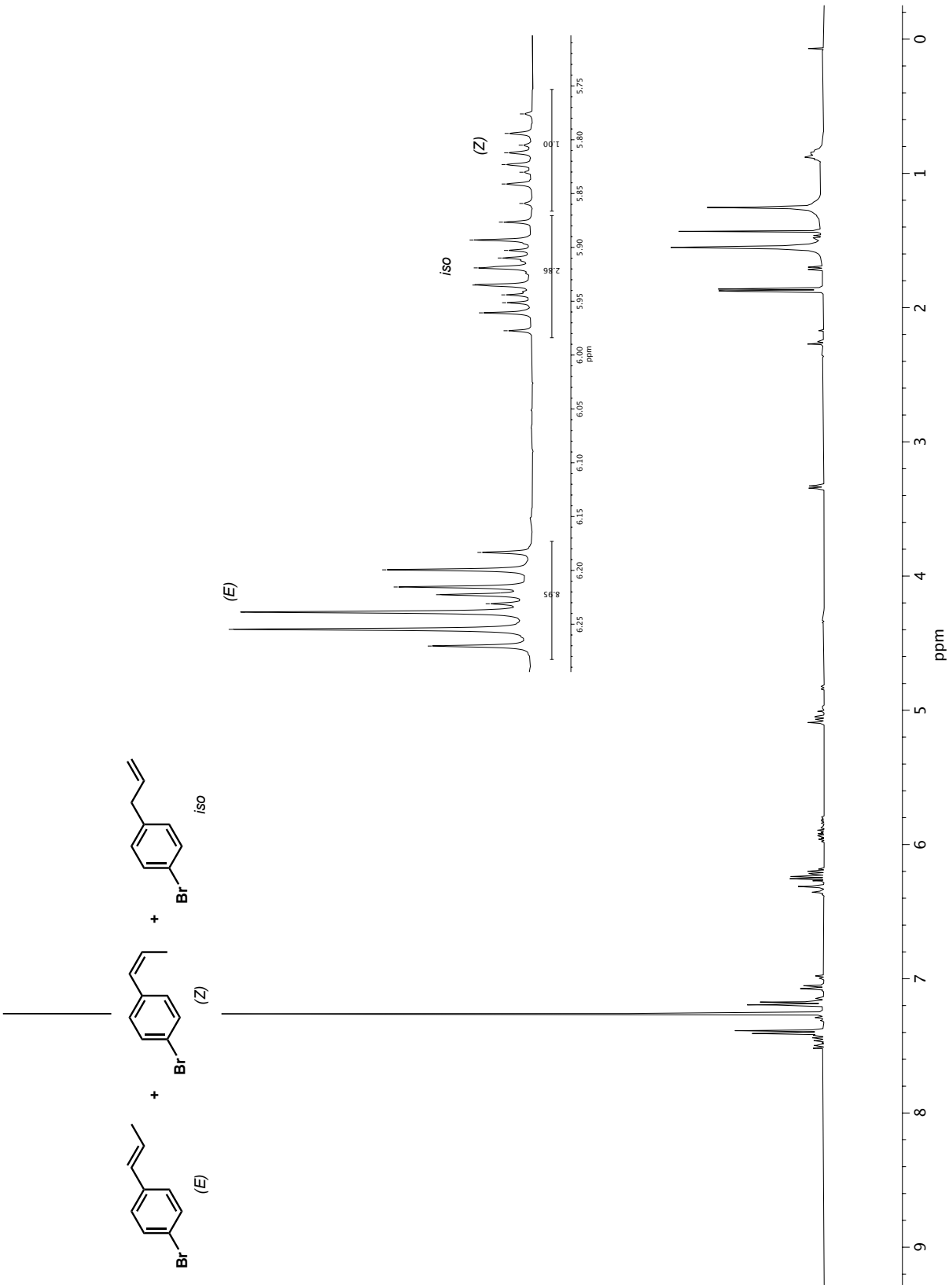


Figure A.4.17. ^{1}H NMR (400 MHz, $CDCl_3$) of **88b**, **88c**, **88d**.

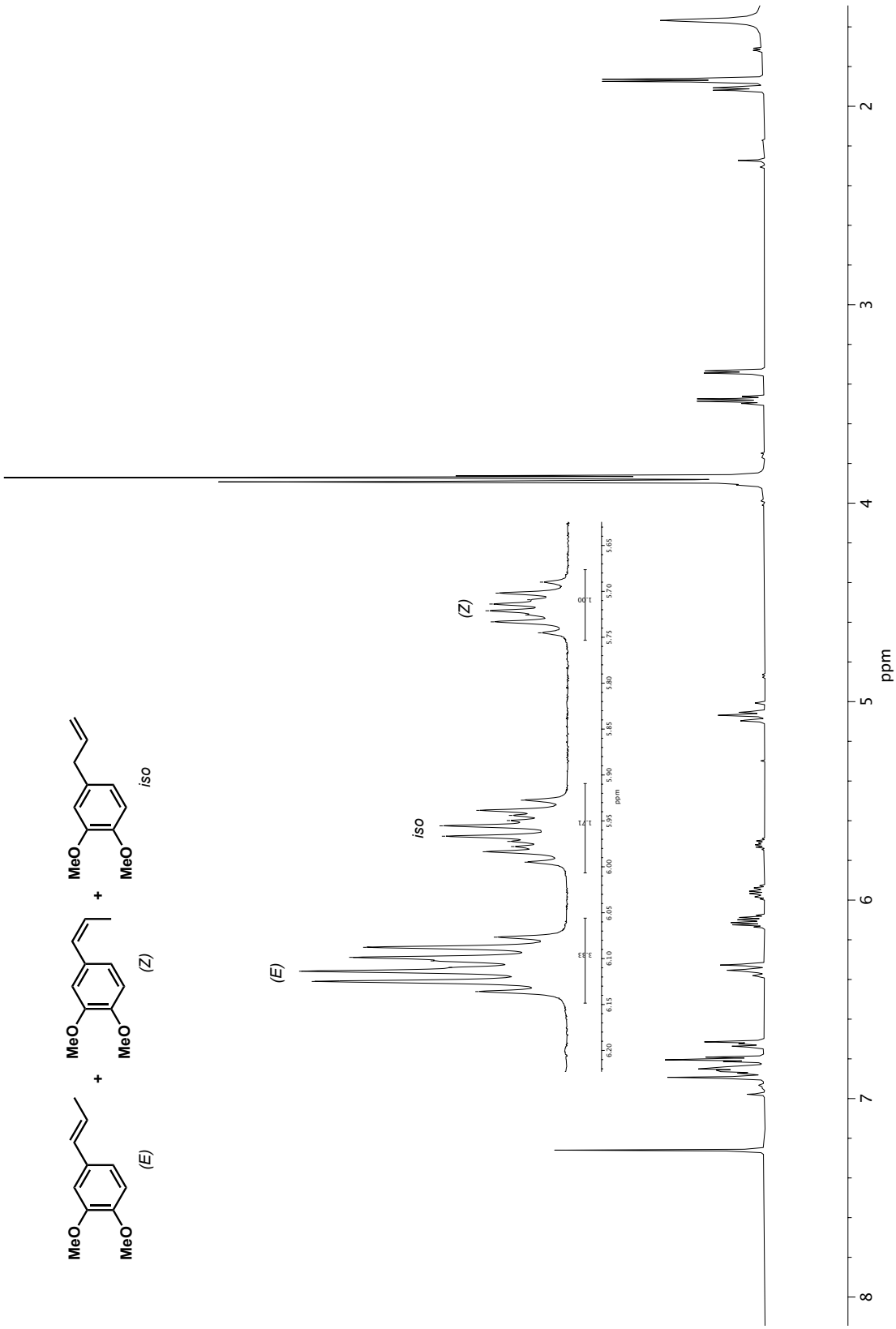


Figure A.4.18. ^{1}H NMR (600 MHz, $CDCl_3$) of **90b**, **90c**, **90d**.

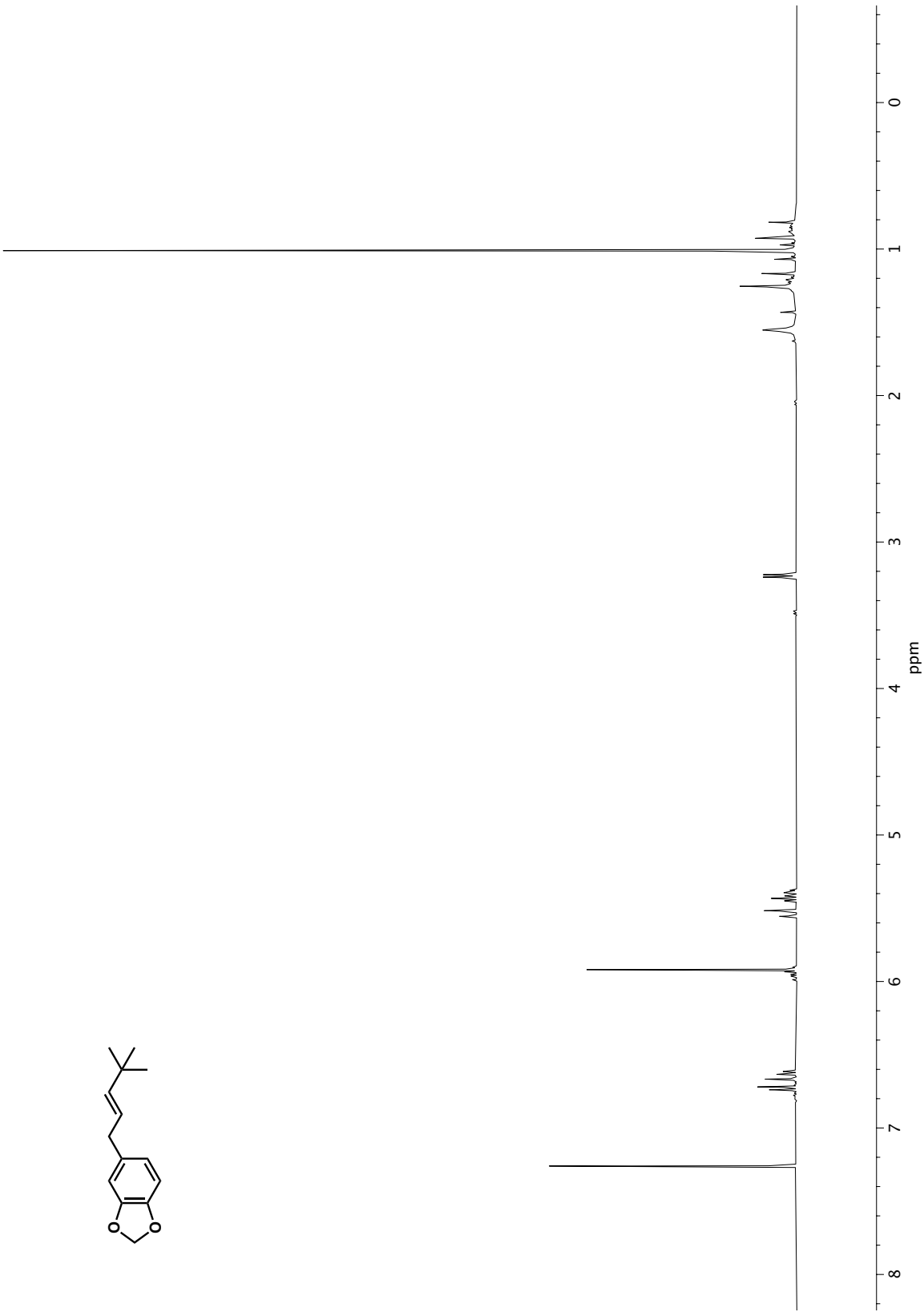


Figure A.4.19. ^{1}H NMR (400 MHz, $CDCl_3$) of **93b**.

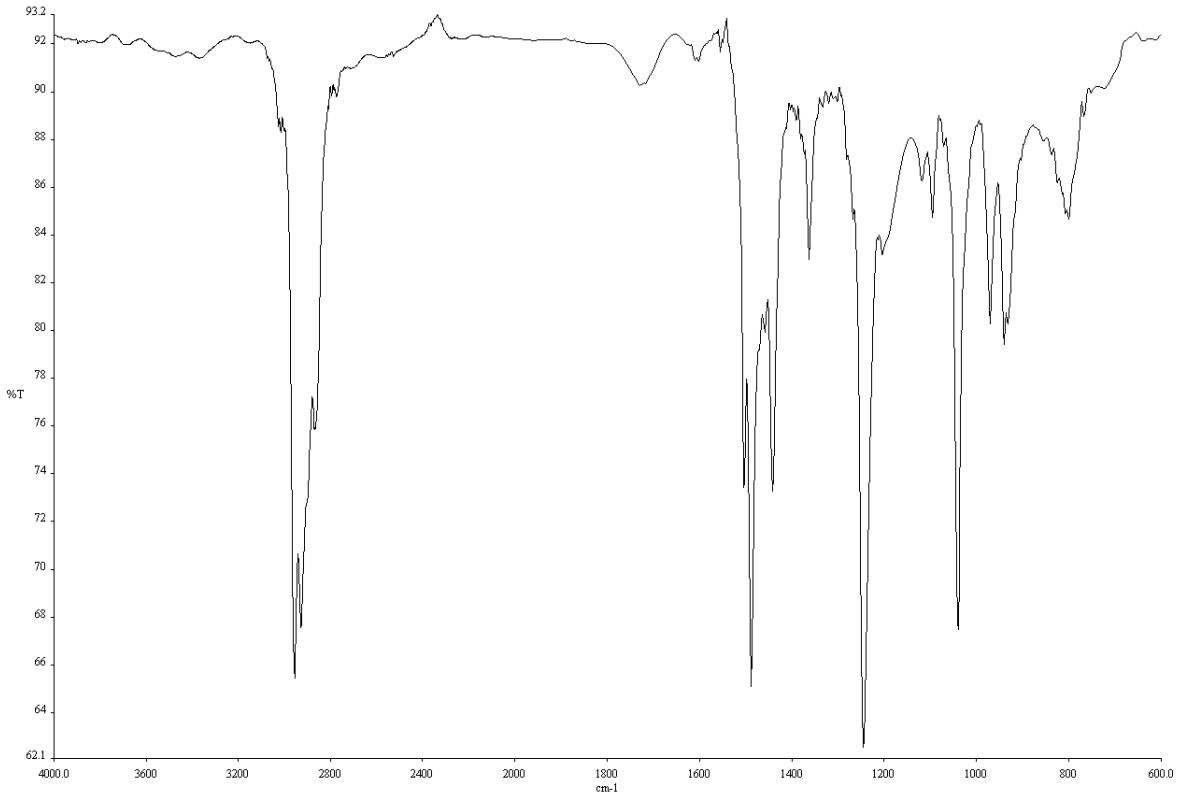


Figure A.4.20. Infrared spectrum (Thin Film, NaCl) of compound **93b**.

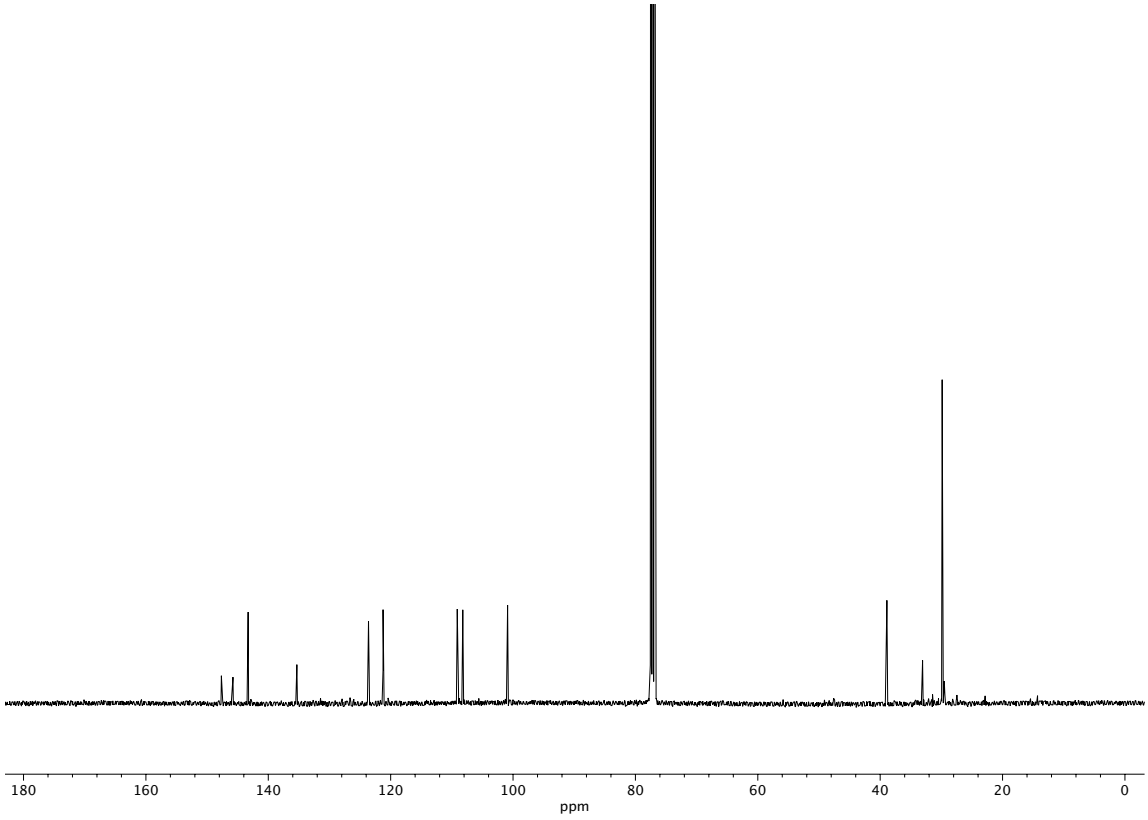


Figure A.4.21. ^{13}C NMR (101 MHz, $CDCl_3$) of compound **93b**.

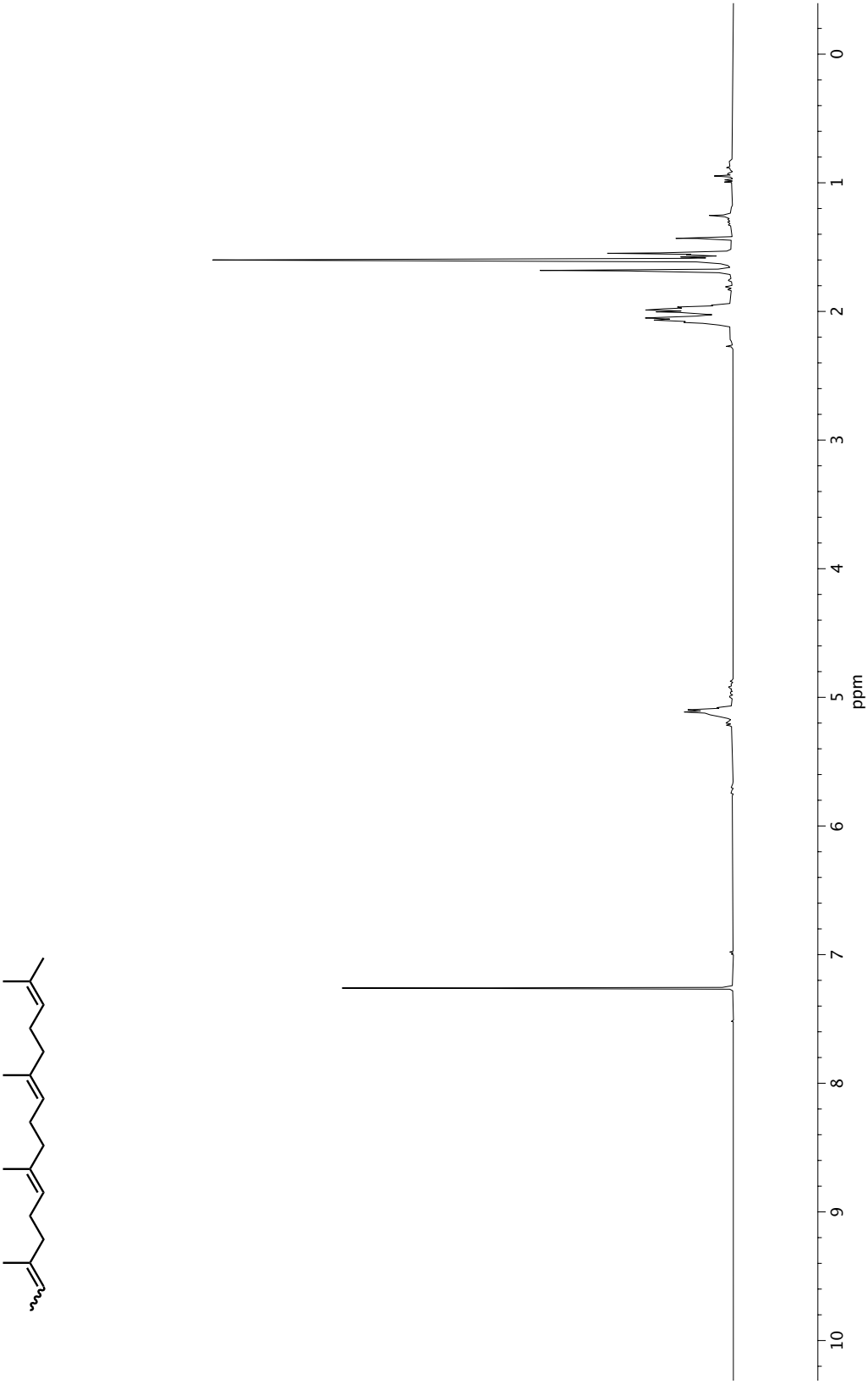


Figure A.4.22. ^{1}H NMR (400 MHz, $CDCl_3$) of **95b**.

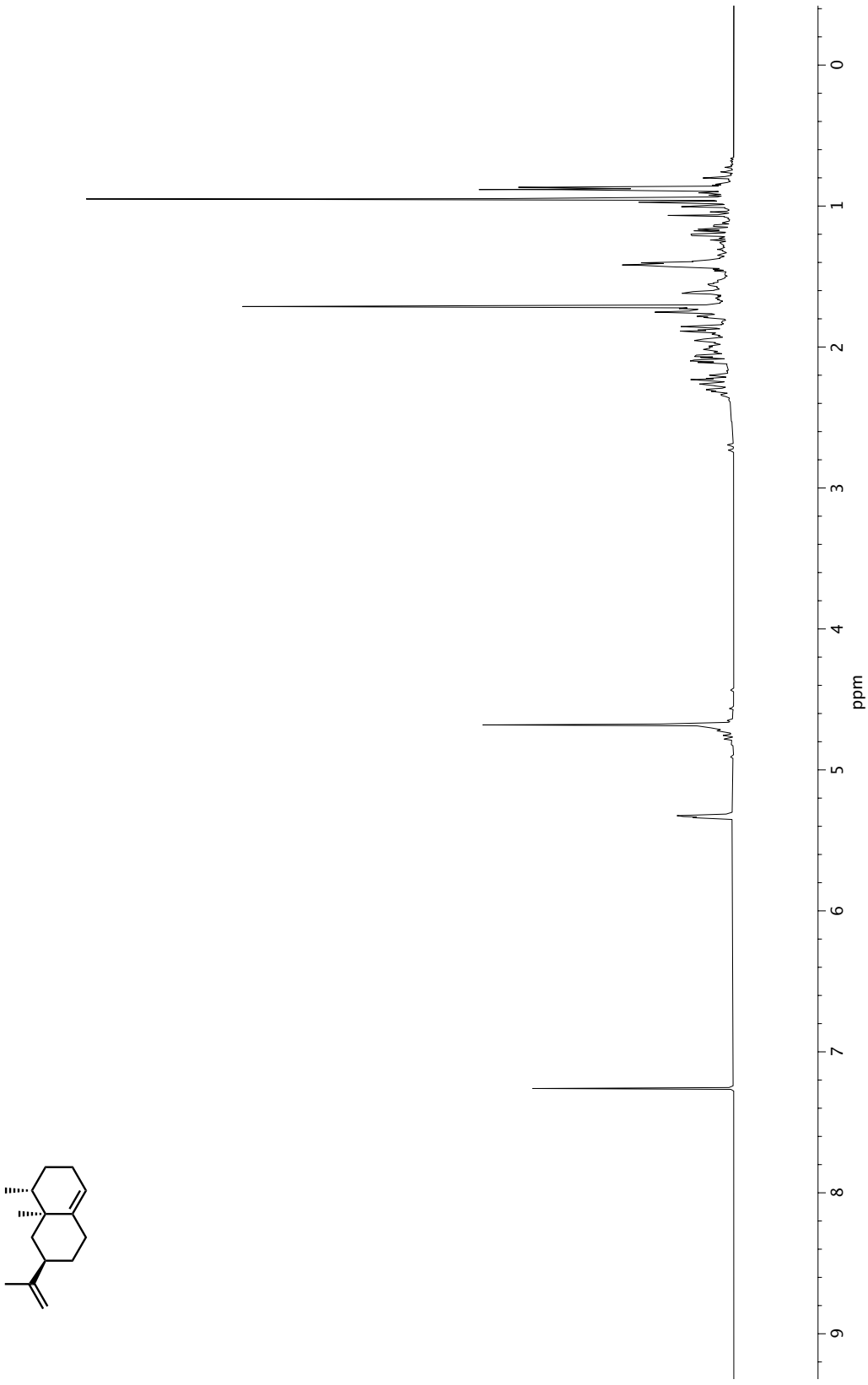


Figure A.4.23. ^{1}H NMR (400 MHz, $CDCl_3$) of **97b**.

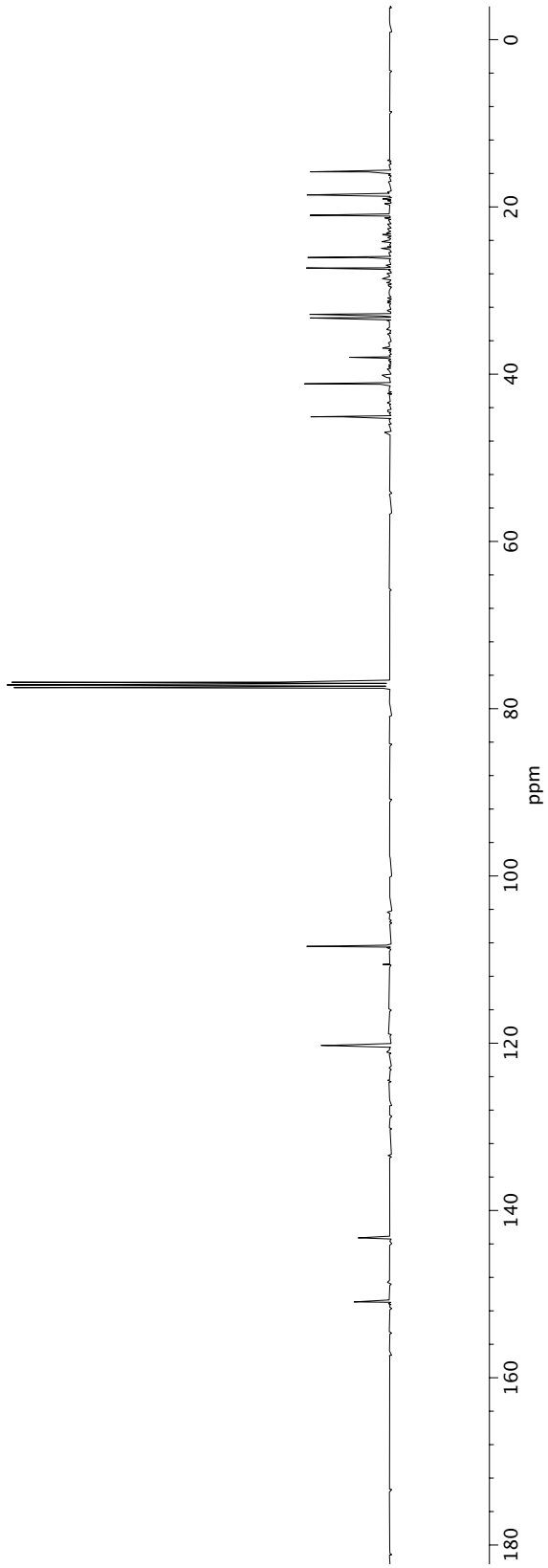


Figure A.4.24. ^{13}C NMR (101 MHz, $CDCl_3$) of **97b**.

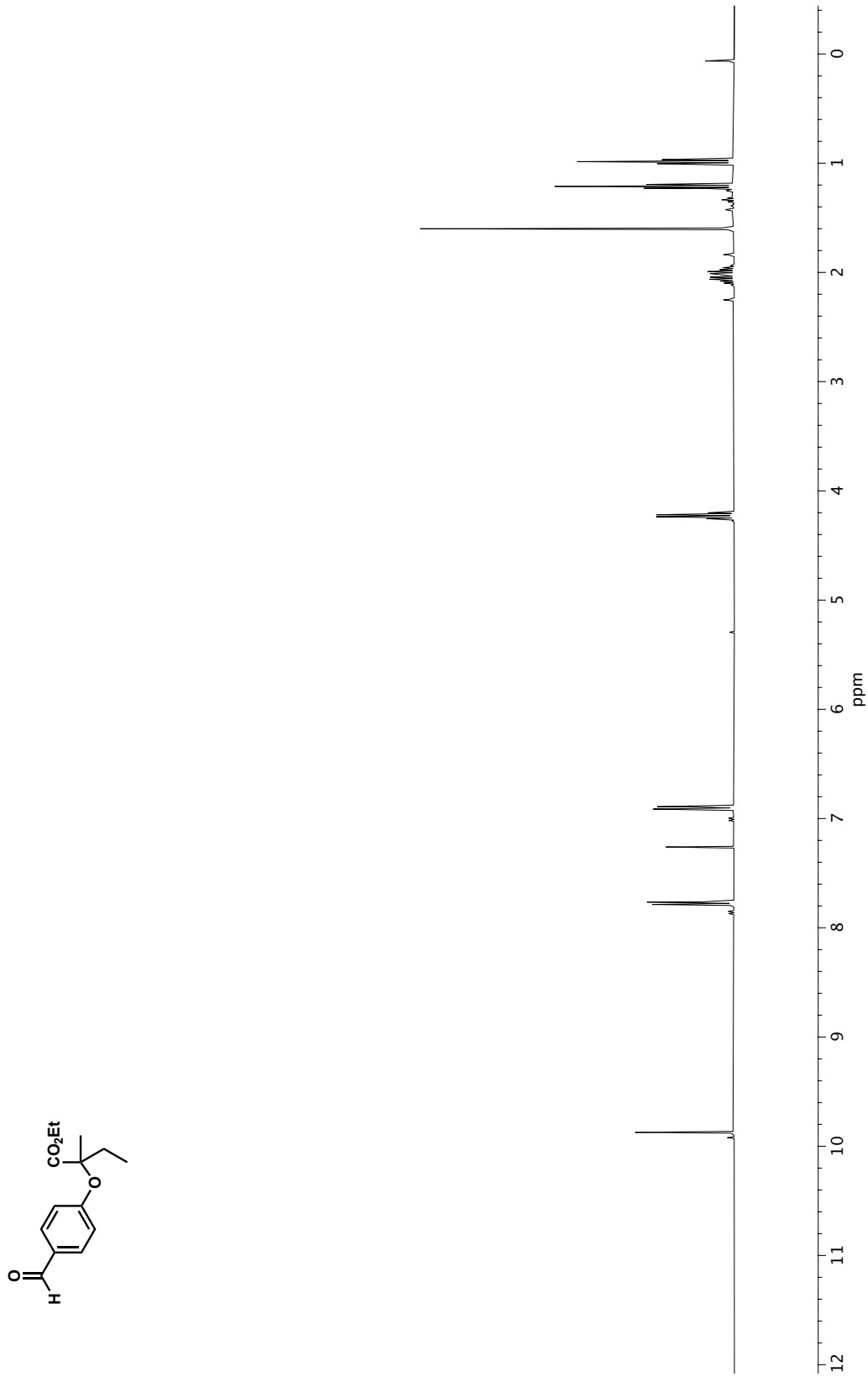


Figure A.4.25. ^{1}H NMR (400 MHz, $CDCl_3$) of **98a**.

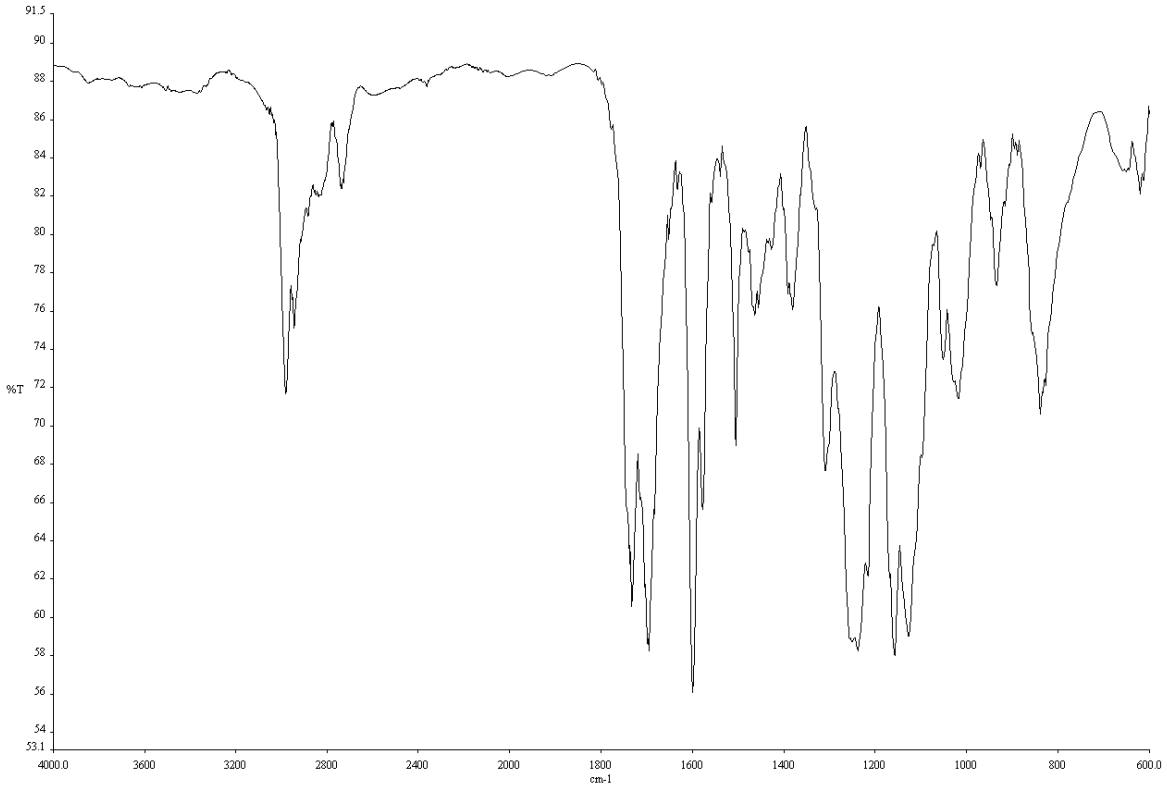


Figure A.4.26. Infrared spectrum (Thin Film, NaCl) of compound **98a**.

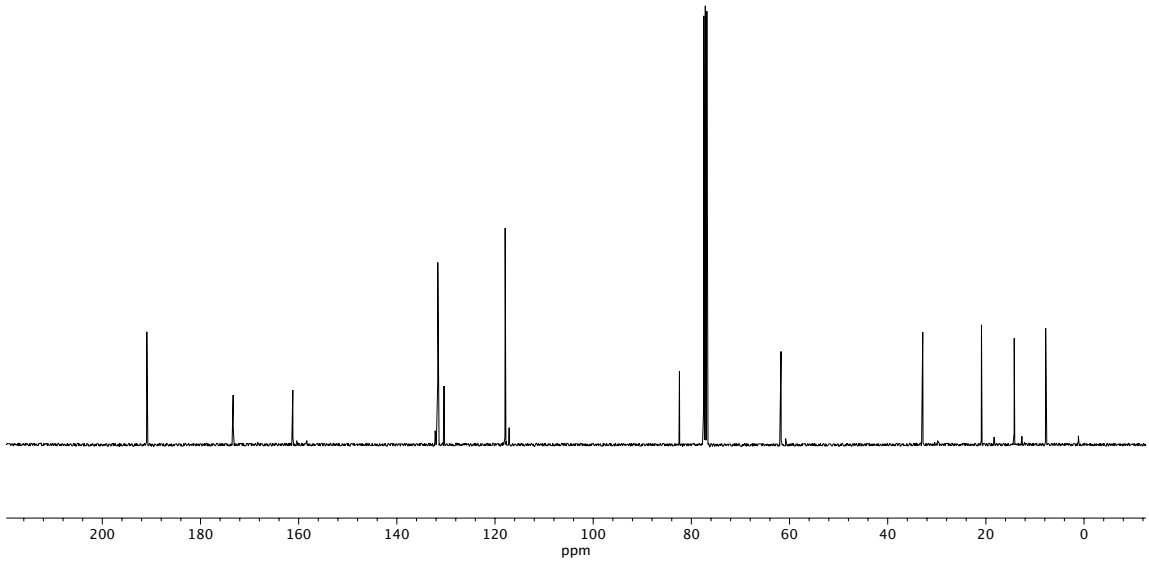


Figure A.4.27. ^{13}C NMR (101 MHz, $CDCl_3$) of compound **98a**.

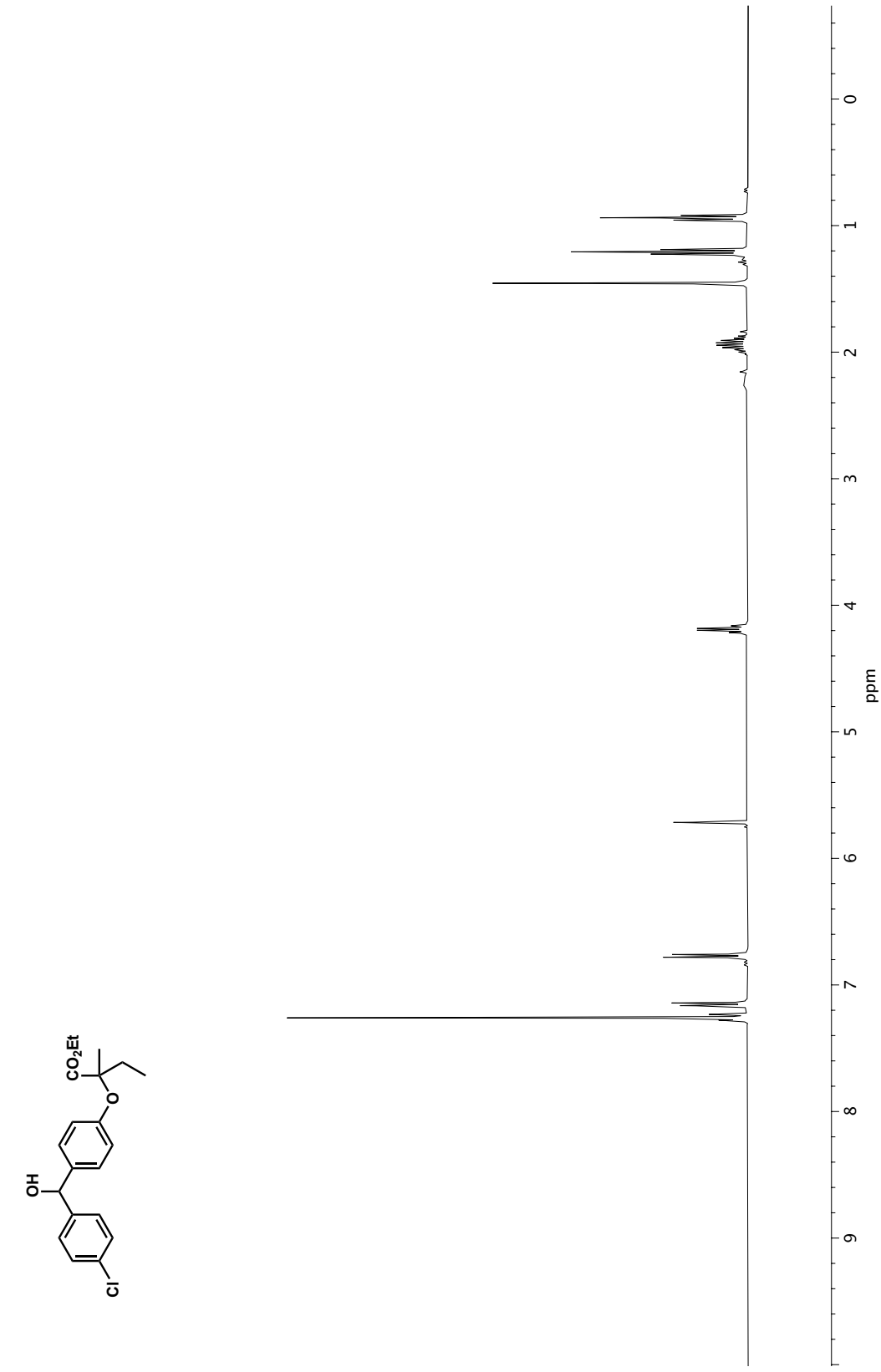


Figure A.4.28. ^{1}H NMR (400 MHz, $CDCl_3$) of **98b**.

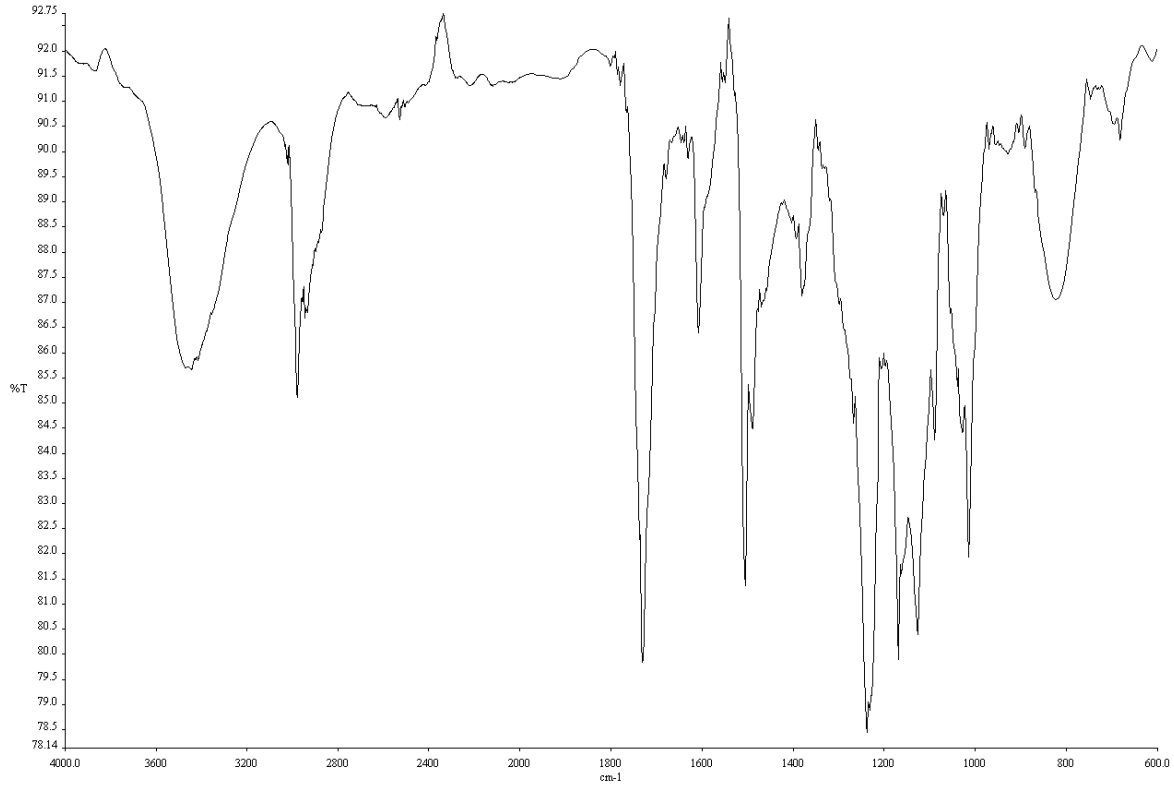


Figure A.4.29. Infrared spectrum (Thin Film, NaCl) of compound **98b**.

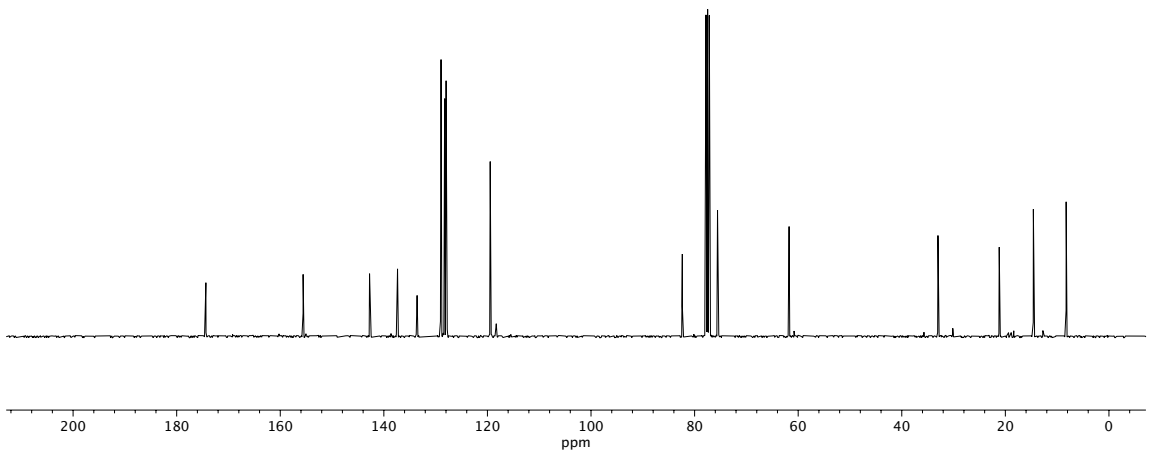


Figure A.4.30. ^{13}C NMR (101 MHz, $CDCl_3$) of compound **98b**.

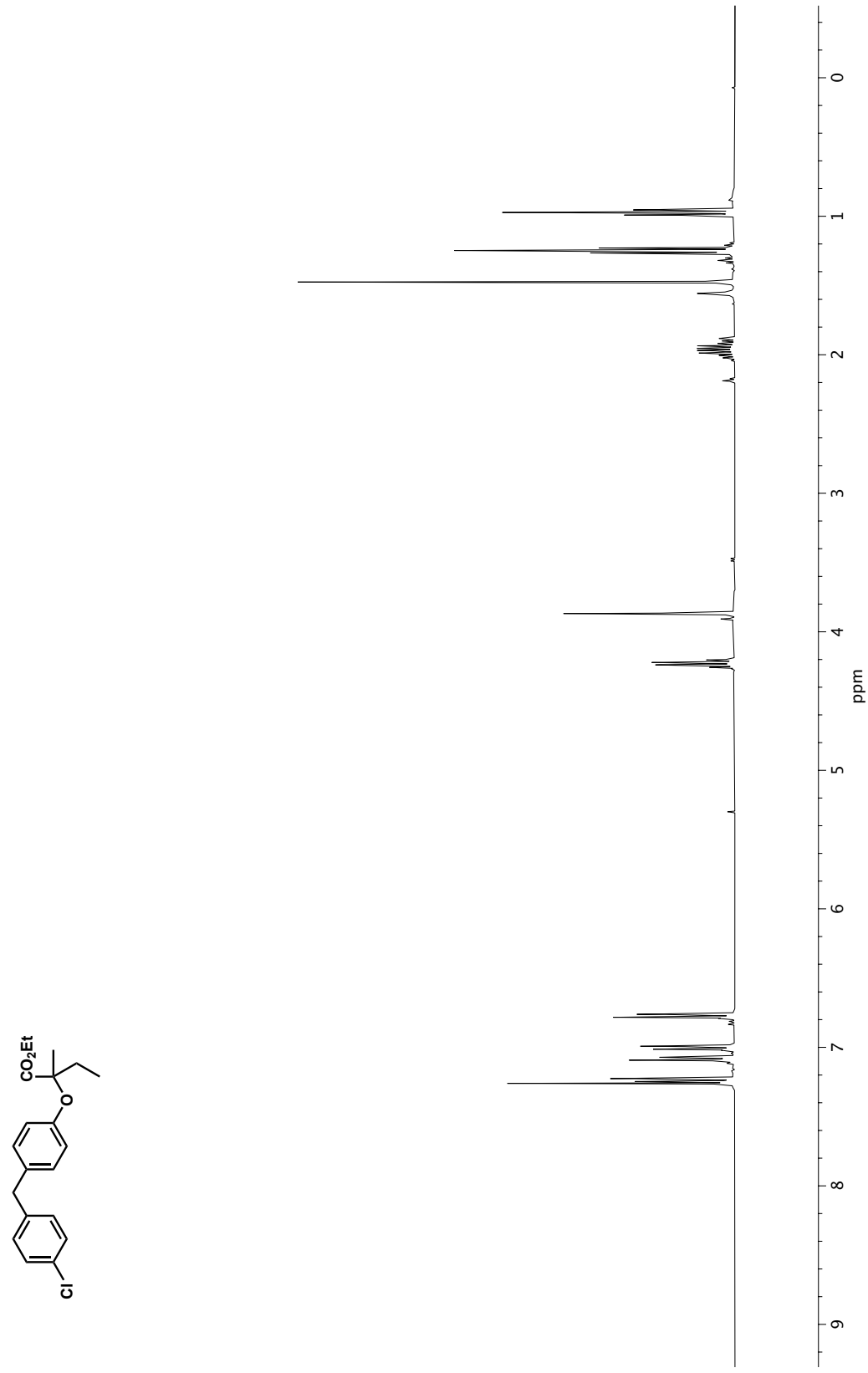


Figure A.4.31. ^{1}H NMR (400 MHz, $CDCl_3$) of **99**.

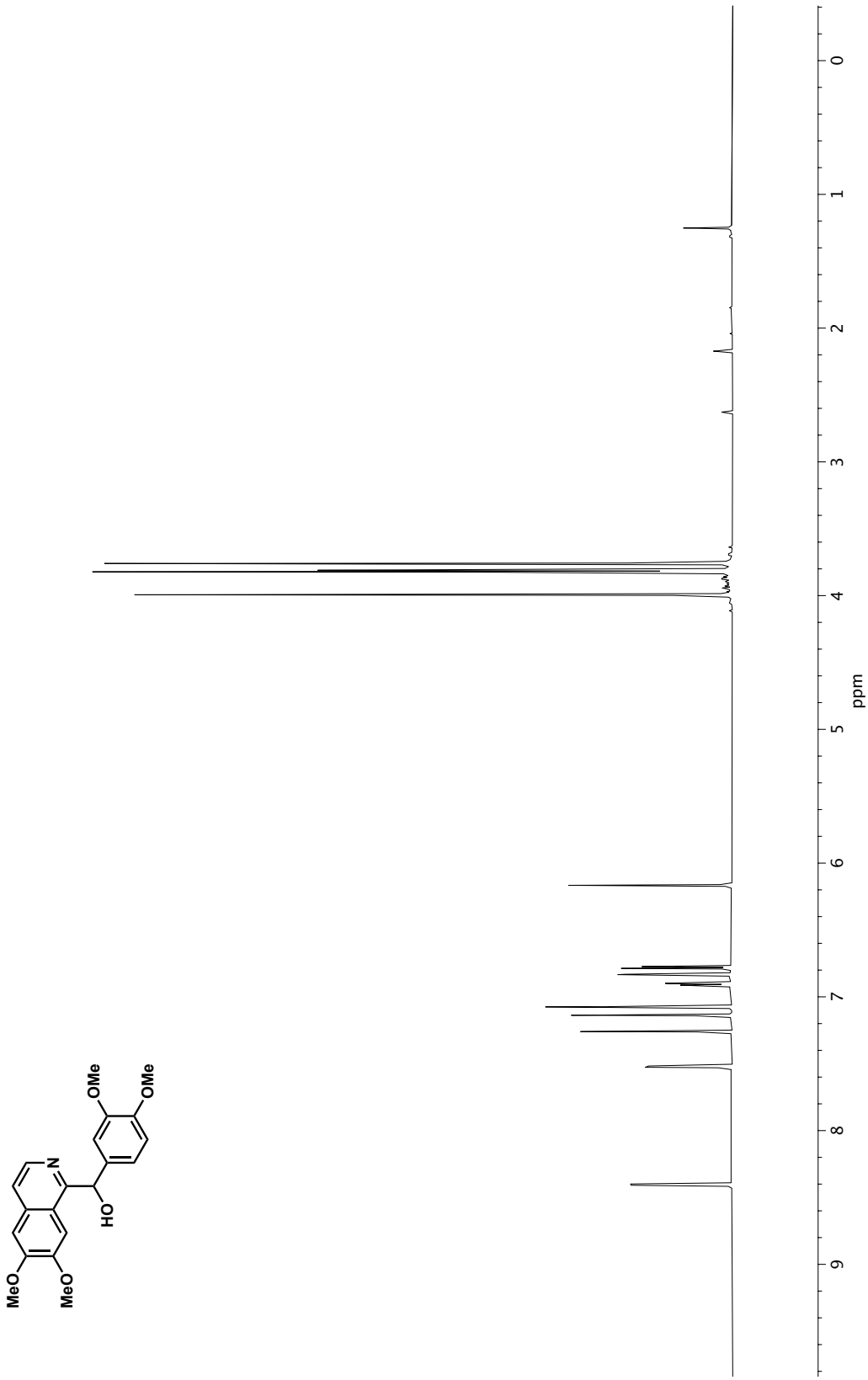


Figure A.4.32. ^{1}H NMR (600 MHz, $CDCl_3$) of **100a**.

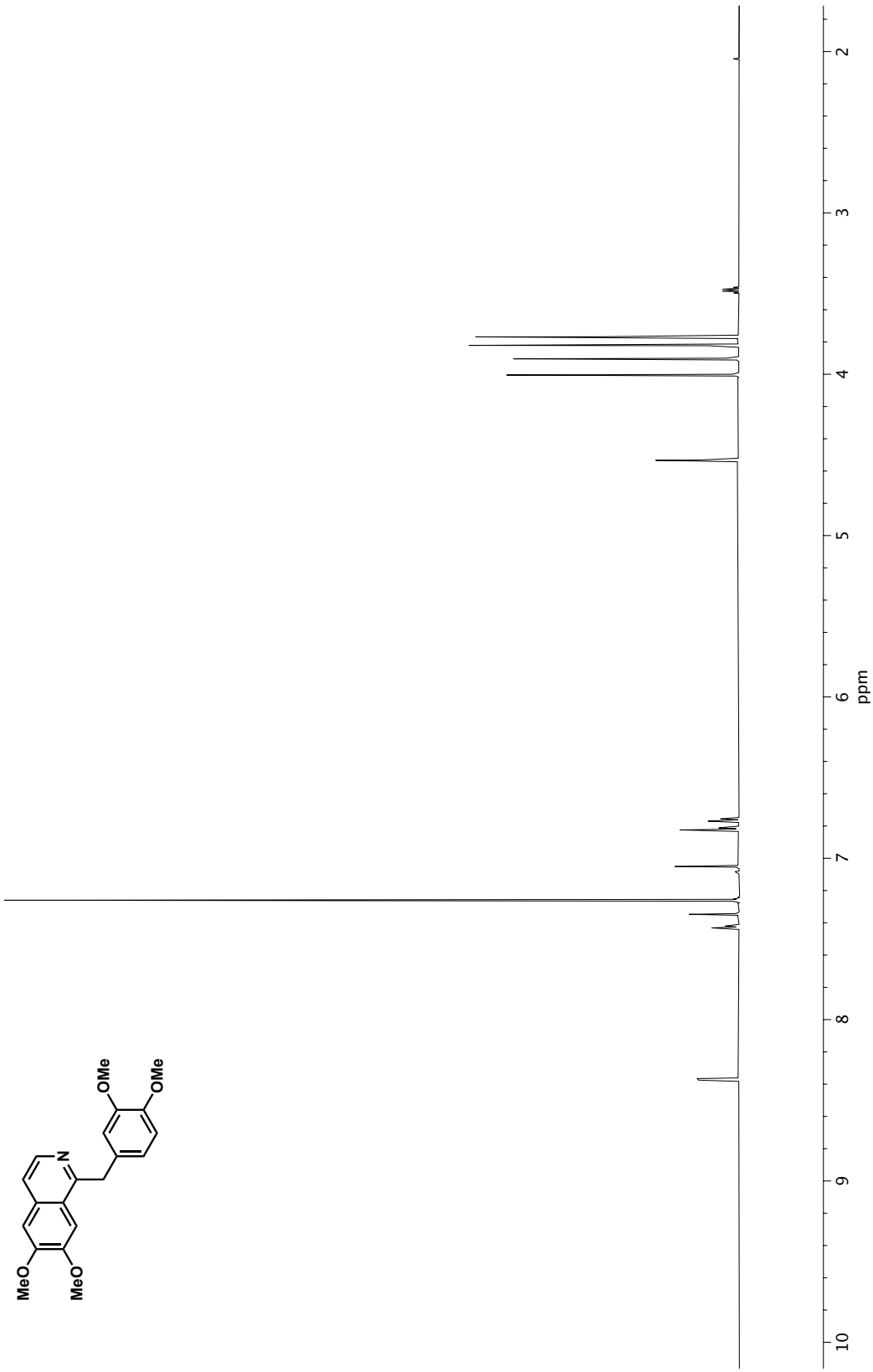


Figure A.4.33. ^{1}H NMR (600 MHz, $CDCl_3$) of **101**.

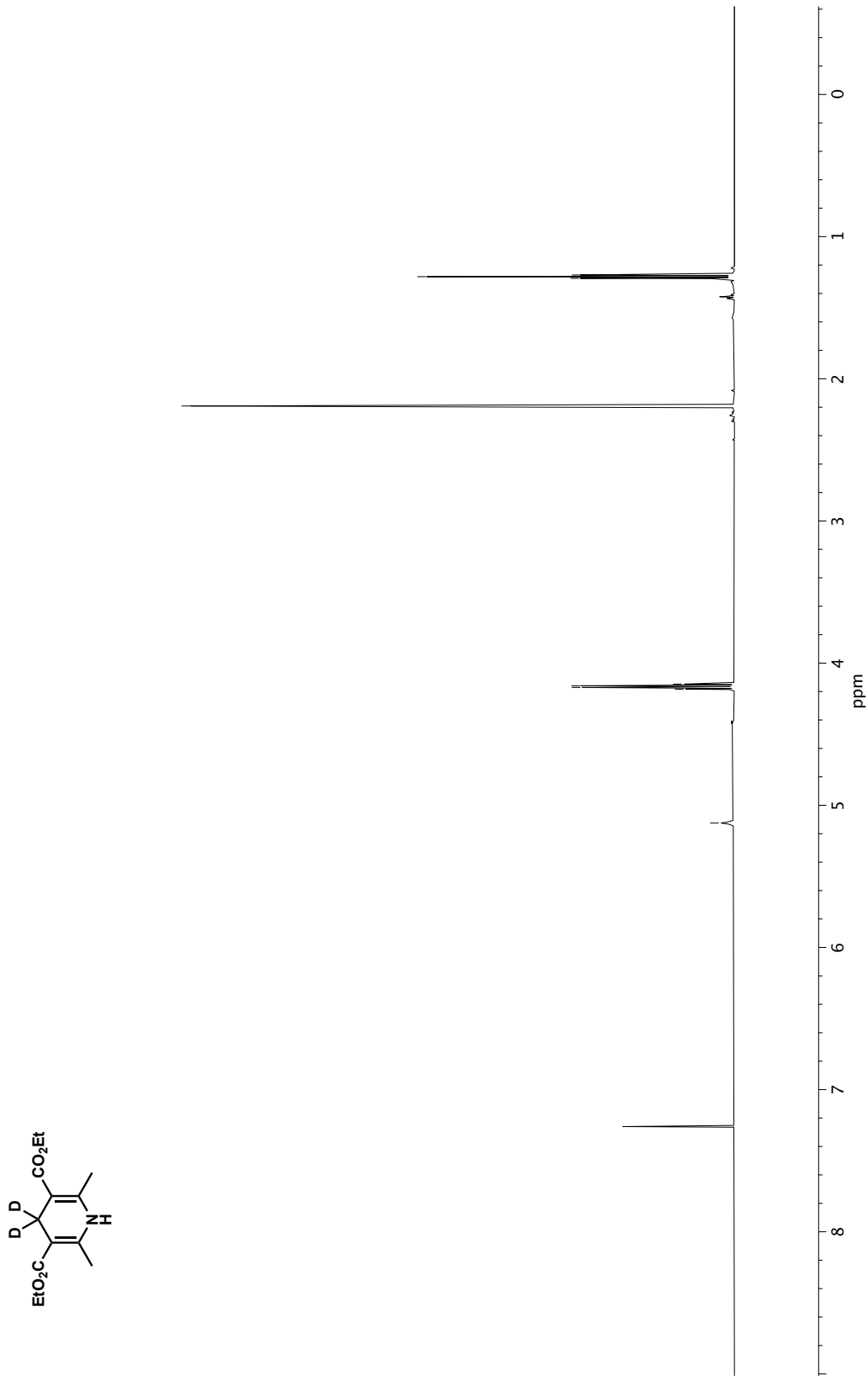


Figure A.4.34. ^{1}H NMR (600 MHz, $CDCl_3$) of **HE-d$_2$**.

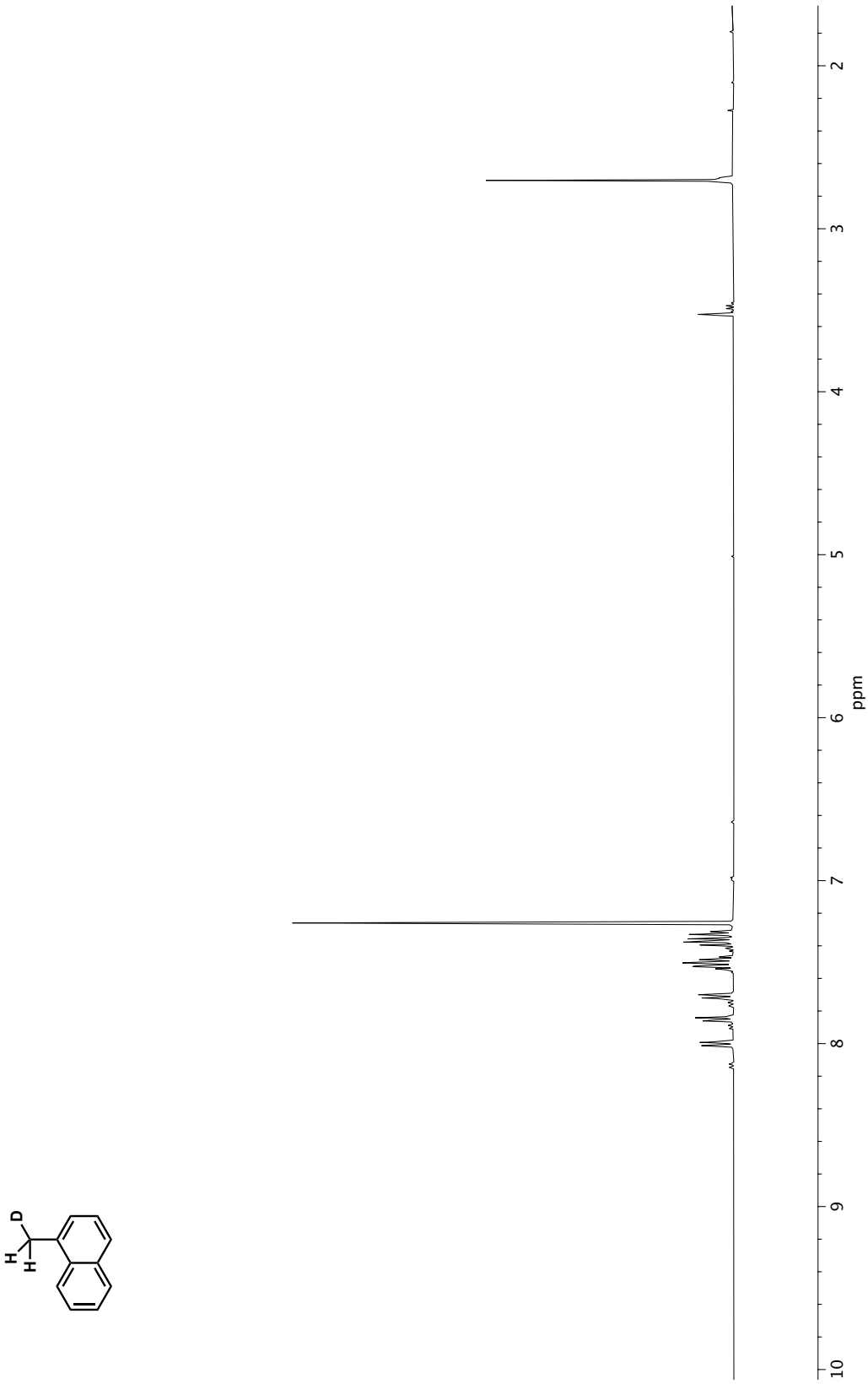


Figure A.4.35. ^{1}H NMR (400 MHz, $CDCl_3$) of **69d**.

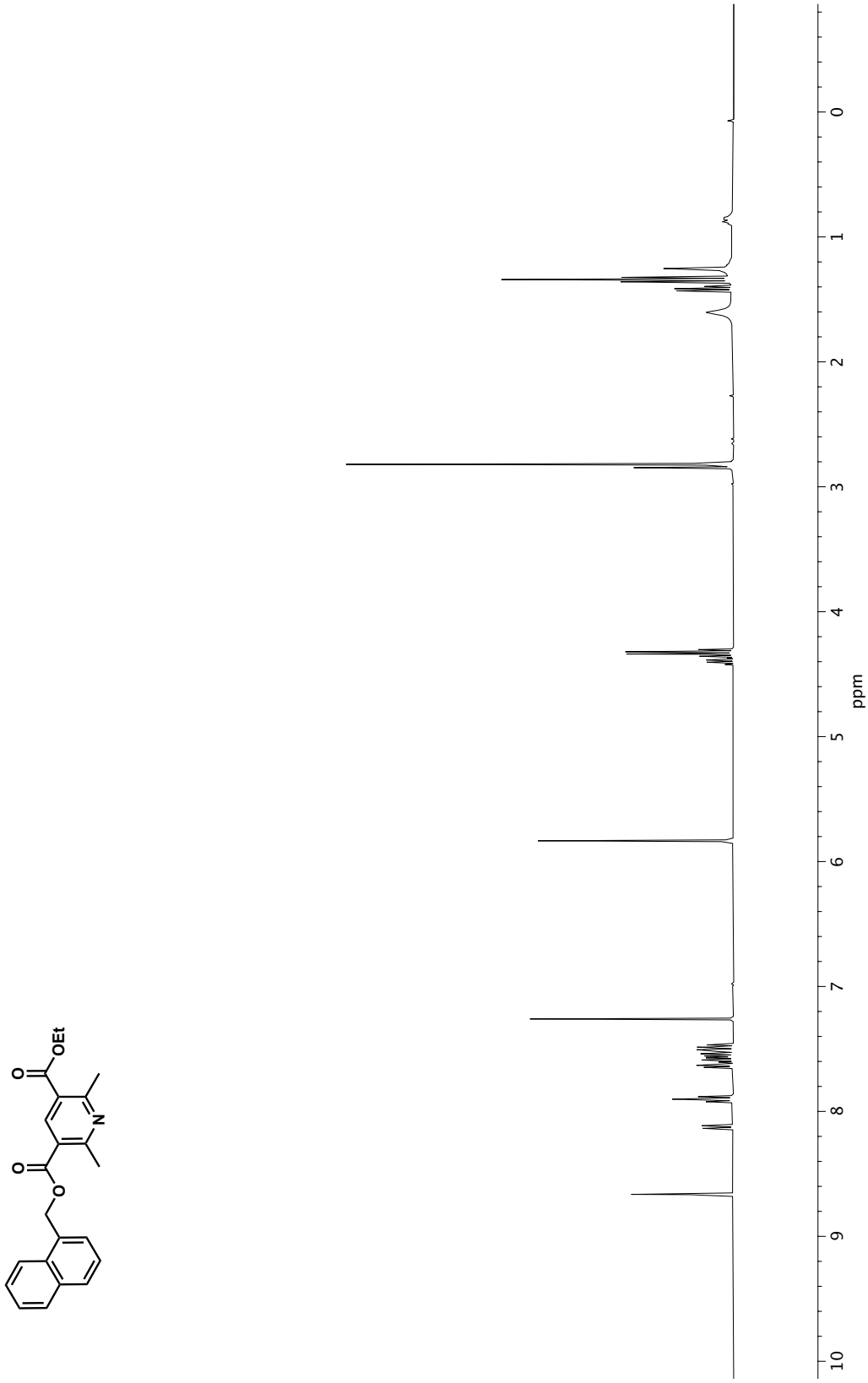


Figure A.4.36. ^{1}H NMR (400 MHz, $CDCl_3$) of **102**.

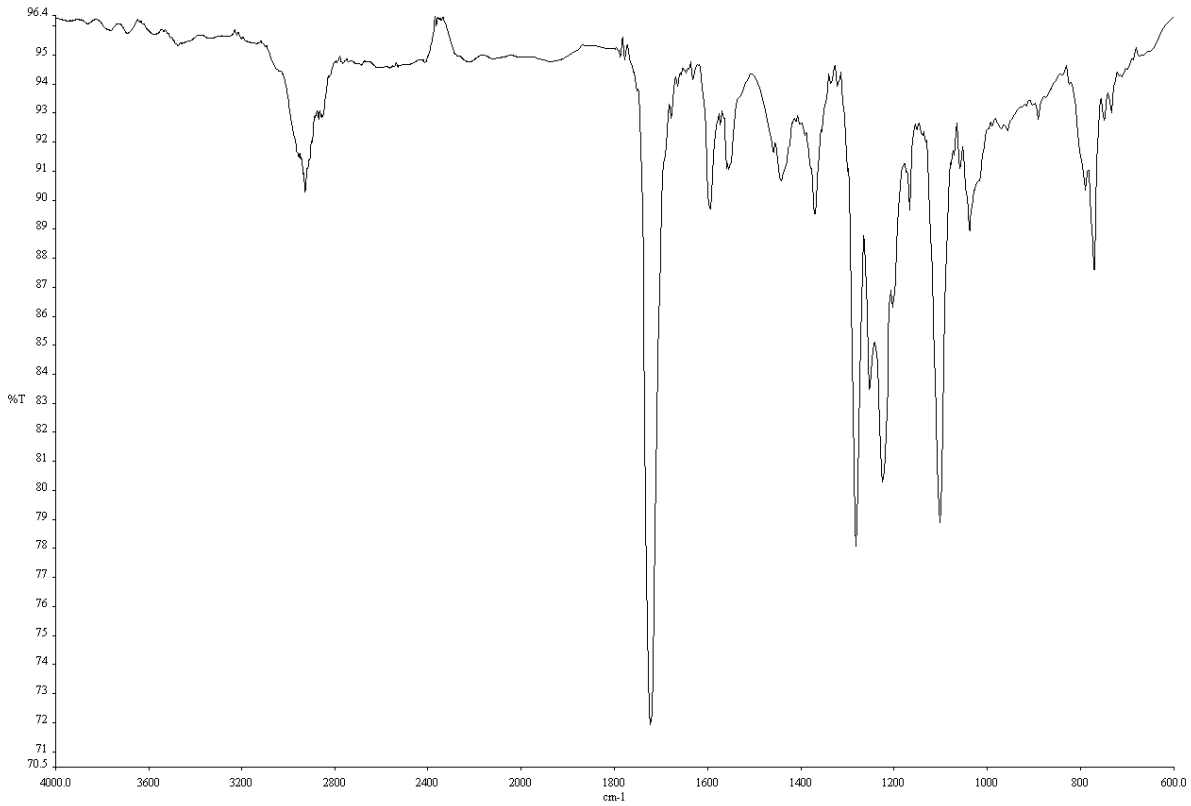


Figure A.4.37. Infrared spectrum (Thin Film, NaCl) of compound **102**.

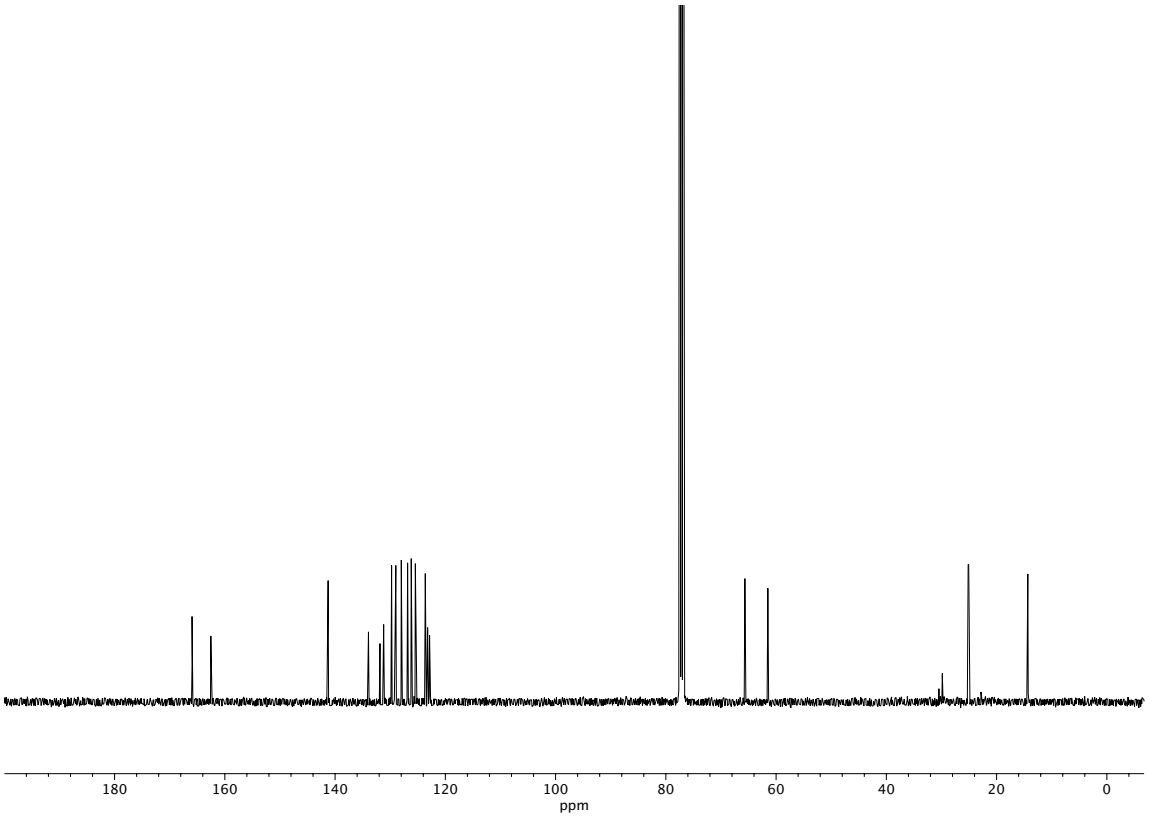


Figure A.4.38. ^{13}C NMR (101 MHz, $CDCl_3$) of compound **102**.

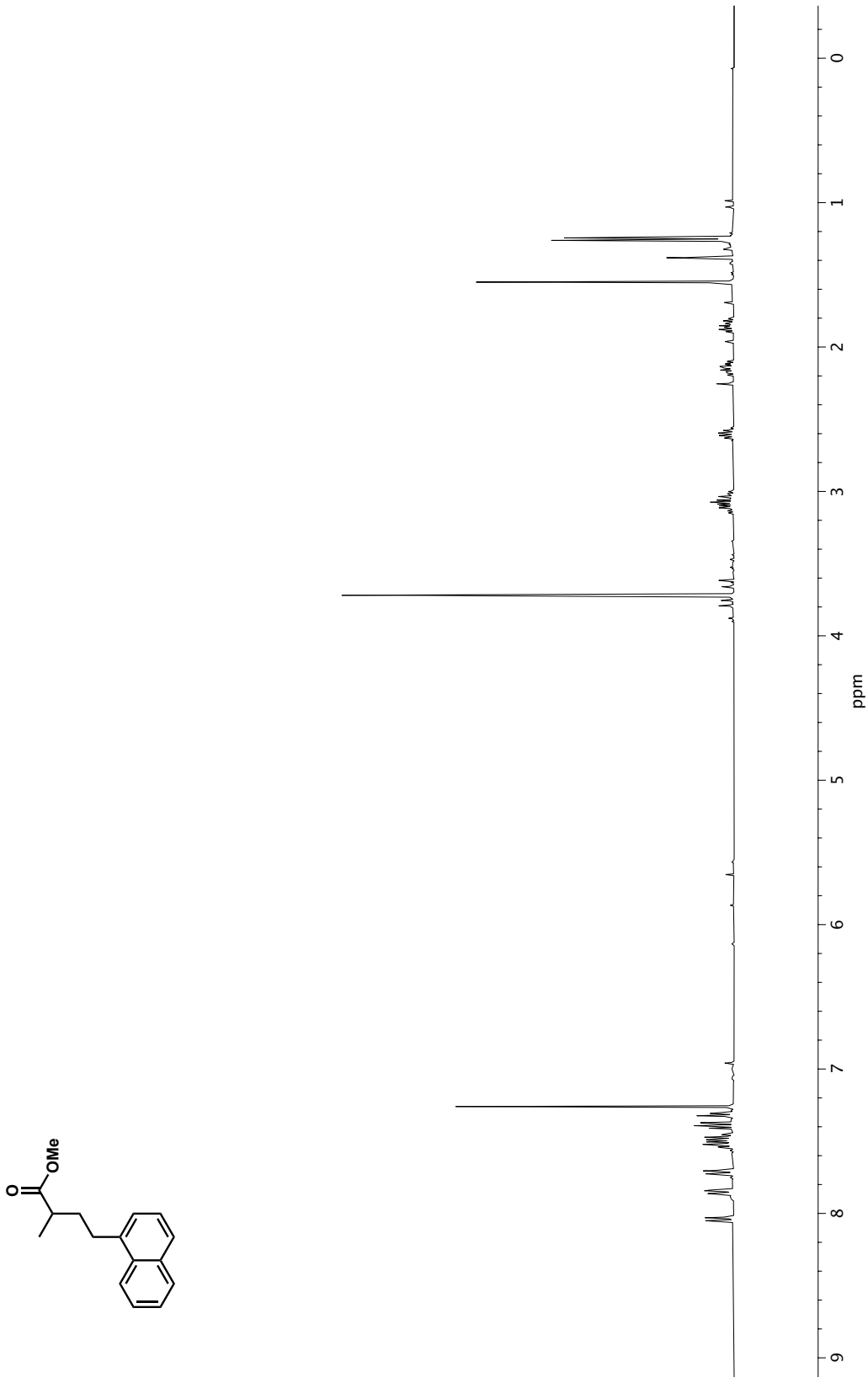


Figure A.4.39. ^{1}H NMR (400 MHz, $CDCl_3$) of **103**.

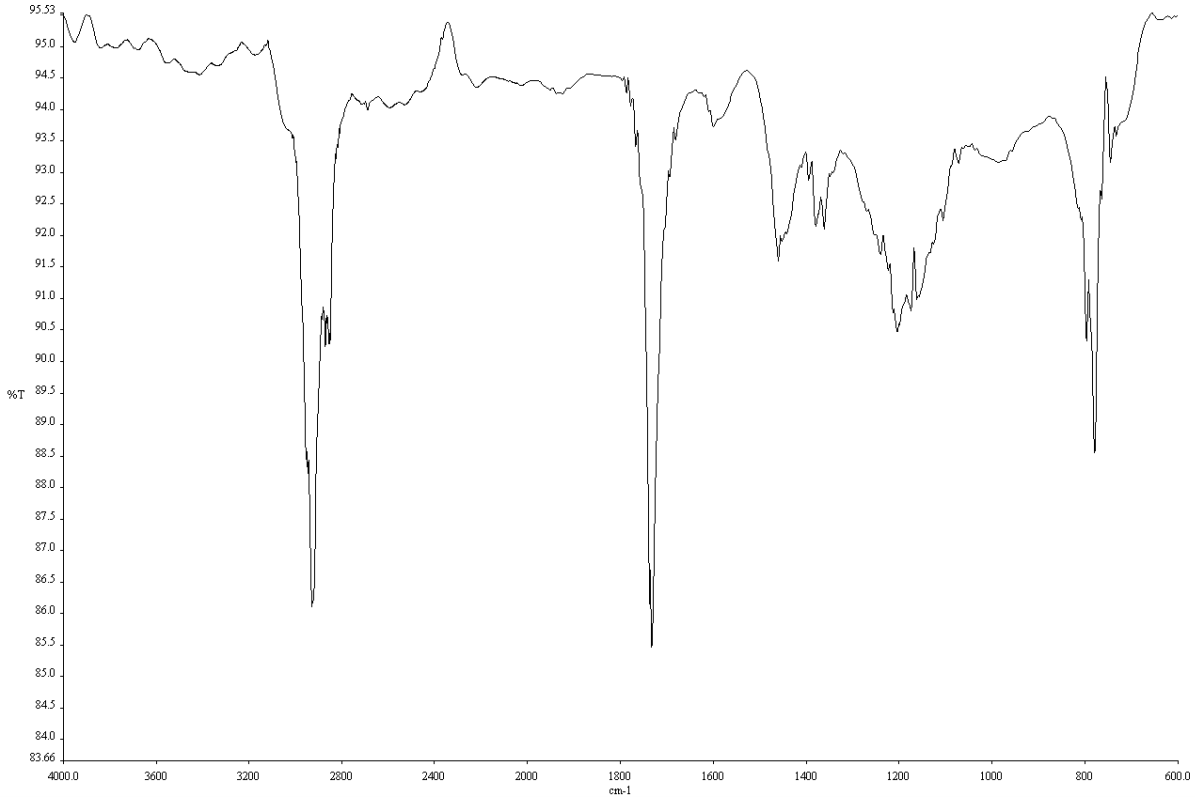


Figure A.4.40. Infrared spectrum (Thin Film, NaCl) of compound **103**.

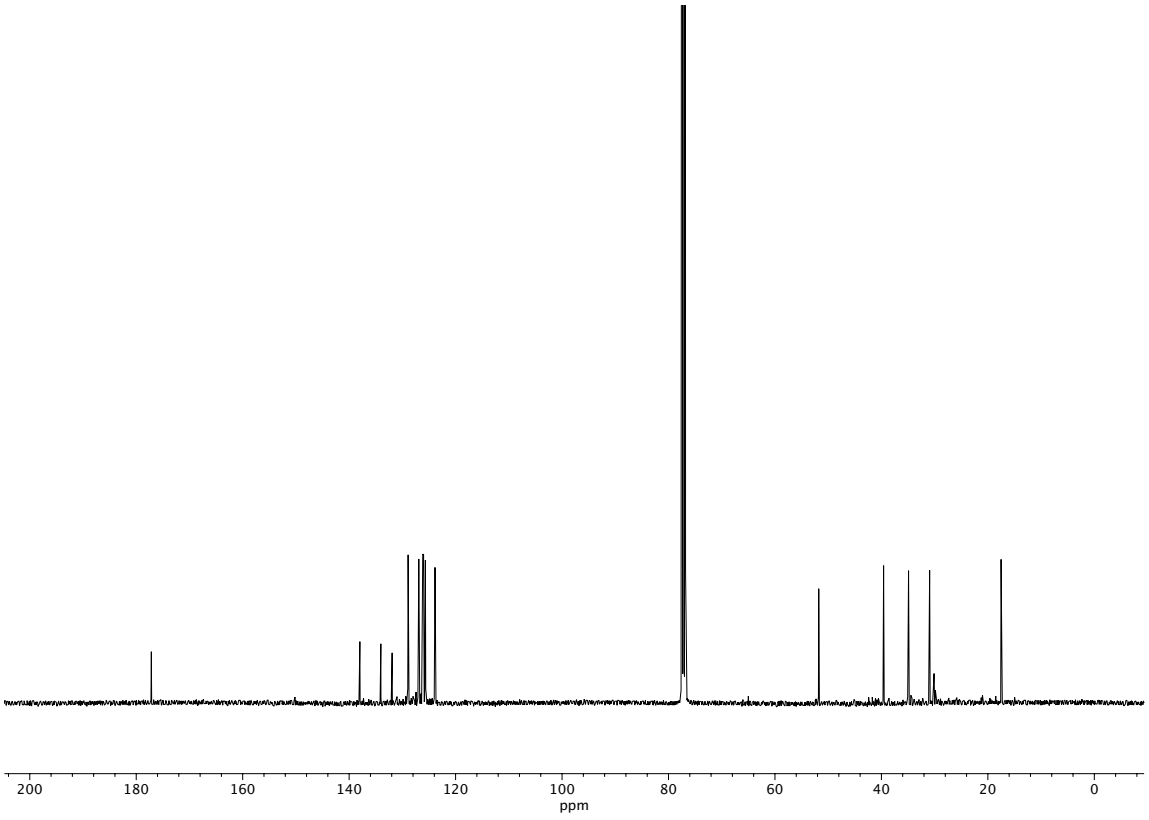


Figure A.4.41. ^{13}C NMR (101 MHz, $CDCl_3$) of compound **103**.

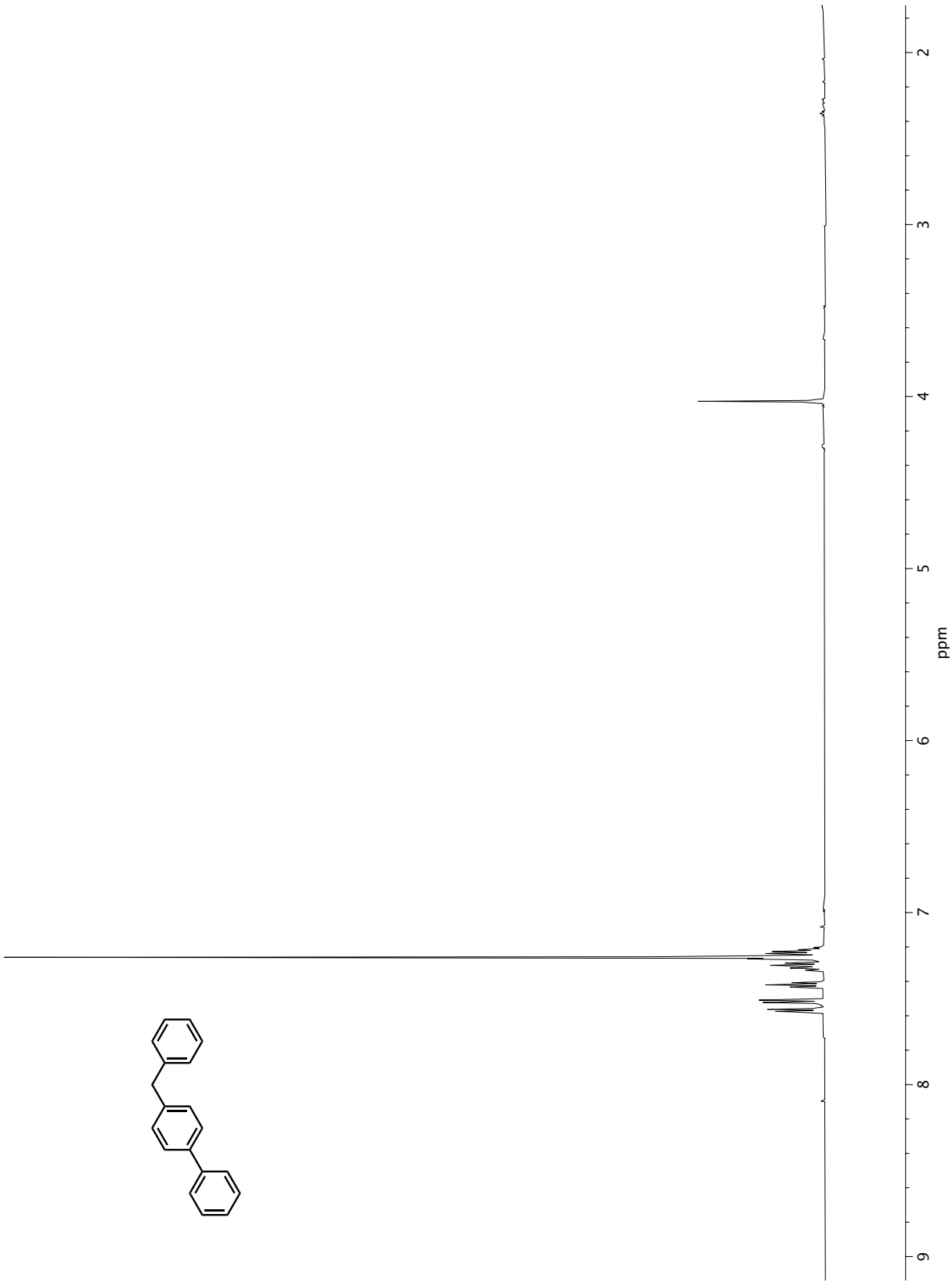


Figure A.4.42. ^{1}H NMR (600 MHz, $CDCl_3$) of **104**.

ABOUT THE AUTHOR

Benjamin Martin Gross was born in Berlin, Germany, where he spent the beginning of his childhood, moving to New York with his family at the age of six. He returned to Berlin to finish high school, graduating from the John F. Kennedy International School with an emphasis in math and physics.

Originally planning to attend medical school, he instead enrolled at the Technische Universität in Berlin as a chemistry undergraduate. He was quickly captivated by the organic chemistry classes taught by Prof. Martin Oestreich and taken under his wing. He completed his bachelor's degree in 2018, where he gained his first research experience in teaching labs and within the research group. He additionally completed a summer stay within the medicinal chemistry department at Merck, KGaA in Darmstadt, Germany.

Staying on for his master's degree in Berlin, he embarked on a five-month research stay with Prof. Christopher D. Vanderwal at the University of California, Irvine. He contributed to the application of a cobalt-catalyzed radical polyene cyclization, further developing his interest in natural product total synthesis. With the start of the COVID pandemic, he returned to Berlin in 2020, completing his master thesis with Prof. Martin Oestreich in the spring of 2021. After a 3-month research internship in medicinal chemistry at the Bayer campus in Berlin, he returned to Southern California in August 2021, to begin graduate studies at Caltech under the guidance of Prof. Brian M. Stoltz. During his PhD, Benjamin further nurtured his passion for the synthesis of complex small molecules and the applications of new reaction development.

Upon completing his PhD, Benjamin will move to South San Francisco to start a job in the medicinal chemistry department at Genentech.